



**HAL**  
open science

# Energy consumption minimization strategy for fuel cell hybrid electric vehicles

Huan Li

► **To cite this version:**

Huan Li. Energy consumption minimization strategy for fuel cell hybrid electric vehicles. Other. Université Bourgogne Franche-Comté, 2018. English. NNT : 2018UBFCA034 . tel-02084175

**HAL Id: tel-02084175**

**<https://theses.hal.science/tel-02084175>**

Submitted on 29 Mar 2019

**HAL** is a multi-disciplinary open access archive for the deposit and dissemination of scientific research documents, whether they are published or not. The documents may come from teaching and research institutions in France or abroad, or from public or private research centers.

L'archive ouverte pluridisciplinaire **HAL**, est destinée au dépôt et à la diffusion de documents scientifiques de niveau recherche, publiés ou non, émanant des établissements d'enseignement et de recherche français ou étrangers, des laboratoires publics ou privés.



SPIM

Thèse de Doctorat



école doctorale sciences pour l'ingénieur et microtechniques

UNIVERSITÉ DE TECHNOLOGIE BELFORT-MONTBÉLIARD

# **Energy consumption minimization strategy for fuel cell hybrid electric vehicles**

 Huan LI



THÈSE DE DOCTORAT DE L'ÉTABLISSEMENT UNIVERSITÉ BOURGOGNE  
FRANCHE-COMTÉ

PRÉPARÉE À L'UNIVERSITÉ DE TECHNOLOGIE DE BELFORT-MONTBÉLIARD

École doctorale n°37

Sciences Pour l'Ingénieur et Microtechniques

Doctorat de Génie Électronique

par

Huan LI

Energy consumption minimization strategy for fuel cell hybrid electric vehicles

Thèse présentée et soutenue à Belfort, le 07/12/2018

Composition du Jury :

BENBOUZID Mohamed	Professeur, Université Bretagne Occidentale	Rapporteur
DIALLO Demba	Professeur, Université Paris Sud-IUT de Cachan	Rapporteur
DJERDIR Abdesslem	Maitre de conférences, Université de Technologie de Belfort-Montbéliard	Directeur de thèse
GUILBERT Damien	Maitre de conférences, Université de Lorraine	Examinateur
OUTBIB Rachid	Professeur, Université Aix-Marseille	Examinateur
N'DIAYE Abdoul	Ingénieur, Université de Technologie de Belfort-Montbéliard	Examinateur
RAVEY Alexandre	Maitre de conférences, Université de Technologie de Belfort-Montbéliard	Codirecteur de thèse
RIU Delphine	Professeur, Ecole ingénieurs énergie eau environnement	Examinatrice



# SPIM

école doctorale sciences pour l'ingénieur et microtechniques





# Acknowledgment

At first, I would like to thank Dr.Benbouzid Mohamed and Dr.Diallo Demba for accepting to review this dissertation, despite their very busy schedules, and for their helpful comments. I also want to thank Dr.Guilbert Damien, Dr.Outbib Rachid, Dr.N'diaye Abdoul and Dr.Riu Delphine for their participation in my dissertation committee.

I would like to express my sincere gratitude to my supervisor, Dr.Djerdir Abdesslem, for the continuous support of my PhD study and research, for his professional guidance throughout the thesis, for his personal help on my future career. I would also like to thank my co-supervisor Dr.Ravey Alexandre, who took much time in providing me with valuable ideas and enlightening suggestions, as well as giving me sincere help. Moreover, I would like to thank Dr.Abdoul N'Diaye for maintaining laboratory equipment, carrying out experiments with me, which is crucial to this thesis.

I also want to thank Mr.Patrice Lubarda, Mr.Abdelmajid Naimi, Mr.Pierre Diebolt, Mr.Djelalli Larioumlil and other staffs of energy department of UTBM for their help on my experimental test.

I would like to thank my friends who started the thesis at the same time as me: Dr.Chen Liu, Dr.Rui MA, Mr.Hailong WU, Mr.Hanqing Wang and Dr.Bei LI. I would like to thanks all the persons that I met and worked with at UTBM: Mr.Hao Bai, Mr.Yang Zhou, Mr.Shengrong ZUO, Mr.Dan Zhu, Mr.shuyao Kong, Mr.Yu wu and Mr.loic vichard.

I want to thank Dr.Fei Gao, Dr.Daniela Chrenko and Dr.Stefan Giurgea for their help on my research and teaching work.

I am thankful for my family support during my abroad study. Thanks for the company of my girlfriend, Mengli Yin.

Finally, financial support of China Scholarship Council is gratefully acknowledged.



# Contents

1	Current context of FCHEV	5
1.1	Introduction	5
1.2	State of the art of fuel cell hybrid electric vehicles	6
1.3	Fuel cell hybrid electric vehicles' research in Belfort-France	13
1.4	Policy supports for fuel cell hybrid electric vehicles	17
1.4.1	US Department of Energy Fuel Cells Program	18
1.4.2	European hydrogen and fuel cell technology platform	19
1.4.3	Japanese New Energy and Industrial Technology Development Organization Fuel Cell Programs	20
1.4.4	Chinese New Energy Vehicle Program	23
1.5	PhD project objectives	24
2	State of the art of energy management strategy	27
2.1	Introduction	27
2.2	Characteristics of power sources	27
2.2.1	Fuel cell	27
2.2.2	Energy storage sources	28
2.3	Energy management strategy	29
2.3.1	Rule based strategy	29
2.3.1.1	Deterministic rule based strategy	29
2.3.1.2	Fuzzy rule based strategy	31
2.3.2	Frequency based strategy	34
2.3.3	Optimization based strategy	35
2.3.3.1	Global optimization based strategy	36
2.3.3.2	Local optimization based strategy	40
2.4	Objectives	45
2.4.1	Drive ability objective	45
2.4.2	Energy storage sources'charge sustenance objective	46
2.4.3	Stability Objective	48

2.4.4	Fuel consumption objective . . . . .	49
2.4.5	Power sources durability objective . . . . .	52
2.4.5.1	Durability of fuel cell . . . . .	52
2.4.5.2	Durability of battery . . . . .	54
2.4.6	Economy objective . . . . .	56
2.4.7	Multiple objectives . . . . .	58
2.5	Analysis of objectives and EMS . . . . .	62
2.5.1	Analysis of objectives . . . . .	62
2.5.2	Analysis of EMS for different objectives . . . . .	66
2.6	Conclusion and suggestion . . . . .	67
<b>3</b>	<b>Energy consumption minimization strategy</b>	<b>69</b>
3.1	Introduction . . . . .	69
3.2	Power train architecture and component modes . . . . .	69
3.2.1	Power train architecture . . . . .	69
3.2.2	Fuel cell stack model . . . . .	72
3.2.3	Fuel cell efficiency model . . . . .	76
3.2.4	Battery model . . . . .	78
3.2.5	Supercapacitor model . . . . .	82
3.2.6	DC/DC converter model . . . . .	83
3.3	Equivalent consumption minimization strategy . . . . .	83
3.3.1	SQP based equivalent consumption minimization strategy (SECMS)	84
3.3.2	Rule based control strategy . . . . .	86
3.3.3	Hybrid ECMS OMCS strategy . . . . .	88
3.4	Simulation results and analysis . . . . .	89
3.5	Conclusion . . . . .	94
<b>4</b>	<b>EMS considering the power sources degradation</b>	<b>95</b>
4.1	Introduction . . . . .	95
4.2	Unscented Kalman filter . . . . .	96
4.3	Fuel cell degradation and on line state of health estimation . . . . .	98
4.4	Battery degradation and on line state of health estimation . . . . .	99
4.5	ECMS with power sources degradation . . . . .	102
4.5.1	The effect of power sources degradation on ECMS . . . . .	102
4.5.2	Adaptive equivalent consumption minimization strategy . . . . .	104
4.6	Simulation results and analyses . . . . .	104

4.7	Conclusion . . . . .	105
5	Experimental validation	109
5.1	Introduction . . . . .	109
5.2	Test bench . . . . .	110
5.2.1	Software system . . . . .	110
5.2.2	Hardware system . . . . .	111
5.3	Experimental validation and analysis . . . . .	115
5.4	Conclusion . . . . .	119
6	General conclusion	125



# General introduction

With the development of society, global warming, environmental pollution and the exhaustion of petroleum energies have risen their attention to human. Electric vehicle (EV), hybrid electric vehicle (HEV) and plug-in hybrid electric vehicle (P-HEV) are thought as the best way to solve these problems in the aspect of the transportation system. Fuel cell hybrid electric vehicle (FCHEV), as one kind of HEV, has many advantages such as zero emission, using the hydrogen as fuel and not relying on oil. A number of automobile manufacturers and various government agencies put forward many projects to develop fuel cell hybrid electric vehicles. Energy management strategy (EMS) plays a key role for FCHEV due to their multiple energy sources composition. Much research is devoted to developing optimal, reliable and applicable control strategies. This PhD dissertation considers a FCHEV with three power sources: fuel cell, battery and supercapacitor, which increases the difficulty to design an energy management strategy to split the power among different power sources. Energy consumption minimization strategy for fuel cell hybrid electric vehicles is designed.

The dissertation is organized in six chapters as follows. In chapter 1, the development history of fuel cell hybrid electric vehicles is introduced. The power sources and the architectures of fuel cell hybrid electric vehicles are also summarized up. The laboratories and universities in Belfort also did much research on fuel cell hybrid electric vehicles and these research projects are introduced. Finally, the future development trends and policy supports of American, European, Japan and China are reviewed.

In chapter 2, a detailed state of the art review is presented for the energy management strategy of FCHEV. The chapter starts by analyzing the characteristics of fuel cell and energy storage sources, which is helpful for the design of energy management strategy to ensure the normal operation of power sources, increase their lifetime and play their full potential. After that, energy management strategies of FCHEV categorized into three kinds: rule based, frequency based and optimization based strategies to analyze the characteristics of every kind of energy management strategy. After that, the objectives and corresponding methods to fulfill these objectives are summarized.

In chapter 3, sequential quadratic programming (SQP) based equivalent consumption minimum strategy (SECMS) is designed for the FCHEV powered by three power sources: fuel cell, battery and supercapacitor. In order to decrease hydrogen consumption and increase the durability of power sources, the fuel cell is chosen as the main power source and supplies steady current, the battery is designed as the main energy buffer and the replacement of fuel cell failure and the supercapacitor is operated to supply peak power. Precise fuel cell stack model and efficiency model of fuel cell system are built to calculate the maximum efficiency point and define its high efficiency zone. By applying the SQP algorithm, the instantaneous equivalent hydrogen consumption is minimized. A rule based control strategy (RBCS) is also designed to compare with SECMS. Power following control strategy (PFCS) as the first part of RBCS to calculate fuel cell reference current and operating mode control strategy (OMCS) as the second part is used to calculate su-

percapacitor reference current. Considering low energy density of supercapacitor, much research neglects supercapacitor equivalent hydrogen consumption in the ECMS objective function where the whole hydrogen consumption including fuel cell hydrogen consumption and equivalent hydrogen consumption of battery and supercapacitor is defined. In order to prove that this simplification can lead to sub-optimal results, a hybrid ECMS and OMCS strategy (HEOS) is designed.

During the lifetime of FCHEV, power sources degradation appears. As the main power source of FCHEV, the output power of fuel cell stack at corresponding current decreases along with degradation and its maximum efficiency point of operation also changes. The capacity of battery decreases and its resistance increases along with its degradation, which decreases the output voltage of battery. In chapter 4, fuel cell and battery aging models are built to monitor their state of health (SOH) to ensure the performance, safety, availability and reliability of power sources. The effects of their degradation on ECMS are analyzed. On the basis of ECMS, adaptive ECMS (AECMS) is designed to adjust equivalent factors and fuel cell dynamical current change rate to ensure the charge sustenance of battery and prolong the lifetime of fuel cell.

In chapter 5, a test bench is built to experimentally validate the presented comparative study of three control strategies. The components of the test bench are introduced in detail. The experimental comparison results show that fuel cell is operated at around maximum efficiency, supercapacitor supplies peak power, battery works as the energy buffer. The battery SOC and supercapacitor SOC are in the limited ranges, the final battery SOC is almost equivalent to initial value. Compared with RBCS and HEOS, SECMS hydrogen consumption decreases 2.16% and 1.47% respectively. SECMS also has the most stable fuel cell current, so the degradation of fuel cell due to dynamical current change is the least.

Lastly, the contributions of this work are overviewed, and the possible future works are listed in chapter 6.

# Nomenclature

## Acronyms

*AC* Alternating Current

*AECMS* Adaptive ECMS

*DC* Direct Current

*DOE* Department of energy

*DP* Dynamical programming

*DRBS* Deterministic rule based strategy

*ECMS* Equivalent consumption minimization strategy

*EKF* Extended Kalman filter

*EMS* Energy management strategy

*ESS* Energy storage source

*FBS* Frequency based strategy

*FCHEV* Fuel cell hybrid electric vehicle

*FCUJU* Fuel Cells and Hydrogen Joint Undertaking

*FCV* Fuel cell vehicle

*FRBS* Fuzzy rule based strategy

*GA* Genetic algorithm

*GOBS* Global optimization based strategy

*HEOS* Hybrid ECMS and OMCS strategy

*HESS* Hybrid energy storage system

*LOBS* Local optimization based strategy

*LP* Linear programming

*MOST* Ministry of Science and Technology

*MPC* Model predictive control

*NEDO* New Energy and Industrial Technology Development Organization

*OBS* Optimization based strategy

<i>OMCS</i>	Operating mode control strategy
<i>PF</i>	Particle filter
<i>PFCHEV</i>	Plug-in fuel cell hybrid electric vehicle
<i>PFCS</i>	Power following control strategy
<i>PMP</i>	Pontryagin's Minimum Principle
<i>PSO</i>	Particle swarm optimization
<i>PWM</i>	Pulse width modulated
<i>RBCS</i>	Rule based control strategy
<i>RBS</i>	Rule based strategy
<i>SECMS</i>	SQP based ECMS
<i>SQP</i>	Sequential quadratic programming
<i>UKF</i>	Unscented Kaleman filter
Symbols	
$ba_{SOC}$	Battery SOC value
$F$	Faraday constant
$I_{FC}$	Fuel cell current
$m_{BA}$	Battery equivalent hydrogen consumption
$m_{FC}$	Fuel cell hydrogen consumption
$m_{SC}$	Supercapacitor equivalent hydrogen consumption
$N_{cell}$	The number of fuel cell stack current
$P_{BA}$	Battery output power
$P_{FC}$	Fuel cell power
$P_{SC}$	Supercapacitor output power
$R$	Ideal gas constant
$S_{fc}$	Fuel cell on/off state
$SOC$	State of charge
$SOC_{bamax}$	Maximum battery SOC value
$SOC_{bamin}$	Minimum battery SOC value
$SOH$	state of health
$T$	The temperature of fuel cell stack
$V_{FC}$	Fuel cell voltage

# Current context of fuel cell hybrid electric vehicles

## 1.1 Introduction

Fossil fuels like oil, coal and natural gas support modernization and economic growth of the world, but they also lead to the serious environmental problem. For the past decades, global warming, ozone layer depletion and air pollution are getting more attention from all over the world. A large amount of fossil fuel consumed by transportation sector accounts for 55% of the world total energy consumption and lead to 30.9% carbon dioxide gas emission in 2014[1]. Reducing the carbon production and saving energy are sought by the vehicle industry. Due to the consumption of gasoline or diesel and air pollution from exhaust gas emission, traditional internal combustion engine based vehicles cannot meet the present requirement any more[2]. Electric vehicle (EV) including pure electric vehicle, hybrid electric vehicle (HEV) and plug-in hybrid electric vehicle (PHEV) is thought a good way to solve these problems[3]. With increasing research on clean energy vehicles, more and more cars, buses, tramway, and trains are designed into electric vehicles.

Regarding pure electric vehicle, the battery packs are the only energy source. Nevertheless, the present energy density of battery technology cannot provide enough energy to run the vehicle for a long trip and long charging time also brings inconvenience to customers[4]. Increasing the number of battery stack or choosing higher energy density batteries are used to solve the problem of short driving distance, but leading to an increase of both weight and price of the vehicle. The present battery technology is still a barrier to the widespread commercialization of pure electric vehicle. For the next following decades, developing higher energy density, lighter, lower price, and faster-charging battery is still an important topic for the researchers. To overcome these shortcomings of a pure electric vehicle, HEV is used, which is composed of at least two power sources. Energy storage source (ESS) as one of the power sources is responsible for supplying energy to the vehicle and can absorb energy during braking phases. Internal combustion engine as another power source cooperates with ESSs to solve the problem of driving distance. Compared to HEV, PHEV also allows charging the vehicle from the public grid. Nevertheless, the use of an internal combustion engine in the vehicle powertrain leads to a trade-off between driving distance and air pollution.

Fuel cell vehicles (FCVs) take fuel cell as the only or one of the power sources of vehicles. Fuel cell stack converts the chemical energy into electrical energy through the reaction between hydrogen and oxygen. The process does not involve high temperature

combustion, and the only production is pollution-free water. As long as hydrogen is supplied, fuel cell can provide continuous electrical energy. In the field of mobile and stationary applications, fuel cell is considered to be one of the future energy solutions. Since the fuel cell system is only working in one way, it cannot recycle braking energy. The starting time to its warm up is long and fuel cell also cannot stand high dynamic power, which limits its usage as the only power source for vehicles. Adding ESSs to work together with the fuel cell as the architecture of fuel cell hybrid electric vehicle (FCHEV) is widely used to overcome these shortcomings. Plug-in fuel cell hybrid electric vehicles (PFCHEV) and fuel cell range extended electric vehicle (FCREEV) are also used in some vehicles[5, 6, 7].

## 1.2 State of the art of fuel cell hybrid electric vehicles

Fuel cell was first invented by Sir William Grove in 1839, which ultimately proved that electric current could be produced from an electrochemical reaction between hydrogen and oxygen over a platinum catalyst[8]. In 1966, fuel cell is used as a power source of vehicle named as GMC Electrovan by General Motors for the first time[9]. Liquid hydrogen and liquid oxygen are used as the fuel. A large room of the Electrovan is taken placed by the tanks containing oxygen and hydrogen, so the six seats van turns into 2 seats one. The top speed of Electrovan is 70 mph and maximum range is 120 miles. Due to high financial cost, heavy weight, large volume, lack of hydrogen infrastructure and low lifetime, the project is stopped.

Due to increasing concerns over energy security, energy efficiency, and carbon dioxide emissions, attention has gradually turned once again to fuel cell as one of the potential technologies capable of delivering high energy efficiency, carbon dioxide saving and reducing dependence on fossil fuels. The decade's development of compressed hydrogen storages, computer-based controllers and low platinum loading catalysts also increase the durability of fuel cell stack and decreases its cost and complexity. The closure of the Apollo program which makes many NASA researchers move to private companies also promote the development of fuel cell technology[10]. A number of automobile manufacturers like Honda, Ford, Toyota and GM take this chance to develop and demonstrate their own fuel cell hybrid electric vehicles in Table1.1. But these fuel cell hybrid electric vehicles are prototypes and only few vehicles are produced and demonstrated in the local region.

Toyota has started the research on fuel cell hybrid electric vehicles since about 1996 and many prototypes are designed such as the RAV 4 FCEV-hybrid (Metal hydride, 1996), RAV 4 FCEV (Methanol, 1997), FCHV-3 (Metal hydride, 2001), FCHV-4 (Compressed H<sub>2</sub>, 2001), and FCHV-5 (reformed gasoline, 2001)[12]. Through the efforts and development for many years, Toyota FCHVs are finally limited sold in USA and Japan in 2002. In 2015, Toyota Mirai shown in Figure 1.1 is sold as the first commercial fuel cell hybrid electric vehicle in the world, which means the development of fuel cell hybrid electric vehicle enters into the early commercialization phase. Following that, Hyundai and Honda also both introduce their fuel cell hybrid electric vehicles: Tucson and Clarity for commercial sale respectively, and several auto manufacturers, including GM, Daimler, and BMW, are working toward commercial production of fuel cell hybrid electric vehicles in the near term[13]. The comparison of three commercial vehicles is shown in Table1.2.

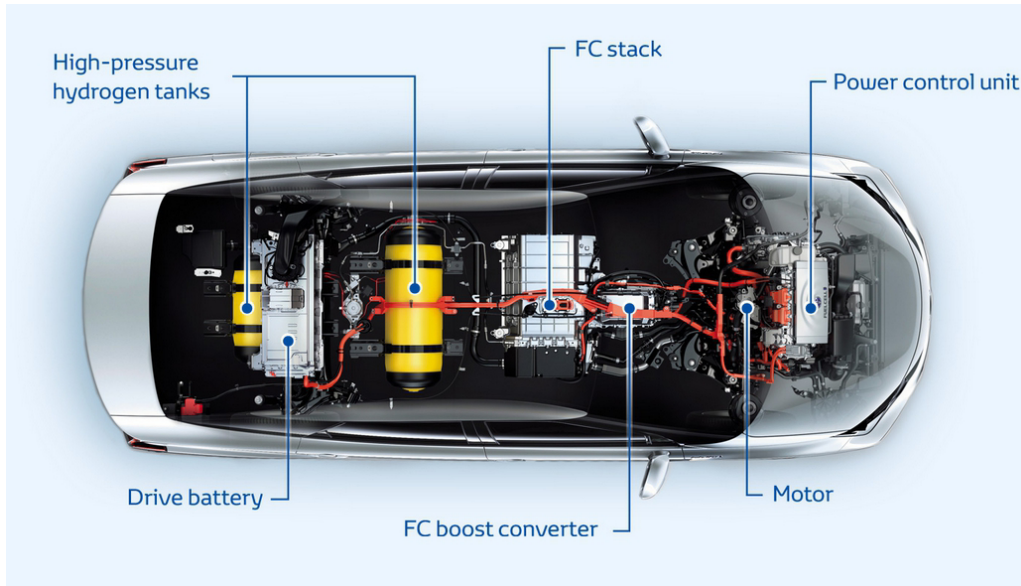
Three commercial vehicles all chose fuel cell and battery as power sources. Fuel cell is an electrochemical device which converts chemical energy into electrical energy. There

Table 1.1: Real-world demonstration projects of fuel cell vehicles and their specifications[11]

Year	Automaker	Model	Engine	FC Power (kW)	Range (miles)	Max speed (mph)	Hydrogen pressure (Bar)	Note
2002	Toyota	FCHV	FC/BA	90	180	96	350	18 leased in California and Japan
2002	Daimler	A-Class F-CELL	FC/BA	85	90	87	700	60 vehicles in US, Japan, Singapore, and Europe in 2003
2002	Ford	Advanced Focus FCV	FC/BA	85	180	-	350	30 fleet vehicles in Sacramento, Orlando, and Detroit
2002	GM	Advanced HydroGen3	FC	94	170	100	700	6 placed in Washington DC
2002	Nissan	X-TRAIL	FC/BA	75	-	78	350	3 leased to Japanese government
2004	Hyundai	Tucson	FC/BA	80	185	93	350	Demonstration project in the US between 2004-2009 and in Korea between 2006-2010
2004	Kia	Sportage	FC	80	185	93	-	Demonstration project in the US between 2004-2009 and in Korea between 2006-2010
2006	GM	Equinox FCEV	FC/BA	93	200	100	-	Leasing in 2007. 100 vehicles in California, New York, and Washington DC
2007	Honda	FCX Clarity	FC	100	354	100	350	Production of 200 vehicles in between 2008-2010, Leasing in Southern California and Japan
2008	Kia	Borrego Mojave FCEV	FC/SC	115	426	93	700	Leasing to Seoul, Korean residents, starting in 2009
2008	Toyota	FCHV-adv	FC/BA	-	97	-	-	Limited leasing in Japan in 2008. More than 100 leased in Connecticut, California and New York.
2009	Daimler	Benz B Class f-cell	FC	90	239	105	-	Small series production started in 2009. 70 Deployed in Los Angeles and San Francisco by 2012
2011	Hyundai	Tucson IX	FC/BA	100	403	-	700	Tested 50 vehicles in 2011
2012	Hyundai	ix35	FC/BA	100	365	100	-	Leasing in Sweden and Denmark started in 2012



(a) Body of Toyota Mirai



(b) Toyota Mirai drive train

Figure 1.1: Toyota Mirai

are several types of fuel cells available in the market today. Based on their electrolyte material, they can be divided into polymer electrolyte membrane fuel cell (PEMFC), direct methanol fuel cell (DMFC), alkaline fuel cell (AFC), phosphoric acid fuel cell (PAFC), molten carbonate fuel cell (MCFC), and solid oxide fuel cell (SOFC)[15]. Different kinds of fuel cells have different characteristics in the aspect of power outputs, operating temperatures, electrical efficiencies, and typical applications and they are used in different applications[16]. The comparison of different kinds of fuel cells is shown in Table 1.3. Compared to other kinds of fuel cells, PEMFC has many advantages like high power density, low weight and volume, low operation temperature and fast startup, which makes it be high potential power source in passenger vehicles and is studied by almost all relevant research on energy management strategy (EMS)[17]. So in this dissertation, only PEMFC

Table 1.2: Comparison of three commercial vehicles[14]

Vehicle		2018 Honda Clarity	2017 Hyundai Tucson Fuel Cell	2018 Toyota Mirai
Fuel Economy (mile/kg)	Combined City Highway	66 67 68	50 49 48	66 66 66
Fuel cell		PEMFC (103kW)	PEMFC (100kW)	PEMFC (113kW)
Range (miles)		366	265	312
Annual Fuel Cost (\$)		1,250	1,700	1,250
Vehicle Class		Midsize Car	Small SUV	Subcompact Car
Motor		AC Permanent Magnet Synchronous (130 kW)	AC Induction (100 kW)	AC Induction (113 kW)
Battery		346 V Lithium Ion	180 V Lithium Ion	245 V Nickel Metal Hy- dride(NiMH)

technology is investigated and "fuel cell" is referring as PEMFC. Hydrogen and oxygen are the fuels of PEMFC. The hydrogen is compressed and stored in the tank. The oxygen from air is compressed through the compressor and imputed into the fuel cell. The schematic diagram of a fuel cell is shown in Figure 1.2. The fuel cell is composed of two electrodes (anode and cathode) and an electrolyte. The operating principle of the electrochemical conversion is shown in equation (1.1)[18].



The hydrogen is imputed into the anode side of the fuel cell and is separated into 2 protons of hydrogen and 2 electrons through catalyst, as shown in equation (1.2).



If a load is connected to the anode and cathode, the electric current is created due to the transportation of free electrons. The hydrogen protons go through the electrolyte to reach the cathode and at the cathode side, the hydrogen protons and electrons merge to create water in equation (1.3)[19]. During the whole process, only water and heat as the wastage of the conversation are produced.



Lead acid battery, Ni-MH battery and the lithium ion battery are the most commonly used energy storage sources and the Ni-MH battery and lithium battery are widely used into electric vehicles due to their high energy density and specific energy [20, 21]. With decades of research on battery and commercial usages, battery performances like capacity,

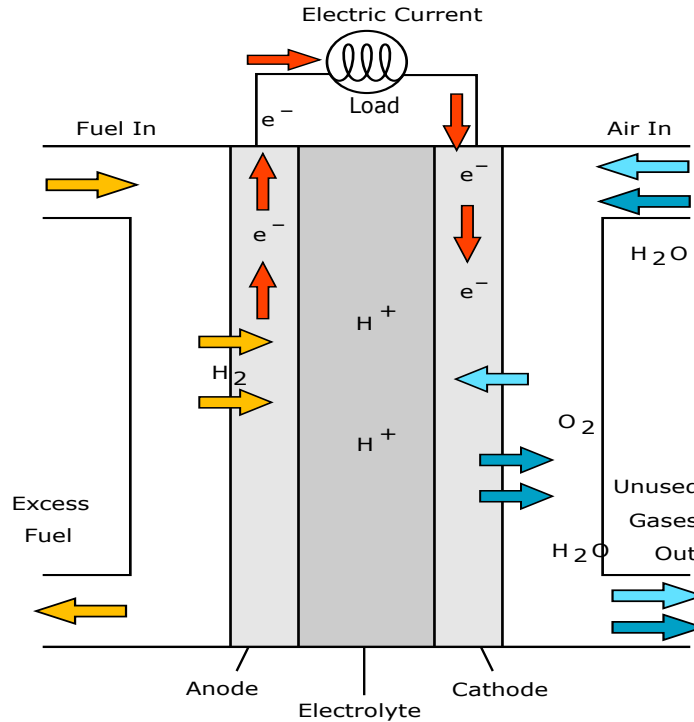


Figure 1.2: The schematic diagram of fuel cell

cycle life, price and charging rate have got dramatic improvement, which allows satisfying the great part of electric vehicle requirement, especially on a suitable driving range[22, 23]. Besides battery, supercapacitor is also chosen as the energy storage source of the vehicle in much research. Because of the high specific active surface area of porous carbon electrodes, supercapacitor has much higher energy storage density than the traditional capacitor, which even can be up to 12 Wh/kg[24]. Compared to battery, supercapacitor has much higher power density and much lower energy density. Supercapacitor also has a wide operating temperature range, lower maintenance cost, high tolerate ability to overcharge and over temperature, long durability and reasonable cost[25]. The comparison of battery and supercapacitor are listed in Table1.4.

Battery or supercapacitor working lonely as the ESS of FCHEV or hybridization of battery and supercapacitor as hybrid energy storage system (HESS) are all well studied by much research. According to the number and kind of power sources, the architecture of FCHEV can be divided into fuel cell-battery HEV, fuel cell-supercapacitor HEV and fuel cell-battery-supercapacitor HEV[1]. Three architectures of FCHEV are listed in Figure 1.3.

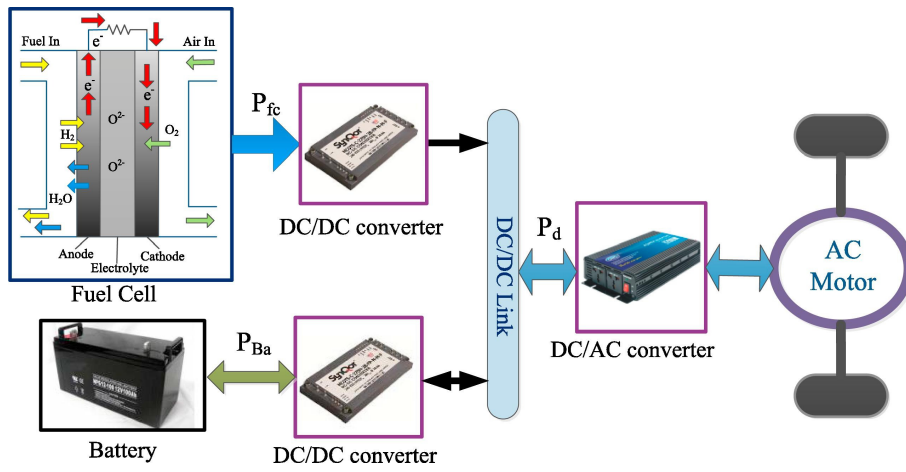
In Figure 1.3 (a), fuel cell is taken as the main power source. Battery supplies the auxiliary power and recycles braking energy for fuel cell-battery HEV. The speed requirement from the driver is transformed into power demand through an electric motor. Due to the low voltage of fuel cell, a unidirectional DC/DC converter is needed to boost its low voltage into the high voltage of DC bus. Battery is also connected to DC bus through a bidirectional DC/DC converter. The DC power supplied by fuel cell and battery is converted to the AC power through DC/AC inverter to drive the AC motor. When the

Table 1.3: Comparison of different kinds of fuel cells [26, 27, 16]

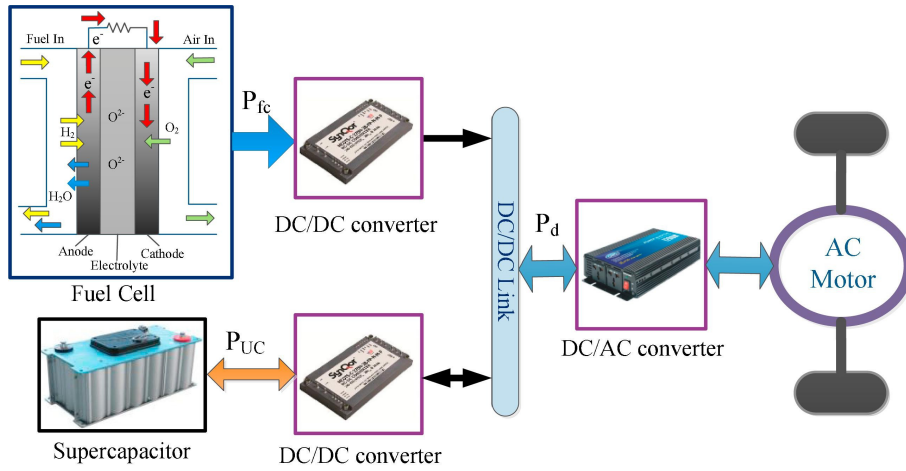
Fuel cell type	Fuel	Cell voltage	Operating temperature(°C)	System output (kW)	Electrical efficiency (%)	Applications
AFC	Pure H <sub>2</sub>	1	90–100	10–100	60	Military, Space
PAFC	Pure H <sub>2</sub>	1.1	150–200	50–1000	>40	Distributed generation
SOFC	H <sub>2</sub> , CO, CH <sub>4</sub> , other	0.8–1.0	600–1000	<1–3000	35–43	Auxiliary power, Electric utility, Large distributed generation
MCFC	H <sub>2</sub> , CO, CH <sub>4</sub> , other	0.7–1.0	600–700	<1–1000	45–47	Electric utility, Large distributed generation
PEMFC	Pure H <sub>2</sub>	1.1	50–100	<1–250	53–58	Backup power, Portable power, Small distributed generation, Transportation
DMFC	CH <sub>3</sub> OH	0.2–0.4	60–200	0.001–100	40	mobiles, computers and other portable devices

Table 1.4: Comparison of batteries and supercapacitor[28]

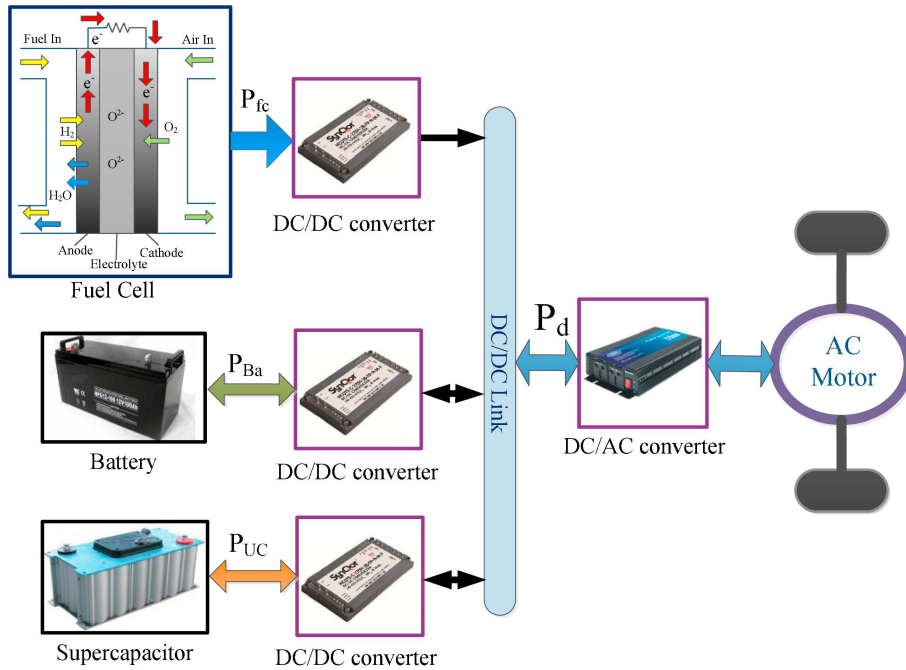
Type	Energy density (Wh/kg)	Power density (W/kg)	Cycle life (Times)	Efficiency (%)	Merits	Drawbacks
Lead-acid battery	30–40	200–300	300–400	75	Low cost, high discharging rate and high recycling rate	Poor performance at low temperature, low lifetime
Ni-MH battery	60–80	800–1500	1000	75	High energy density, high charging and discharging speed and long life	High self-discharging rate, need for cooling system and higher manufacturing cost
Lithium ion battery	100–120	600–2000	1000	90	High voltage, high energy density, lightweight, long cycle life, low self-discharging rate, no memory effect and no pollution	Life reduced at high temperature, non-overcharge, non-over discharge and high security requirement
supercapacitor	4–15	1000–10,000	100,000	85–98	Fast charging and discharging speed, pollution-free and extremely long life	Low energy density



(a) Architecture of fuel cell-battery HEV



(b) Architecture of fuel cell-supercapacitor HEV



(c) Architecture of fuel cell-battery-supercapacitor HEV

Figure 1.3: Three architectures of FCHEV [29]

vehicle is in braking state, the AC motor is switched into the generator to recycle the braking energy and the braking energy is stored in the energy storage sources. When fuel cell is initially started, battery works solely as the power source until fuel cell is warm up. The bidirectional DC/DC converter connected to the battery is not needed in some research which is dependent on the battery voltage and DC bus voltage. High dynamical power change rate on fuel cell accelerates its degradation and failure, therefore fuel cell mostly works in steady state. The battery is responsible for the dynamical power due to acceleration or braking in drive situation, which results in the negative effect on its efficiency, internal resistance and durability[30].

In Figure 1.3 (b), fuel cell is still the main power source and supercapacitor replaces battery as the auxiliary power source. Supercapacitor has high power density, which can remedy the shortcoming of fuel cell on high dynamical power. The operation of fuel cell-supercapacitor HEV is similar to fuel cell-battery HEV. Fuel cell and supercapacitor supply power to the DC bus through respective DC/DC converters and the electric energy is transformed into AC through DC/AC inverter to drive the AC motor. State of charge (SOC) of supercapacitor has a linear relationship with its output voltage. If supercapacitor is directly connected to the DC bus without the corresponding bidirectional DC/DC converter, the variation of supercapacitor SOC under its full exploitation condition leads to the high variation of DC bus voltage. Therefore, supercapacitor is rarely connected to the DC bus directly like battery. Supercapacitor has the low energy density, therefore, compared to the battery, more numbers of supercapacitor are needed to keep the long driving range of the vehicle and this also brings a challenge to the financial cost of the whole vehicle.

In order to overcome the shortcoming of single ESS as the power source of FCHEV except for fuel cell, in Figure 1.3 (c), battery and supercapacitor are combined as the hybrid energy storage system, which can overcome the shortcoming of low lifetime of battery and low energy density of supercapacitor and meets the dual requirements of high specific energy capacities for long driving distances and high specific power capacities for acceleration, braking and climbing[31]. But this topology also complicates the power-train of the FCHEV and brings a challenge to the design of energy management strategy. The retain or remove of bidirectional DC/DC converter connected to hybrid energy storage system is similar to the above two architectures.

### 1.3 Fuel cell hybrid electric vehicles' research in Belfort-France

FEMTO-ST laboratory of Université Bourgogne Franche-Comté and two industrial partners, HELION and PANHARD General Defense cooperate to develop an Electrical Chain Components Evaluation vehicle (ECCE). The project is financially fund by French Directorate General of Armaments (DGA). The first prototypical vehicle is built and driven in 2003, which is shown in Figure 1.4.

ECCE is a hybrid electric vehicle, which is designed to evaluate the components of hybrid electrical vehicles under real operation. The components of its drive train include electrical machines, power converters, energy sources and energy management systems. Four independently controlled electrical machines drive the four wheels respectively which act both as the motors and generators. The energy sources can be chosen from fuel cell system, internal combustion engine, supercapacitor, battery and flywheel. Different energy management strategies according to different hybrid configurations can be validated



Figure 1.4: Electrical Chain Components Evaluation vehicle

using the ECCE. The project can be divided into two phases. From 1997 to 2005 is the first phase of ECCE, which focuses on the design, construction and evaluation of the vehicle. The second phase is from 2008 to 2012. All possible energy sources are integrated into the vehicle and corresponding control systems are developed. In this period, two other partners joined the project. Panhard General Defense (Saint Germain-Laval, Loire, France) supplied military vehicles and was responsible for the mechanical integration and the flywheel system development. Helion Hydrogen Power (Aix-en-Provence, France) subsidiary of Areva group, supplied fuel cell systems.

F-CITY H2, a range extender vehicle, is developed by the French automotive producer FAM Automobiles, EVE Systems, FC LAB and the Institute Pierre Vernier. F-CITY H2 takes the battery as the main power source. Fuel cell is taken as the range extender. It is the first urban electric vehicle in France. Fifteen prototypes have already been produced by FAM Automobiles and were tested in 2012. The rated power of fuel cell stack is 4 kW. Lithium-ion batteries have 2.4 kWh energy density. The range of the F-City H2 is 150 km (93 miles). The F-City H2 vehicle is shown in Figure 1.5.

MobyPost is a European project aimed at developing a sustainable mobility concept by delivering a solar-to-wheel solution. The first core element of this environmentally friendly and novel project is developing and instrumenting a fleet of ten hybrid hydrogen vehicles powered by fuel cell for postal delivery applications. The powertrain is designed using series architecture by operating the fuel cell as a range extender. The nominal power of the fuel cell is 1kW. The battery pack is composed of four modules (U24- 12XP) connected

### 1.3. FUEL CELL HYBRID ELECTRIC VEHICLES' RESEARCH IN BELFORT-FRANCE<sup>15</sup>



Figure 1.5: F-CITY H2

in series and manufactured by Valence. Those modules present a nominal voltage of 12.8V and a nominal capacity of 110Ah. The MobyPost vehicles are shown in Figure 1.6



Figure 1.6: 3 vehicles of the MobyPost fleet

The second core element of MobyPost project is the development of two hydrogen production and refueling stations. These stations are built in the French region Franche-Comté. Photovoltaic generators were installed on two buildings owned by project partner La Poste. One station is composed of one photovoltaic generator which feeds an electrolyzer where hydrogen is produced. Hydrogen is then stored on site in gaseous form in a low-pressure tank where vehicles can directly be refilled. Vehicles are then ready for postal delivery. The whole hydrogen production chain and the vehicles equipped during a testing phase in real working conditions are shown in Figure 1.7.

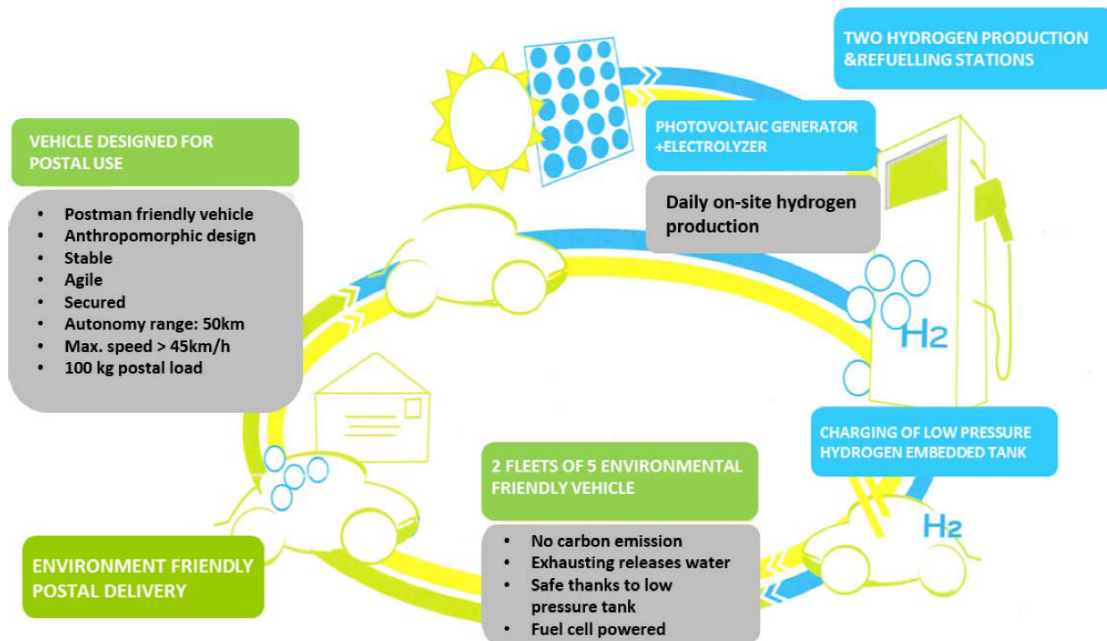


Figure 1.7: MobyPost project

The project is carried out by 9 partners coming from four different European countries (Germany, France, Switzerland and Italy). The role of each partner is clearly defined and the complementarities are evident. Institut Pierre Vernier, Université de Technologie Belfort-Montbéliard, European Institute for Energy Research are academia-research partners and are recognized players in their respective field of expertise. DUCATI Energia, Mahytec Sarl, H2Nitidor and MES are responsible for the development of vehicles and infrastructures. Institut Pierre Vernier and Steinbeis-Europa-Zentrum are regional institutes for transfer of technology. DUCATI Energia and La Poste are mainly responsible for demonstration, field test and training activities as well as raising awareness of the usage of hydrogen-propelled vehicles.

MobyPost follows a global approach by taking a wide range of aspects into consideration to develop a unique autonomous system. The aims of the project can be summarized as follows:

Enable a sustainable mobility concept based on a solar-to-wheel solution by developing ten fuel cell electric vehicles meeting ecological requirements for the future.

Develop a concept for fuel cell electric vehicles aimed at improving the ergonomics of postal delivery vehicles.

Design and build two autonomous stationary hydrogen production and refueling in-

frastructure sites. Each of them is able to feed 5 fuel cell electric vehicles all year round.

Demonstrate the relevance and reliability of the system, improve the lifetime of the developed solution in real working conditions.

Reducing the carbon footprint of postal delivery.

## 1.4 Policy supports for fuel cell hybrid electric vehicles

In more recent years, a number of automobile manufacturers and various government agencies put forward many projects to develop fuel cell technology for use in the transportation system and other applications. Since hydrogen has attracted global attention as next-generation energy, not only western developed countries but also China and other emerging countries with continually increasing energy demands are promoting hydrogen use initiatives.

Current fuel cell hybrid electric vehicle development shows major international automakers generally have completed fuel cell hybrid electric vehicle functional and performance development. Major technical issues identified during the demonstration stage have been solved. Future research and development will focus on fuel cell power density and lifespan, cold start performance, fuel cell system cost reduction, hydrogen infrastructure scale up, and fuel cell application expansion and commercialization. Technical targets of integrated transportation fuel cell power systems from Department of energy (DOE), New Energy and Industrial Technology Development Organization (NEDO), Fuel Cells and Hydrogen Joint Undertaking (FCU JU) and Ministry of Science and Technology (MOST) in American, Japan, Europe and China respectively are listed as Table1.5.

Table 1.5: Technical targets of integrated transportation fuel cell power systems[32]

Characteristic	USA DOE	Japan NEDO	EU FCU JU	China MOST
Peak power efficiency (%)	65	60	55	55
Rated power efficiency (%)	–	–	40 (NEDC)	50
Power density ( $WL^{-1}$ )	650	–	–	60
Specific power ( $Wkg^{-1}$ )	650	–	–	–
Cold start-up time (seconds)	30	30	–	–
Cold start-up temperature ( $^{\circ}C$ )	–30	–40	–25	–30
Durability in automotive drive cycle (hours)	5000	5000	5000	5000
Start-up/shutdown durability (cycles)	5000	–	–	–
Top operation temperature ( $^{\circ}C$ )	90	95	–	–
Storage hydrogen pressure (MPa)	70	70	70	70
Cost (/kW)	\$ 40	\$ 97	€100	–

### 1.4.1 US Department of Energy Fuel Cells Program

The United States is striving to continue to be a global leader in hydrogen and fuel cell technology development and commercialization. So the U.S.DOE Hydrogen and Fuel Cells Program is formed to integrate the DOE's efforts in hydrogen and fuel cells to enable the widespread commercialization of hydrogen and fuel cell technologies across diverse applications[13]. The Program is coordinated across the DOE, incorporating activities in the offices of Energy Efficiency and Renewable Energy (EERE)—led through the Fuel Cell Technologies Office —Science, Nuclear Energy, and Fossil Energy[33]. The Program works with partners in state and federal agencies, foreign governments, industry, academia, non-profit institutions, and national laboratories[34]. In order to achieve the goal of the program, a robust, comprehensive research and development portfolio that balances short-term objectives with long-term needs and sustainability is designed and every year a large number of budget is set.

The EERE has spent an average of about \$139 million per year (about 0.5% of the average DOE budget) since 2004 on fuel cell and hydrogen research, development, and demonstration. This investment has led to more than 650 U.S. patents, approximately 30 commercial technologies being developed by industry and being introduced into the market, and more than 75 emerging technologies that are anticipated by industry to be in the market within the next several years[35]. Budget information for hydrogen and fuel cell research, development, and other activities at the U.S. Department of Energy (DOE) is provided in Figure 1.8 including budgets from DOE's offices of Energy Efficiency and Renewable Energy, Fossil Energy, Nuclear Energy, and Science[36].

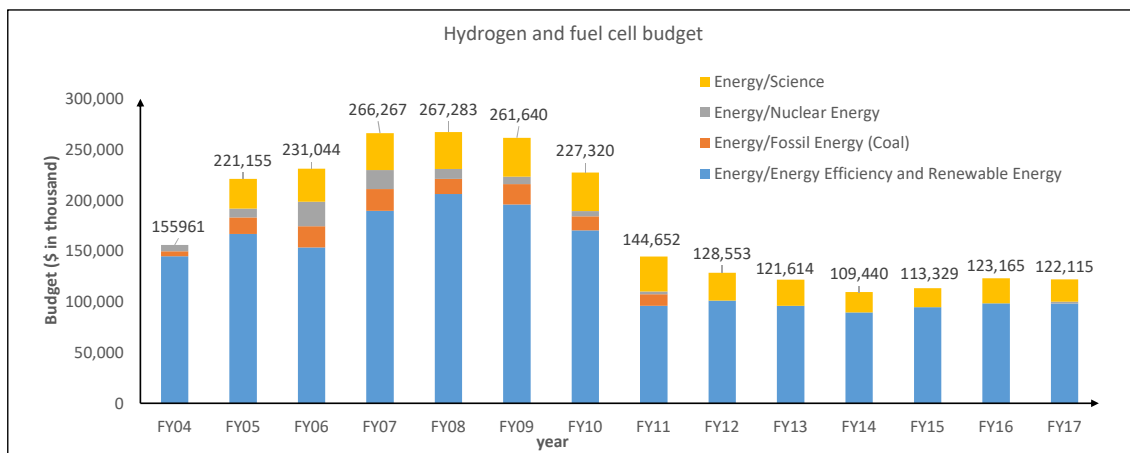


Figure 1.8: Hydrogen and fuel cell budget

Developing a 65% peak-efficient, direct hydrogen fuel cell power system for transportation that can achieve 5,000-hour durability (ultimate 8,000 hours) and be mass produced at a cost of \$40/kW by 2020 (ultimate \$30/kW) are the technical objectives of fuel cell section for Multi-Year Research, Development, and Demonstration Plan of DOE[37]. According to the Plan, fuel cell research and development (R&D) emphasizes activities aimed at achieving high efficiency and durability along with low material and manufacturing costs for the fuel cell stack. Developing lower cost, better performing system balance of plant components such as air compressors, fuel processors, sensors, and water and heat management systems are also included in R&D activities.

National Hydrogen Fuel Cell Electric Vehicle Learning Demonstration project was

initiated in 2004 to implement complete integrated systems including hydrogen production facilities and FCEVs and collect data to determine whether the technical targets have been met under real-world conditions. The project brought together teams of automotive and energy companies that worked to address FCEV and hydrogen infrastructure interface issues and to identify future research needs. Fuel cell bus development and demonstration activities have been primarily funded by the Department of Transportation's Federal Transit Administration through the National Fuel Cell Bus Program as well as a number of congressionally directed fuel cell bus (FCB) projects. Through the activities, the FCB data including operational, maintenance, reliability, and cost are compared to data from conventional buses (diesel or compressed natural gas) to track progress over time. The results are used to identify key areas of R&D focus to speed the progress toward full market introduction.

#### 1.4.2 European hydrogen and fuel cell technology platform

The potential of fuel cell and hydrogen to enhance energy security and mitigate climate change was recognized in 2003 with the creation of the Hydrogen and Fuel Cell Technology Platform in Europe. The platform brings together key stakeholders in the fuel cell and hydrogen fields who jointly develop an implementation plan. Published in 2007, the plan addressed the technological and non-technological barriers to deployment of these disruptive technologies. It has identified key issues and priorities for accelerating deployment of portable, stationary and transport applications. The platform leads to the formation of a Public Private Partnership - the 'Fuel Cells and Hydrogen Joint Undertaking' (FCH JU). In future, the European Commission will channel support for fuel cell and hydrogen research and demonstration through the JU. For the period 2007-2013, European Commission supports amounts to €470 million[38].

The JU is a unique public private partnership supporting research, technological development and demonstration activities in fuel cell and hydrogen energy technologies in Europe. Its aim is to accelerate the market introduction of these technologies, realizing their potential as an instrument in achieving a carbon-clean energy system. The three members of the FCH JU are the European Commission, fuel cell and hydrogen industries represented by Hydrogen Europe and the research community represented by Hydrogen Europe Research. On 6th May 2014, the Council of the European Union formally agreed to continue the Fuel Cells and Hydrogen Joint Technology Initiative under the EU Horizon 2020 Framework[39].

The phase (from 2014 to 2020) will have a total budget of €1.33 billion, provided on a matched basis between the EU represented by the European Commission, industry, and research. The second phase of the FCH JU (though the "FCH 2 JU") will reinforce this commitment to a real, strong, reliable European platform on fuel cells and hydrogen in which Industry, Research, and Local, National and European officials act together to address major socio-economic and environmental challenges through the technology. The projects under FCH 2 JU will improve performance and reduce the cost of products as well as demonstrate on a large scale the readiness of the technology to enter the market in the fields of transport (cars, buses and refueling infrastructure) and energy (hydrogen production and distribution, energy storage and stationary power generation). The FCH 2 JU is set up for a period lasting until 31 December 2024. It brings public and private interests together in a new, industry-led implementation structure, ensuring that the jointly defined research program better matches industry's needs and expectations, while focusing on the

objective of accelerating the commercialization of fuel cell and hydrogen technologies.

### 1.4.3 Japanese New Energy and Industrial Technology Development Organization Fuel Cell Programs

Japan has strong global competitiveness in the field of fuel cells. For example, Japan has filed the world's largest number of patent applications for the technology: five times the number of those filed by second or lower-placed countries, leaving other countries far behind. In addition, Japan's regional resources and renewable energy, can be utilized to manufacture hydrogen for fuel cells[40]. In June 2014, Japanese Ministry of Economy, Trade and Industry compiled the "Strategic Road Map for Hydrogen and Fuel Cells" toward the realization of a "hydrogen society." This road map states how Japan would be able to make use of hydrogen, what are goals to be achieved in each step of production, transportation, storage and utilization of hydrogen, and what kind of collaborative efforts could be possible among industry, academia and government for achieving these goals.

To realize a "hydrogen society", related systems will be formulated on a large scale, which may be accompanied by changes in the current social structure, and long-term, continuous measures for realizing such a society will be taken. In addition, the imbalance between the supply side and demand side issues will be resolved, while academia, government and industry will collaborate to protectively engage in measure for utilizing hydrogen. To achieve this goal, Japan will aim to achieve a hydrogen society through the following step-by-step process in Figure 1.9. The fuel cell electric vehicle and hydrogen station part of road map is shown in Figure 1.10.

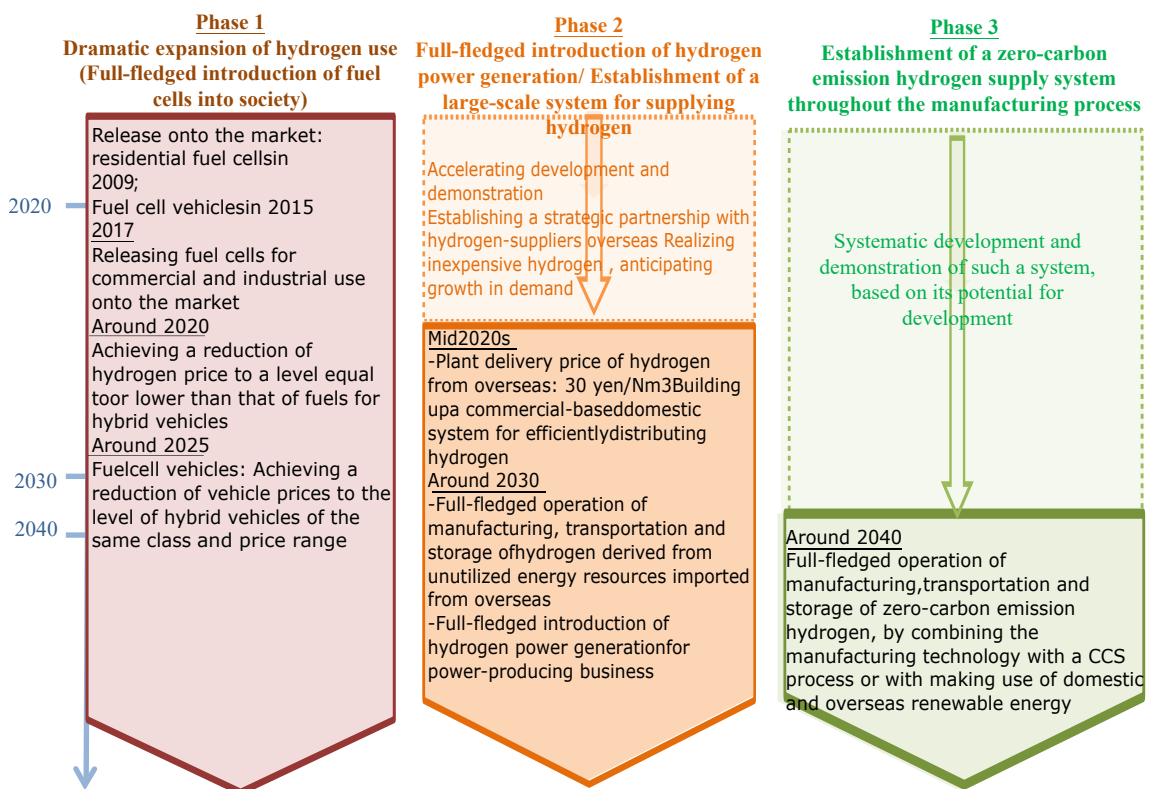


Figure 1.9: Hydrogen/Fuel cell Strategy Road map[41]

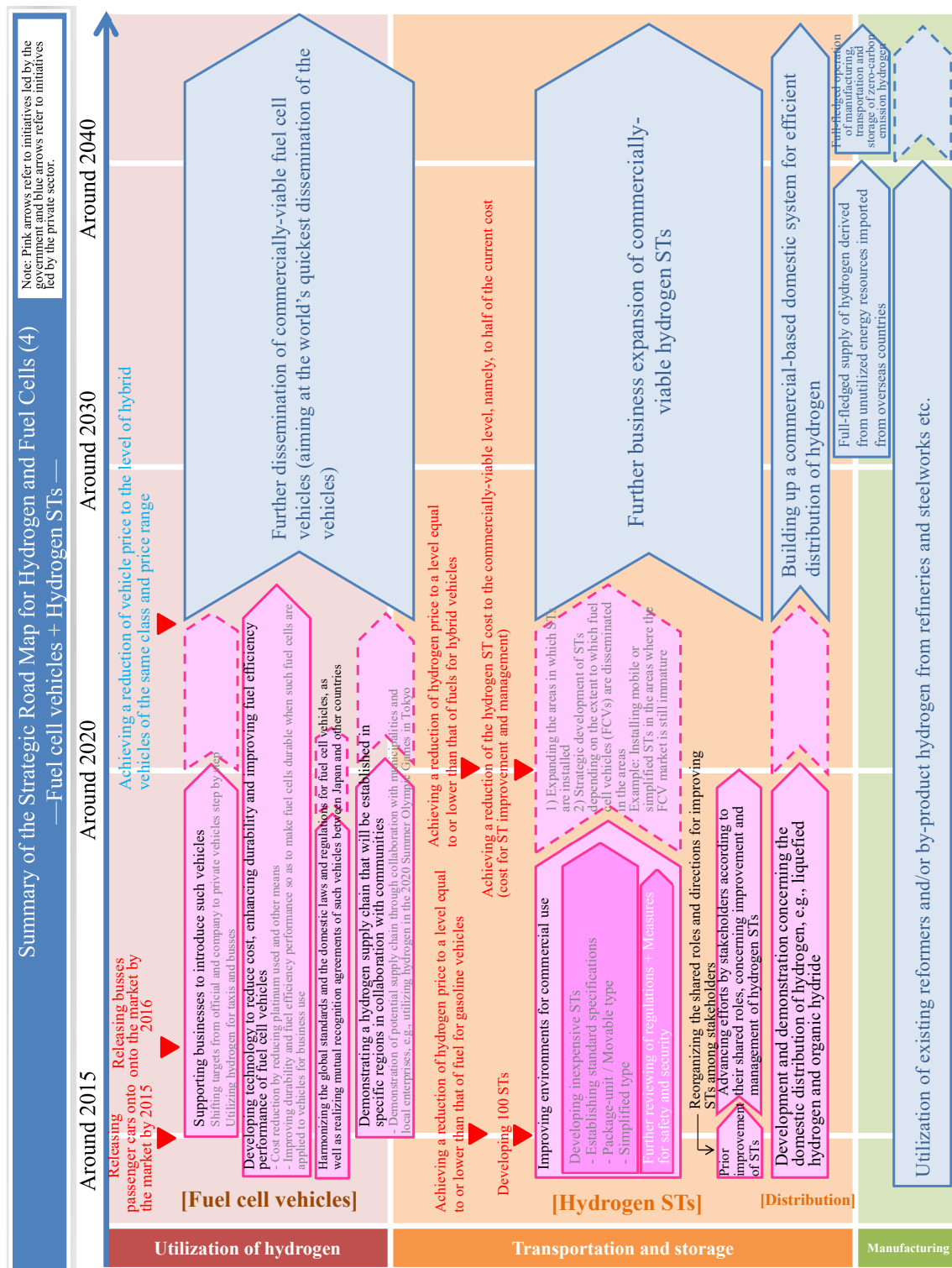


Figure 1.10: Hydrogen/Fuel cell Strategy Road map about FCV and hydrogen stations[42]

Phase 1 (Dramatic expansion of hydrogen use): Dramatically expanding the use of stationary fuel cells and fuel cell vehicles, which are in the process of being realized, leading to the successful acquisition of a global market in the field of hydrogen and fuel cells, in which Japan leads the world;

Phase 2 (Full-fledged introduction of hydrogen power generation/Establishment of a large-scale system for supplying hydrogen): Further expanding the demand for hydrogen, while widening the scope of hydrogen sources to include unutilized energy, so as to establish a new secondary energy structure in which hydrogen will be added to existing resources, namely electricity and heat (gas);

Phase 3 (Establishment of a zero-carbon emission hydrogen supply system throughout the manufacturing process): Combining the technology for manufacturing hydrogen with a CCS process, or with making use of hydrogen derived from a renewable energy resource, so as to establish a zero-carbon-emission system for supplying hydrogen throughout the manufacturing process.

In light of recent circumstances, in which various efforts have been advanced since the formulation of the Road Map, including the increased dissemination of fuel cells for households, the launch of fuel cell vehicles onto the market, and steady progress in the construction of hydrogen stations, in 2016 the Council revised the contents of the Roadmap, set new targets, and specified efforts to be made[43].

(1) The future price targets for household fuel cells were clarified: PEMFC: 800 thousand yen by 2019, SOFC: one million yen by 2021.

(2) Targets for the dissemination of fuel cell vehicles were set: About 40 thousand vehicles by 2020, about 200 thousand vehicles by 2025, and about 800 thousand vehicles by 2030, in total.

(3) Targets for the construction of hydrogen stations were set: About 160 stations by 2020 and about 320 stations by 2025.

(4) Descriptions concerning hydrogen power generation were fleshed out.

(5) Concerning the utilization of hydrogen generated using renewable energy, it was decided that technical and economic challenges would be discussed.

In December 2017, the “Basic Hydrogen Strategy” was formulated and published, which defines the direction or vision for realizing a hydrogen-based society with an eye on 2050 and provides an action plan for its realization. In order to make hydrogen a new energy alternative, the strategy aims to make hydrogen affordable and cost-competitive in comparison to conventional energy sources such as natural gas. The target number of applications to be installed such as fuel cell electric vehicles, Hydrogen Refueling Stations, and stationary fuel cells is indicated. To enhance the introduction of hydrogen energy, the Ministry of Economy, Trade and Industry of Japan has a budget of around US\$300 million for FY2018 by which various demonstration projects including a hydrogen power generation plant, an international hydrogen supply chain, and power-to-gas as well as financial incentives for hydrogen utilization including mobility sectors are being implemented. In February 2018, Japan H2 Mobility was initially established by eleven leading companies aiming to accelerate the dissemination of fuel cell electric vehicles and the development of hydrogen stations.

The NEDO has been conducting comprehensive technology development and demonstrative research programs on hydrogen energy. The most recent result from NEDO’s program such as new materials for PEMFC, analysis technology of morphology, electrochemical reaction and mass transfer in MEA, evaluation technology for long time fuel cell durability will be addressed. Following current topic, NEDO’s future challenge to develop hydrogen energy demand will be presented. NEDO just started R&D program to develop

large scale hydrogen supply chain with long-distance transportation of hydrogen and hydrogen gas turbine technology. NEDO is now also conducting Power to Gas which is a key technology to provide CO<sub>2</sub> free hydrogen in the future.

Japan traditionally places a high value on close collaboration among the government, industry, and academia. In addition, Japan's industry consists mainly of major corporations with deep pockets that are willing to go beyond their co-share responsibilities. Indeed, it is acknowledged that Japanese automakers have spent a substantial amount of their own funds to develop fuel cell vehicle technology without government assistance. According to interviews and site visits conducted by one of the co-authors in the late 1990s, we assess that the Japanese corporations that participated in government projects invested at least twice as much as the government (Williams, 1996) and that the Japanese government and corporate cumulative combined fuel cell R&D spending for the 2003–2015 period likely amounted to \$12.3 billion, including government funding (\$4.1 billion), corporate cost-share (\$4.1 billion), and additional corporate R&D spending (\$4.1 billion)[44].

#### 1.4.4 Chinese New Energy Vehicle Program

China became the largest car producer a decade ago, set to overtake the USA as the world's biggest oil importer in 2017. Since the 2000s, several national and local policies for New Energy Vehicles (NEVs) are proposed by the Chinese Government. The NEVs refer to vehicles that are partially or fully powered by electricity, such as battery electric vehicles and fuel cell hybrid electric vehicles. In recent years, China has made tremendous progress in the development and demonstration of electric vehicles which is helpful for China to meet international climate change obligations greenhouse gas emission reduction targets[45]. Chinese incentives for fuel cell electric vehicles currently extend beyond those offered for battery NEVs. On February 11, 2018, an interdisciplinary, cross-industry, inter-agency national alliance: the National Alliance of Hydrogen and Fuel Cell was founded in Beijing to develop the hydrogen relevant technologies and fuel cell electric vehicle technologies[46].

From first New Energy Vehicle Program in China's 9th five-year plan to the latest 13th five-year plan proposed by the Ministry of Science and Technology of China, fuel cells are considered as one of the most important high technologies. Ministry of Finance, Ministry of Industry and Information Technology, Ministry of Science and Technology and National Development and Reform Commission cooperate to provide continuous policy support on finance and taxation of new energy vehicle: the standard financial support for fuel cell passenger vehicle is 749 €/kW (power rating) (Ren Min Bi (RMB) is transformed into Euro with ratio 8.01); light-weight bus and truck maximum 37453 €/vehicle; large and medium bus and medium and heavy truck maximum 62422 €/vehicle[47].

Based on China's Key Fields Technology Road map of "Made in China 2025", the Hydrogen Fuel Cell Vehicle Technology Road map describing China's overall objectives and strategies, along with corresponding technical innovation requirements and priority action plans for its fuel cell electric vehicle development is determined in Figure 1.11. China's overall development pathway of fuel cell electric vehicle is through three "Five-Year Plans" in technology R&D, demo and evaluation, and expanding fuel cell industrial applications, to achieve the following objectives:

- Capable of the design and system integration of fuel cell buses and passenger cars;
- Establishment of an entire fuel cell electric vehicle technology and industry chain, including fuel cell stacks and key materials, fuel cell system and core components, fuel cell

electric vehicles and critical parts, and hydrogen supply infrastructure; and

- Realization of the overall development of future clean, low carbon, high-efficient fuel cell electric vehicle R&D and application system.

## 1.5 PhD project objectives

In this dissertation, fuel cell, battery and supercapacitor are chosen as the power sources of FCHEV. As described before, the fuel cell-battery-supercapacitor architecture takes fuel cell as the main power source and cooperates the battery and supercapacitor as the hybrid storage system of the vehicle to use their specify characteristics at best and overcome their shortcomings: fuel cell cannot stand high dynamical change rate, supercapacitor has high power density but low energy density, battery has high energy density but low power density. Fuel cell could be set to supply steady power to the vehicle and charge the state of charges of battery and supercapacitor back to their initial value. The hybrid energy storage system allows a reduction of the size, efficiency or cost of the embedded energy storage sources. Peak power demand during ascent or accelerating can be supplied by supercapacitor. The current fluctuation on the battery is reduced and its durability is increased. But the complex architecture of three power sources also increases the difficulty in splitting power demand of the vehicle among different power sources. An energy management strategy is needed to play the full potential of every power source and reach certain purposes, like minimizing hydrogen consumption, increase the lifetime of power sources and keep charge sustenance of energy storage sources. Through the review of energy management strategy, an equivalent consumption minimization strategy (ECMS) is going to be designed in the dissertation. The validation of the designed energy management strategy needs to be verified. Therefore a test bench to valid the energy management strategy should be studied in the dissertation. Along with the operation of vehicle, the degradation of power sources appears, which not only affects the optimal solution of energy management strategy but also brings risk to the stability of the control system. Then the method that can estimate the degradation degree of power sources is needed and the effects of power sources degradation on energy management strategy should also be considered. Finally, on the basis of the designed ECMS and analysis of power sources degradation on energy management strategy, the adaptive equivalent consumption minimum strategy (AECMS) will be designed.

		2020	2025	2030	
Overall objective		Small scale public sector demonstration in selected areas (5,000 FCVs)	Large scale deployment of FC passenger cars and service vehicles in urban areas (50,000 FCVs)	Large scale commercial deployment of passenger cars and commercial vehicles (one million FCVs)	
		Fuel cell system production capacity > 1,000 units per enterprise	Fuel cell system production capacity > 10,000 units per enterprise	Fuel cell system production capacity > 100,000 units per enterprise	
Hydrogen Fuel Cell Vehicles *	Functional Requirements	Cold start -30°C, power system structure optimization, FCV cost close to all-electric vehicles	Cold start -40°C, small volume production, FCV cost similar to hybrid vehicles	FCV overall performance comparable with traditional ICE vehicles - achieving competitive advantage	
	Commercial vehicle	Cost ≤ RMB 1.5 million	Cost ≤ RMB 1.0 million	Cost ≤ RMB 600,000	
	Passenger car	Max speed ≥ 160km/h Lifespan 200,000 km Cost ≤ RMB 300,000	Max speed ≥ 170km/h Lifespan 250,000 km Cost ≤ RMB 200,000	Max speed ≥ 180km/h Lifespan 300,000 km Cost ≤ RMB 180,000	
Key common technologies	Fuel cell stacks	Cold start < -30°C Power density 2.0kW/kg Lifespan 5,000 hrs	Cold start < -40°C Power density 2.5kW/kg Lifespan > 6,000 hrs	Lifespan > 8,000 hrs	
	Critical materials	High performance membrane materials, Low platinum catalysts, metal bipolar plates	Membrane reliability improvement, catalysts and bipolar plates	Low cost membrane electrode assemblies and bipolar plates	
	Control tech	Fuel cell system control optimization	Fuel cell control reliability improvement	Fuel cell cost reduction and control integration	
	Hydrogen storage		Key component development of Hydrogen supply system	Key component reliability improvement of hydrogen supply system	Key component cost reduction of hydrogen supply system
			High pressure hydrogen storage and safety	Hydrogen storage reliability	Cost reduction of hydrogen storage
Critical components	Key system components (incl. high speed oil-free air compressors, hydrogen recirculation system, and 70MPa hydrogen cylinders) to meet vehicle specifications; system cost below RMB200/kW				
H2 infrastructure	H2 supply	Decentralized hydrogen production from renewable sources; industrial by-products such as coke-oven gas		Decentralized H2 production from renewable sources	
	H2 delivery	High pressure hydrogen storage and delivery	Cryogenic liquid hydrogen delivery	High density organic liquid hydrogen storage and delivery at normal pressure	
	HRS	100 stations	350 stations	1,000 stations	

\* Note: In this Chapter, unless otherwise specified, all studies use 12-meter city bus for commercial vehicles, and class B car for passenger vehicles

Figure 1.11: Development objectives of hydrogen fuel cell vehicles in China



# State of the art of energy management strategy

## 2.1 Introduction

Every power source has different physical characteristics. They play different roles in different architectures of FCHEV. So the objectives and methods of EMS should be adapted according to their roles. Being familiar to the characteristics of power sources is helpful to run the full potential of each source and reach the objectives of EMS. Therefore, it is necessary to analyze their characteristics.

EMS not only meets the power demand of vehicle but also plays the full potential of power sources and cooperates them together to minimize fuel consumption, extend the lifetime of components, reducing economic cost and so on. Each kind of EMS has its own specific operation methods, the range of application, advantages and drawbacks, therefore energy management strategies applied into FCHEV in recent years are categorized and reviewed. When designing an EMS, the objectives should be set in advance. These objectives are summarized and methods to fulfill these objectives for different kinds of energy management strategies are also reviewed.

This chapter is organized as follows: section two describes the characteristics of power sources. In the third section, a review of EMS according to their control technique is described. In the fourth part, all the objectives for energy management strategies and methods to reach each objective are summarized up. Based on the review of EMS in the third section, objectives in the fourth section and statistic of references for EMS, energy management strategies and objectives are analyzed in the fifth section. Finally, conclusions are drawn.

## 2.2 Characteristics of power sources

### 2.2.1 Fuel cell

PEMFC operates through the electrochemical conversion process, which converts chemical energy into electrical energy through the reaction between hydrogen and oxygen. Through the reaction, only water and heat as wastage of the reaction are produced[48]. Cost, performance, and durability are still key challenges to widespread commercialization of FCHEV[49]. 65% peak-efficient, 5000-hour durability (ultimate 8000 hours) and cost

of \$40/kW (ultimate \$30/kW) under mass production are set the technique goals of 2020 for transportation usage of fuel cell[37]. Increasing the percentage of operation points in high efficiency zone during the operation time, decreasing hydrogen consumption and prolonging the lifetime of fuel cell and reducing overall cost can be done through operation control under the guidance of EMS.

Different from other objectives, increasing the durability of fuel cell is complicated due to the unknown degradation mechanism of fuel cell. The operating lifetime of the fuel cell is defined as the state at which the voltage drops by 10% from its initial value[50]. With the operation of fuel cell stack, the membrane electrode assembly including membrane, electrodes and gas diffusion layers degrade, leading to the decrease of fuel cell performance[51]. Many researchers have reviewed the degradation mechanism of fuel cell stack where most of experimentation is based on ideal environmental test condition or accelerated stress test which do not represent a realistic usage. The degradation mechanism of fuel cell is complicated and precise quantification of fuel cell service lifetime is difficult[52]. The operating conditions of fuel cell that may accelerate the degradation are reviewed as follows[53, 54, 55, 56]:

- 1) Start up and shut down of fuel cell may result in the localized starvation.
- 2) Very low required power from fuel cell can lead to the catalyst layer degradation.
- 3) Very high power demand exceeding the oxygen and hydrogen maximum supply rate will result in the reduction of electrochemical active surface area.
- 4) Large transient power change rate will also lead to the localized starvation.

Thermal and humidity management is also important for fuel cell degradation, but for this dissertation, we just consider the effect of power demand on fuel cell degradation. All the listed following constrains should be carefully taken into account when designing EMS:

- 1) Reducing the number of fuel cell start-stop.
- 2) Minimum fuel cell current is set up.
- 3) The fuel cell power (including voltage, current) must be in the range of their maximum and minimum values.
- 4) The dynamic change rate of fuel cell power must be limited.

### 2.2.2 Energy storage sources

Reliable energy storage systems like battery and supercapacitor are the key elements to enable evolutions of electric vehicles. Battery and supercapacitor can work alone as the energy storage sources of FCHEV. Cooperating battery with supercapacitor together as hybrid energy storage system also is a good choice for much research, which can meet both high energy densities and power densities requirement for FCHEV.

Battery is an electrochemical device that converts chemical energy into electric energy and is mostly chosen as an assistant power source to supply the peak power and recycle the braking energy. Battery can also be considered as the main power source to supply main power demand and fuel cell just acts as a steady power source to charge the battery state of charge (SOC) back to initial value, especially for plug-in fuel cell hybrid electric vehicle. Li-ion and NiMH battery are mostly used in electric vehicles[57]. Increasing

battery performance, prolonging its lifetime, decreasing charge time and reducing its cost are main research targets for battery. When designing EMS, increasing lifetime, reducing electric consumption from battery and reducing its cost is related to this topic.

Compared to battery, supercapacitor has high power density and low energy density[58]. The life cycle of supercapacitor is very long (over  $10^6$  cycles)[59]. The advantage of ultra-rapid charging and delivery of high current on demand makes the supercapacitor an ideal candidate as a peak-load supplier for FCHEV. Supercapacitor can provide vehicles additional power during acceleration and hill climbing and help recover braking energy.

## 2.3 Energy management strategy

EMS can be divided into rule-based strategies (RBS), frequency-based strategies (FBS) and optimization-based strategies (OBS). RBS also can be divided into deterministic rule based strategy (DRBS) and fuzzy rule based strategy (FRBS). The control rules of RBS are designed according to human intelligence and experience and generally without prior knowledge of a drive cycle[60]. Frequency based strategies are specialized for FCHEV due to low dynamical characteristic of fuel cell. Optimization based strategy can be divided into local optimization based strategy (LOPS), also called real-time optimization strategy or online optimization strategy, and global optimization based strategy (GOBS), also called offline optimization strategy[61]. Energy management strategies are classified in the following Figure 2.1. The widely used energy management strategies are introduced in the following section.

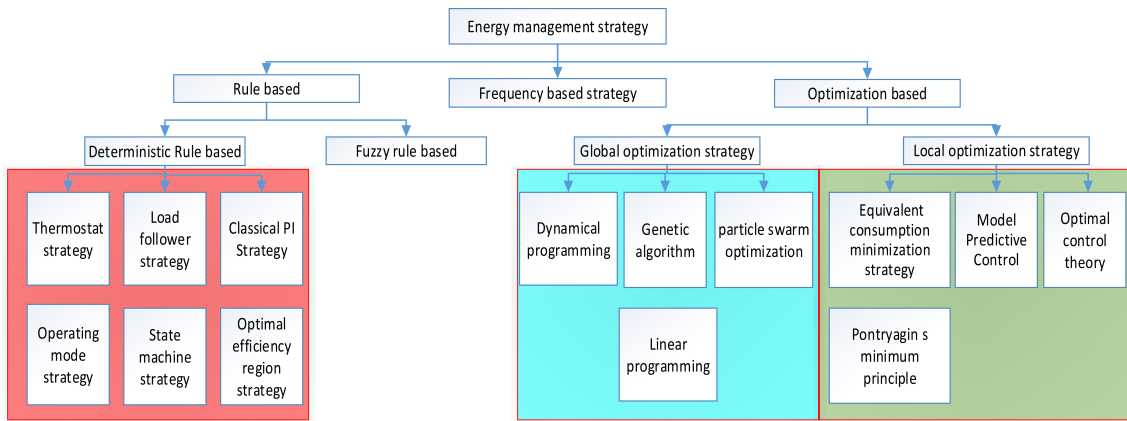


Figure 2.1: Energy management strategy

### 2.3.1 Rule based strategy

#### 2.3.1.1 Deterministic rule based strategy

Deterministic rule based strategy relies on deterministic rules to control the split of power requirement among different power sources, which are designed according to the designer's experience. Deterministic rule based strategy is simple and can easily be applied into the reality, but optimal results are hardly reached.

Thermostat control strategy is one simple deterministic based strategy, which tries to operate the fuel cell at high efficiency point to charge the energy storage sources when their SOC is under the lower threshold[62]. When SOC is over the upper threshold, fuel cell stops working. This strategy leads to frequent start/stop of fuel cell and deep discharge of battery, resulting in the reduction of their lifetime.

Load follower strategy takes consideration of SOC and load power to operate fuel cell to follow the load power. On one hand, when load power is small and SOC of energy storage source is high, energy storage source supplies more power or all power. On the other hand, when load power is high and SOC is low, fuel cell meets the load power demand[63]. Regarding the load follower strategy of [64], Maximum efficiency power point and high efficient regions of fuel cell are defined in advance. According to mode selection hysteresis cycles and real values of battery SOC and load power, fuel cell is operated at three different regions: minimum power to highest efficient power region, highest efficient power point and highest efficient power to maximum power region to reduce hydrogen consumption and avoid the frequent mode switch.

In [65], PID control approach is used. Two PID controllers shown in Figure 2.2 are designed to calculate battery current and fuel cell current. Aiming to maintain the battery SOC at its nominal value, the difference between battery reference SOC and real SOC is taken as the input of the first PID controller to decide battery reference current. Based on the difference between battery reference current and real current, the fuel cell current is calculated through the second PID controller.

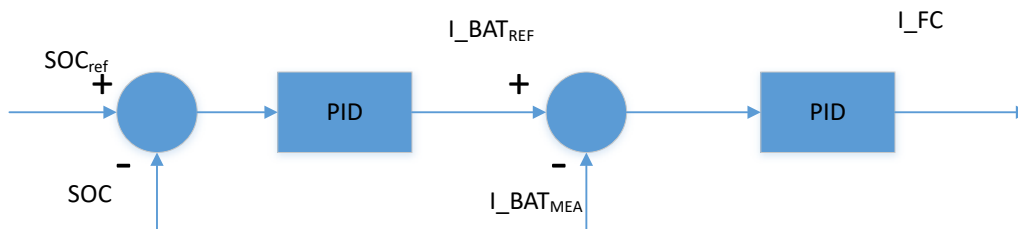


Figure 2.2: PID control strategy

In [66, 67], operating mode control (OMC) is proposed in Figure 2.3. It is similar to load follower strategy, the fuel cell reference power is decided by the supercapacitor SOC and vehicle speed. This strategy is divided into 5 modes to filter power vibration of fuel cell and limit its power dynamic change rate to increase the fuel cell lifetime.

[68] proposes a stiffness coefficient model (SCM). This SCM is based on the battery SOC and comparison of load power demand and fuel cell power at maximum efficiency point to make fuel cell work in high efficiency area. The charge and discharge powers of battery are also decided by stiffness coefficient, which changes with battery SOC value.

[69] proposes a state machine strategy (SMS) which is divided into 5 states according to the SOC values of battery and supercapacitors. For every state, fuel cell power is decided by the value of load power. SMS combining with the droop control strategy operates the fuel cell to supply the low frequency power, battery to charge and discharge power on middle frequency power and supercapacitor to meet high frequency power. Through this strategy, the overall efficiency and lifetime of battery and fuel cell can be improved.

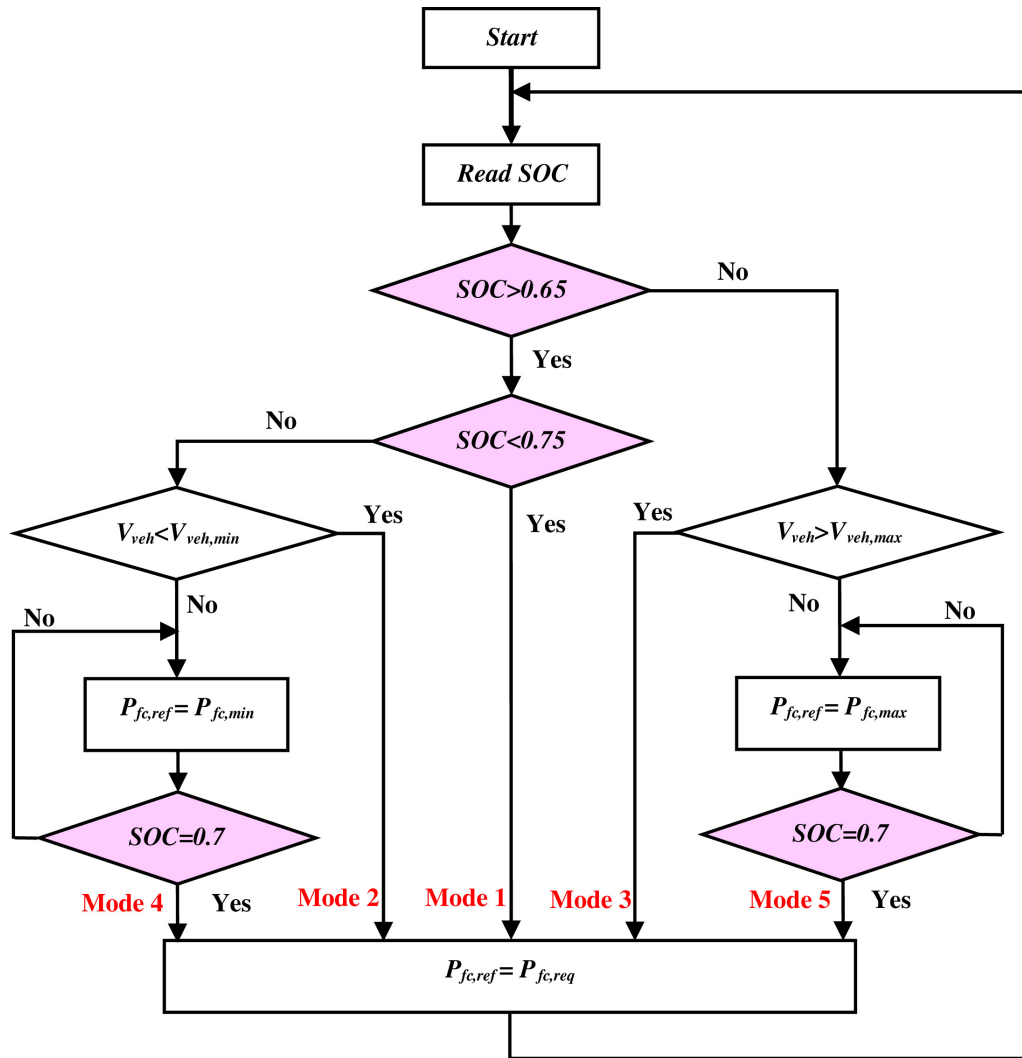


Figure 2.3: Operating mode control

### 2.3.1.2 Fuzzy rule based strategy

Fuzzy rule based strategy is similar to deterministic rule based strategy. But its rules are in form of “if-then” and its states are described by different membership functions. The judgemental conditions are not decided by deterministic criteria like minimum battery SOC or maximum fuel cell current, which are replaced with probability in the certain range of criteria. Fuzzy rule based strategy doesn't rely on precise system model, particularly suitable for the nonlinear, uncertain and time varying systems like vehicle dynamical system.

In [6], fuzzy rule based strategy for a fuel cell-battery range extend HEV is proposed. Battery SOC and distance are taken as input variables. The fuzzy membership function of battery SOC is shown in Figure 2.4. Fuel cell power and pedal's duty ratio are outputs. Fuzzy rules are shown in Figure 2.5. Pedal time-sharing concept is used to prevent quick SOC loss and reduce the times of start-stop situation of fuel cell, which is helpful for prolonging battery lifetime and improving the energy efficiency. NEDC drive cycle is used to validate the fuzzy logic control strategy. The speed response of fuzzy rule based

strategy is shown in Figure 2.6 and comparative simulation results of designed fuzzy rule based strategy and thermostat strategy are shown in Figure 2.7. It can be observed that compared to the thermostat control strategy, the quick loss problem of the system's SOC is solved by fuzzy rule based strategy and it can offer a longer driving range than the thermostat control strategy.

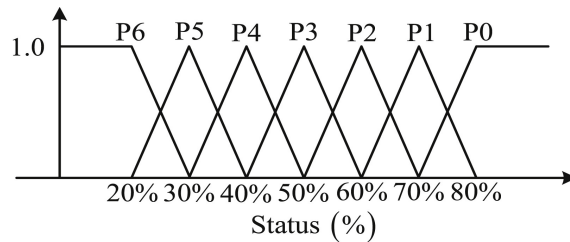


Figure 2.4: Fuzzy membership function of battery SOC

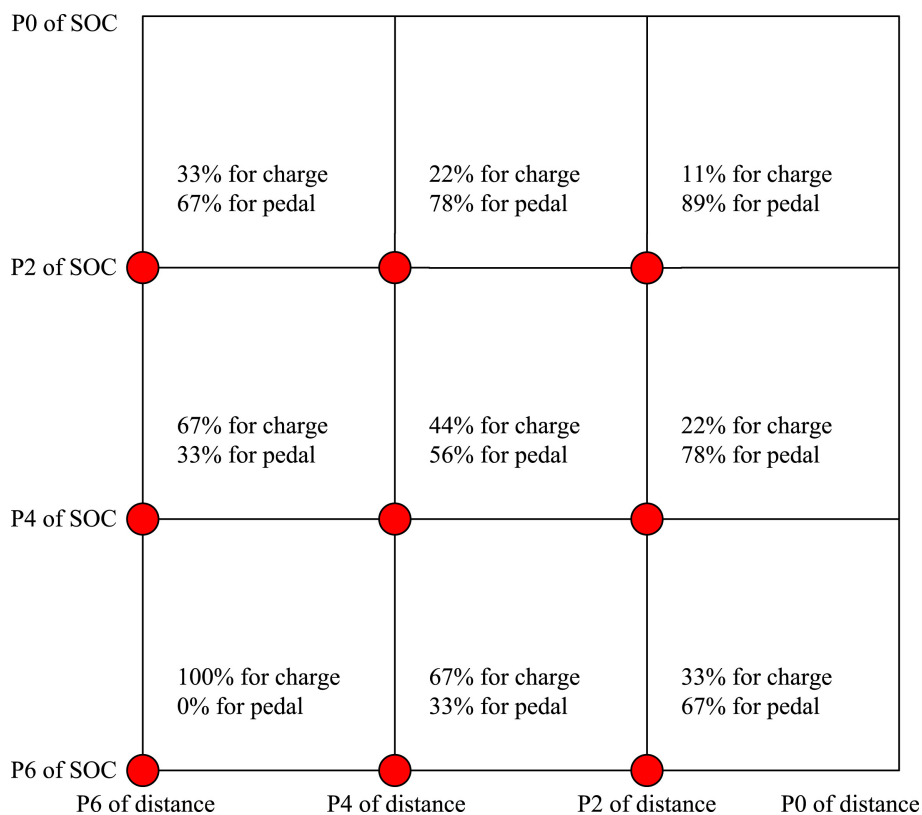


Figure 2.5: Fuzzy rules

[70] designs two fuzzy logic strategies for fuel cell battery HEV and fuel cell battery supercapacitor HEV respectively to improve fuel economy. The two strategies take load power and SOC of energy storage source as inputs and fuel cell power as the output. Two fuzzy logic controllers are designed for fuel cell battery supercapacitor HEV. The first one is to get the fuel cell power and the second one is to get the battery and supercapacitor power. Simulation results show that FCHEV with two energy storage sources has better fuel economy.

The input variables, output variables and their corresponding membership functions of fuzzy logic controller are determined by researchers. Supercapacitor SOC and remaining

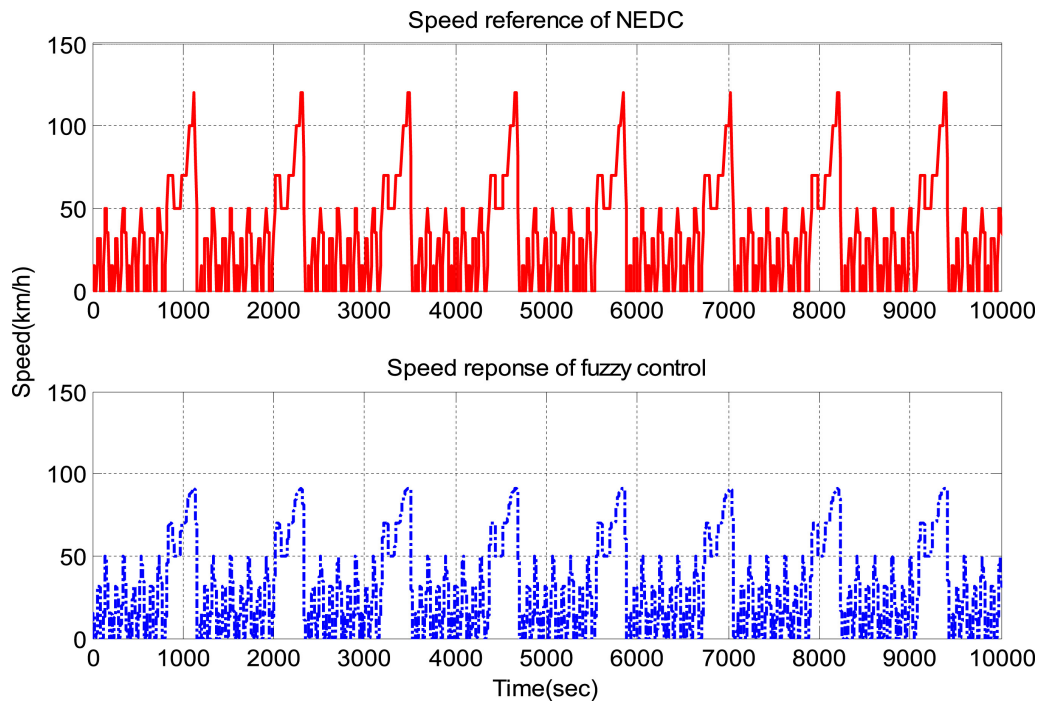


Figure 2.6: Speed profile of drive cycle

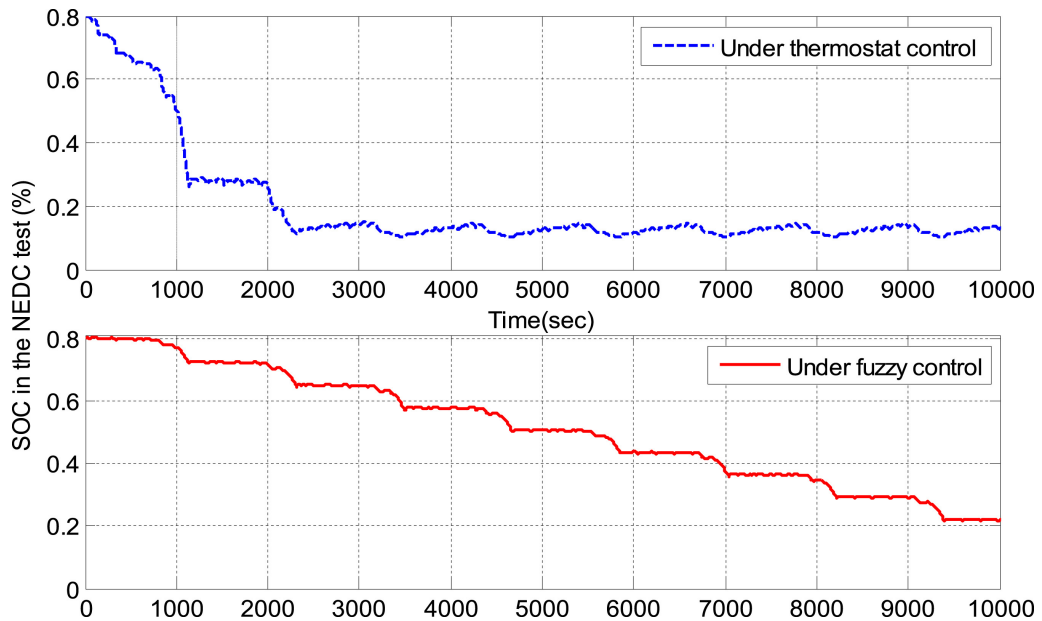


Figure 2.7: Comparative simulations of SOC

hydrogen quality are taken as input variables in [71] and supercapacitor reference current as output. The fuel cell reference current is decided by the difference between power demand and supercapacitor current. [72] chooses the battery SOC and fuel cell degradation as inputs and fuel cell current as the output. The membership functions and fuzzy rules are designed based on the experience of researchers and can be quite arbitrary.

Limited by their own features and control techniques, optimal results are hardly reached for deterministic rule based strategy and fuzzy rule based strategy. In order to get

better in the fuel consumption and durability of energy sources or economy, membership functions or fuzzy rules could be optimized by optimization algorithms.

In [73], genetic algorithm (GA) is used to optimize the membership functions of inputs (battery SOC and power demand) and output (power of DC/DC converter). Every membership function is defined by four parameters. Through the optimization of these parameters, better fuel economy is obtained.

In [64], the upper and lower limit values of hysteresis cycles of operating mode control are optimized by the genetic algorithm to minimize the equivalent consumption. [74] and [75] also use genetic algorithm to optimize membership functions of fuzzy controller, while the direct algorithm is used in [76]. These optimization strategies rely on road information and optimization results are affected by the kind of driving cycles. So some intelligent control strategies such as artificial neural network, machine learning strategy and drive cycle recognition strategy are used to improve rule based strategy robustness and adaptability ability for different road conditions.

### 2.3.2 Frequency based strategy

Fuel cell has slow transient response characteristic which cannot cover the fast power variation of power demand[77]. Frequency based strategy (FBS) decomposes the load power into high frequency power and low frequency power. Low frequency power is supplied by fuel cell and energy storage source meets high frequency power demand, which can seriously increase fuel cell lifetime.

[78] uses Haar wavelet transform to separate different frequency power demands. The wavelet filtering operation of a digital signal includes two phases: the decomposition in Figure 2.8 and the reconstruction in Figure 2.9. The decomposition levels of fuel cell and battery are different according to their physical characteristics of power sources. Through this strategy, the power demand of drive cycle is separated into low frequency power for fuel cell, middle frequency power for battery and high frequency power for supercapacitor in Figure 2.10. This method can help both fuel cell and battery to be protected from high dynamic power and increase their durability.

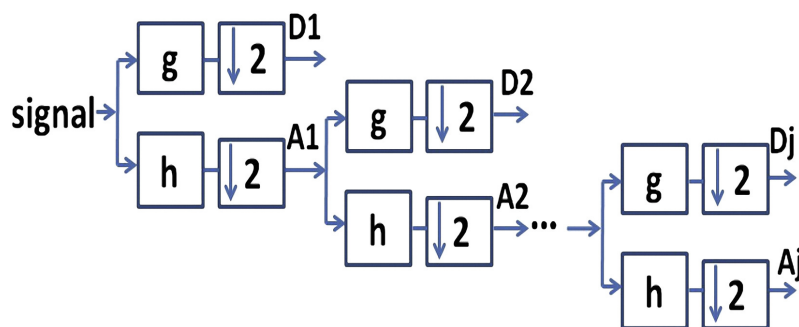


Figure 2.8: n level filtering: decomposition [78]

In [79, 80, 81], a low pass filter is used to get fuel cell power and battery power to improve the fuel cell lifetime. [82] uses two low pass filters to split power among three power sources. The first filter is used to get fuel cell current and the second one is used to split the current between battery and supercapacitor, where each filter has its own characteristics.

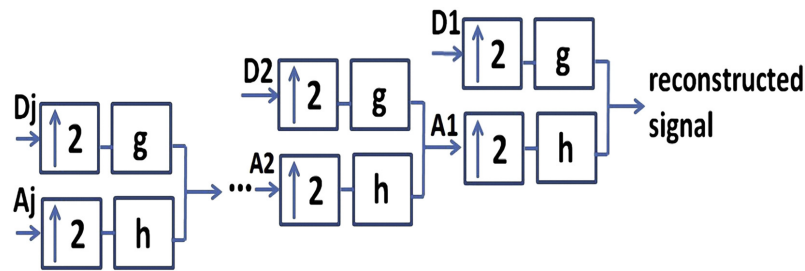


Figure 2.9: n level filtering: reconstruction [78]

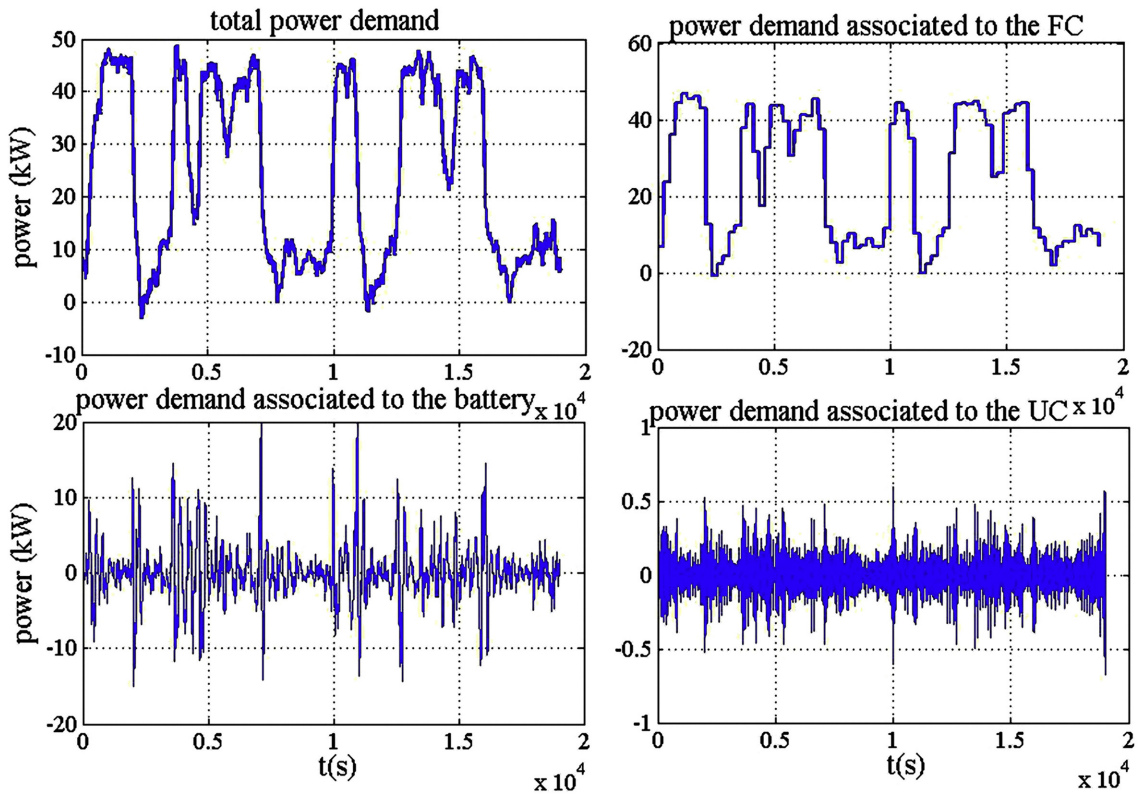


Figure 2.10: Wavelet transform for the Fuel cells-batteries-supercapacitors-architecture [78]

[83] proposes a power-sharing control strategy based on wavelet transform and fuzzy logic. The Haar-wavelet transform is utilized in this work for load profile decomposition to obtain the transients corresponding to sharp peak power demand which are assigned for the ESS. In order to raise the efficiency of the hybrid system, a control system based on fuzzy logic controller is developed for keeping the output power and power changing rate of the fuel cell system in a suitable range while maintaining the SOC of the battery and the supercapacitor in predefined limits.

### 2.3.3 Optimization based strategy

The interest of research on optimization based strategy is increasing due to its ability to reach optimal results. The optimal results are calculated through optimization based strategy by minimizing the sum of the objective function over time (global optimization) or by instantaneously minimizing the objective function (local optimization) [84]. The

objectives of these strategies can be quantified through a cost function which can represent fuel economy, durability of power sources, economy cost and other objectives. Equality constraints and inequality constraints are set in the optimization function to keep the normal operation of whole control system and power sources. The optimization problem for FCHEV is a nonlinear continuous constrained objectives problem, which can be described as the following equation (2.1) :

$$\begin{aligned} & \min f(x) \\ & \text{s.t.} \quad \begin{cases} g_k(x) \leq 0, k = 1, 2 \cdots n \\ h_j(x) = 0, j = 1, 2 \cdots m \\ x_i^{\min} \leq x_i \leq x_i^{\max}, i = 1, 2 \cdots I \end{cases} \end{aligned} \quad (2.1)$$

$f(x)$  is the objective function with variable  $x$ ,  $x_i^{\min}$  and  $x_i^{\max}$  are lower and upper values respectively,  $g_k(x)$  represents inequality function,  $n$  the number of inequality functions,  $h_j(x)$  equality function,  $j$  the number of equality functions. Through penalty factors, these constraints can also be transformed into one part of  $f(x)$ .

### 2.3.3.1 Global optimization based strategy

Global optimization based strategy takes whole drive cycle as the optimization period to find the optimal values. The drive cycle should be known in advance. But in reality, precise road information is hard to get. Meanwhile, the large computation burden also brings a serious challenge to the storage and calculation of vehicle controller. Even though global optimization based strategy is difficult to be used in reality, it is a perfect control benchmark to compare with other control strategies and it is also useful for the determination of judgemental parameters of rule based strategy and optimization of power train component size.

#### 1) Linear programming (LP)

LP, also called linear optimization, is principally used for determining the best allocation of limited resources either by maximizing the profits or by minimizing the costs and is particularly suitable for the optimization problem that has linear relationship[85].

[86] simplifies the non-linear fuel cell power-hydrogen consumption relation into three linear parts. Its cost function is defined by three linear fuel cell powers, battery power and their cost efficiencies to minimize hydrogen, electric energy consumption and overall cost. The constraints of designed LP include battery SOC, power balance constraint, fuel cell and battery ramp rate constraint, power and SOC limits and hydrogen storage capacity constraint.

[87] proposes a combinatorial optimization approach for FCHEV to split the power among main power sources: fuel cell and ESS: supercapacitor. The optimization problem with system constraints is non-linear due to the non-linear characteristics of fuel cell efficiency and supercapacitor power losses. Traditional optimization algorithms are time consuming to solve this non-linear problem. In order to solve this problem, a novel approach is proposed. The energy management problem is transformed into a combinatorial optimization problem through the piecewise linearization of the supercapacitor power losses and discretization of the fuel cell space. After the transformation of the problem from non-linear into linear, mixed integer linear programming is used to optimize the

power requirement of two power sources. Simulation results show that the novel strategy has low energy consumption and less time consumption.

LP algorithm has advantages of rapid calculation even with large problems containing a significant number of variables and constraints. Minimizing hydrogen consumption is mostly chosen as the objective of LP. Nevertheless, FCHEV is a complicated nonlinear system and the approximations used for transformations from non-linear into linear may increase inaccuracy which prevents the extensive application of LP on EMS[88].

## 2) Dynamical programming (DP)

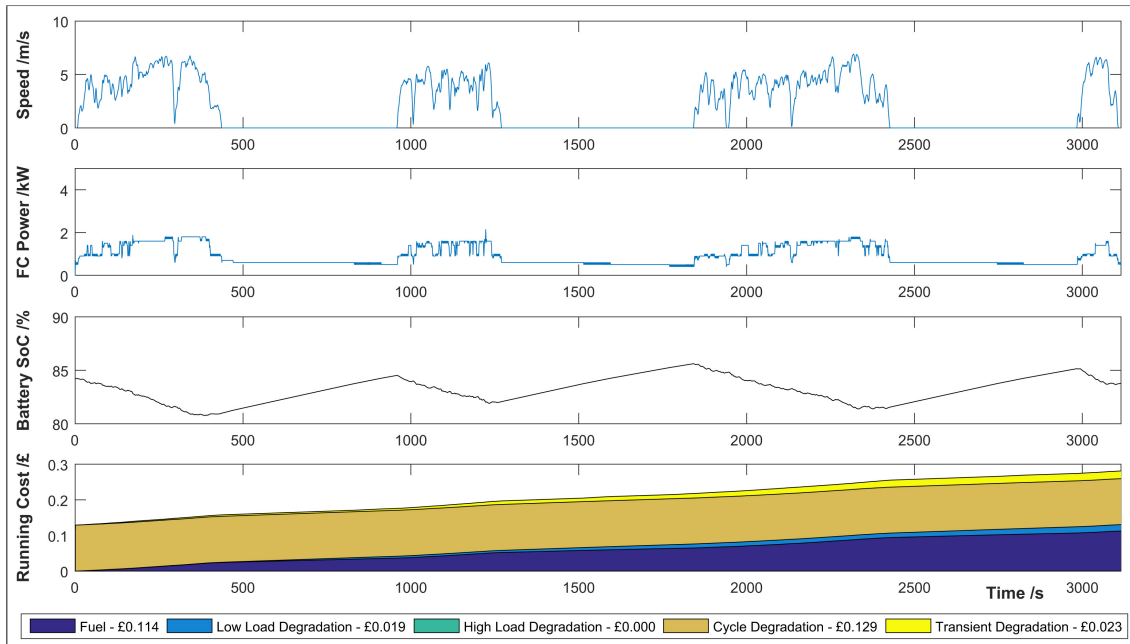
DP has been used in many different fields by engineers and mathematicians to solve engineering and other optimization problems and it is also one of the most effective strategy to solve the global optimization problem of EMS[89]. The complex optimization problem is disassembled into sub-problems by DP and the optimal results of the sub-problems are used to calculate the global optimal solution of the initial problem[90].

[91] designs a stochastic dynamic programming (SDP) considering the fuel economy and the durability of power sources. Firstly, the fuel cell degradation mechanism is reviewed and the operation actions of fuel cell that cause degradation are summarized. The cost function is described including the fuel consumption and fuel cell degradation. Voltage degradation rate under each condition is set in advance and battery voltage bounds are also limited. The final cost function is defined by the fuel consumption, fuel cell degradation, battery voltage limitation and their corresponding weightings respectively. The simulation results of the baseline controller and degradation optimized controller by SDP are shown in Figure 2.11. It can be observed that fuel cell has more stable power requirement. Fuel cell lifetime has increased 14%, but fuel consumption only has 3.5% decrease.

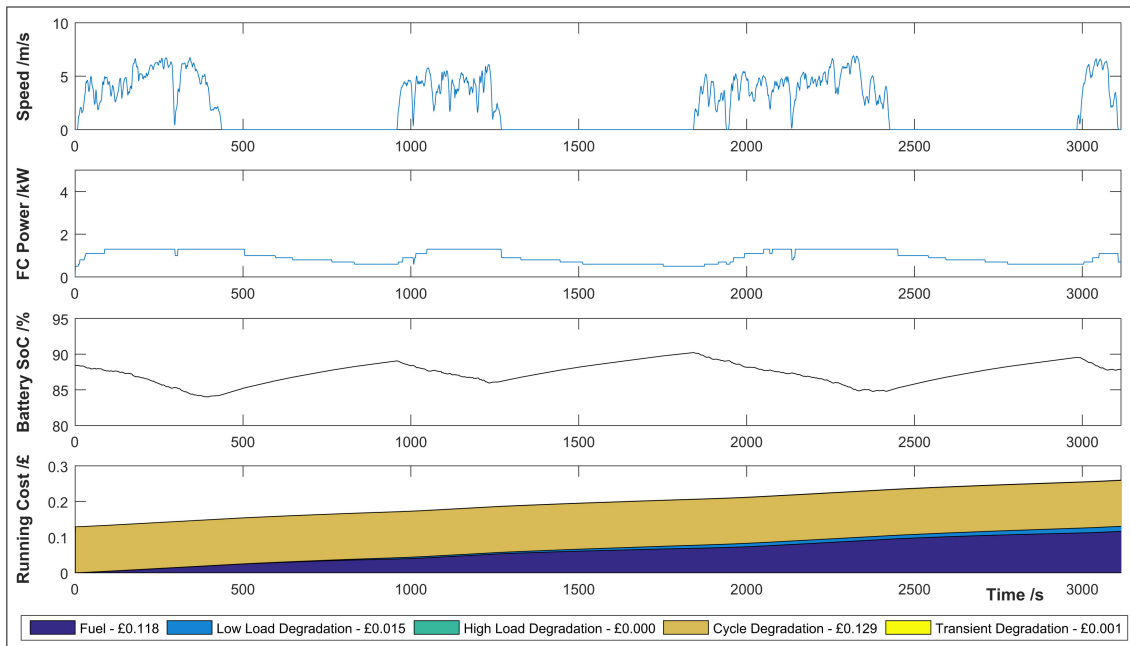
[92] described a discrete dynamic programming (DDP) for a PFCHEV. Battery is the main power source and its degradation severely affects the normal operation of the whole system and overall financial cost. The aim of the strategy is to minimize the overall cost including hydrogen consumption, battery degradation and grid recharge expense. A battery degradation model is designed to predict the battery performance loss and remaining useful lifetime. Every objective cost of DDP is not weighted towards a specific goal but each state/economic cost is sought to be zero. Constraints are set on power sources to ensure the normal operation of the whole system, including battery SOC bound, battery power bound, fuel cell power, vehicle speed and hydrogen reserve bound. Based on [92] and [93], the long-term effect of battery degradation management on the economic performance of PFCHEV is studied.

[94] proposes a weighted improved dynamic programming approach (WDP) and its cost function is composed of several parts: the square of fuel cell power multiplied by its weight to minimize hydrogen consumption, battery power limits and battery SOC bounds. Fuel cell power, battery power, battery SOC, fuel cell ramp rate and battery ramp rate are constrained to increase their lifetime. Brute-force search algorithm is used to find optimal weights.

DP is a powerful tool to realize optimal control and it can be applied to the nonlinear constrained complex problem of vehicle EMS. But DP also has some shortcomings. DP needs to know the whole drive condition in advance to achieve the optimal control which is difficult to obtain in the real driving scenarios. The high computational burden of searching for optimal results also prevents DP being used in the real car. Nevertheless, DP can be



(a) Baseline Controller



(b) Degradation Optimised Controller

Figure 2.11: Accumulated running cost of each controller[91]

used as the optimal benchmark for other control strategies or as an effective method as a basis for the development and improvement of other sub-optimal controllers[95].

### 3) Genetic algorithm (GA)

GA is based on Darwin’s evolution theory and is often used to search for optimal results for optimization and search problems. A set of candidate solutions called population are evolved to form new optimal population relying on bio-inspired operators including mutation, crossover and selection[96]. At the process of evolution, the fitness is used to

evaluate the objective function. The fitter the pollution is, the more chance is it chosen to produce a new population. The iteration will continue until the optimal solution is found.

In [64], GA is used to optimize fuzzy rule based strategy and operating mode control strategy. Regarding fuzzy logic part, GA optimizes membership functions of the power demand, fuel cell power and battery SOC. Operating mode control strategy has three modes and the mode selection hysteresis cycle is set to judge the operating mode according to the values of power demand and battery SOC. The upper and lower limit values of each cycle are optimized by GA. The objective is to minimize equivalent fuel consumption, increase average efficiency of fuel cell and battery, maintain SOC at the end of the cycle same as the initial value. The penalty function is used to add constraints to the final fitness function. In [97], the membership functions of fuel cell reference current are accurately adjusted by the GA. [59] also uses GA to optimize control parameters of PI. The objective is minimum hydrogen consumption and average absolute power of the battery.

GA is proven to be effective to solve complex engineering optimization problems, characterized by nonlinear, multi-modal objective functions [60]. GA is also widely used to optimize the control parameters of other rule based strategies. GA is good at searching the global optima, but easily getting stuck in local optima and it also has the common disadvantages of global optimization strategy: relying on previous knowledge of whole drive cycle, high computation cost and cannot be applied in real-time energy management.

#### 4) Particle swarm optimization (PSO)

PSO is a stochastic population-based optimization method proposed by Kennedy and Eberhart [98]. This algorithm is inspired by the information circulation and social behavior observed in bird flocks and fish schools and it is successfully applied to many problems such as fuzzy control, artificial neural network training, function optimization, and pattern classification [99]. The learning process of PSO relies on the experience of particle's own and other most successful particles. For the N-dimensional global optimization problem, a swarm with N particles is defined. Each candidate solutions for the optimization problem is called a particle. The particles are assigned random positions in the n-dimensional space. Each particle has its own trajectory: position and velocity and moves in the search space by successively updating its trajectory [100]. The trajectories of particles are modified by populations of particles based on the best positions visited earlier by themselves and other particles. The fitness function is defined to calculate the fitness values of all particles. Each particle moves towards its previously best position and the global best position in the swarm to seek the optimal solution [101].

In [102], an online rule based strategy is designed for fuel cell battery electric vehicle, and the ideal choice of its control parameters is difficult: fuel cell maximum power, fuel cell minimum power, battery maximum power, battery minimum power and battery SOC inferior and superior limits. PSO is used to optimize these control parameters under the objective of minimizing hydrogen consumption.

[103] proposes a double layer meta-heuristic based EMS for fuel cell ultra-capacitor HEV. The rule based strategy as the first layer is a strategic layer to decrease computational effort and time and restricts the search space of the second layer. PSO as the second layer is integrated into rule based strategy to search optimal fuel cell reference net current at the target of minimizing hydrogen consumption. Integrated PSO algorithm achieves lower computational time with an average of 0.65 ms versus 43.09 ms for the integrated GA for each time step, which makes it more suitable for real-time applications. Besides hydrogen consumption, the durability of the fuel cell system is considered as an important

performance criterion by limiting the fuel cell power variation rate in both layers using falling and rising limit values.

[104] pretenses a PSO-PID based maximum power point tracking for PEMFC. The maximum power point of fuel cell system changes according to fuel cell system parameters: cell temperature, the oxygen partial pressure, the hydrogen partial pressure and the membrane water content. PSO takes output power of fuel cell as the objective function to calculate the optimal output voltage with the changes of fuel cell system parameters, which is used to adjust the boost converter duty cycle connected to fuel cell through PID controller. The results show that compared with Perturb and Observe method and sliding mode algorithm, PSO has high accuracy, good time response and very low power fluctuations on tracking the real peak power point under different temperature and membrane water content.

PSO is a global optimization algorithm which is particularly suited to solve problems where the optimal solution is a point in a multidimensional space of the parameter [105] and it has fast computing speed and parallel processing ability. But PSO also has the disadvantages that it is easy to fall into local optimum in high-dimensional space and has a low convergence rate in the iterative process[106].

### 2.3.3.2 Local optimization based strategy

Global optimization based strategy relies on a predefined driving cycle to search for the global optimal results for the drive cycle. High computational effort is requested for global optimization strategy which means that it cannot be used in real time control of the vehicle. But global optimization based strategy can be a good benchmark for other energy management strategies and give insights for the development of simple and implementable strategies[107]. Local optimization based strategy replaces the optimization period of whole drive cycle for global optimization strategy into the instantaneous sampling time to calculate instantaneous optimal power split scheme among different power sources[108]. Equivalent consumption minimization strategy (ECMS), Pontryagin's Minim Principle (PMP), Model predictive control (MPC) are widely used local optimization based strategies.

#### 1) Equivalent consumption minimization strategy

The idea of ECMS is transforming electric energy stored by energy storage sources into equivalent hydrogen consumption and minimizing the sum of hydrogen consumption consumed directly by fuel cell and equivalent hydrogen consumption from energy storage sources. ECMS calculates the optimal reference power of power sources at every sampling time. No future predictions and previous drive cycle knowledge are necessary and only a few control parameters are required.

A control strategy designed in the two-level architecture for fuel cell supercapacitor HEV is developed in [109]. ECMS as the up-level calculates the fuel cell and supercapacitor optimal powers at each sampling time minimizing the hydrogen mass consumption, and PI controllers as the low level are designed to regulate the fuel cell and supercapacitor currents to their reference values respectively. Some physical limits including fuel cell power boundary, supercapacitor power boundary, state of energy boundary of supercapacitor are set to ensure the normal operation of the vehicle.

In [110], An ECMS for fuel cell/battery/supercapacitor tramway is developed in Fig-

ure 2.12. Supercapacitor has low energy density and its equivalent consumption is considered as null when whole hydrogen consumption of objective function is defined. Through ECMS, the fuel cell and battery powers can be calculated shown in Figure 2.13 for the real drive cycle of Urbos 3 tramway. It can be observed that fuel cell almost works as a constant power, around 95 kW. An additional PI controller is used to control supercapacitor SOC and get a reasonable reference power in Figure 2.14. Supercapacitor is designed to work during the high acceleration or braking in order to generate or absorb the power that either the fuel cell or the battery are not able to generate or absorb. Less power is dissipated by the braking resistor.

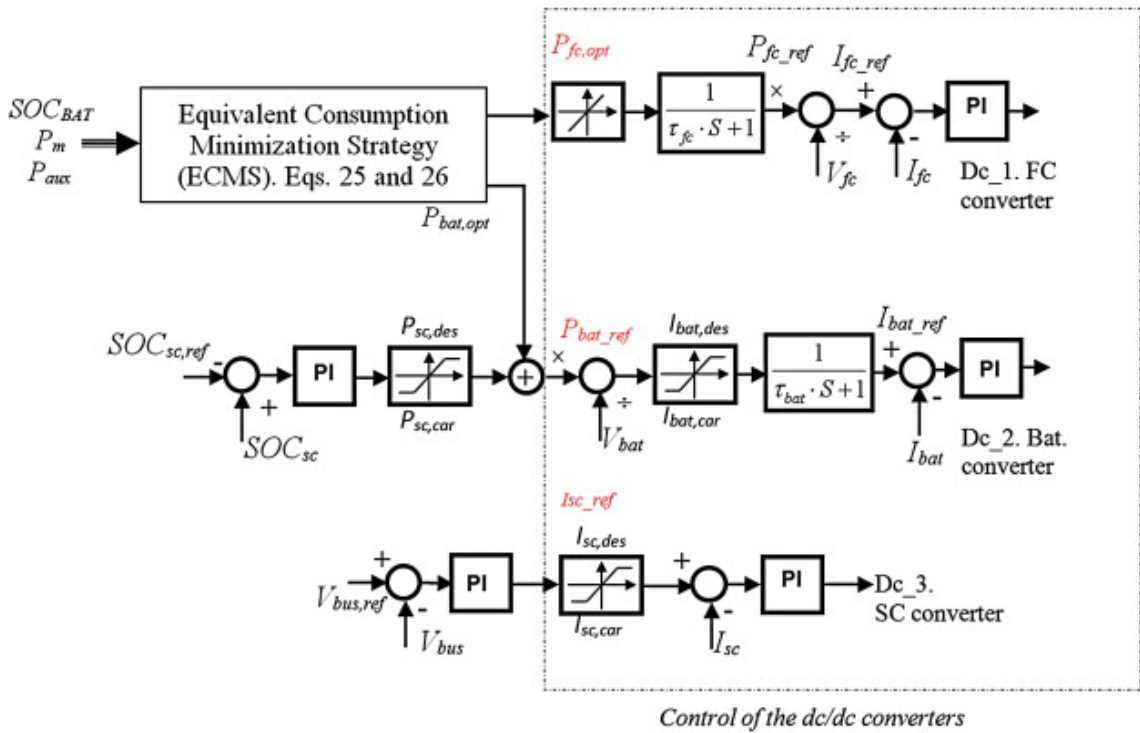


Figure 2.12: Energy management system proposed for the hybrid tramway[110]

[111] proposes a two-stage control strategy to minimize hydrogen consumption and protect fuel cell health. For the first stage, it uses telemetry equivalent consumption minimization strategy (T-ECMS) to calculate the fuel cell and battery reference power without considering fuel cell health. For the second stage, a tracking controller is used to track the fuel cell reference power. During the tracking process, the constraints are guaranteed to keep fuel cell healthy. The two-stage strategy reaches the aim of minimizing fuel consumption and prolonging fuel cell lifetime.

Equivalent factor is important for ECMS and its value is affected by driving cycle, battery SOC bound limits and others[112]. Through adjusting equivalent factor, we can achieve both aims of reducing the fuel consumption and prolonging the lifetime of power sources. In [113], a Hamiltonian function is defined as equivalent fuel consumption with equivalent factor. Equivalent factors for different drive cycles are pre-set as different constant values. Through pattern recognition algorithm and comparison result between the predicted battery mode and the desired battery mode, the equivalent factor that is good for the battery lifetime can be decided.

## 2) Pontryagin's Minim Principle

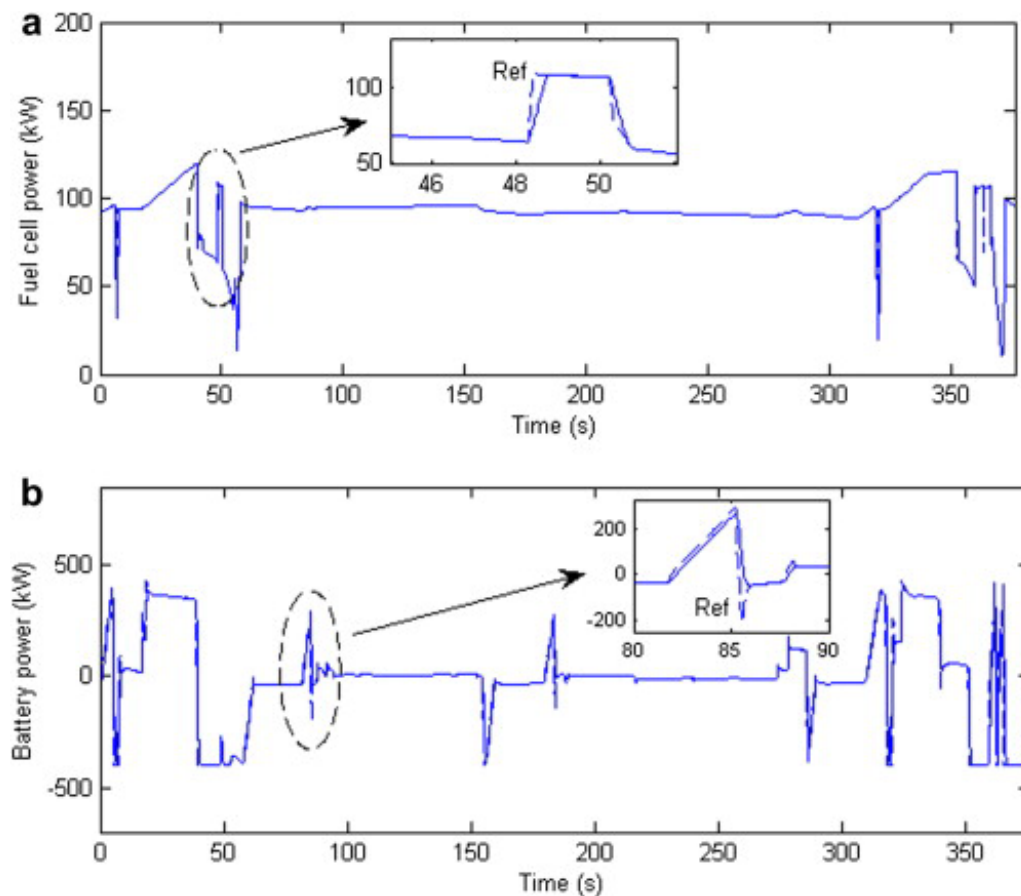


Figure 2.13: Simulation results for fuel cell and battery power[110]

PMP is based on optimal control strategy and its optimization result is close to dynamical programming. PMP is realized by an instantaneous minimizing Hamiltonian function and is in the form of a set of optimization conditions and its state variables are constrained in limited boundaries[114]. In PMP, the number of nonlinear second-order differential equations is decided by the problem dimension so the control based on PMP takes less computational time for getting optimal results. Under certain assumptions, PMP also can be used as a global optimal strategy[115].

In [116], a PMP based EMS is proposed. Firstly, the objective function that can describe hydrogen consumption and fuel cell lifetime is designed. Compared to the PMP only considering hydrogen consumption in the objective function, the designed novel PMP can prolong the fuel cell lifetime but hydrogen consumption has increased. In order to find a suitable optimal criterion to analyze the trade-off between hydrogen consumption and fuel cell stack lifetime, fuel cell stack cost, hydrogen cost, the lifetime growth factor, fuel cell consumption rate and fuel cell stack lifetime are chosen as the factors of evaluating function. Simulation results indicate that the designed PMP is superior on the fuel consumption and fuel cell stake lifetime.

[117] divides the control strategy into three typical processes: startup process, normal process and stop process. Different energy management strategies are designed for each process. In the normal process, the PMP strategy is used to keep fuel cell in the high efficiency zone, the change rate of fuel cell output power is limited to increase the fuel cell lifetime. The battery current is also limited to prolong the battery lifetime. During

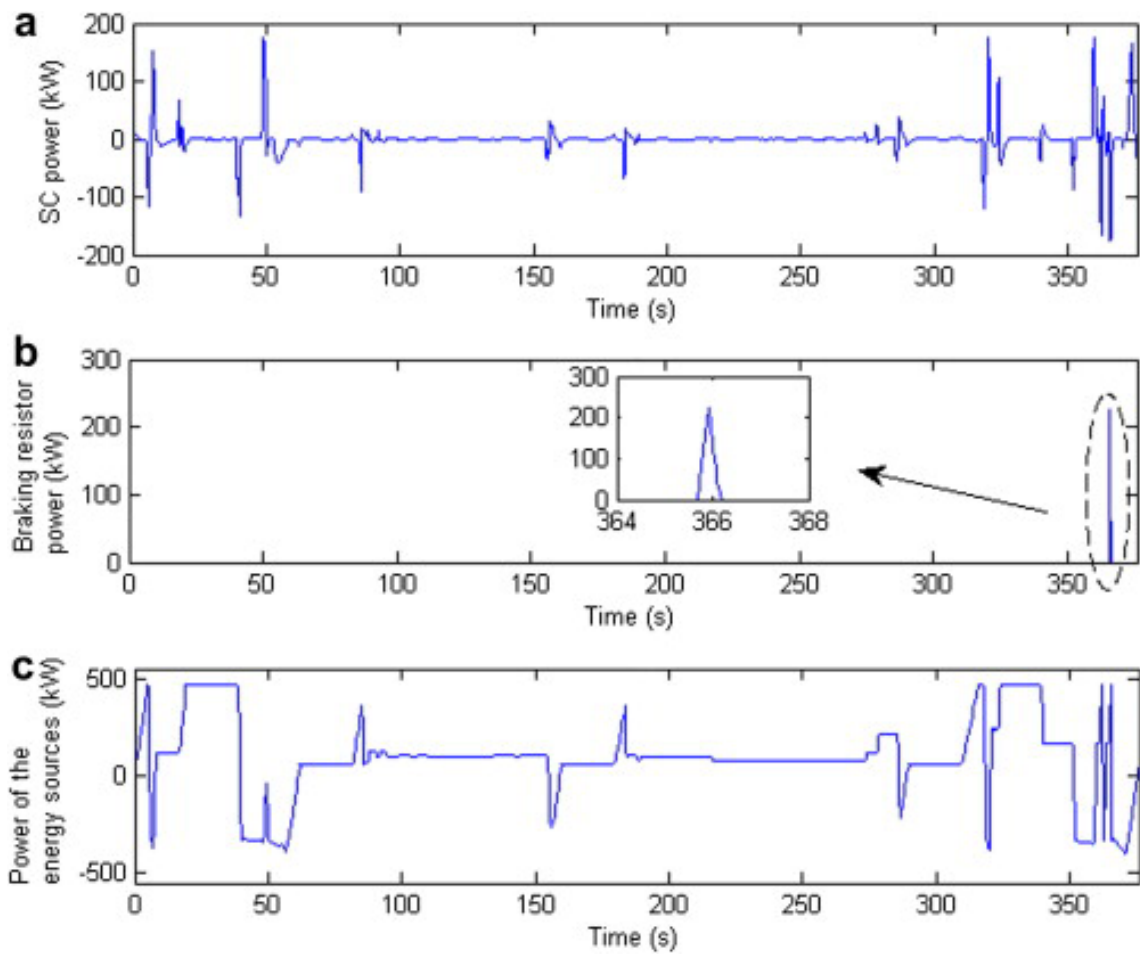


Figure 2.14: (a) Supercapacitor power, (b) Power dissipated in the braking resistor dissipated power, and (c) total power of the energy sources[110]

the shutting down process, fuel cell decreasing rate is limited to avoid water flooding or drying. At last the battery degradation rate decreased from  $37 \text{ mVh}^{-1}$  to  $75 \text{ mVh}^{-1}$ .

In [118], the objective of PMP is to minimize hydrogen consumption, maintain battery SOC in limits, meet the power demand of drive cycle and get optimal fuel cell power. Many constraints including fuel cell power, fuel cell power change rate, and battery SOC are set to PMP. Penalty functions are used to transform these constraints as the part of optimization function. Considering the effect of degradation on fuel cell performance, the adaptive recursive least square is used to identify the variation of fuel cell performance.

[119] takes the minimization of fuel consumption, limitation on battery SOC and increase of fuel cell lifetime as aims through PMP approach. PMP transforms battery SOC limitation and fuel cell power change rate into a new cost function and adds the new cost function into the objective function.

Even though PMP has good control performance similar to the DP, the co-state of the Hamiltonian function are determined by a trial-and-error method, therefore PMP cannot be applied directly[120, 121]. PMP is based on optimal control theory and also can be used to solve global optimization problem through taking whole drive cycle as the optimization period.

In [122], the design process of an on-board EMS is divided into two steps. In the first step, PMP is developed to solve global optimization problem taking minimization of fuel consumption as the objective. In the second step, according to the optimal solutions calculated in the first step, an Auto-Regressive Moving Average controller is designed.

### 3) Model predictive control

MPC is a model-based control methodology and the built system model is used to solve an open-loop optimal control problem in limited time horizons[123]. The cost function that represents the required behavior of the system is proposed to obtain the control law[124]. MPC is good to deal with the optimization problem that has many kinds of constraints and it also can predict future changes through the current values, dynamic state, predictive model and the process variable targets and limits[125].

[126] uses MPC to split power demand among fuel cell, battery and supercapacitor. The inputs are power demand, battery SOC and supercapacitor SOC and outputs are fuel cell reference power and battery reference power. Some constraints also are set such as fuel cell current bound, fuel cell current slope limitation, battery SOC and supercapacitor SOC.

In order to minimize hydrogen consumption, improve the durability of fuel cell system and maintain the supercapacitor SOC, MPC is developed as the EMS of fuel cell supercapacitor HEV in [127]. In the MPC framework, the Markov chains and neural networks as the power demand prediction methodologies are compared and neural network power predictors have better prediction ability than Markov chains. Based on the prediction results, the optimal fuel cell net power trajectory is calculated by DP.

In [128], a hybrid predictive control strategy is proposed for the fuel cell battery HEV to enhance the performance of both power sources and decrease the hydrogen consumption under the condition of reducing the degradation of power sources. The novel strategy is designed to track power demand of drive cycle and keep battery close to the desired state of charge. Some constraints like fuel cell power threshold and time limitation between fuel cell start-ups and shutdown to increase fuel cell durability. Fuel cell reference power is smoothed through a reference governor and battery is controlled to supply peak power during sharp power dynamics. An explicit controller is also designed into the MPC to decrease the execution time.

MPC is widely used to predict the power requirement of the vehicle and then applies various optimization methods to solve the optimization problem on the basis of the predicted power demand[129]. The prediction methods could be neural network algorithm, Markov Chain method and torque requirement exponentially decreasing model. The optimization methods could be the Pontryagin's Minimum Principle, equivalent consumption minimization strategy, dynamic programming or quadratic programming algorithm. MPC has the obvious advantages such as it is simple, robust and stable, and it can deal with multi-variable and constrained problems effectively and can stand the uncertainty caused by the model mismatch. But MPC relies on a plant model that can describe the real system very accurately and the high computational effort for the optimization[130, 131, 132].

### 4) Optimal control theory

OCT is a mathematical optimization approach based on control strategy. In [133], an EMS based on OCT is proposed. Its objective is the minimization of fuel consumption. The fuel cell power range, supercapacitor power range and fuel cell power change rate are constrained. The supercapacitor SOC is the state variable. At the final Hamiltonian

function, minimization of hydrogen consumption is replaced by minimizing fuel cell power. A Thermostat control strategy is also proposed to compare with OCT. The simulation results show that the EMS based on OCT has about 18% fuel reduction and has better good control of SOC and durability of fuel cell, but it relies on the knowledge of whole drive cycle. [134] proposes an adaptive optimal control algorithm. It minimizes fuel consumption subjected to an equality constraint that load power demand is supplied and some inequality constraints: fuel cell power bound limitation, fuel cell power change rate limitation, battery SOC upper and lower boundaries.

## 2.4 Objectives

When an EMS has to be designed, the objective of EMS should be set in advance. These objectives not only include basic objectives which ensure the normal operation of the vehicle and its power sources like drive ability, charge sustenance of energy storage sources and stability of EMS but also include optimal objectives like minimizing fuel consumption, increasing the durability of power sources and improving the economy. The EMS of FCHEV is a complex nonlinear problem with multiple variables. Multiple objectives are sought at the same time. As reviewed in Section 2.3, each kind of energy management strategy has different characteristics and when they are chosen to fulfill these objectives, different methods are used. In this part, the objectives of EMS and the methods to fulfill these objectives are reviewed for different kinds of energy management strategies.

### 2.4.1 Drive ability objective

Under the control of EMS, power sources should cooperate to ensure the normal operation of FCHEV. Meeting the power demand of drive cycle is the basic and mandatory objective that should be achieved. Limited by physical characteristics of power sources and other components like DC/DC converters, DC/AC converters and motor of FCHEV, the operation range of components should be limited in the objectives or constraints of EMS. Taking fuel cell as an example, the referenced power demand from fuel cell should not be larger than its maximum power value, otherwise, serious damage to the fuel cell stack will be led. High dynamical power change rate also should be limited to increase the fuel cell durability. All these basic requirements for drive ability objective can be described in equation (2.2) and met by all EMSs in the published articles.

$$\left\{ \begin{array}{l} P_{demand} = P_{fc} * \eta_{DCFC} + P_{ESS} * \eta_{DCSS} \\ I_{com}^{min} \leq I_{com} \leq I_{com}^{max} \\ V_{com}^{min} \leq V_{com} \leq V_{com}^{max} \\ P_{com}^{min} \leq P_{com} \leq P_{com}^{max} \\ SOC_{ess}^{min} \leq SOC_{ess} \leq SOC_{ess}^{max} \\ -dP_{fc} \leq \frac{P_{fc}(t) - P_{fc}(t-1)}{T} \leq dP_{fc} \\ -dP_{ess} \leq \frac{P_{ess}(t) - P_{ess}(t-1)}{T} \leq dP_{ess} \end{array} \right. \quad (2.2)$$

where,  $P_{demand}$  is power demand,  $P_{fc}$  and  $\eta_{DCFC}$  is fuel cell power and its efficiency respectively,  $P_{ess}$  and  $\eta_{DCSS}$  is the power of energy storage sources and their efficiency respectively,  $I_{com}$ ,  $V_{com}$  and  $P_{com}$  are the operation range requirement on drivetrain components like power sources and motor,  $T$  is sampling time, and dynamical change rate

of fuel cell and energy storage sources  $dP_{fc}$  and  $dP_{ess}$ ,  $SOC_{ess}$  is SOC of energy storage source.

### 2.4.2 Energy storage sources' charge sustenance objective

Charge sustenance means that the net energy consumption from energy storage sources is zero at the end of the drive cycle, meaning that the final state of charge of energy storage sources should be equal to its initial value at the beginning of drive cycle[135]. On the contrary, charge depletion means maximum energy consumption supplied by energy storage sources, which is only adopted by Plug-in HEV. Charge sustenance should be considered in the EMS of FCHEV. It is not only convenient for the next usage of the vehicle in reality but also facilitates the comparison of different energy management strategies. If the final SOC of energy storage source is different from the initial value, when hydrogen consumption is compared for different energy management strategies, the difference between initial energy consumption and final energy consumption from energy storage sources should be converted into equivalent hydrogen consumption to ensure the fairness of comparison. This can be avoided by taking charge sustenance as an objective.

In [135], charge sustenance is limited through a "soft" constraint: a penalty function based on the difference between the final SOC of energy storage sources and initial value is added as the part of the objective function in equation (2.3). Other components of the objective function are the hydrogen consumption from fuel cell and the decreasing frequency of fuel cell operation through reducing frequent fuel cell on/off cycle to increase its durability. DP is used to solve this problem directly. The simulation results are shown in Figure 2.15. The charge sustenance of the battery and supercapacitor is met. In [102, 64], the charge sustenance is also met through the added penalty function.

$$J = \underbrace{w_{bt} (x_{bt}^N - x_{bt}^1)^2}_{\text{Battery}} + \underbrace{w_{uc} (x_{uc}^N - x_{uc}^1)^2}_{\text{Ultracapacitor}} + \underbrace{\Delta t \sum_1^{N-1} \dot{m}_f(u_{fc})}_{\text{Fuel cell consumption}} + \underbrace{\lambda \sum_1^{N-1} \dot{m}_f(\text{Sign}(u_{fc}^k) - \text{Sign}(u_{fc}^{k+1}))^2}_{\text{On /off frequency}} \quad (2.3)$$

*Charge sustaining penalty*

In [87] integer linear programming is designed to optimize the hydrogen consumption. The charge sustenance is reached through the direct equivalence constraint on the optimization problem:  $SOC_{fin} = SOC_{ini}$ . As one kind of global optimization strategy, the solutions that cannot meet the constraint of charge sustenance are discarded directly. The method through equivalence constraint of battery SOC also is used in [117].

It should be mentioned that the methods: adding the penalty function method in [135] and the equivalence constraint method in [87] to ensure the charge sustenance of energy storage sources can only be used in global optimization strategy. Because the final SOC of energy storage sources can be calculated directly for every possible solution under the condition of known knowledge of drive cycle. But the final SOC is not available for other kinds of energy management strategies due to the lack of known drive cycle.

In [136], equivalent consumption minimization strategy is designed for the FCHEV powered by fuel cell, battery and supercapacitor. Minimizing the whole hydrogen consumption including direct hydrogen consumption from fuel cell and equivalent hydrogen consumption from energy storage sources. In order to reach the objective of charge suste-

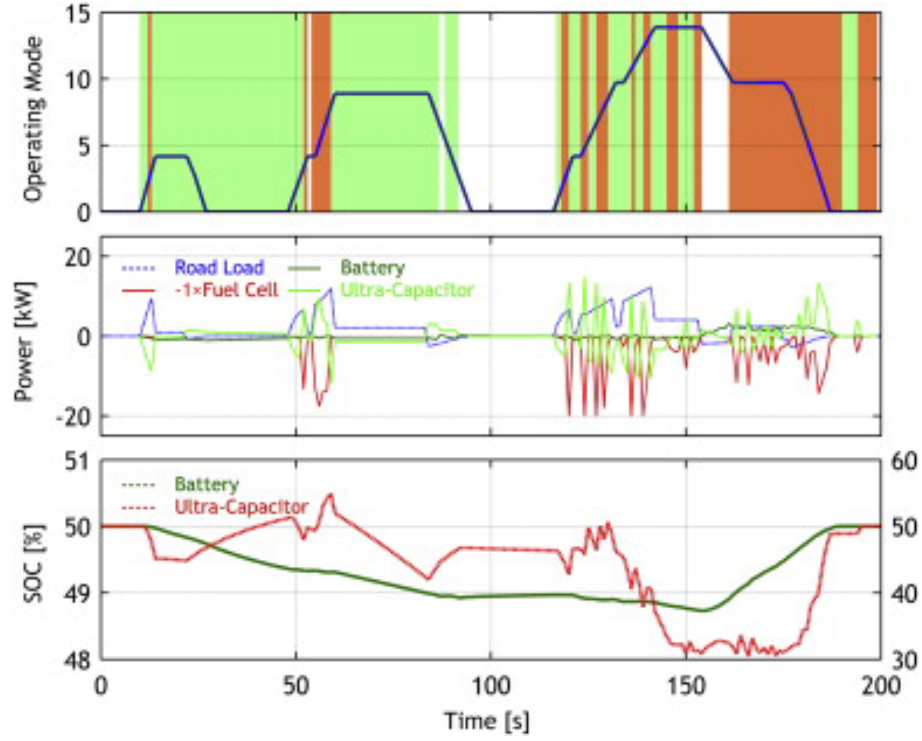


Figure 2.15: Response of fuel-cell hybrid vehicle with hybrid storage system[135]

nance, battery SOC penalty coefficient  $K_{BA}$  is added as the equation (2.4).

$$m_w(t) = K_{FC}m_{FC}(t) + K_{BA}m_{BA}(t) + K_{SC}m_{SC}(t)$$

$$K_{BA} = \begin{cases} \left(1 - \frac{2*(u-B_{ini})}{B_{max}-B_{min}}\right)^8 & B_{min} \leq u \leq B_{max} \\ \left(1 - \frac{2*(u-B_{ini})}{B_{max}-B_{min}}\right)^{16} & u < B_{min}, u > B_{max} \end{cases} \quad (2.4)$$

where  $m_w(t)$  is whole hydrogen consumption,  $m_{FC}(t)$  fuel cell hydrogen consumption,  $m_{BA}(t)$  battery equivalent hydrogen consumption,  $m_{SC}(t)$  supercapacitor equivalent hydrogen consumption,  $K_{BA}$  and  $K_{SC}$  are penalty coefficients,  $K_{FC}$  is the fuel cell efficiency penalty coefficient that operates fuel cell at high efficiency point,  $u$  is the present instantaneous battery SOC,  $B_{ini}$  is initial battery SOC,  $B_{max}$  the maximum battery SOC,  $B_{min}$  the minimum battery SOC.

Although penalty function method is also used in this local optimization strategy, different from global optimization strategy, the present battery SOC is sought to be equal to the initial value and the degree that its SOC approaches the initial value is decided by power demand, fuel cell power at last sampling time and supercapacitor SOC. Similar method is also used in [137]. The method can promote the charge sustenance of energy storage sources but cannot guarantee the total equivalence between the final and initial value.

Regarding rule based strategy, the charge sustenance is tried to be held through letting the fuel cell supply additional power to charge the energy storage source under precondition of meeting power demand when its SOC is less than the initial value and on the contrary letting energy storage source supply more power when its SOC is larger than the initial one.

In [68] a stiffness coefficient model (SCM) is designed for the fuel cell battery HEV. The battery SOC is regulated by the SCM through the dynamic charging/discharging coefficient which simulates the compression/stretching characteristics of a spring. when power demand  $P_{demand}$  is larger than fuel cell power at the maximum efficiency point  $P_{peak}$ , the fuel cell power  $P_{set}$  is set in equation (2.5)

$$\begin{cases} P_{set} = P_{peak} & SOC \geq 50\% \\ P_{set} = P_{peak} + K_{discharge}(P_{demand} - P_{peak}) & SOC < 50\% \end{cases} \quad (2.5)$$

where the dynamical discharging coefficient  $K_{discharge}$  is defined as the equation (2.6)

$$K_{discharge} = a \times \left( \frac{0.5 - SOC}{0.5 - SOC_{mn}} \right)^{k1}, \quad 1 \leq k1 \leq 10 \quad (2.6)$$

where  $a$  is a constant,  $k1$  is the stiffness coefficient of discharging and  $SOC_{mn}$  is the minimum value of battery SOC. Through the stiffness coefficient, the battery SOC is hoped to hold a reasonable state. The similar rules under the condition of  $P_{demand} < P_{peak}$  is also defined.

### 2.4.3 Stability Objective

Besides the normal operation of FCHEV, the energy management strategy should also maintain the stability of the system under the special conditions such as accelerations and decelerations of the vehicle, degradation and failure of power sources, short circuit or open circuit caused instability of the dynamic power system [138].

In [139, 140], a fuzzy rule based strategy is firstly designed for the FCHEV powered by fuel cell, battery and supercapacitor. Fuel cell and supercapacitor are connected to the DC bus through DC/DC converters. Battery is connected to the DC bus directly to hold the DC bus voltage. On the basis of the designed fuzzy control strategy, the failures of fuel cell and supercapacitor are considered to maintain the stability of EMS. Considering that the failure of battery leads to the non operation of the vehicle, so EMS only considers the failures of fuel cell and supercapacitor. Experimental results are shown in Figure 2.16 and Figure 2.17 for failure conditions of supercapacitor and fuel cell respectively. It can be observed that modified EMS can ensure the normal operation of vehicle under the conditions of the respective failures of fuel cell and supercapacitor.

Fuel cell and Li-ion batteries are used as the power sources of FCHEV in [141]. The thermal management system of fuel cell stack can make sure that the temperature of fuel cell stack varies in a certain range. However, the battery temperature is affected by the external environment and increases during its operation. In order to achieve the stability objective of EMS under varying temperature, the battery temperature is taken as the second-state variable of designed Pontryagin's Minim Principle strategy and a new co-state is defined for it in the Hamiltonian function. The optimal surface representing the relationship of final battery SOC value, battery temperature and the final hydrogen consumption is built through the extended Pontryagin's Minim Principle strategy. According to the simulation results, the Pontryagin's Minimum Principle strategy considering battery temperature not only reduces the final hydrogen consumption but also increases the battery lifetime.

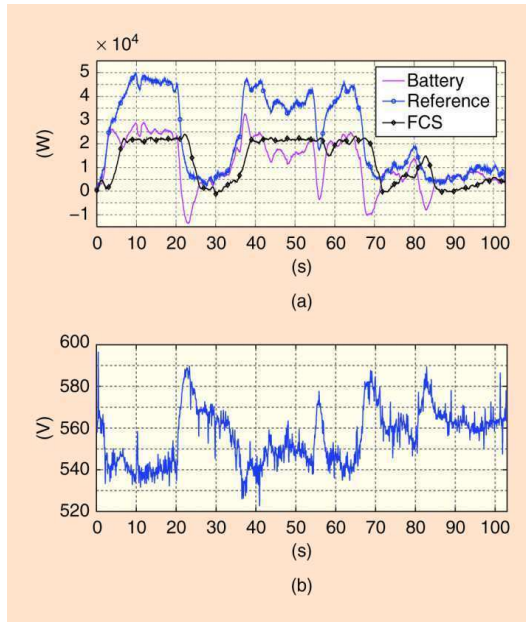


Figure 2.16: The experimental results of EMS without a supercapacitor. The (a) power distribution and (b) battery voltage[139, 140]

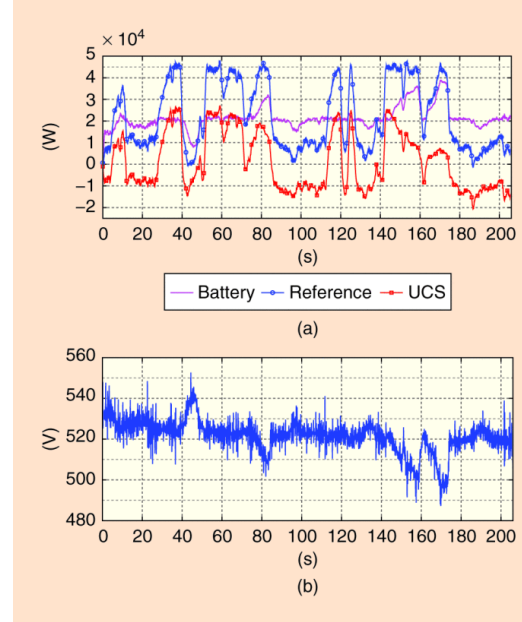


Figure 2.17: The experimental results of EMS without a supercapacitor. The (a) power distribution and (b) battery voltage[139, 140]

In [67], fuel cell and supercapacitor are taken as the power sources. The supercapacitor power is indirectly controlled by the regulation of DC bus voltage and fuel cell reference power is determined by the filtering power demand and supercapacitor SOC. Two five-phase permanent magnetic synchronous machines (PMSM) are used in the vehicle. There is a possibility that the phases of PMSM are out of action along with its operation. A current control strategy is designed to avoid the vibration of power demand and eliminate the possible damage to fuel cell system under the condition of sudden phases failure of PMSM.

In [72] a fuzzy rule based strategy taking account of the fuel cell degradation is designed. Battery SOC and fuel cell degradation degree are taken as the inputs of fuzzy logic controller. The fuel cell in healthy state, 50% degradation state and 20% degradation state due to the failure of some cells are simulated respectively. The results show the good behavior of the controller, proving its adaptation to the fuel cell degradation and failure.

In [142], an equivalent consumption minimization strategy is developed for fuel cell hybrid electric vehicle powered by fuel cell, battery and supercapacitor. An adaptive dynamical change rate is limited based on the degradation degree of fuel cell. Three conditions: fuel cell in healthy state, half degradation state and full degradation state simulate. Simulation results show that the equivalent consumption minimization strategy can properly provide the power demand by the driving cycle regarding the fuel cell degradation.

#### 2.4.4 Fuel consumption objective

Minimization of fuel consumption including fuel cell hydrogen consumption and electric energy consumption is the most studied objective. Electric energy is often transformed

into an equivalent hydrogen consumption. The sum of hydrogen consumption from fuel cell directly and equivalent hydrogen consumption is defined as the whole hydrogen consumption. The methods to minimize fuel cell hydrogen consumption and whole hydrogen consumption are summarized in this section.

Fuel cell hydrogen consumption can be calculated through two methods: the fitting function from experimental data and theoretical function based on fuel cell theory. The fitting function can be defined in equation (2.7) in [143] or equation (2.8) in [144]. The equation form is decided by different real experiment test data.

$$H_{fc} = a_1 P_{fc}^3 + a_2 P_{fc}^2 + a_3 P_{fc} + a_4 \quad (2.7)$$

$$H_{fc} = a P_{fc}^2 + b P_{fc} + c \quad (2.8)$$

where  $H_{fc}$  is the hydrogen consumption rate,  $P_{fc}$  fuel cell power,  $a_1$ ,  $a_2$ ,  $a_3$ ,  $a_4$ ,  $a$ ,  $b$ ,  $c$  are fit coefficients from the experimental data.

The theoretical function can be described as the equation (2.9) [143, 136]

$$J_{fc} = \int_0^t \frac{M_{H_2} n_c}{2 F} I_{FC}(t) dt \quad (2.9)$$

where  $J_{fc}$  represents the hydrogen mass rate,  $n_c$  is the number of cells,  $M_{H_2}$  is the hydrogen molar mass (2.02g/mol),  $I_{FC}$  represents the fuel cell current and  $F$  represents the Faraday constant (96,487 C).

According to the specified hydrogen consumption rate function, minimizing hydrogen consumption can be chosen as all or part of the objective function for optimization based strategy. [73, 122, 145] takes the quantified hydrogen consumption as the only objective function. Besides the quantified hydrogen consumption, the charge sustenance of battery is also taken as part of the objective in [102].

Using quantified hydrogen consumption function as the method to minimize hydrogen consumption is popular for optimization based control strategy, but it is difficult to be applied into rule based strategy. Limiting fuel cell working in high efficiency zone even seeking maximum efficiency point is a way that can be used in all kinds of energy management strategies. Consequently, finding its best operation point with high precision is vital, which directly leads to the reliability of the designed energy management strategy. Different methods to define the fuel cell system efficiency are introduced.

[117, 119] defines the fuel cell system efficiency  $\eta_{fcs}$  in equation (2.10), it is simple but not precise. Auxiliary power consumed by auxiliary equipment such as electrical control board, cooling fan and air compressor which ensure the normal operation of fuel cell system is not considered.

$$\eta_{fcs} = \frac{P_{fcs}}{m_{H_2} * LHV} \quad (2.10)$$

where  $P_{fcs}$  fuel cell system power,  $m_{H_2}$  fuel consumption rate from fuel cell,  $LHV$  is the low heating value of hydrogen.

A more precise fuel cell efficiency model is built and the whole fuel cell stack efficiency is defined in section 3.2.3

In [64], 50kW PEMFC is used and the overall efficiency map along with fuel cell current is defined. According to the efficiency map, the fuel cell high efficiency zone and maximum efficiency point are defined. Operating mode control strategy as one kind of rule based strategy is designed for the fuel cell hybrid electric vehicle. According to the battery SOC and the gap between fuel cell maximum efficiency point and power demand of the vehicle, the control system is operated in different modes. The calculation of fuel cell and battery reference powers is defined for different modes.

In [68], a novel stiffness coefficient model is developed. The reference powers of power sources are decided by the logic relationship between the fuel cell maximum efficiency point and the power demand of the drive cycle. The degree of how fuel cell power follows the power demand is regulated by the battery SOC and stiffness coefficient of charging and discharging.

Regarding optimization-based strategy, the function to calculate hydrogen consumption and fuel cell system efficiency can be chosen as one part of the objective function directly. Hydrogen consumption rate is defined as the above equation (2.7) or (2.9). Fuel cell efficiency can be defined as above equation (2.10). In [146, 147, 148], the global extreme seeking optimization algorithm is designed. The optimization function ( $J$ ) is defined as the sum of fuel cell net power  $P_{net}$ , which represents the objective of minimizing hydrogen consumption, and fuel cell system efficiency  $Fuel_{eff}$  with respectively weighting coefficients  $K_{net}$  and  $K_{fuel}$  as the equation (2.11)

$$J = K_{net}P_{net} + K_{fuel}Fuel_{eff} \quad (2.11)$$

Load following strategy is firstly designed to adjust the fuel cell power level to the dynamic load request. When the weighting coefficients  $K_{net}$  and  $K_{fuel}$  are defined, a global extreme seeking algorithm is designed to locate and track the global maximum point of fuel cell system and calculate air flow rate and fuel flow rate to the optimal operation point of the fuel cell system. The fuel cell system efficiency and fuel consumption efficiency are defined as the equation (2.12) and equation (2.13)

$$Fuel_{eff} = \frac{P_{net}}{FuelFr} \quad (2.12)$$

$$\eta_{sys} = \frac{P_{fc} - P_{aux}}{P_{fc}} \quad (2.13)$$

The auxiliary power is defined as the power consumed by air compressor as the equation (2.14)

$$P_{aux} = (a_2AirFr^2 + a_1AirFr + a_0)(b_1I_{FC} + b_0) \quad (2.14)$$

where  $a_2, a_1, a_0, b_1, b_0$  are fit coefficients,  $AirFr$  is air flow rate,  $I_{FC}$  fuel cell current.

Electric energy consumption as one kind of fuel consumption is always transformed into equivalent hydrogen consumption through equivalent factor and the sum of hydrogen consumption from fuel cell and equivalent hydrogen consumption from energy storage

sources is minimized in the objective function of EMS. There is not relevant research that minimizes the electric energy consumption alone for FCHEV.

In[110], an ECMS is designed for a fuel cell-battery-supercapacitor tramway and the objective function is defined as the equation (2.15),

$$J = C_{fc} + K_1 C_{ba} + K_2 C_{sc} \quad (2.15)$$

where  $C_{fc}$  is fuel cell hydrogen consumption,  $C_{ba}$  and  $C_{sc}$  are battery equivalent hydrogen consumption and supercapacitor equivalent hydrogen consumption respectively, since supercapacitor has low energy density and is used to generate the power peaks of power demand of drive cycle during the accelerations or braking, therefore its contribution to hydrogen consumption will be minimum and  $C_{sc}$  can be neglected and the objective function can be defined as the equation (2.16). The objective function of [137] is also defined as the equation (2.16).

$$J = C_{fc} + K_1 C_{ba} \quad (2.16)$$

In [149, 109], the objective function includes fuel cell hydrogen consumption and equivalent supercapacitor hydrogen consumption in equation (2.17).

$$C = \dot{M}_{H_2}(t) + \lambda P_{sc}(t) \quad (2.17)$$

where  $\dot{M}_{H_2}$  hydrogen consumption rate,  $P_{sc}$  supercapacitor power,  $\lambda$  equivalent factor.

### 2.4.5 Power sources durability objective

During FCHEV's lifetime, power sources degradation appear. As the main power source of FCHEV, the output power of fuel cell stack at corresponding current decreases along with degradation and its efficiency map of operation also changes. The capacity of battery decreases and its internal resistance increases along with its degradation, which decreases the output voltage of battery[150]. Supercapacitor lifetime is far larger than the vehicle and other power sources, so the durability of power sources is defined as the durability of fuel cell and battery in the following parts of dissertation[151].

#### 2.4.5.1 Durability of fuel cell

High cost of fuel cell systems and low lifetime are the main challenges of commercially used of fuel cell stack on the vehicles. Increasing the durability of fuel cell stack is one of the most important objectives for EMS. Comprehensive research and reviews have been published in an attempt to understand the degradation mechanisms of fuel cell components such as electrocatalysts, membranes, and bipolar plates based on the experimental test[152]. But for the whole stack, the degradation rate is difficult to be quantified for specific operation of fuel cell.

[153] has developed a quick evaluating method for automotive fuel cell lifetime. Based on the practical operation data of fuel cell hybrid bus, the operation of fuel cell is divided into four typical operation cycles: load changing cycles, start-stop cycles, idling time and high power load driving conditions and their degradation rate are decided through the

respective test results of a fuel cell stack in laboratory. This method is used in the EMS of [93]. The fuel cell overall degradation is calculated in equation (2.18)

$$\delta_{fc}(k+1) = \delta_{fc}(k) + \frac{\sum_k^{k+1} K_{fc} (n_1 V'_1 + n_2 V'_2 + U'_{load} \Delta t)}{V_{nom,cell}(1 - EOL_{fc})} \quad (2.18)$$

where a relative voltage loss percentage is  $\delta_{fc}$ ,  $K_{fc}$  experimental difference factor,  $V'_1$  and  $V'_2$  are event counters and instantaneous voltage degradation rates for start-stop and drastic load changes, respectively,  $U'_{load}$  continuous load-dependent degradation rate,  $V_{nom,cell}$  fuel cell nominal voltage,  $EOL_{fc}$  fuel cell end-of-life voltage loss level over a step  $k$  of length  $\Delta t$ . The degradation rate of different operations are  $V'_1 = 13.79\mu V/cycle$  for start-stop,  $V'_1 = 0.4185\mu V/cycle$  for load change,  $U'_{load} = 8.662\mu V/h$  for low power idling,  $U'_{load} = 10\mu V/h$  for high power load and 1.72 for  $K_{fc}$  factor.

In [117, 91], the relationship between degradation rate of fuel cell  $\delta_{fc}$  and cycle information is defined in equation (2.19)

$$\delta_{fc} = K_p (P_1' N_1 + P_2' N_2 + P_3' T_1 + P_4' T_2) \quad (2.19)$$

where  $K_p$  is accelerating coefficient by reasons of air quality,  $P_1'$ ,  $P_2'$ ,  $P_3'$ , and  $P_4'$  are degradation rates for large load change cycling, start-stop cycling, idle condition and high-power load condition, separately.  $N_1$  and  $N_2$  are operating times,  $T_1$  and  $T_2$  are time.

The gas supply system of fuel cell stack cannot respond to high dynamical power requirement. The high dynamical variation can seriously decrease the fuel cell lifetime and even damage the fuel cell. Except for quantification of fuel cell degradation rate under different load conditions, setting the limitations on fuel cell current-changing rate, current value and power-changing rate to reduce the dynamical change of fuel cell is a widely used method to prolong its durability and this method can be used in all kinds of energy management strategies.

In [154, 116], the designed Pontryagin's Minimum Principle as one kind of optimization strategy not only decreases the hydrogen consumption but also increases the lifetime of fuel cell through Hamiltonian function in equation (2.20)

$$H(S\dot{OC}(t), P_{FC}(t), t) = m_{H_2}(P_{FC}(t)) + \lambda(t)S\dot{OC}(t) + S(P_{FC}(t)) + L(P_{FC}(t)) \quad (2.20)$$

Where  $m_{H_2}(P_{FC}(t))$  hydrogen consumption rate,  $P_{FC}$  fuel cell net power,  $\lambda(t)$  a co-state variable,  $S\dot{OC}(t)$  is state equation of supercapacitor,  $L(P_{FC}(t))$  and  $S(P_{FC}(t))$  are cost functions to limit the operation of fuel cell and supercapacitor SOC in equation (2.21) and (2.22)

$$\begin{aligned} L(P_{FC}(t)) &= L_1(P_{FC}(t)) + L_2(P_{FC}(t)) + L_3(P_{FC}(t)) \\ \begin{cases} L_1(P_{FC}(t)) &= \gamma_1 (P_{FC}(t) - P_{FC}(t - \Delta t))^2 \\ L_2(P_{FC}(t)) &= \begin{cases} \gamma_2 P_{FC}(t), & \text{if } I_{FC}(t) \geq I_{FC,large} \\ 0, & \text{otherwise} \end{cases} \\ L_3(P_{FC}(t)) &= \gamma_3 (I_{FC}(t) - I_{FC}(t - \Delta t))^2 \end{cases} \end{aligned} \quad (2.21)$$

Where  $\gamma_1$ ,  $\gamma_2$  and  $\gamma_3$  are constant tuning parameters,  $L_1$ ,  $L_2$  and  $L_3$  are parts of objective functions to make the optimal trajectory of the fuel cell power smooth, limit the fuel cell working range, and current change rate of fuel cell respectively,  $t$  time step,  $I_{FC}$  fuel cell current,  $I_{FCLarge}$  fuel cell maximum current.

$$S(P_{FC}(t)) = \begin{cases} \alpha P_{FC}(t) & SOC(t) \leq SOC_L \\ 0 & SOC_L < SOC(t) < SOC_H \\ \beta P_{FC}(t) & SOC(t) \geq SOC_H \end{cases} \quad (2.22)$$

Where  $\alpha$  and  $\beta$  are constant parameters,  $SOC_L$  and  $SOC_H$  are the minimum and maximum SOC values.

Through the objective function, the fuel cell power range, current changing rate and power changing rate are constrained to smooth the fuel cell power and current to increase the durability of fuel cell. This method is also used in the rule based strategy of [69, 67] through minimizing the fuel cell power demand transitions.

Regarding the ability to stand dynamical power variation, supercapacitor is higher than battery and battery is higher than fuel cell. Therefore frequency based strategy decomposes the power demand into low frequency power, medium frequency power and high frequency power, which are supplied by fuel cell, battery and supercapacitor respectively in Figure 2.18 [80]. This method also belongs to the limitation on fuel cell power variation.

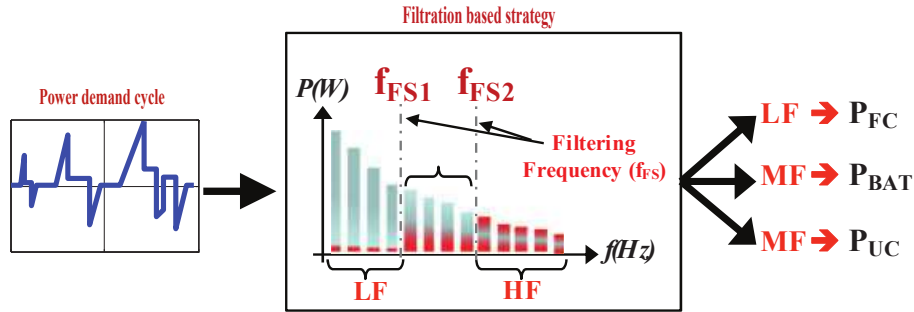


Figure 2.18: Frequency decomposing technique for frequency based strategy [82]

#### 2.4.5.2 Durability of battery

Battery is widely chosen as the main energy storage source and its durability is important. Quantifying battery lifetime and taking it as the part of the objective function is a good method to prolong the durability of battery. A lifetime model built for the EMS of FCHEV is introduced in this section

In [92] and [93], a battery degradation model is built according to the Ah-throughput technique and Arrhenius time-temperature reaction rates in equation (2.23)

$$\delta_b(I_b, DOD, \theta_b, k) = \delta_b^l + \delta_b^\theta \quad (2.23)$$

Both partial degradation rate  $\delta_b^l$  and  $\delta_b^\theta$  are modelled in equation (2.24) and (2.25)

$$\delta_b^l(I_b, DOD, k) = \frac{\sum_{k=t_0}^{t_f} (I_b(k) \phi(DOD, k) \Delta t)}{k_{max}} \quad (2.24)$$

$$\delta_b^\theta(DOD, \theta_b, k) = \frac{\sum_{k=t_0}^{t_f} \left( A e^{\frac{-E_a}{R(\theta_b(k) - \theta_{b,ref})}} \phi(DOD, k) \Delta t \right)}{\lambda_b} \quad (2.25)$$

where  $I_b$  is discharge current of battery, DOD is depth of discharge,  $k$  and  $k_{max}$  are battery lifetime recoverable energy values for instantaneous and optimal conditions,  $\phi(DOD, k)$  is the discharge level stress factor,  $\Delta t$  is sample time,  $A$  exponential factor,  $R$  the universal gas constant,  $\theta_b$  and  $\theta_{b,ref}$  are instantaneous and reference values for electrolyte temperature,  $\lambda_b$  is a battery lifetime estimate.

The discharge level stress factor  $\phi(DOD, k)$  is defined in equation (2.26) according to the discharge level of battery based on the battery life-cycle data shown in Figure 2.19

$$\phi(DOD, k) = 1 + \frac{k_{max} - k(DOD, k)}{k_{max}} \quad (2.26)$$

$$k(DOD, k) = C_\delta(k) \times DOD(k) \times n_{cycles}(DOD) \quad (2.27)$$

$$k_{max} = \max(k(DOD, k)) \quad (2.28)$$

where  $n_{cycles}$  is the number of cycles achievable at a given DOD level.

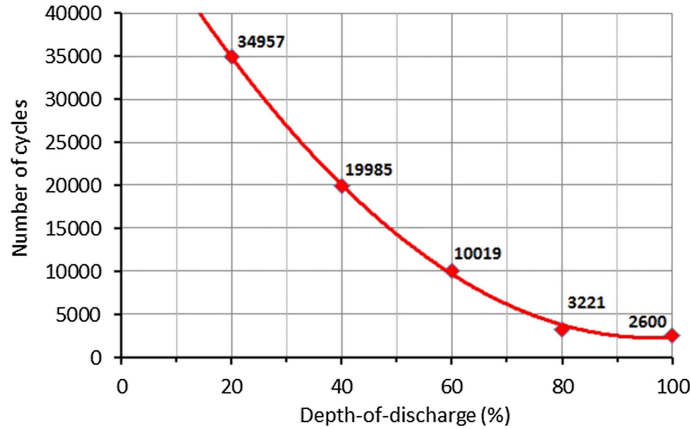


Figure 2.19: Lithium-ion battery experimental lifecycle according to DOD [93]

According to the above equations, the degradation degree of battery capacity is calculated in equation (2.29).

$$C_\delta(k) = C_b(k) - (C_{nom} (1 - EOL_b) \delta_b(k)) \quad (2.29)$$

where  $C_b$  is battery instantaneous capacity at sampling time  $k$ ,  $C_{nom}$  is nominal capacity of battery,  $EOL_b$  is the battery 80% capacity end of lifetime condition.

In[113], rain flow counting method is taken as another method to define the battery lifetime through counting the number of cycles for different DOD levels and the losses of battery lifetime, which is defined in equation (2.30).

$$LOL = \sum_{DOD_{min}}^{DOD_{max}} \frac{N_{cyc}(DOD)}{N_{ctf}(DOD)} \quad (2.30)$$

where  $N_{cyc}$  is the number of cycles,  $N_{ctf}$  is the maximum number of cycles as cycle to failure in datasheet of the battery.

#### 2.4.6 Economy objective

The economic criteria for FCHEV involves many factors like the construction cost, hydrogen consumption cost, electric consumption cost, replacement cost, maintenance cost and lifetime cost. It is particularly important to assess the cost of fuel cell and energy storage sources per unit energy consumed over their lifetime. Optimization based strategy is the best method to fulfill this objective.

[155] minimizes the economical cost including hydrogen consumption, the cost of fuel cell stack and the battery cost in equation (2.31)

$$F = \frac{c_h}{C_h} \int_{t_0}^{t_f} P_h(t) dt + c_{be}n + c_{fcsbe}S_{fcs} \quad (2.31)$$

where  $c_h$  hydrogen price per gram (0.00444€/g),  $C_h$  the lower heating value of hydrogen (120000J/g),  $c_{be}$  the equivalent cost of the battery and  $c_{fcsbe}$  the cycle normalized cost of fuel cell are defined in equation (2.32)

$$c_{be} = 1.075c_b E_{cb} \frac{L_d}{S} \quad (2.32)$$

$$c_{fcsbe} = 1.075c_{fcs} P_{max,fcsb} \frac{L_d}{S} \quad (2.33)$$

where  $c_b$  is the battery price per kilowatt hour (900€/kWh),  $c_{fcs}$  is the fuel cell system price per kilowatt (34.78€/kW),  $E_{cb}$  the nominal cell energy in kilowatt hour,  $L_d$  and  $S$  are the length of drive cycle and total bus mileage in kilometre.

In [94], the life-cycle cost of the fuel cell system ( $\gamma_{sl-fc}$ ) is 0.01\$/kWh, which is determined by the current production cost 50\$/kW for volume manufacturing of 500000 units per year and 5000h service life hour for automotive fuel cells. The hydrogen cost ( $\gamma_{fc}$ ) is 0.81\$/kWh. The battery life cycle cost ( $\gamma_{bt}$ ) is 0.6 \$/kW. The final cost objective is defined as the equation (2.34). The simulation results of the designed energy management strategy using a weighted improved dynamic programming for FUDS drive cycle is shown in Figure 2.20. The comparative results of improved dynamic programming and rule based strategy are shown in Table 2.1. The energy management strategy developed by improved dynamic programming not only can make sure the normal operation of the vehicle but also has lower costs and hydrogen consumption levels compared to rule based strategy.

$$C = \sum_{t=1}^T ((\gamma_{fc} + \gamma_{sl-fc}) P_{fc}(t) + \gamma_{bt} P_{bt}(t)) \Delta t \quad (2.34)$$

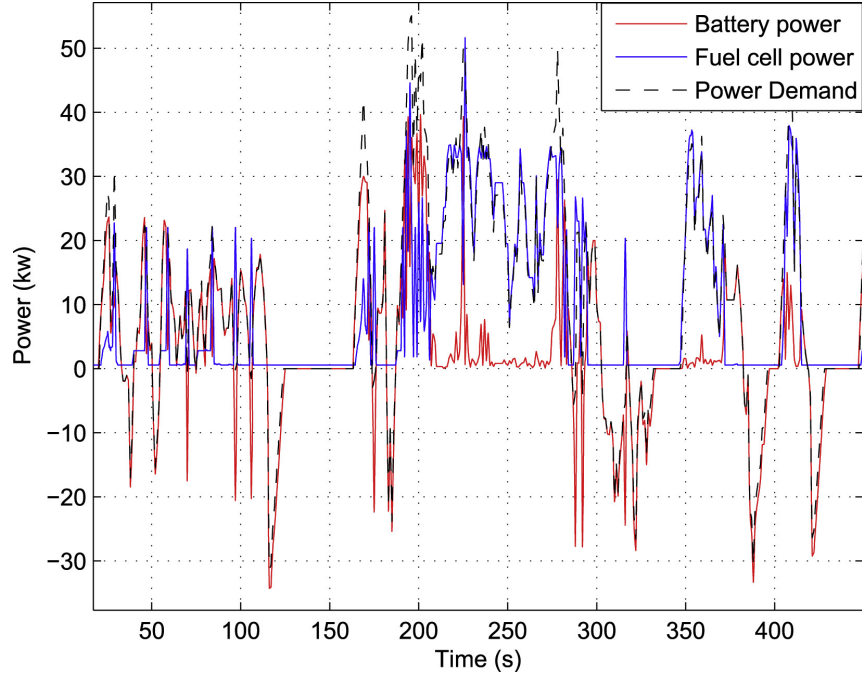


Figure 2.20: FUDS cycle-sprinter power allocation of the sources[94]

Table 2.1: Highway/FUDS driving cycle comparative results

	Highway		FUDS	
	Improved dynamic programming	Rule based strategy	Improved dynamic programming	Rule based strategy
Operational cost (\$)	2.7	3.2	1	2.2
H2 consumption (g)	179	211	65.2	143
Runtime (s)	10	3	14	3

where  $P_{fc}$  is fuel cell power,  $P_{bt}$  is battery power.

In [93], the objective function is defined as the equation (2.35), which is the summed monetary cost of each decision relative to each state variable. These monetary expenses for each decision are hydrogen consumption cost, fuel cell lifetime cost, battery lifetime cost and grid-based recharge cost.

$$C = \sum_{k=0}^N \left( C_{H2}(x_{H2}, u, k) + C_{\delta_b}(x_{\delta_b, k}) + C_{\delta_{fc}}(x_{\delta_{fc}}, u, k) \right) + C_{Qe}(x_{Qe, N})$$

$$\begin{cases} C_{H2}(x_{H2}, u, k) &= \left[ x_{H2}(k) + \sum_{i=0}^M \dot{m}_{H2} \Delta t \right] \alpha_{H2} \\ C_{\delta_b}(x_{\delta_b}, k) &= \left[ x_{\delta_b}(k) + \sum_{i=0}^M \delta_b \Delta t \right] \alpha_b \\ C_{\delta_{fc}}(x_{\delta_{fc}}, u, k) &= \left[ x_{\delta_{fc}}(k) + \sum_{i=0}^M \delta_{fc} \Delta t \right] \alpha_{fc} \\ C_{Qe}(x_{Qe}) &= x_{Qe}(N) \alpha_{Qe} \end{cases} \quad (2.35)$$

where the subscript  $H2$  is hydrogen consumption,  $\delta_b$  battery degradation,  $\delta_{fc}$  fuel cell degradation,  $Qe$  remaining battery charge,  $x$  are state variables for each consumable

$H_2$ ,  $\delta_b$ ,  $\delta_{fc}$  and  $Q_e$ .  $u$  is the control variable at step,  $K$  representing the power demand to the PEMFC,  $\alpha$  is a economical weight and the cost values are 2.88\$/kg, 500\$/kWh, 0.11\$/kWh and 55\$/kW for  $\alpha_{H_2}$ ,  $\alpha_b$ ,  $\alpha_{Q_e}$  and  $\alpha_{fc}$ . Similar to [93], the objective function of [92] includes hydrogen consumption cost, battery lifetime cost and public grid recharge cost of the battery pack.

In [91], the objective function includes the hydrogen consumption cost and the degradation cost of fuel cell in equation (2.36). The voltage degradation rate under different operating conditions is quantified.

$$C_{total} = -\left(H_{fc}V_{fuel} + D_{fc}V_{fc} + \alpha C_v\right) \quad (2.36)$$

where  $H_{fc}$  fuel cell hydrogen consumption,  $V_{fuel}$  hydrogen cost (2.88\$/kg),  $D_{fc}$  fuel cell degradation rate,  $V_{fc}$  fuel cell cost (47.97\$/kW),  $\alpha$  is high penalty cost,  $C_v$  is battery voltage constrain function to avoid the over discharge and overcharge, which is in equation (2.37)

$$C_v = \begin{cases} \int (V_{min} - V_{bat}) dt, & \text{if } V_{bat} < V_{min} \\ \int (V_{bat} - V_{max}) dt, & \text{if } V_{bat} > V_{max} \\ 0 & \text{otherwise} \end{cases} \quad (2.37)$$

In [86], the economic objective is defined as the energy cost from fuel cell and battery in equation (2.38)

$$J = \sum_{t=1}^T (C_1 P_{FCa}(t) + C_2 P_{FCb}(t) + C_3 P_{FCc}(t) + C_{BT} P_{BT}(t)) f(t) \quad (2.38)$$

where  $P_{FCa}$ ,  $P_{FCb}$  and  $P_{FCc}$  are fuel cell power for three parts,  $P_{BT}$  battery power,  $C_1$ ,  $C_2$ ,  $C_3$ , and  $C_4$  are corresponding cost.

#### 2.4.7 Multiple objectives

The power splitting problem for the fuel cell hybrid electric vehicles needs to achieve several objectives at the same time. If just one objective as presented objectives is considered, the optimal solution for this objective means the "sacrifice" of other objectives. Multiple objectives which are achieved simultaneously in order to get optimal results are increasing the attention of researchers. As an example: Minimizing hydrogen consumption and increasing the lifetime of fuel cell and energy storage sources are hoped to reduce the commercial cost of the vehicle. Solving a single objective function by using the presented method is easily achievable but using multiple objectives, a set of possible solutions are found and these solutions are conflicting for different objectives. The most straightforward method to solve multiple objective problems is to weigh each object and add them up as the objective function (2.39) of [64]

$$J = W_1 \int \frac{mpgge}{mpgge} + W_2 \int \frac{mpg}{mpg} + W_3 eff_{fc} + W_4 eff_{es} + W_5 \overline{\Delta SOC} - W_6 \left| \frac{\Delta V}{\Delta V} \right| \quad (2.39)$$

where  $W_1 \cdots W_6$  are the weighting factors of corresponding objective functions,  $mpg$  (mile per gallon) and  $mpgge$  (mile per gallon gasoline equivalent) representing fuel economy parameters,  $eff_{fcs}$  and  $eff_{es}$  are the average efficiency of the fuel cell stack and battery respectively,  $\overline{\Delta SOC}$  the difference between final battery SOC and initial value,  $\Delta V$  is the difference of required and achieved speed,  $\overline{mpgge}$ ,  $\overline{mpg}$  and  $\overline{\Delta V}$  are target values.

The importance of each objective is decided by corresponding weighting factors. For equation (2.39), minimizing fuel consumption is chosen as the main target. Other objects like  $eff_{fcs}$ ,  $eff_{es}$ ,  $\overline{\Delta SOC}$  and  $\Delta V$  are set with low weights in the fitness function.

In [102], the particle swarm optimization is used to optimize the power control limits of fuel cell and battery for rule based strategy. Its objective function is a combination of two terms: the hydrogen consumption and battery charge sustenance in equation (2.40)

$$J = m_{H_2} + K |SOC_{t_i} - SOC_{t_f}| \quad (2.40)$$

Where  $m_{H_2}$  hydrogen consumption rate,  $SOC_{t_i}$  battery initial value,  $SOC_{t_f}$  battery final value,  $K$  weighting coefficient.

In [59], the method of adding relevant weighting coefficient into different objective is not used. Its two objectives are defined in equation (2.41): the first one is total hydrogen consumption over the driving cycle and the second one is the average absolute power of the battery to minimize the battery contribution through letting the supercapacitor supply most of the transient power.

$$\begin{aligned} J_1 &= \int_0^{t_f} m_{H_2} dt \\ J_2 &= \frac{1}{t_f} \int_0^{t_f} |P_{ba}(t)| dt \end{aligned} \quad (2.41)$$

where  $t_f$  is duration time of drive cycle,  $P_{ba}$  is battery power.

Regarding these two objectives, there are a set of solutions called non-dominated solutions or Pareto front. These solutions are compared according to whether one dominates the other or not. If the following two conditions are filled, it proves that the solution X1 dominates solution X2. Two conditions are: X1 is no worse than X2 in all the objectives and X1 is strictly better than X2 in at least one objective. PI controller is firstly designed as the energy management strategy of the vehicle to control the battery and supercapacitor states around the constant references. Non-dominated Sorting Genetic Algorithm  $\Pi$  is used to optimize the control parameters of PID controller. Optimization results of EMS and experimental evaluation of the power management strategy over Manhattan drive cycle are shown in Figure 2.21 and Figure 2.22 respectively.

The standard optimization problem can be converted into an unconstrained optimization problem through penalty functions like [117]. In order to reduce the hydrogen consumption and increase the durability of battery and fuel cell, an optimization problem with constraints is defined in equation (2.42), which can be transformed into an unconstrained multiple objectives problem as (2.43)

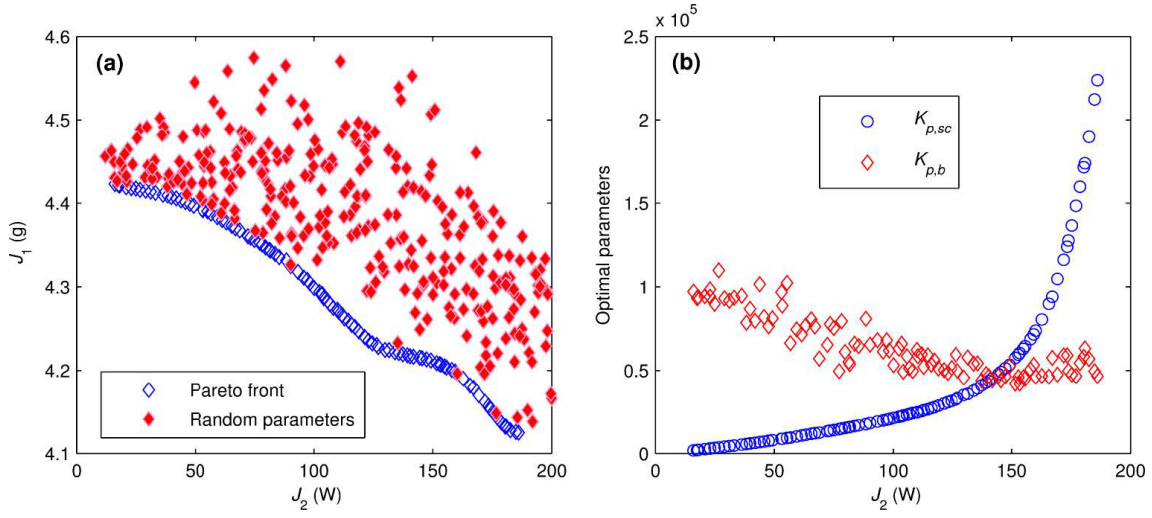


Figure 2.21: Optimization results of EMS [59]. (a) Comparison between the Pareto front and the performance of randomly tuned parameters; (b) Optimal strategy parameters for the Pareto front

$$\min J = \sum_{k=0}^{N-1} (\dot{m}_{H_2}(u(k)) \Delta T)$$

$$s.t. \begin{cases} V_{lowerbat} \leq V_{bat}(k) \leq V_{upperbat} \\ I_{lowerbat} \leq I_{bat}(k) \leq I_{upperbat} \\ V_{lowerfc} \leq V_{fc}(k) \leq V_{upperfc} \\ SOC(N) = SOC_{tg} \\ |\Delta u(k)| \leq \Delta P_{fc} \end{cases} \quad (2.42)$$

$$\min J = \sum_{k=0}^{N-1} \left( \dot{m}_{H_2}(u(k)) \Delta T + L_1(k) + L_2(k) + P_1 (\Delta u(k) - \Delta P_{fc})^2 \right) + P_2 (SOC(N) - SOC_{tg})^2 \quad (2.43)$$

where

$$\begin{cases} L_1(k) = R_1 (V_{bat}(k) - V_{upperbat})^2 + R_2 (V_{bat}(k) - V_{lowerbat})^2 \\ \quad + R_3 (I_{bat}(k) - V_{maxdis})^2 + R_4 (I_{bat}(k) - V_{maxchg})^2 \\ L_2(k) = Q_1 (V_{fc}(k) - V_{upperfc})^2 + Q_2 (V_{fc}(k) - V_{lowerfc})^2 \\ \Delta u(k) = u(k) - u(k-1) \\ \Delta u(0) = 0 \end{cases} \quad k \geq 1 \quad (2.44)$$

where  $\dot{m}_{H_2}$  is hydrogen consumption,  $V_{bat}$ ,  $I_{bat}$ ,  $SOC$ ,  $\Delta P_{fc}$  and  $V_{fc}$  are battery voltage, battery current, battery SOC, fuel cell dynamical change rate and fuel cell power respectively,  $Q_1$ ,  $Q_2$ ,  $R_i$ ,  $i = 1 - 4$  are weight coefficients.

In [118], the whole equivalent hydrogen consumption is set as the objective and the constraints of fuel cell power range, battery SOC range, and fuel cell dynamical change rate are transformed into parts of the objective function in equation (2.45).

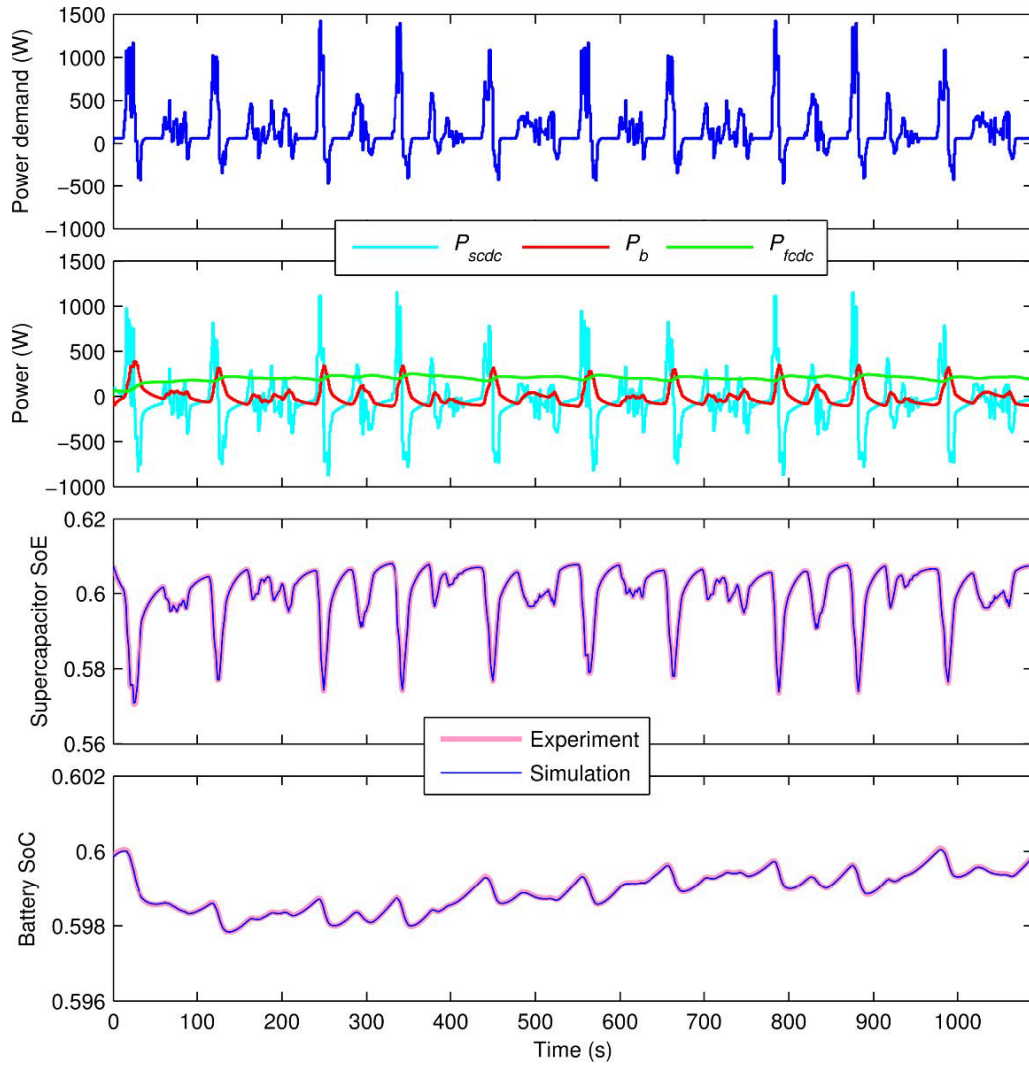


Figure 2.22: Experimental evaluation of the power management strategy over Manhattan drive cycle [59]

$$\begin{aligned}
 \min J' &= \min J + \frac{s}{2} \sum_{i=1}^6 \int_{t_0}^{t_f} g_i(P_{bat}(t), soc(t), t) h(g_i) dt \\
 &\begin{cases}
 g_1(t) = \frac{P_{load}(t) - P_{bat}(t)}{\eta_{dc}} - P_{fc,min}(t) \geq 0 \\
 g_2(t) = P_{fc,max}(t) - \frac{P_{load}(t) - P_{bat}(t)}{\eta_{dc}} \geq 0 \\
 g_3(t) = soc(t) - soc_{min} \geq 0 \\
 g_4(t) = soc_{max} - soc(t) \geq 0 \\
 g_5(t) = \frac{d}{dt} \frac{P_{load}(t) - P_{bat}(t)}{\eta_{dc}} - \Delta P_{fc,decrease} \geq 0 \\
 g_6(t) = \Delta P_{fc,increase} - \frac{d}{dt} \frac{P_{load}(t) - P_{bat}(t)}{\eta_{dc}} \geq 0
 \end{cases} \quad (2.45)
 \end{aligned}$$

## 2.5 Analysis of objectives and EMS

### 2.5.1 Analysis of objectives

A summary of energy management strategies for different objectives is listed as Table 2.2

Table 2.2: EMS for different objectives

Number	Power sources	Strategy	Objective	Method
[72]	FC/BA	Fuzzy rule based strategy	Stability objective	Degradation and failure of fuel cell
[67]	FC/SC	Operating mode control	Stability objective	Phase failure of five-phase permanent magnetic synchronous machines
[141]	FC/BA	Pontryagin's Minim Principle	Stability objective	Variational battery temperature
[139]	FC/BA /SC	Fuzzy rule based strategy	Stability objective	Failure of fuel cell and supercapacitor
[142]	FC/BA /SC	Equivalent consumption minimization strategy	Stability objective	Fuel cell degradation
[149]	FC/SC	Equivalent consumption minimization strategy	Fuel consumption	Objectives: Quantified whole hydrogen consumption
[73]	FC/BA	Pontryagin's Minim Principle	Fuel consumption	Objectives: Quantified hydrogen consumption
[109]	FC/SC	Equivalent consumption minimization strategy	Fuel consumption	Objectives: Quantified whole hydrogen consumption
[118]	FC/BA	Pontryagin's Minim Principle	Fuel consumption	Objectives: Quantified whole hydrogen consumption
[122]	FC/BA	Pontryagin's Minim Principle	Fuel consumption	Objectives: Quantified hydrogen consumption
[145]	FC/BA	Adaptive Pontryagin's Minim Principle	Fuel consumption	Objectives: Quantified hydrogen consumption

Number	Power sources	Strategy	Objective	Method
[156]	FC/BA	Equivalent consumption minimization strategy	Fuel consumption	Objectives: Quantified whole hydrogen consumption
[113]	FC/BA	Equivalent consumption minimization strategy	Fuel consumption	Objectives: Quantified whole hydrogen consumption
[157]	FC/BA	Equivalent consumption minimization strategy	Fuel consumption	Objectives: Quantified whole hydrogen consumption
[110]	FC/BA /SC	Equivalent consumption minimization strategy	Fuel consumption	Objectives: Quantified whole hydrogen consumption
[102]	FC/BA	Particle swarm optimization	Fuel consumption, Charge sustenance	Objectives: Quantified hydrogen consumption, charge sustenance
[133]	FC/SC	Pontryagin's Minim Principle	Fuel consumption, Charge sustenance	Objectives: Quantified hydrogen consumption, Constraints: Charge sustenance
[137]	FC/BA	Equivalent consumption minimization strategy	Fuel consumption, Charge sustenance	Objectives: Quantified whole hydrogen consumption
[119]	FC/BA	Pontryagin's Minim Principle	Fuel consumption, Charge sustenance	Objectives: Quantified hydrogen consumption, Constraints: charge sustenance
[87]	FC/SC	Linear programming	Fuel consumption, Charge sustenance	Objectives: Quantified hydrogen consumption, Constraints: Charge sustenance
[68]	FC/BA	Stiffness coefficient model	Fuel consumption, Charge sustenance	Seeking for maximum efficiency penalty coefficient
[64]	FC/BA	Genetic algorithm	Fuel consumption, Charge sustenance	Objectives : minimize hydrogen consumption, average efficiency of the FC and BA, battery charge sustaining , difference of required and achieved speed

Number	Power sources	Strategy	Objective	Method
[94]	FC/BA	Improved dynamic programming	Economical objective	Objectives: hydrogen consumption cost , life cycle cost of fuel cell and battery cost
[93]	plug-in FC/BA	Discrete dynamic programming	Economical objective	Objectives: hydrogen consumption cost , fuel cell degradation cost, battery degradation cost and battery charge cost from grid
[92]	plug-in FC/BA	Discrete dynamic programming	Economical objective	Objectives: hydrogen consumption cost, battery lifetime cost and public grid recharge cost
[158]	FC/BA	Discrete dynamic programming	Economical objective	Objectives: hydrogen consumption cost, electric cost
[91]	FC/BA	Stochastic dynamic programming	Economical objective	Objectives: hydrogen consumption cost , degradation cost of fuel cell battery voltage constraint
[155]	FC/BA	The convex optimization algorithm	Economical objective	Objectives Minimum the hydrogen cost, the FCS cost, and the battery cost
[86]	FC/BA	Linear programming	Economical objective	Objectives: hydrogen consumption cost, battery lifetime cost
[154]	FC/SC	Pontryagin's Minim Principle	Fuel consumption, Durability of fuel cell	Objectives: Quantified hydrogen consumption, reduing dynamic of fuel cell
[116]	FC/BA	Pontryagin's Minim Principle	Fuel consumption, Durability of fuel cell	Objectives: Quantified hydrogen consumption reduing dynamic of fuel cell
[127]	FC/SC	Model predictive control	Fuel consumption, Durability of fuel cell	Objectives: Quantified hydrogen consumption, Constraints: dynamical rate
[80]	FC/BA /SC	Frequency based strategy	Durability of fuel cell Durability of battery	Frequency split
[83]	FC/BA /SC	Frequency based strategy	Durability of fuel cell Durability of battery	Frequency split

Number	Power sources	Strategy	Objective	Method
[81]	FC/BA	Frequency based strategy	Durability of fuel cell	Frequency split
[79]	FC/BA	Frequency based strategy	Durability of fuel cell	Frequency split
[78]	FC/BA /SC	Frequency based strategy	Durability of fuel cell, Durability of battery	Frequency split
[82]	FC/BA /SC	Frequency based strategy	Durability of fuel cell, Durability of battery	Frequency split
[117]	Plug-in FC/BA	Operating mode control	Fuel consumption, Durability of fuel cell, Charge sustenance	Objectives: Quantified hydrogen consumption, reducing dynamic of fuel cell, charge sustenance
[135]	FC/BA /SC	Dynamical programming	Fuel consumption, Charge sustenance, Durability of fuel cell	Objectives: Quantified hydrogen consumption, Charge sustenance, on/off frequency

The objective of drive ability and charge sustenance as the basic requirement for EMS of FCHEV are not fully listed in the table. Charge sustenance is listed only in the reference articles that meet it through taking it as one part of objective functions and is not required by Plug-in FCHEV. Monitoring the health and performance of drive-train components especially power sources is important for FCHEV. From Table 2.2, it can be observed that even though the objective of stability is important, it is rarely studied. NASA's Mars Global Surveyor stopped operating due to the battery overheating which led to the loss of capacity. The AFRL ARGOS satellite, the Viking 2 Mars Lander and Boeing Dream-liner aircraft also suffered battery failures [159]. Fuel cell cannot stand high dynamical power and has more strict requirements on temperature, air quality and humidity of hydrogen and air. Compared to other components of drive train, fuel cell is easier to occur degradation and failure. In that case, how to keep the stability of EMS under the conditions of performance decrease and even failure is especially important. It needs to pay more attention by researchers.

Fuel consumption is mostly studied both in single objective and multiple objective studies. Hydrogen consumption is easily quantified through relevant functions. Limiting fuel cell to operate at high efficiency and seek for maximum efficiency point is also taken as the method to minimize hydrogen consumption. The precision of the fuel cell efficiency map decides the final hydrogen consumption result. Electric consumption is often transformed into the equivalent hydrogen consumption through equivalent factor and is added to the hydrogen consumption to get the whole hydrogen consumption which is taken as

the objective function. Electric consumption is not taken as the objective alone. The equivalent factor is affected by the drive train of the vehicle, drive cycle, SOC of energy storage sources and health state of power sources, which should be paid more attention.

Reducing the dynamical variation of fuel cell is widely used to increase its durability. Quantifying fuel cell degradation for every operation is difficult due to its complicate degradation mechanism. Dividing operation into four typical operation cycles: load changing cycles, start–stop cycles, idling time and high power load driving conditions and defining their degradation rate based on the real operation data of vehicle is the only way to do that. Durability of battery is only studied in few papers through quantified function. The degradation process of battery is complicated and many factors affect its lifetime.

Cost reduction as well as the hydrogen infrastructure extension are the most important tasks to widely commercial usage of FCHEV[160]. Hydrogen consumption cost, fuel cell lifetime cost and battery lifetime cost are the main factors that could be considered in the design of EMS. The electric cost from the public grid is also considered for Plug-in FCHEV. When the lifetime cost of fuel cell and battery is determined, the degradation rate of power sources should be quantified which is similar to the objective of durability.

When an EMS is designed, several objectives are sought at the same time and, in general, parts of them are contradictory[161]. As an example: decreasing hydrogen consumption and increasing durability of fuel cell cannot be maximized both at the same time. Compromising multiple objectives in the EMS is a typical solution. The above presented objectives can be fulfilled with two methods weighted sum method and constraint method. Through the weighted sum method, multiple objectives are weighted and are summed up into an aggregated objective function by multiplying each objective function by a weighting factor[162]. Constraint method directly sets limitations on control parameters of rule based strategy and constraints in optimization functions to reach corresponding objectives like limiting fuel cell dynamical change rate to increase fuel cell durability. The constraint method also can be transformed into weighted sum method by transmitting it into part of the objective function.

### 2.5.2 Analysis of EMS for different objectives

Deterministic rule based strategy belongs to the supervisory strategy. Some variables (mostly state of charge of energy storage sources and load power demand) are chosen as the judgment criteria and according to different input values, the reference powers of fuel cell and energy storage sources are calculated. Quantified objectives like fuel consumption and durability of power sources are hardly used into deterministic rule based strategy. Restricting the fuel cell to operating in high efficiency zone and limiting its dynamical change rate can be used to decrease the hydrogen consumption and increase its durability. The control rules are designed according to experience and it is simple and easily applicable in reality. But optimal results and other objectives are hardly reached, that is also why it is widely used in real vehicles but is rarely studied in recent research. The control parameters of deterministic rule based strategy could be optimized through optimization algorithms like genetic algorithm and particle swarm optimization to get optimal results. All the objectives that can be filled through optimization based strategy can be fulfilled in this way.

Fuzzy rule based strategy is similar to deterministic rule based strategy and the specific values of control variables are just transformed into membership functions. Quantified

objective function method is difficult being applied to fuzzy rule based strategy. Considering more inputs and outputs into the fuzzy controller to describe whole control system more precisely, constraining operation of power sources according to their physical properties, optimization by other optimal control strategy and cooperation with other intelligent control strategies to increase its robustness and adaptability are the research trends of fuzzy rule based strategy. These methods will increase the complexity of the control system and limit their application on real vehicles, which should be taken into account in the process of designing new fuzzy rule based strategy.

Frequency based strategy decomposes power demand into different frequent powers, which is supplied by different power sources. It is particularly suitable for fuel cell hybrid electric vehicle. Frequency based strategy plays important role in the objective of the durability of power sources, but it is difficult to fulfill other objectives like charge sustenance of energy storage sources and reducing the fuel consumption. The decision for decomposition depth is also arbitrary. Cooperation with other control strategies to overcome these shortcomings is the trend of frequency based strategy.

Regarding optimization based strategy, all the objectives could be achieved through two ways. The first one is quantifying these objectives and adding them as part of the objective function to achieve their aims, like quantified hydrogen consumption and durability of power sources. The second one is setting constraints on physical properties of power sources into optimization function, like charge sustenance of energy storage sources and fuel cell dynamical change rate. local optimization based strategy can fulfill these objectives like global optimization based strategy and the only difference is it just transforms whole drive cycle optimization situation into instant optimization.

## 2.6 Conclusion and suggestion

When the architecture and power-train of FCHEV are decided, an EMS is needed to ensure the normal operation of the vehicle and guide the energy distribution among power sources. Characteristics of fuel cell and energy storage sources are analyzed to let EMS ensure their operation, increase their lifetime and play their full potential. Energy management strategies of FCHEV are summarized and categorized to analyze the characteristic of every kind of EMS. Through the category and summarization of energy management strategies, the objectives and corresponding methods to fulfill these objectives are summarized. These methods also depend on the kind of energy management strategies. The category of EMS and summarization of objectives can supply good guidance to design EMS for FCHEV. Based on the review of different kinds of EMSs, objectives and methods, following suggestion for EMS of FCHEV are put forward:

- 1) Equivalent consumption minimization strategy and Pontryagin's Minim Principle are mostly used in relevant research and they have the potential to reach commercial applications. The new design energy management strategies that are tested on a test bench or a real vehicle account a small proportion, so experimental validation of EMS should be strengthened.

- 2) The objective of stability is rarely studied, but it is crucial to FCHEV. Special external factors like weather, temperature, region and altitude and insider factors of vehicle components like battery temperature and degradation of power sources which directly affect the performance of components of drive-train, should be considered into EMS. Fault

diagnosis and fault tolerance control of components are also important as part of EMS.

3) Increasing the durability of power sources is an important objective. The precision of quantified degradation function used in the EMS should be increased. Quantifying power sources degradation relies on the continuous research on its degradation mechanism.

4) The economy should consider the cost changes of fuel and power source in the future due to the improvement of technology.

5) Single objective is hard to meet the development of FCHEV, multi-objective are sought simultaneously and the optimization algorithms to solve it is increasing the interest of researchers.

# Energy consumption minimization strategy

## 3.1 Introduction

As concluded in the last chapter, equivalent consumption minimization strategy as a kind of local optimization strategy doesn't rely on the knowledge of drive cycle and can reach optimal results at every sampling time, which is chosen as the energy management strategy of FCHEV in the dissertation. Low energy density of supercapacitor lets its equivalent hydrogen consumption be taken as zero for much research on equivalent consumption minimization strategy. This simplification leads to suboptimal fuel economy and increases the complexity of the control system. A sequential quadratic programming (SQP) based Equivalent Consumption Minimization Strategy (ECMS) (SECMS) is proposed in this section to consider the energy cost of all three power sources into the objective function. A rule based strategy is designed as a benchmark for SECMS. In order to prove that neglecting supercapacitor equivalent hydrogen consumption in ECMS objective function cannot reach the optimal result for three power sources power train, a Hybrid ECMS Operating mode control strategy (OMCS) (HEOS) is also designed. In order to validate the built energy management strategy, the vehicle model including main components is built firstly with software Matlab/Simulink.

This chapter is organized as follows: section two gives the vehicle architecture and the model of power train components including fuel cell, battery, supercapacitor and DC/DC converters. In the third section, SECMS, rule based control strategy and HEOS are explained. In the fourth part, the simulation results are compared for different control strategies. Finally, conclusions are drawn.

## 3.2 Power train architecture and component modes

### 3.2.1 Power train architecture

The series architecture is chosen for FCHEV, as shown in Figure 3.1. Proton Exchange Membrane Fuel Cell (PEMFC) is the main energy source to supply steady state power and is connected to the DC bus via a unidirectional DC/DC power converter. Battery as the main energy storage source is directly connected to DC bus to hold the bus voltage. Supercapacitor as a peak power supplier is connected to the DC bus through a bidirectional

DC/DC power converter. The DC energy supplied by three power sources is converted into AC energy through DC/AC inverter to drive the AC motor and further to propel the vehicle. AC motor also can work as a generator to recycle braking energy of the vehicle.

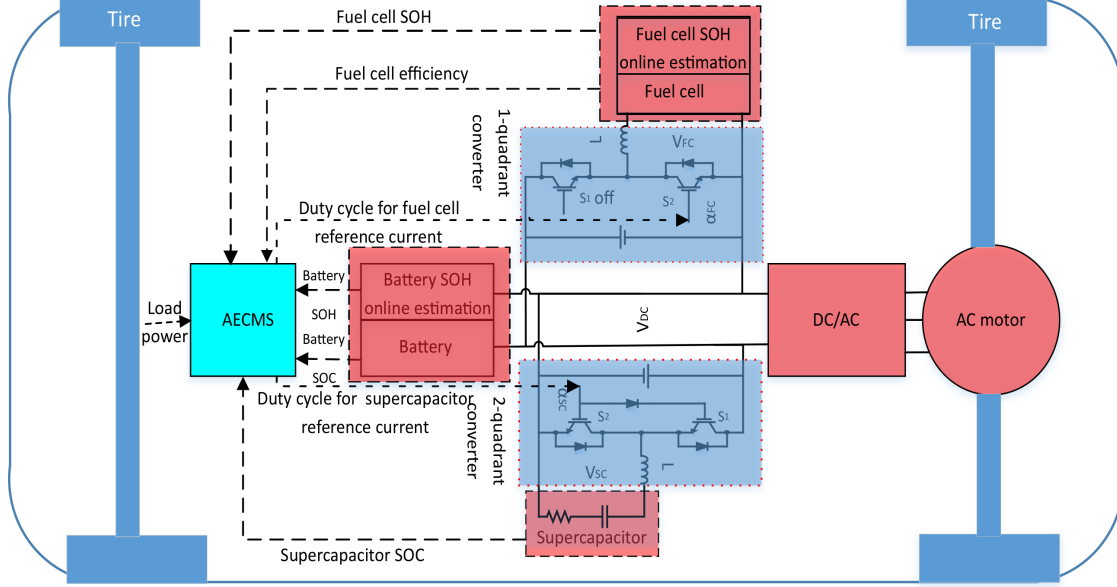


Figure 3.1: Powertrain architecture

The power demand of motor to meet the speed requirement of drive cycle can be calculated through dynamic vehicle model. The vehicle can be considered as a mass point and its motion equation can be written in equation (3.1) from the forces shown in Figure 3.2.

$$m_v(t) \frac{d}{dt} v(t) = F_t(t) - (F_a(t) + F_r(t) + F_d(t) + F_g(t)) \quad (3.1)$$

where,  $m_v$  is the mass of the vehicle,  $v(t)$  is the speed of the vehicle,  $F_t$  is the vehicle traction force on the wheel which is equal to the difference between tractive force generated by the power train and the brakes at the wheels,  $F_a$  is the aerodynamic friction,  $F_r$  is the rolling friction,  $F_d$  is the disturbance force that summarizes all other effects and  $F_g$  is the force caused by gravity when driving on slope road.

The reasons that lead to the aerodynamic friction  $F_a$  include the viscous friction of the surrounding air on the vehicle surface and the losses caused by the pressure difference between the front and the rear of the vehicle, generated by a separation of the air flow. The vehicle body, the wheel housings, the exterior mirrors, window housings, even ventilation, and the engine ventilation all can cause the aerodynamic resistance force. Usually, the aerodynamic resistance force is approximated by simplifying the vehicle to be a prismatic body with a frontal area. The force caused by the stagnation pressure is multiplied by an aerodynamic drag coefficient  $C_x$  that models the actual flow conditions. The aerodynamic friction can be calculated in equation (3.2).

$$F_a = \frac{1}{2} \rho A C_x v^2 \quad (3.2)$$

where,  $\rho$  the density of the ambient air,  $A$  the front surface of the vehicle,  $C_x$  the

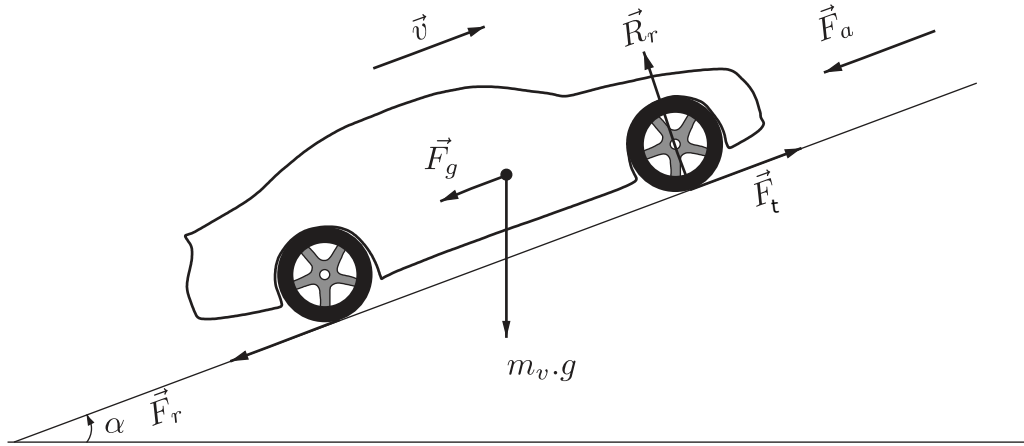


Figure 3.2: Schematic representation of the forces acting on a vehicle in motion

aerodynamic drag coefficient,  $v$  the speed of the vehicle.

The rolling friction  $F_r$  can be calculated through equation (3.3).

$$F_r = m_v C_r g \cos(\alpha) \quad (3.3)$$

where  $m_v$  the vehicle mass,  $g$  gravitational acceleration,  $\alpha$  the angle defining the slope of the road,  $C_r$  the rolling friction coefficient, which is determined by many variables. Vehicle speed, tire pressure and road surface conditions are three important factors to decide the value of  $C_r$ . In most case,  $C_r$  is assumed to be a constant value or an affine function of the vehicle speed. The order of magnitude of  $C_r$  is 0.01–0.03[163].

The grade force  $F_g$  is the horizontal component of the vehicle weight, which opposes (or facilitates) vehicle motion only if the vehicle is moving uphill (or downhill) in equation (3.4):

$$F_g = m_v g \sin(\alpha) \quad (3.4)$$

Through the calculated traction force on the wheel, the power required to drive the vehicle can be calculated in equation (3.5).

$$\begin{aligned} P_{cycle} &= F_t v \\ &= v * \left( m_v(t) \frac{d}{dt} v(t) + F_a(t) + F_r(t) + F_d(t) + F_g(t) \right) \end{aligned} \quad (3.5)$$

where  $P_{cycle}$  the required power at wheel,  $F_t$  traction force on the wheel,  $v$  the speed of the vehicle.

The power demand on the DC bus from the fuel cell, battery and supercapacitor is given in equation (3.6)(3.7).

$$P_{demand} = \frac{P_{cycle}}{\eta_{DC/AC} * \eta_{motor}} \quad (3.6)$$

$$P_{demand} = P_{FC} * \eta_{DCFC} + P_{SC} * \eta_{DCSC} + P_{BA} \quad (3.7)$$

where  $P_{demand}$  is power demand,  $\eta_{DC/AC}$  is converter efficiency of DC/AC connected to motor,  $\eta_{motor}$  is motor efficiency,  $\eta_{DCFC}$  is unidirectional DC/DC converter efficiency connected to fuel cell,  $\eta_{DCSC}$  is bidirectional DC/DC converter efficiency connected to supercapacitor.

The parameters of the vehicle used in the dissertation are shown below:

- Mass ( $m_v$ ): 530 kg;
- Front surface ( $A$ ): 2.56 m<sup>2</sup>;
- Drag coefficient ( $C_x$ ): 0.8;
- Rolling coefficient ( $C_r$ ): 0.02;
- Density of the ambient air ( $\rho$ ): 1.25kg/m<sup>3</sup>;
- Gravity force  $g$ : 9.8m/s<sup>2</sup>.

### 3.2.2 Fuel cell stack model

PEMFC as the main power source for the FCHEV transforms the chemical energy into electrical energy through the reaction between hydrogen and oxygen [164]. The voltage of a single cell of the fuel cell stack is very low (between 0.4 and 1V), far from enough to power a fuel cell hybrid electric vehicle. Therefore PEMFC is built in a stack in order to provide the power with a voltage enabling them to operate at a reasonable current. In general, each cell in the stack has the same geometric structure and material properties. A PEMFC stack can be broken down as shown in Figure 3.3[165].

Fuel cell stack is assembled from multiple cells. The voltage of a stack can be calculated through a simple multiplication of cell numbers and single cell voltage in equation (3.8).

$$E_{stack} = N_{cell} * E_{cell} \quad (3.8)$$

Where  $E_{stack}$  the voltage of fuel cell stack,  $N_{cell}$  the number of cells in the stack,  $E_{cell}$  voltage of single cell.

The electrochemical process within fuel cells is associated with many losses as shown in Figure 3.4. The causes of losses are activation losses, ohmic losses, and concentration losses.

The variation of the individual cell voltage can be calculated from the maximum cell voltage and the various voltage losses in equation (3.9)[166].

$$E_{cell} = E_{rev} - E_{act} - E_{ohm} - E_{con} \quad (3.9)$$

where  $E_{rev}$  is the thermodynamic reversible potential and is also the maximum performance that can be obtained from a fuel cell,  $E_{act}$  the activation losses due to the activation

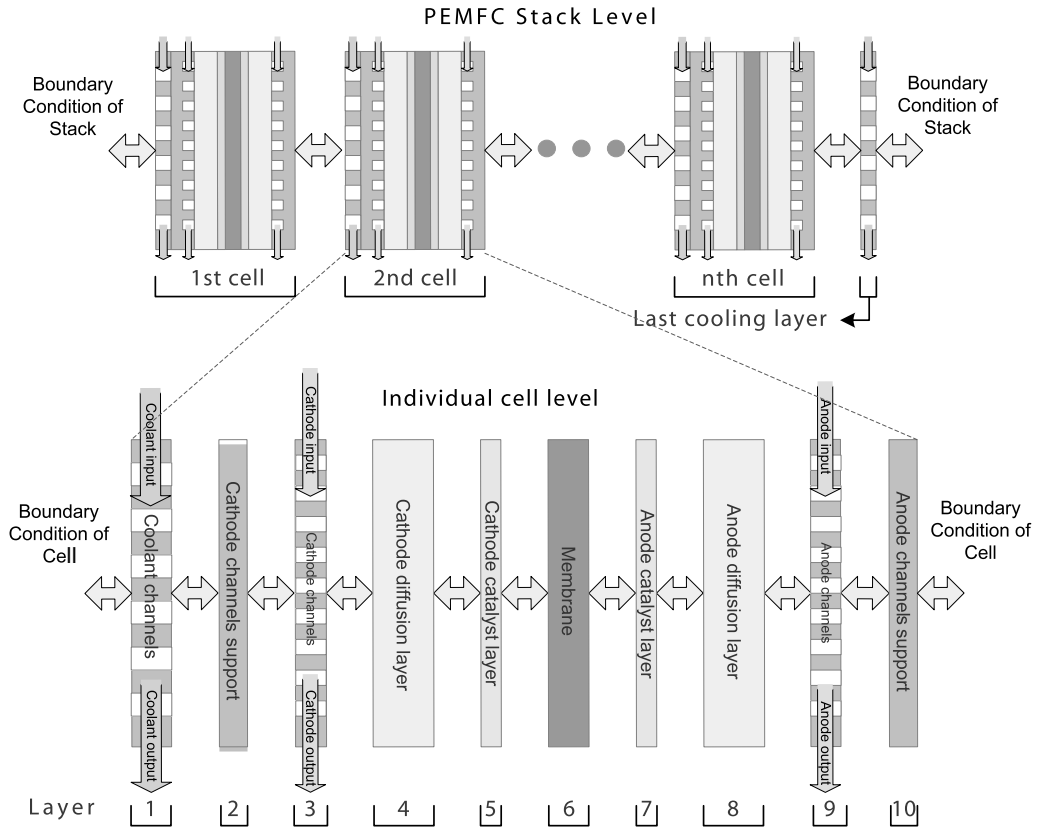


Figure 3.3: Structural and functional decomposition of a fuel cell stack[165]

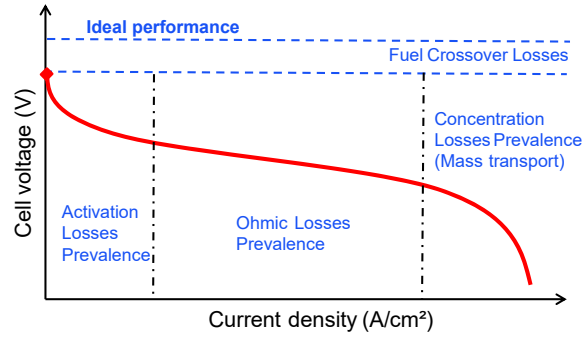


Figure 3.4: Representation of the different losses on the polarization curve[165]

of the anode and cathode,  $E_{ohm}$  the ohmic losses related with the conduction of the protons through the solid electrolyte and electrons through the internal electronic resistances,  $E_{con}$  the concentration losses due to the concentration or mass transportation of the reacting gases[167].

The thermodynamic reversible potential is the voltage that would be obtained if all the Gibbs free energy was converted into electricity without any loss. It can be calculated in equation (3.10) [168].

$$E_{rev} = E_0 - 0.85e^{-3}(T - T_c) + \frac{RT}{2F} \ln(\sqrt{P_{O_2}} P_{H_2}) \quad (3.10)$$

where  $E_0$  is the reversible nearest potential for single cell,  $T$  is the temperature of cell,

$T_c$  is the temperature correction offset,  $P_{O_2}$  and  $P_{H_2}$  are partial pressure of oxygen and hydrogen.

The activation losses  $E_{act}$  are due to the slowness of reactions which are taking place at the surface of the electrodes. A proportion of the voltage generated is lost in driving the chemical reaction that transfers the electrons to or from the electrode. This voltage drop is highly non-linear, as shown in Figure 3.4. However, the reaction of hydrogen oxidation at the anode is very rapid while the reaction of oxygen reduction at the cathode is much slower than hydrogen oxidation. Thus, the voltage drop resulting from activation losses is dominated by the cathode reaction conditions.

The dynamical activation losses  $E_{act}$  can be described in equation (3.11).

$$\frac{dE_{act}}{dt} = \frac{I_{FC}}{C_{dl}} \left( 1 - \frac{E_{act}}{\eta_{act}} \right) \quad (3.11)$$

where  $C_{dl}$  is the single-fuel cell double-layer capacitance.

The cell static activation losses  $\eta_{act}$  can be calculated based on the well-known Butler–Volmer potential equation (3.12).

$$I_{FC} = I_0 S \left( e^{\frac{\alpha n F}{RT} \eta_{act}} - e^{-\frac{(1-\alpha)nF}{RT} \eta_{act}} \right) \quad (3.12)$$

where  $I_{FC}$  fuel cell stack current,  $S$  is the catalyst layer section area,  $n$  is the number of electrons involved in the reaction,  $\alpha$  the symmetry factor, and  $I_0$  the exchange current density.

Equation (3.12) can be simplified in equation (3.13), when  $\eta_{act}$  is large.

$$\eta_{act} = \frac{RT}{n\alpha F} \ln \left( \frac{I_{FC}}{I_0 S} \right) \quad (3.13)$$

The ohmic losses  $E_{ohm}$  due to the electrical resistance of the electrodes, and the resistance to the flow of ions in the electrolyte are the simplest to understand and to model. This voltage drop is proportional to current density and it is linear. The ohmic losses can be obtained through equation (3.14).

$$E_{ohm} = I_{FC} * R_{FC} \quad (3.14)$$

where  $R_{FC}$  is the internal resistance.

Concentration losses  $E_{con}$  is related to the change in concentration of reactants at the surface of electrodes. As pure hydrogen diffuses better than oxygen in the nitrogen and water, the concentration losses at the anode can be neglected. Concentration losses  $E_{con}$  can be defined in equation (3.15).

$$E_{con} = -B * \ln \left( 1 - \frac{I_{FC}}{I_{max}} \right) \quad (3.15)$$

where  $B$  is an empirical constant,  $I_{max}$  is the maximum allowed current.

All the potentials in the equation (3.9) have been defined. In order to determine the relationship between fuel cell current and its voltage, the parameters of the above model should be determined like parameters  $E_0$ , empirical constant  $B$  and resistance  $R_{FC}$ .

The Ballard NEXA TM fuel cell stack is used in the vehicle as shown in Figure 3.5. Its parameters are shown in Table 3.1.

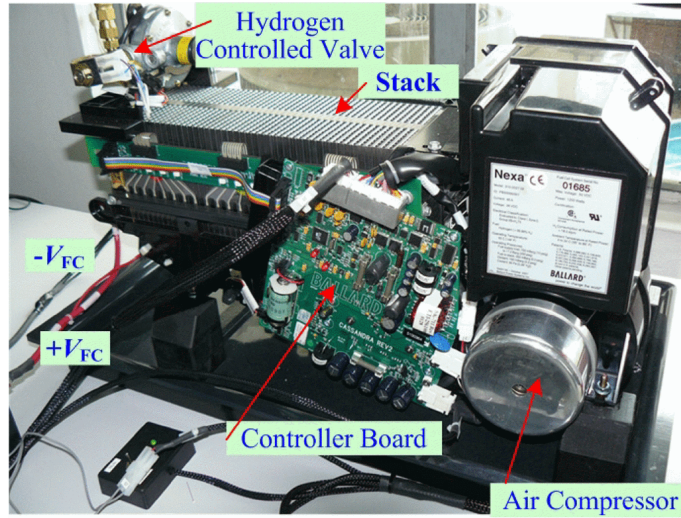


Figure 3.5: Ballard NEXA TM fuel cell stack

Table 3.1: Fuel cell parameters

Company	Ballard NEXA PEMFC
Cell number	47
Rated power (W)	1200
Operating voltage range (V)	[22,50]
Maximum current (A)	46
Air supply	Air blower + filter
Cooling	Air fan cooled
Fuel supply	99.99% dry $H_2$ @1.2 bar

Static measurements of Ballard NEXA TM fuel cell stack are performed. The fuel cell stack current, stack voltage, load voltage, load current and stack temperature are recorded to validate the fuel cell stack model. As a commonly used strategy, Genetic algorithm is chosen to identify the initial value of the model and demonstrate the modeling accuracy. Genetic algorithm is particularly suitable for such multi-parametric and nonlinear system. The main idea of genetic algorithm is to generate a population of solutions and then to improve it using techniques of natural evolution, such as inheritance, mutation, selection, and crossover method. This generational process is repeated until an appropriate solution can satisfy (optimize) the objective function [169]. Minimizing the root mean squared error (RMSE) is chosen as the objective function of genetic algorithm. RMSE is defined as the accuracy between the estimated value from the built model and real experimental value, which is defined as (3.16) [170].

$$RMSE = \sqrt{\frac{1}{N} \sum_{i=1}^N (y_i - \tilde{y}_i)^2} \quad (3.16)$$

where  $y_i$  is actual experimental voltage value,  $\tilde{y}_i$  is the estimated voltage from number,  $N$  is the total number of test data.

The comparative results between experimental results and simulation results through the built model are shown in Figure 3.6. It can be observed that the difference is small and the validation of fuel cell stack model is verified.

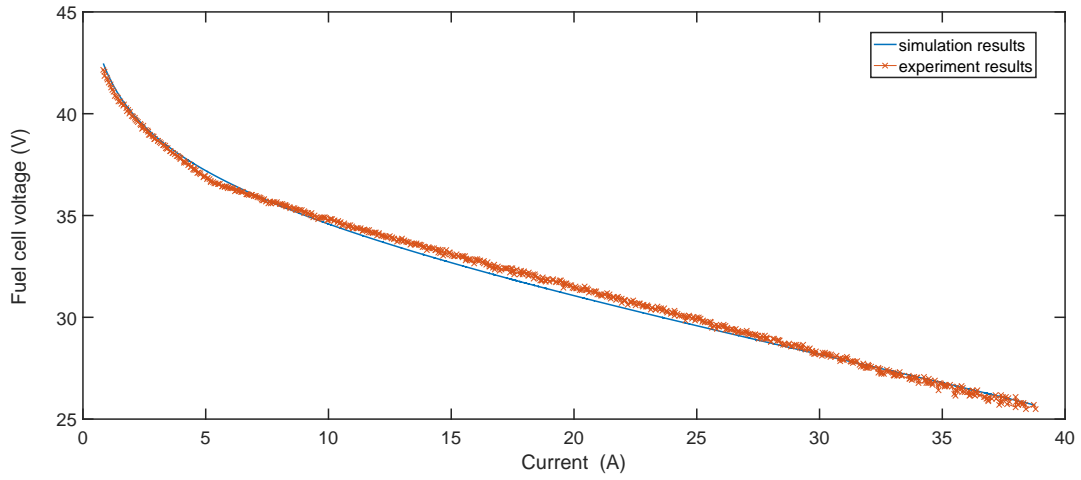


Figure 3.6: Fuel cell polarization curve

### 3.2.3 Fuel cell efficiency model

In order to minimize fuel cell hydrogen consumption, fuel cell stack should be operated to seek maximum efficiency point at high efficiency region, so a precise fuel cell efficiency model is needed.

Fuel cell transforms the chemical energy into electrical energy through the reaction between hydrogen and oxygen [136]. The theoretical efficiency of energy conversion is defined as the ratio between the useful energy output and the energy input. The energy output of fuel cell is the output electrical energy and the energy input is the energy contained in the mass of hydrogen supplied in equation (3.17) [171] [172]

$$\eta_{LHV} = \frac{P_{FC}}{P_{H_2}} = \frac{V_{FC} I_{FC}}{-\Delta H_{LHV} I_{FC}} = \frac{V_{FC}}{1.254} \quad (3.17)$$

where  $\eta_{LHV}$  is fuel cell theoretical efficiency,  $\Delta H_{LHV}$  is the lower heating value of hydrogen.

Some auxiliary systems are needed to ensure the normal operation of fuel cell system, such as electrical control border, cooling fan and air compressor. As the result, the

efficiency of fuel cell system is decided by fuel cell theoretical efficiency and real auxiliary efficiency, which can be calculated in equation (3.18)

$$\eta_{FCS} = \eta_{LHV} * \eta_{aux} = \frac{V_{FC}}{1.254} \left( \frac{P_{FC} - P_{AUX}}{P_{FC}} \right) \quad (3.18)$$

where  $\eta_{FCS}$  is fuel cell system efficiency,  $\eta_{LHV}$  is fuel cell theoretical efficiency,  $\eta_{aux}$  fuel cell real auxiliary efficiency,  $P_{AUX}$  fuel cell power consumed by the auxiliary system.

According to the study of [156], the compressor power is up to 93.5% of the total auxiliary power, so a precise compressor model to calculate its power variation along with fuel cell current is built and the other auxiliary power is set as a constant value. The power consumed by the air compressor is shown in equation (3.19)

$$P_{cp} = \frac{C_P T_{air}}{\eta_{mec} \eta_{mot}} \left( \left( \frac{P_{out}}{P_{in}} \right)^{\frac{\gamma-1}{\gamma}} - 1 \right) F_{cp} \quad (3.19)$$

where  $P_{cp}$  is air compressor power,  $C_P$  is heat capacity of air,  $T_{air}$  inlet air temperature,  $\eta_{mec}$  is compressor mechanical efficiency,  $\eta_{mot}$  is the efficiency of compressor motor,  $P_{in}$  is input air pressure,  $P_{out}$  is output air pressure,  $\gamma$  is ratio of the specific heat of air.  $F_{cp}$  is the compressor air flow rate which can be defined according to the fuel cell current as the equation (3.20)

$$F_{cp} = S * M_{air} \frac{N_{cell} * I_{FC}}{4X_{O_2} * F} \quad (3.20)$$

where  $S$  is the stoichiometric ratio,  $M_{air}$  is the number of air moles,  $X_{O_2}$  oxygen molar fraction.

From the experimental measurement, the speed of controlled cooling fan is divided into a constant speed zone and regulated zone, depending on the stack temperature, as shown in the Table 3.2.

Table 3.2: Cooling fan speed and stack temperature

In nonregulated zone	
Stack temperature range	Fan speed (%)
to 50.5 °C	35
From 50.5 °C to 53.5 °C	36
From 53.5 °C to 55.5 °C	37
From 55.5 °C to 58.5 °C	38
From 58.5 °C to 60.5 °C	39
From 60.5 °C to 63.5 °C	40
From 63.5 °C to 65.5 °C	41
From 65.5 °C to 67.5 °C	42
In regulated zone	
Fan speed regulator start temperature: 67.5 °C	
Fan speed regulator stop temperature: 65.0 °C	

It should be noticed the DC/DC converter connected to fuel cell stack affects the output power of fuel cell stack on DC bus. So, its efficiency is also included into fuel cell

system. According to equation (3.18), the fuel cell system efficiency can be calculated and shown in Figure 3.7.

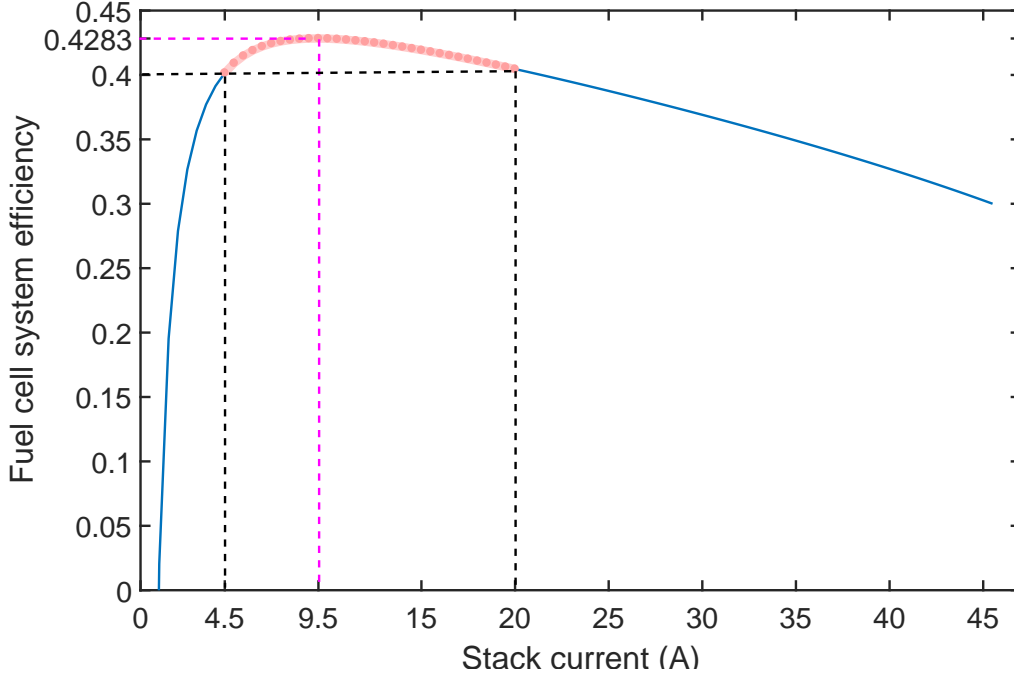


Figure 3.7: Fuel cell system efficiency curve along with stack current

It can be observed that the maximum efficiency point 42.83% occurs at fuel cell current 9.5A. From 4.5A to 20A in red color, the fuel cell system efficiency is above 40% which is defined as a high efficiency zone. To reduce the final hydrogen consumption, fuel cell should be operated to seek maximum efficiency point within this zone.

Minimizing hydrogen consumption is often set as the objective of energy management strategy, which is also one of the most important part of the objective function of designed energy management strategy in the dissertation. In order to minimize the hydrogen consumption quantificationally, the calculation of hydrogen consumption rate is defined by fuel cell current in equation (3.21) [173]:

$$m_{H_2} = \int_0^t \frac{M_{H_2} N_{cell}}{2F} I_{FC}(t) dt \quad (3.21)$$

where  $m_{H_2}$  represents the hydrogen mass rate,  $M_{H_2}$  is the hydrogen molar mass.

### 3.2.4 Battery model

Battery is the main energy storage source of the vehicle. An electrochemistry-based lithium-ion battery model is built in the dissertation. Compared to the empirical model, the multi-physical model and equivalent circuit battery model, the new model not only can ensure the low cost of computation but also meets the high accuracy requirement [174]. The electrochemistry-based battery model is also helpful to analyze the degradation process of the battery.

Li-ion battery is composed of positive electrode, negative electrode and electrolyte. During discharge process, lithium ions ( $Li^+$ ) de-insert from the negative electrode consisting of lithiated carbon ( $Li_xC$ ), diffuse through the separator consisting of electrolyte towards the positive electrode and intercalate in the positive electrode consisting of lithium cobalt oxide ( $Li_xCoO_2$ ) [175]. The charging process is the reverse of discharging process. The voltage terms of the battery are summarized in Figure 3.8. The overall voltage of battery  $V(t)$  is the difference between the positive current collector potential and negative current collector potential. Resistance losses at the current collectors are taken as zero [176]. According to the Figure 3.8, battery voltage can be expressed in equation (3.22).

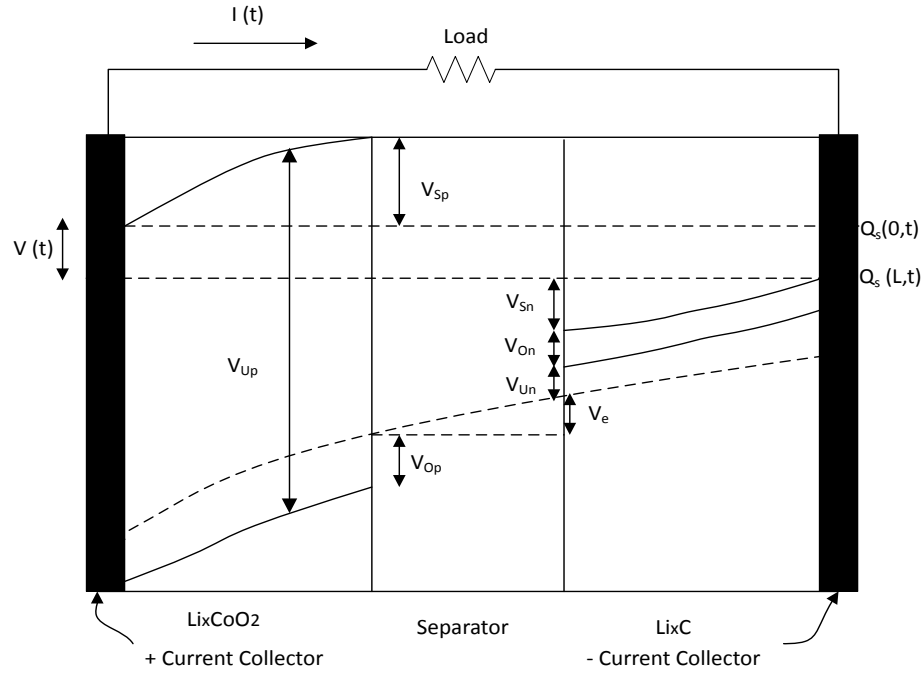


Figure 3.8: Battery model

$$V(t) = V_{U,p} - V_{U,n} - V_{S,p} - V_{S,n} - V_e - V_{O,n} - V_{O,p} \quad (3.22)$$

where  $V_{U,p}$ ,  $V_{U,n}$  are equilibrium potentials at the positive current collector and the negative current collector respectively,  $V_{O,n}$  and  $V_{O,p}$  are surface over-potentials due to charge transfer resistance at the positive and negative current collector,  $V_{S,p}$ ,  $V_{S,n}$  and  $V_e$  are the voltage drop due to solid phase ohmic resistance at the positive and negative current collector and the electrolyte ohmic resistance respectively. Each of these voltages is described in detail in the following parts.

Equilibrium potential can be calculated from the Nernst equation (3.23):

$$V_{U,i} = U_0 + \frac{RT}{nF} \ln\left(\frac{1-x_i}{x_i}\right) + V_{act,i} \quad (3.23)$$

where  $i$  stands for the electrode ( $n$  for negative and  $p$  for positive),  $U_0$  is reference voltage,  $T$  is electrode temperature,  $n$  the number of electrons transferred in the reaction,  $V_{act,i}$  the activity correction term (0 in the ideal condition), which can be defined in equation (3.24) [177].

$$V_{act,i} = \frac{1}{nF} \left( \sum_{k=0}^{N_i} A_{i,k} \left( (2x_i - 1)^{k+1} - \frac{2x_i k (1 - x_i)}{(2x_i - 1)^{1-k}} \right) \right) \quad (3.24)$$

$x_i$  can be defined in equation (3.25).

$$x_i = \frac{q_i}{q_{max}} \quad (3.25)$$

where  $q_i$  the amount of Li ions in electrode  $i$ ,  $q_{max} = q_p + q_n$ , the total amount of Li ions.  $x_p + x_n = 1$ , when fully charged  $x_p = 0.4$  and  $x_n = 0.6$ . When fully discharged,  $x_p = 1$  and  $x_n = 0$ .

The equilibrium voltage is directly decided by the amount of charge in the electrodes. Each electrode can be divided into surface layer (subscript  $s$ ) and buck layer (subscript  $b$ ). So the relationship can be determined by:

$$q_p = q_{s,p} + q_{b,p} \quad (3.26)$$

$$q_n = q_{s,n} + q_{b,n} \quad (3.27)$$

$$q_{max} = q_{s,n} + q_{b,n} + q_{s,p} + q_{b,p} \quad (3.28)$$

In the buck layer, the concentration of Li ion is nearly even but inside the surface layer, the concentration changes drastically. The concentrations of Li ions in the surface layers are described as:

$$c_{b,i} = \frac{q_{b,i}}{v_{b,i}} \quad (3.29)$$

$$c_{s,i} = \frac{q_{s,i}}{v_{s,i}} \quad (3.30)$$

where  $q_{s,i}$  and  $q_{b,i}$  are the charge at different layers,  $v_{b,i}$  and  $v_{s,i}$  are the volume of layers. The diffusion rate from the bulk to the surface is:

$$q_{bs,i}' = \frac{c_{b,i} - c_{s,i}}{D} \quad (3.31)$$

Where  $D$  is the diffusion constant. So the charge variables are calculated as:

$$q_{s,p}' = i_{app} + q_{bs,p}' \quad (3.32)$$

$$q_{b,p}' = i_{app} + q_{bs,p}' - i_{app} \quad (3.33)$$

$$q_{b,n}' = i_{app} + q_{bs,n}' - i_{app} \quad (3.34)$$

$$q_{s,n}' = -i_{app} + q_{bs,n}' \quad (3.35)$$

where  $i_{app}$  is the applied electric current, the mole fraction in the surface and buck can be calculated based on the charge:

$$x_i = \frac{q_i}{q_{max}} \quad (3.36)$$

$$x_{s,i} = \frac{q_{s,i}}{q_{s,i,max}} \quad (3.37)$$

$$x_{n,i} = \frac{q_{n,i}}{q_{n,i,max}} \quad (3.38)$$

According to above function the value of  $V_{U,p}$  and  $V_{U,n}$  can be calculated. Regarding to  $V_{S,p}$ ,  $V_{S,n}$ ,  $V_e$ , they can be categories as the Ohmic potential:

$$\begin{aligned} V_r &= V_{S,p} + V_{S,n} + V_e \\ &= i_{app} (R_{S,p} + R_{S,n} + R_e) \\ &= i_{app} R \end{aligned} \quad (3.39)$$

The surface potentials  $V_{O,n}$  and  $V_{O,p}$  are due to charge transfer resistance and solid-electrolyte interface (SEI) kinetics can be calculated as the simplified Butler-Volmer equation (3.40).

$$V_{O,i} = \frac{RT}{F\alpha} \arcsin\left(\frac{J_i}{2J_{i0}}\right) \quad (3.40)$$

where  $\alpha$  is the symmetry factor,  $J_i$  is the current density,  $J_{i0}$  is the exchange current density.

Now that, all potentials at equation (3.22) are defined. Regarding the battery dynamical changes can be calculated as:

$$V(t) = V_{U,p} - V_{U,n} - V_r' - V_{O,n}' - V_{O,p}' \quad (3.41)$$

$$V_r'' = \frac{V_r - V_r'}{\tau_r} \quad (3.42)$$

$$V_{o,i}'' = \frac{V_{o,i} - V_{o,i}'}{\tau_{o,i}} \quad (3.43)$$

where  $\tau$  are empirical time constants.

The SOC of battery can be calculated according to the charge on the buck and surface layer and the whole amount of charge, scaled from 0 to 1 in equation (3.44).

$$SOC = \frac{q_n}{0.6q_{max}} \quad (3.44)$$

The measured battery voltage and the estimated value from battery model for a variable loading scenario are shown in figure 3.9. The variable loading scenario is tested under a random sequence of charging and discharging currents among (-4.5A, -3.75A, -3A, -2.25A, -1.5A, -0.75A, 0.75A, 1.5A, 2.25A, 3A, 3.75A, 4.5A)[178]. In order to save time and reduce experiment cost, only one cell of battery sack is tested. It can be observed that the model fits very well with the measured values. The voltages of the model are fairly

accurate in response to changes in load. Some errors are still present that may possibly be accounted for temperature effects. The model described here can also be applied to a battery pack by multiplying the number of cells as a lumped equivalent single-cell model.

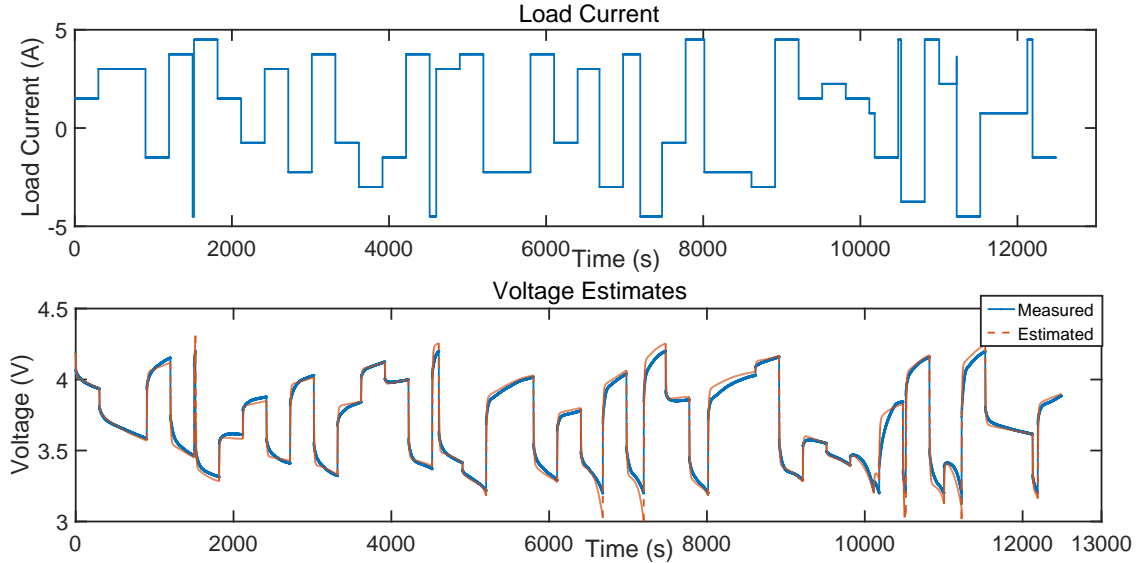


Figure 3.9: Model validation for variable loading

The precise electrochemical-based battery model has been built in this section, which is helpful for the validation of the designed energy management strategy in the latter section. The model described here can also be applied to analyze the battery degradation and estimate its state of health.

### 3.2.5 Supercapacitor model

Supercapacitor is a high-capacity capacitor with 10 to 100 times more energy per unit volume or mass than electrolytic capacitors[179]. Supercapacitor has high peak power density. It can accept and deliver charge much faster and tolerates many more charge and discharge cycles than battery. These advantages make it wide applications in vehicles as the power source to supply peak power demand like fast acceleration and deceleration. As one important peak power source of vehicle, supercapacitor can be modeled as a capacitor and an equivalent resistance[180] as shown in Figure 3.10. Capacitor represents supercapacitor performance at discharge and charge state and resistance represents the supercapacitor ohmic losses. The open circuit voltage of supercapacitor has linear relationship with its SOC, so the supercapacitor SOC can be calculated in equation (3.45). The supercapacitor current can be calculated through the following equation (3.46).

$$SOC = \frac{V_{oc} - V_{min}}{V_{max} - V_{min}} \quad (3.45)$$

$$I = \frac{V_{oc} - \sqrt{V_{oc}^2 - 4R_{SC}P_{SC}}}{2R_{SC}} \quad (3.46)$$

where  $V_{max}$  is supercapacitor maximum voltage,  $V_{min}$  output minimum voltage,  $V_{oc}$  capacitor voltage,  $R_{SC}$  equivalent resistance.

Through the built supercapacitor model, the supercapacitor SOC, current and voltage can be calculated and these parameters are important for the energy management strategy.

### 3.2.6 DC/DC converter model

Fuel cell stack is connected to DC bus through a 1-quadrant DC/DC boost converter and supercapacitor is connected to DC bus through a 2-quadrant DC/DC buck/boost converter with boost operation for discharging mode and buck operation for charging mode. Each converter consists of two IGBT transistors which are controlled by two complementary pulse width modulated (PWM) signals. Two DC/DC converters have the same architecture, which are shown in Figure 3.11. Different from buck/boost converter for supercapacitor, the  $S_1$  IGBT transistors of fuel cell 1-quadrant DC/DC boost converter is always set in the state of off.

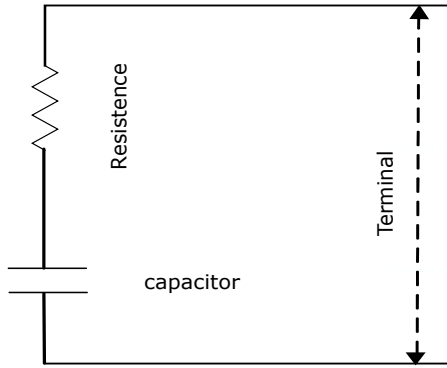


Figure 3.10: Supercapacitor model

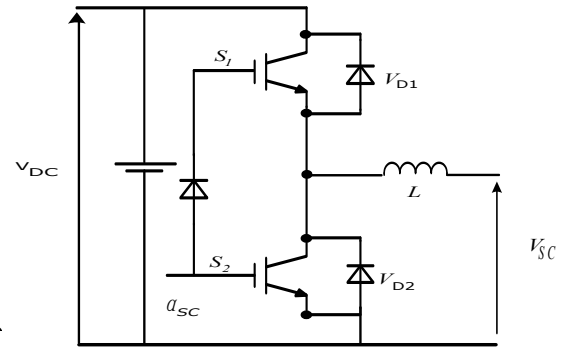


Figure 3.11: 2-quadrant DC/DC buck/boost converter for supercapacitor

The relationship between input and output power of two converters is described in the following equation (3.47)

$$I_{out} = \eta_{conv} \frac{P_{in}}{U_{out}} \quad (3.47)$$

where  $P_{in}$  represents input power,  $U_{out}$  is output voltage and  $\eta_{conv}$  is DC/DC converter efficiency.

## 3.3 Equivalent consumption minimization strategy

The fuel cell hybrid electric vehicle in the dissertation has three power sources: fuel cell, battery and supercapacitor, which increase the difficulty to design an energy management strategy for it. Up to now, few papers focus on building energy management strategy which takes into account more than two power sources. State machine control strategy of [69] and fuzzy logic strategy of [70, 181, 182] are used to control the power split among three power sources. But they belong to rule based strategy which is hard to reach optimal results. As concluded in the last chapter, equivalent consumption minimization strategy as one kind of local optimization strategy doesn't rely on the prior knowledge of drive cycle and can reach optimal results at instantaneous time, which is chosen as the energy management strategy of FCHEV in this dissertation. There is lesser research

evaluating the fuel economy potential of supercapacitor and battery combination for equivalent consumption minimization strategy. Two-level control structure, where the first level calculates the optimal results between fuel cell and battery and the second one lets supercapacitor improve the battery performance, are widely used for three power sources like [183]. Equivalent consumption minimization strategies in [184, 185, 143] are designed as two-level architecture and take equivalent hydrogen consumption of supercapacitor as zero, which not only runs directly counter to the aim of minimizing whole hydrogen consumption but also increases the complication of energy management strategy due to the need of an additional energy management strategy to calculate supercapacitor power demand. Thus, a sequential quadratic programming (SQP) based Equivalent Consumption Minimization Strategy (ECMS) (SECMS) is proposed to consider energy cost of all three power sources into the objective function to solve this problem.

Fuel cell is operated to seek for the maximum efficiency point in high efficiency zone by the novel designed SECMS. Meanwhile, fuel cell dynamical current change rate is limited to increase the lifetime of fuel cell. The supercapacitor is operated to supply peak power to decrease the maximum transient current of battery to increase its lifetime. SOC values of battery and supercapacitor are kept within a reasonable range and the terminal battery SOC is close to the initial one.

### 3.3.1 SQP based equivalent consumption minimization strategy (SECMS)

All energy needed by vehicle is supplied indirectly by the fuel cell system at last. In order to minimize hydrogen consumption, the instantaneously consumed electrical energy from battery and supercapacitor can be equivalent to the chemical energy from fuel cell. The instantaneous hydrogen consumption composes of direct hydrogen consumption from fuel cell system and indirect equivalent hydrogen consumption from battery and supercapacitor, as shown in equation (3.48),

$$\begin{aligned} m_w(t) &= m_{fc}(t) + m_{BA}(t) + m_{SC}(t) \\ &= m_{fc}(t) + \lambda_{ba}P_{ba}(t) + \lambda_{sc}P_{sc}(t) \end{aligned} \quad (3.48)$$

where  $m_w(t)$  is the whole hydrogen consumption.  $\lambda_{ba}$  and  $\lambda_{sc}$  are battery and supercapacitor equivalent factor for equivalent hydrogen consumption.

In order to keep fuel cell working in high efficiency zone, battery SOC of end cycle same as start value, supercapacitor supplying peak power, the relevant penalty coefficients are added into equation (3.48), and the objective function is defined in equation (3.49),

$$\begin{aligned} f_w(t) &= K_{eff}m_{fc}(t) + K_{ba}m_{BA}(t) + K_{sc}m_{SC}(t) \\ &= K_{eff}m_{fc}(t) + K_{ba}\lambda_{ba}P_{ba}(t) + K_{sc}\lambda_{sc}P_{sc}(t) \end{aligned} \quad (3.49)$$

where  $K_{ba}$  and  $K_{sc}$  are penalty coefficients which limit battery and supercapacitor SOC range and variation between instantaneous SOC and initial SOC,  $K_{eff}$  is the fuel cell efficiency penalty coefficient that urges fuel cell to operate at maximum efficiency in high efficiency zone [186].

According to equation (3.21), fuel cell hydrogen consumption  $m_{fc}(t)$  can be computed directly. The equivalent hydrogen consumption of battery is calculated through equation (3.50):

$$m_{BA}(t) = P_{ba}(t) * \frac{m_{average}}{P_{average}} * \eta_{ba} \quad (3.50)$$

for supercapacitor in equation (3.51):

$$m_{SC}(t) = P_{sc}(t) * \frac{m_{average}}{P_{average}} * \eta_{sc} \quad (3.51)$$

where  $\eta_{ba}$   $\eta_{sc}$  is battery and supercapacitor equivalent transform efficiency,  $m_{average}$  is fuel cell average hydrogen consumption,  $P_{average}$  is fuel cell average power.

Fuel cell efficiency penalty coefficient  $K_{eff}$  is defined in equation (3.52):

$$K_{eff} = \begin{cases} (1 - 2 * \frac{\eta - \eta_{opt}}{\eta_{max} - \eta_{min}})^2 & \eta \geq 0.4 \\ (1 - 2 * \frac{\eta - \eta_{opt}}{\eta_{max} - \eta_{min}})^4 & \eta < 0.4 \end{cases} \quad (3.52)$$

where  $\eta$  is the instantaneous efficiency,  $\eta_{opt}$  is optimal efficiency (0.4283),  $\eta_{max}$  the maximum efficiency (0.4283),  $\eta_{min}$  the minimum efficiency (0.4), which define the zone described in section 3.2.3. When fuel cell system efficiency is below than 0.4, a large penalty value  $K_{eff}$  is calculated to shut fuel cell stack down or operate fuel cell stack to meet power demand by drive cycle when battery and supercapacitor SOC are less than limited SOC range.

Regarding battery SOC penalty coefficient  $K_{ba}$ , it is defined in equation (3.53):

$$K_{ba} = \begin{cases} (1 - \frac{2*(u-B_{int})}{B_{max}-B_{min}})^4 & B_{min} \leq u \leq B_{max} \\ (1 - \frac{2*(u-B_{int})}{B_{max}-B_{min}})^{20} & u < B_{min}, u > B_{max} \end{cases} \quad (3.53)$$

where  $u$  is the instantaneous battery SOC,  $B_{int}$  is battery initial SOC,  $B_{max}$  the maximum SOC,  $B_{min}$  the minimum SOC.  $K_{ba}$  operates the battery SOC to return back to its initial SOC. When battery SOC reaches  $B_{min}$  or  $B_{max}$ , high  $K_{ba}$  value is defined as the penalty factor to avoid the battery continues to discharge and charge respectively.

Supercapacitor penalty coefficient  $K_{sc}$  is composed of SOC coefficient  $S_{eff}$  and peak power coefficient  $S_{peak}$ .  $S_{eff}$  is familiar to  $K_{ba}$  to restrict supercapacitor SOC value at reasonable range.  $S_{peak}$  is used to let supercapacitor supply peak power firstly. In order to avoid the frequent on/off cycles of fuel cell and frequent charge/discharge cycles of supercapacitor due to the large amplitude changes of supercapacitor SOC in short time, supercapacitor SOC is equivalent to battery SOC to define  $S_{eff}$ .  $K_{SC}$ ,  $S_{eff}$  and  $S_{peak}$  can be defined in equation (3.54), (3.55), (3.56) respectively:

$$K_{SC} = S_{eff} * S_{peak} \quad (3.54)$$

$$S_{eff} = \begin{cases} (1 - 2 \frac{ax+b-S_{opt}}{S_{max}-S_{min}})^2 & S_{min} \leq x \leq S_{max} \\ (1 - 2 \frac{ax+b-S_{opt}}{S_{max}-S_{min}})^{20} & x < S_{min}, x > S_{max} \end{cases} \quad (3.55)$$

$$S_{peak} = \begin{cases} 1 & 0 \leq I_{load} \leq 30 \\ -0.01 * I_{load} + 1 & I_{load} < 0, I_{load} > 30 \end{cases} \quad (3.56)$$

where  $x$  is the instantaneous supercapacitor SOC,  $S_{opt}$  is optimal SOC,  $S_{max}$  the maximum SOC,  $S_{min}$  the minimum SOC,  $I_{load}$  is load current demand on the DC bus,  $a$  and  $b$  are the transform coefficients from supercapacitor SOC to equivalent battery SOC and their values are decided by battery minimum SOC and maximum SOC.

As described in the above content, all the factors of the objective function  $f_w$  can be decided. In order to limit the working point of fuel cell, battery and supercapacitor to increase their lifetime, play their full character potential and meet the power demand, some constraints have been set. Higher current than 46A is not allowed for fuel cell, otherwise, the lifetime of fuel cell will be reduced and even permanent damage will be caused. When fuel cell current is less than 4.5A, the efficiency is less than 40%. In order to operate fuel cell at high efficiency point, the lowest current is set to 4.5A. When current is smaller than that, the fuel cell will be shut off. The fuel cell current change rate is also considered. High current change rate on fuel cell results into fuel starvation problem and increase the fuel cell degradation. Therefore, its current change rate (A/s) is limited to [-1,1]. The initial SOCs of battery and supercapacitor are set 0.8. The constraints on power sources in the vehicle are shown as Table 3.3 :

Table 3.3: Constraints for battery and supercapacitor

constraint parameters	value
Fuel cell current(A)	[4.5, 46]
battery SOC	[0.2, 0.8]
battery current	[-50A, 50A]
supercapacitor SOC	[0, 0.9]
supercapacitor current	[-18A, 18A]

The ECMS strategy is transformed into a non-linear programming problem, which has fuel cell reference current and supercapacitor reference current as variables, equivalent hydrogen consumption as weighting function and subjects to several constraints and inequality constraints. Sequential quadratic programming is one of the most successful methods for the numerical solution of constrained nonlinear optimization problems[187]. Therefore, sequential quadratic programming is programmed in C language to solve ECMS optimization problem in real time.

### 3.3.2 Rule based control strategy

A rule based control strategy is designed as the benchmark for SECMS. The rule based control strategy is divided into two parts: load following control strategy (LFCS) to decide what current the fuel cell should be operated according to power demand by drive cycle and battery SOC, and , operating mode control strategy to calculate supercapacitor current according to supercapacitor SOC and the difference between fuel cell supplied power and load power. The architecture of the rule based control strategy is shown in Figure 3.12

Load following control strategy belongs to deterministic rule based strategy. The main idea of load following control strategy is that fuel cell as the main power source is

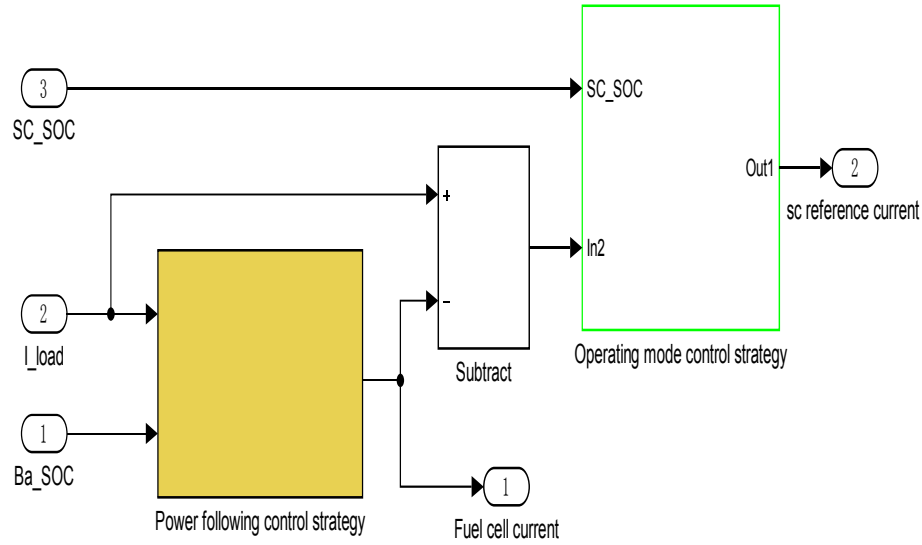


Figure 3.12: Architecture of rule based control strategy

operated in high efficiency zone same as SECMS, and its power changes follow the load power demand on DC bus. Frequent fuel cell on/off cycles degrade fuel cell more seriously, so it is operated at on state until battery SOC is above maximum value or power demand value is very low. The conditions that set fuel cell on or off are listed as following, where  $S_{fc} = 0$  means fuel cell is off,  $S_{fc} = 1$  means fuel cell is on,  $I_d$  current demand on the DC bus,  $t_{offtime}$  is the fuel cell minimum off time that means since the fuel cell was last on, the restart should not be less than this time.  $t_{ontime}$  is similar to  $t_{offtime}$  means the fuel cell minimum on time.

Condition 1: if the fuel cell is off and  $ba_{SOC} < SOC_{bamin}$ , fuel cell is turned on immediately, which is not limited by  $t_{offtime}$ . The current of fuel cell is set as  $I_{fcmax}$ .

Condition 2: if the fuel cell is on and  $ba_{SOC} > SOC_{bamax}$ , fuel cell is turned off, which is not limited by  $t_{ontime}$ . The current of fuel cell is 0.

Condition 3: if the fuel cell is on and  $SOC_{bamin} < ba_{SOC} < SOC_{baint}$ , the fuel cell current is adjusted according to load power.

Condition 4: if the fuel cell was previously off, and the average of the last 5 seconds of  $I_d$  is larger than fuel cell maximum efficiency point  $I_{opt}$  and the time since the fuel cell was last on is larger than  $t_{offtime}$ , the fuel cell is started.

Condition 5: if the fuel cell was previously on, and the average of the last 5 seconds of  $I_d$  is less than fuel cell maximum efficiency current  $I_{opt}$  and the time since the fuel cell was last off is larger than fuel cell minimum on time  $t_{ontime}$ , the fuel cell is off.

Condition 6: if  $I_d$  on the bus is greater than ESS maximum current on the bus  $I_{essmax}$ , the fuel cell stays on or is turned on.

Fuel cell current  $I_{fc}$  is decided by current demand on DC bus  $I_d$  and battery SOC value in equation (3.57). Fuel cell current is limited to high efficiency zone (4.5A, 20A). Beside meeting  $I_d$ , fuel cell also tries to charge the battery to its SOC initial value. The charge current is calculated according to the SOC value.

$$I_{fc} = \begin{cases} I_{min} & I_{ch} + I_d < I_{min} \\ I_{ch}(ba_{SOC}) + I_d & I_{min} \leq I_{ch} + I_d \leq I_{max} \\ I_{max} & I_{ch} + I_d > I_{max} \end{cases} \quad (3.57)$$

when fuel cell reference current is decided by equation (3.57), the difference current  $I_{di}$  between  $I_d$  and  $I_{fc}$  is supplied by battery and supercapacitor, which is decided by operating mode control strategy. The flow chart of the operating mode control strategy is shown in Figure 3.13.

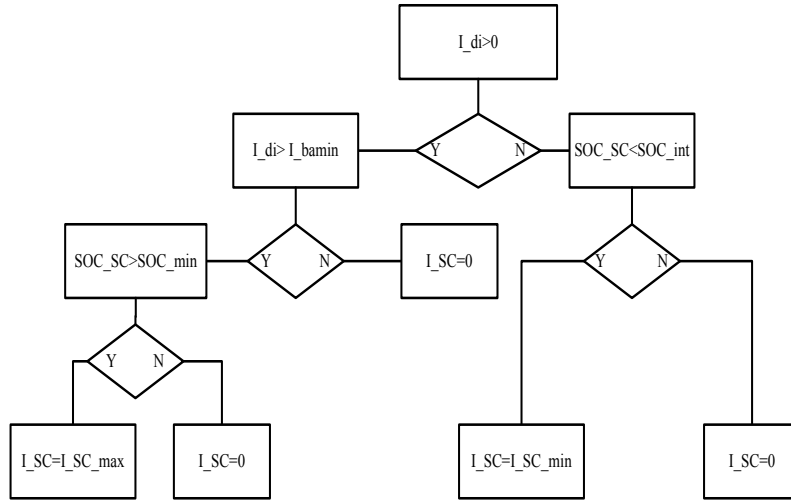


Figure 3.13: Flow chart of operating mode control strategy

The main idea of the operating mode control strategy is when  $I_{di} < 0$  and supercapacitor SOC  $SOC_{sc}$  is smaller than initial supercapacitor SOC  $SOC_{int}$ , supercapacitor firstly be charged at the maximum charge current  $I_{SC_{min}}$ . When supercapacitor discharge, its current  $I_{SC} > 0$ , when it is charged, its current  $I_{SC} < 0$ . when  $I_{di} > I_{bamin}$  and  $SOC_{sc}$  in the range of minimum SOC and maximum SOC, the supercapacitor supplies maximum discharge current. Otherwise supercapacitor current is zero. Battery current is passively decided by the difference between current demand by drive cycle, fuel cell current and supercapacitor current on DC bus.

### 3.3.3 Hybrid ECMS OMCS strategy

Due to low energy density and the role of supercapacitor as peak power supplier, much research on ECMS simplify the equivalent hydrogen consumption of supercapacitor into zero. Based on equation (3.49) of SECMS, a new objective function is defined as (3.58) due to the simplification of supercapacitor equivalent consumption. Other constraints are same as SCEMS. Therefore, the two degrees nonlinear constraint optimization problem of SECMS is simplified into one degree nonlinear constraint problem. The solving of the optimization function is easier.

$$\begin{aligned} m_w(t) &= m_{fc}(t) + m_{BA}(t) \\ &= m_{fc}(t) + \lambda_{ba} P_{ba}(t) \end{aligned} \quad (3.58)$$

Trough the simplified ECMS, the fuel cell current is calculated. But another energy management strategy is needed to determine the supercapacitor reference current, like PI-based control strategy and filter based control strategy. In order to prove that the simplification of ECMS cannot reach the optimal resolution, a HEOS strategy is designed to compare with SECMS in the dissertation. The first part of HEOS is simplified ECMS to calculate fuel cell current and the second part is operating mode control strategy (OMCS) to calculate supercapacitor current. The architecture of HEOS is shown in Figure 3.14

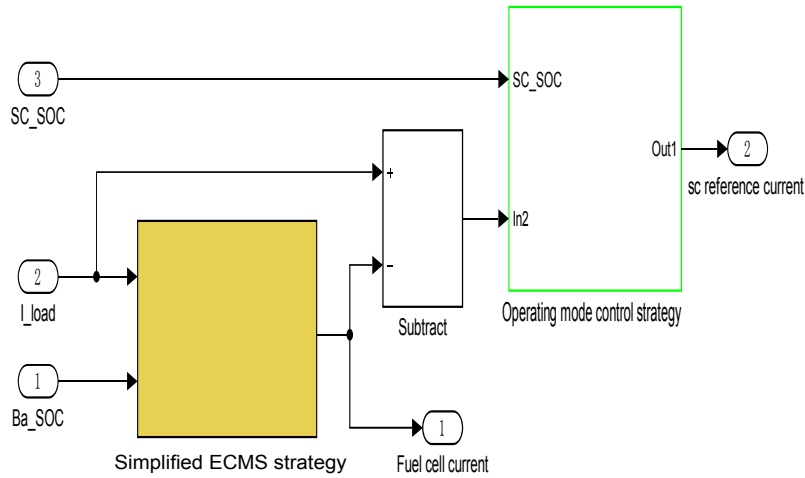


Figure 3.14: HEOS architecture

### 3.4 Simulation results and analysis

A driving cycle is a series of data points representing the speed of a vehicle versus time. Driving cycles are produced by different countries and organizations to assess the performance of vehicles in various ways, as for example fuel consumption and polluting emissions[188]. The propulsion system of vehicle operates to match the speed of the drive cycle. The power profile along with drive cycle can be determined by the built vehicle model and the chosen drive cycle.

WVUCITY drive cycle is shown in Figure 3.15, which is a composite drive cycle of various micro-trips pulled from on-road test data. It represents typical city driving for a heavy vehicle.

New York Bus drive cycle is shown in Figure 3.16 which represents actual driving patterns of transit buses in New York City. The test developed by the United States Environmental Protection Agency attempts to simulate some of the toughest bus driving conditions that existed in the United States in the 1980s. The data for this cycle was collected from a mid-town Manhattan route in New York City. The New York Bus drive cycle simulates rapid stop-and-go traffic with long passenger transfer times. The cycle consists of very rapid accelerations, followed by rapid decelerations to idle and long idling periods.

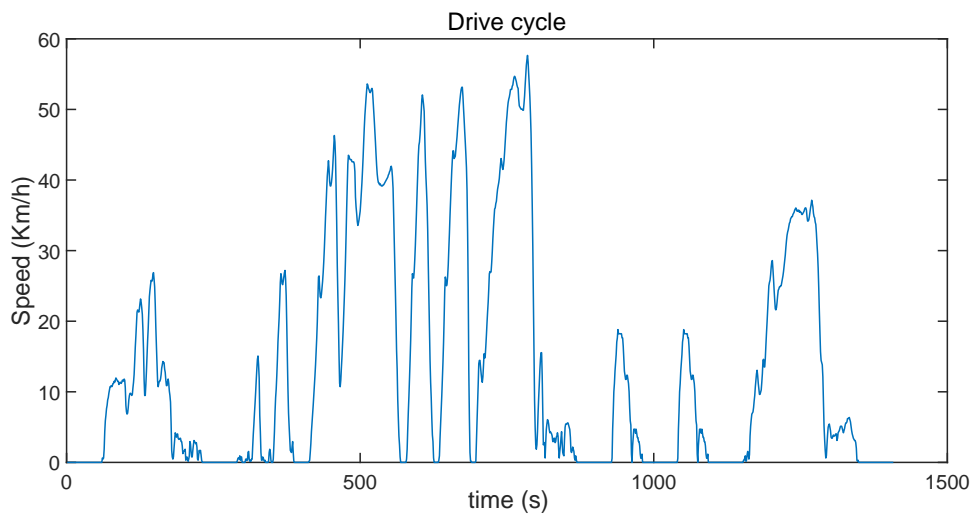


Figure 3.15: WVUCITY drive cycle

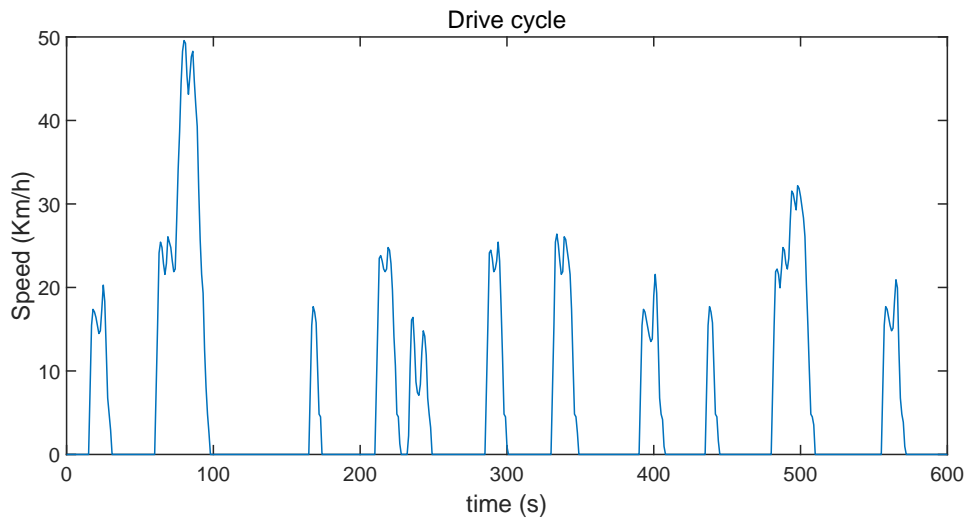


Figure 3.16: New York Bus drive cycle

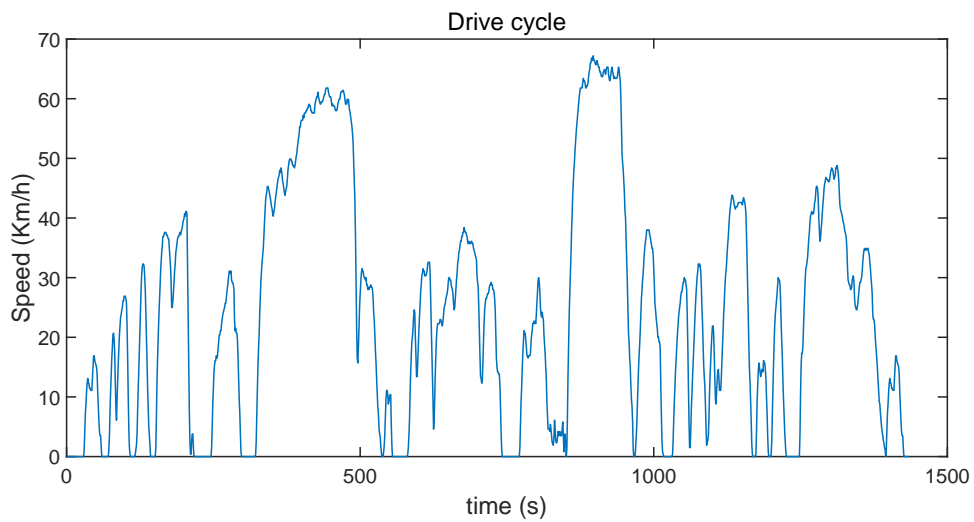


Figure 3.17: LA92 drive cycle

LA92 drive cycle also called California Unified Cycle, is a driving schedule for light-duty vehicles developed by the California Air Resources Board. It has higher speed, higher acceleration, fewer stops per mile, and less idle time. Table 3.4 includes a summary of selected parameters for the WVUCITY, New York Bus and LA92 drive cycles.

Table 3.4: Parameters for three drive cycles

	WVU drive cycle	New York Bus drive cycle	LA92 drive cycle
Time (s)	1408	600	1435
Distance (km)	5.32	0.99	15.8
Max speed (km/h)	57.65	49.57	108.15
Average speed (km/h)	13.59	5.93	39.6
Max acceleration ( $m/s^2$ )	1.14	2.77	3.08
Max deceleration ( $m/s^2$ )	-3.24	-2.06	-3.93
Idle time (s)	427	404	234
Stop numbers	14	11	16

The vehicle used in the dissertation is a light duty urban vehicle and is designed for the postal delivery service in the city communities. A postal delivery mission not only has a lot of start/stop sequences conditions, where the mean value of speed over time is very small but also has long time high speed driving conditions from community to community. In order to reproduce the behavior of such application, WVUCITY and New York Bus drive cycle are chosen for simulation purposes of first condition due to their similarities with the required average speed and start/stop numbers. LA 92 drive cycle simulates the second high speed conditions. The WVUCITY, New York Bus and LA92 drive cycle are connected together to test the performance of three designed energy management strategies. The whole drive cycle time is 3443s and the distance is 22.11Km. According to the built vehicle model, Load power profile for the composite drive cycle of WVUCITY, New York Bus and LA92 drive cycle is shown in Figure 3.18.

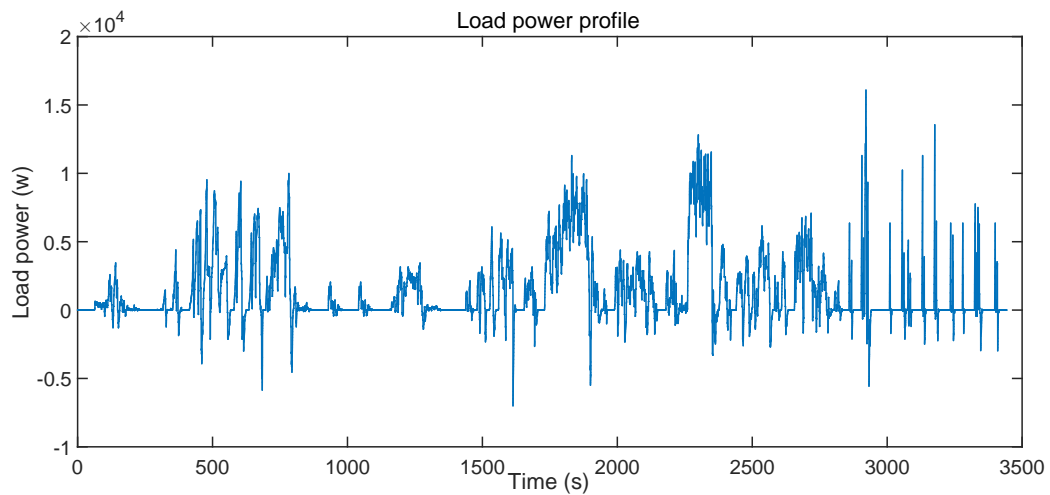


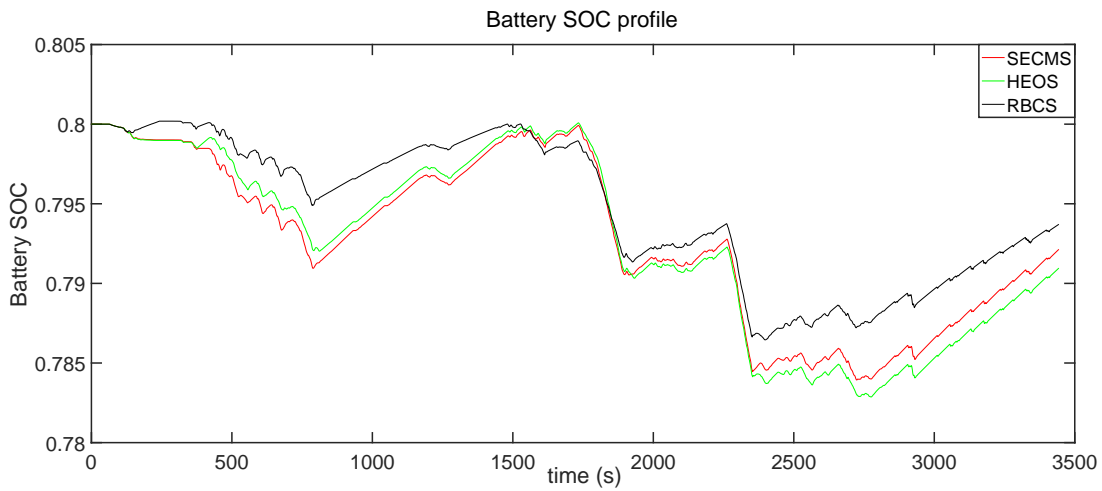
Figure 3.18: Load power profile for composite drive cycle of WVUCITY, New York Bus and LA92 drive cycle

The simulation results of three energy management strategies are shown as Table 3.5.

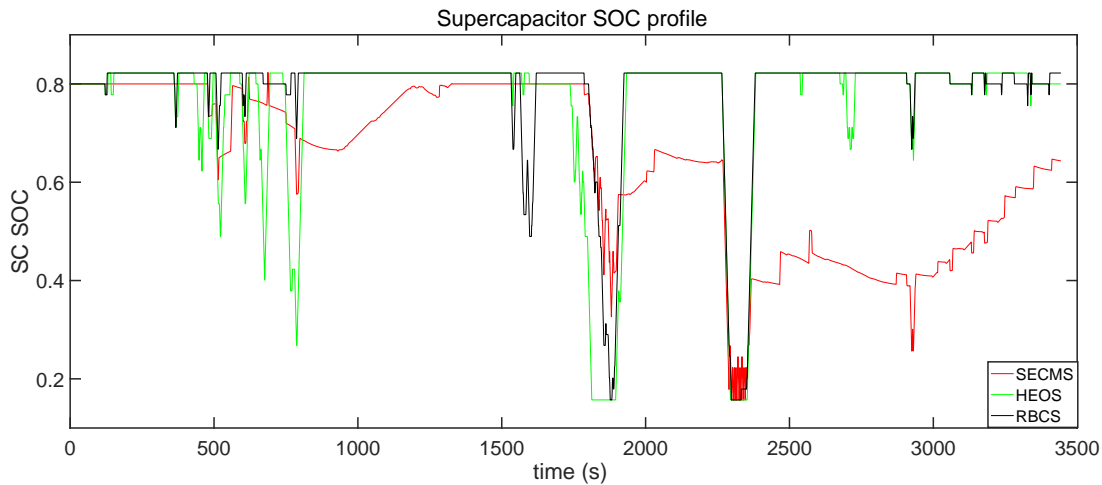
The battery SOC, supercapacitor SOC, fuel cell current, battery current and supercapacitor current for three control strategies are shown in Figure 3.19 and Figure 3.20.

Table 3.5: Comparative results for three EMSs

EMSs	ECMS	RBCS	HEOS
Initial supercapacitor and battery SOC	0.8	0.8	0.8
Final supercapacitor SOC	0.6436	0.8222	0.8000
Variation of supercapacitor SOC	-0.1564	+0.0222	0
Final battery SOC	0.7921	0.7937	0.7910
Variation of battery SOC	-0.0079	-0.0063	-0.009
Hydrogen consumption (g)	15.83	17.00	16.17



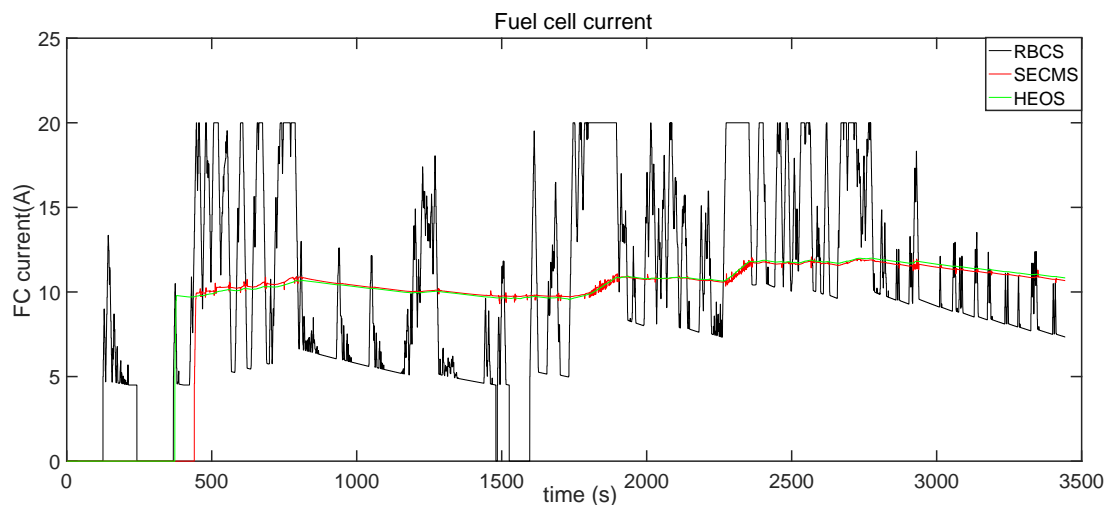
(a) Simulation results of battery SOC



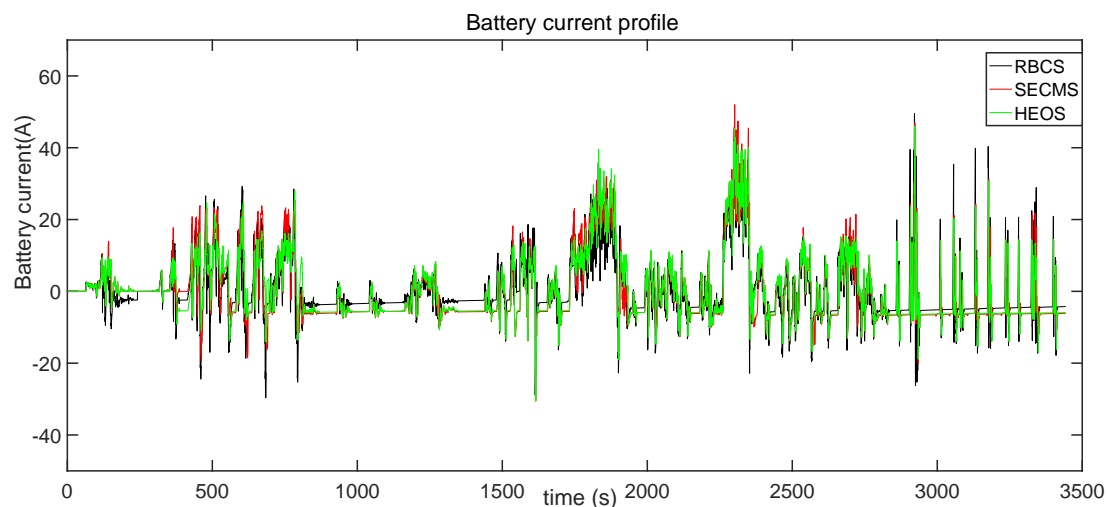
(b) Simulation results of supercapacitor SOC

Figure 3.19: Simulation results of battery SOC and supercapacitor SOC

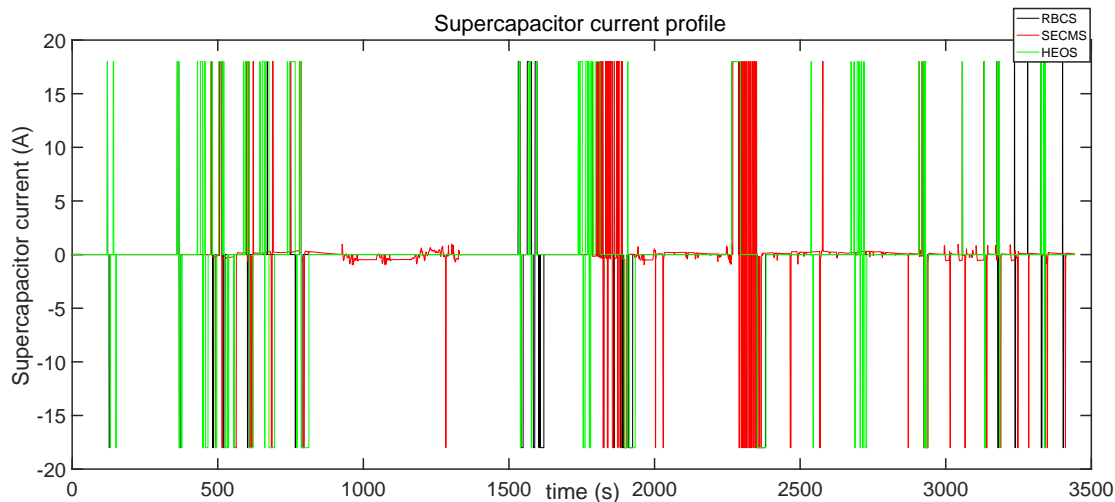
Variation of supercapacitor SOC and variation of battery SOC in Table 3.5 are defined as the subtraction between final values and initial values. As shown in Figure 3.19, battery SOC and supercapacitor SOC of three control strategies are in the limited range (0.2,



(a) Fuel cell current



(b) Battery current



(c) Supercapacitor current

Figure 3.20: Simulation results of fuel cell, battery and supercapacitor currents for three control strategies

0.8) and (0.1, 0.9) respectively. According to Table 3.20, the final battery SOC of three control strategies are almost equal to the initial value. The difference between initial battery SOC and final battery SOC of HEOS is the largest among three control strategies. Supercapacitor has low energy capacity and it is not designed as the energy storage source. Therefore the charge sustenance is not required on supercapacitor.

From Figure 3.20, fuel cell of RBCS operates in the defined high efficiency zone from 4.5A to 20A. But compared to SECMS and HEOS, the fluctuation of fuel cell current is the largest. When fuel cell current is lower than 4.5A, the fuel cell stack is turned off. Three on/off cycles also appear which increases the degradation of fuel cell. Battery works as the main energy storage source to buffer the power demand of drive cycle and supercapacitor supplies peak power. RBCS has the lowest battery SOC variation.

The fuel cell currents of HEOS and SECMS are similar due to the low energy density of supercapacitor. Fuel cells of both energy management strategies operate around maximum efficiency point in high efficiency zone. Their current fluctuation is small. The fuel cell stack of HEOS starts at 373s earlier than SECMS at 440s due to lower supercapacitor SOC value at sample time. Supercapacitor also supplies peak power for HEOS and SECMS. Table 3.5 shows that SECMS has the least hydrogen consumption. Its battery SOC fluctuation is also smaller than HEOS.

From the simulation results of three control strategies, the normal operation of fuel cell hybrid electric vehicle and charge sustaining of battery can be ensured, which means that they have the potential to be tested in the test bench or real vehicle. In order to prove the possible validation of energy management strategies on real vehicle application, analyze the priority of SECMS in more detail and let the final operation results be more convincing, a test bench for the experimental test of three energy management strategies is needed. In Section 5, experiment validation through the test bench will be introduced and the final experimental results will be analyzed in detail.

### 3.5 Conclusion

The components of the drive train of FCHEV are modeled in this chapter and A SECMS strategy is proposed for FCHEV supplied by three power sources: fuel cell, battery and supercapacitor. Fuel cell is operated to seek for the maximum efficiency point in the defined high efficiency zone, while the battery assumes as the main energy storage source to buffer energy demand by vehicle and the supercapacitor dedicates to provide the peak power. This work originally takes into account the hydrogen consumption of all three components in the adopted objective function of energy management strategy. In order to prove the superiority of the new approach, the rule based control strategy and HEOS have also been implemented. The WVUCITY, New York Bus and LA92 drive cycles have been simulated with the three above control strategies. The simulation results show that the three energy management strategies can ensure the normal operation of vehicle and they can be tested in the test bench or real vehicle further.

# Energy management strategy considering the power sources degradation

## 4.1 Introduction

Along with the operation of FCHEV, fuel cell and battery degrade. As the main power source of FCHEV, the output power of fuel cell stack decreases along with degradation. The maximum efficiency point also changes. Battery capacity decreases which increases battery state of charge fluctuation at certain current and its resistance also increases, which decreases battery output voltage [150]. Without correct estimation of fuel cell and battery degradation states and continually using per-set control parameters cannot get optimal results for EMS and even cannot ensure the normal operation of the vehicle. As one of the most important control parameter, battery SOC seriously affects the EMS. Precise estimation of battery SOC is not possible without considering its degradation. Based on imprecise SOC, EMS cannot make better use of power potential of battery, may overcharge/overdischarge the battery and even brings catastrophic hazards. Therefore fuel cell and battery ageing models are needed to monitor their state of health (SOH) to ensure performance, safety, availability and reliability of power sources[189]. Supercapacitor lifetime is far larger than the vehicle and other power sources, so its degradation can be neglected compared to the degradation rate of both other components.[151]. Degradation of power sources is defined as fuel cell degradation and battery degradation in the following parts of the dissertation to facilitate the description.

The health management of power sources can be solved through prognostic approaches, which can be broadly classified into the data-driven approach and model-based approach[190]. Data-driven techniques mainly exploit evolution trends of the tracked variable observed from training or archived data under similar operational conditions. Domain expertise and model development are not needed, but the precision of data-driven approach relies on a larger number of data which cannot get for some systems due to some reasons like high experimental test cost and long time to run to failure. This disadvantage motivates the development of model-based techniques where domain expertise may be brought to bear and this approach also can be used in an online system. So, in the dissertation, model based approach is used. The prognostic technique that can track the nonlinear dynamics of power sources health while using a lower-order system representation is introduced and based on this representation, state of health estimation is determined.

This chapter is organized as follows: section two describes the on-line state of health estimation of power sources. In the third part, the effects of fuel cell degradation and bat-

tery degradation on SECMS results are analyzed respectively and new adaptive equivalent consumption minimization strategy is designed. Finally, conclusions are drawn.

## 4.2 Unscented Kalman filter

Model based prognostic approach is used to assess the power sources degradation. Domain knowledge about the system, its components and its degradation process including failure, derived from first principles that capture the underlying physical phenomena, are needed. This method does not require a lot of data and can be used in real time application such as vehicles' control units. Model-based prognosis can be used to solve the joint state-parameter estimation problem, like the determination of system health based on the observations. It also can be used to solve the prediction problem, in which, the state-parameter distribution is simulated forward in time to compute end of life (EOL) and remaining useful life (RUL). The two problems are generally in the proper sequence in Figure 4.1[191]. In this chapter, the online estimation of power sources' degradation belongs to joint state-parameter estimation problem, which is typically solved through the usage of a state observer or filter to estimate the changeable state parameters based on the degradation model[192].

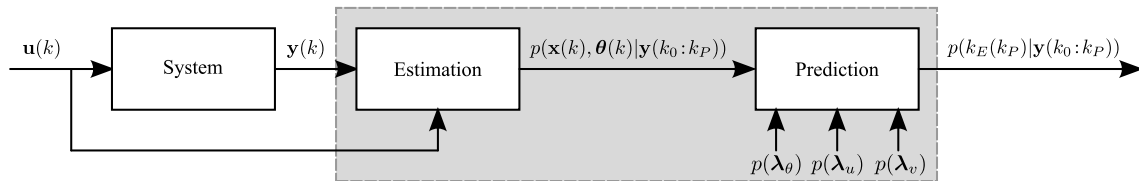


Figure 4.1: Model-based prognostics architecture.

Kalman filter as the most well-known filter is used for the prognostics problems in [193] and [194]. But Kalman filter can only be used in linear systems, which is not the case of most prognostic problems. Approximate filters like extended Kalman filter (EKF) and unscented Kalman filter (UKF), and another nonlinear filter: particle filter (PF) are widely used in the nonlinear prognostic problem. EKF has become a standard technique for performing recursive nonlinear estimation and used for estimating the state of a nonlinear dynamic system, estimating parameters for nonlinear system identification, and dual estimation where both states and parameters are estimated simultaneously[195]. The propagation of a Gaussian random variable (GRV) through the system dynamics is the key operation for the Kalman filter. The state distribution of EKF is approximated by a GRV and is propagated analytically through the first-order linearization of the nonlinear system to solve the nonlinear prognostics problem, which leads to large errors in the true posterior mean and covariance of the transformed GRV and finally may result in sub-optimal performance and sometimes divergence of the filter[196].

Particle filter method, also known as a Sequential Monte Carlo method, is widely used to solve the nonlinear non-Gaussian problem. The core idea of the degradation state estimation is to construct a probability density function (PDF) of the state based on all available information. For particle filter approach, the PDF is approximated by a set of particles (points) representing sampled values from the unknown state space, and a set of associated weights denoting discrete probability masses[197]. The particles are generated and recursively updated from a nonlinear process model that describes the evolution in time of the system under analysis, a measurement model, a set of available measurements

and a prior estimate of the state PDF. The main shortcoming of the usage of particle filter on the on-line estimation of degradation is the computational complexity because the number of particles needed for joint state parameter estimation is typically large and this number increases with the dimension of state parameter space[198]. UKF replaces propagating the Gaussian variables through the first-order linearization model as EKF with the Unscented Transformation (UT) to handle the nonlinear plant directly to overcome the large errors problem of EKF. Remarkably, the computational complexity of the UKF is the same order as that of the particle filter. In summary, UKF has not only higher accuracy than EKF but also lower computational cost than particle filter[191]. Therefore in this dissertation, UKF is chosen to estimate the battery state of health and fuel cell state of health. The UKF is introduced in brief in this section.

The basic framework for UKF estimation of the state of a discrete-time non-linear dynamical system is in equation (4.1) and (4.2) [199].

$$x_{k+1} = F(x_k, u_k, v_k) \quad (4.1)$$

$$y_k = H(x_k, n_k) \quad (4.2)$$

where  $x_k$  is the unobserved state of system,  $u_k$  is input,  $v_k$  is the process noise,  $y_k$  is the observed measurement signal,  $n_k$  the observed noise.

Given the observation  $y_k$ , estimation of state  $x_k$  is the goal. UT is used for UKF to approximate the distribution. UT calculates the mean output variable  $\bar{y}$  and its covariance  $P_{yy}$  through  $x$ , with mean  $\bar{x}$  and covariance  $P_{xx}$ . The mean and covariance of  $x$  are determined by deterministically selected sample points, called sigma points[200].

$$\chi_0 = \bar{x} \quad (4.3)$$

$$\chi_i = \bar{x} + \left( \sqrt{(l + \lambda) P_x} \right)_i, \quad i = 1 \cdots L \quad (4.4)$$

$$\chi_i = \bar{x} - \left( \sqrt{(l + \lambda) P_x} \right)_{i-L}, \quad i = L + 1 \cdots 2L \quad (4.5)$$

where  $\chi_i$  the  $i$  th sigma point of  $x$ ,  $L$  the dimension of  $x$ .

The corresponding value, mean and covariance of  $y$  for sigma points can be calculated through the following equations.

$$y_i = f(\chi_i) \quad i = 0 \cdots 2L \quad (4.6)$$

$$\bar{y} = \sum_{i=0}^{2L} W_i^{(m)} y_i \quad (4.7)$$

$$P_y = \sum_{i=0}^{2L} W_i^{(c)} (y_i - \bar{y})(y_i - \bar{y})^T \quad (4.8)$$

weights decided by

$$w_0^m = \frac{\lambda}{L + \lambda} \quad (4.9)$$

$$w_0^c = \frac{\lambda}{L + \lambda} + 1 - \alpha^2 + \beta \quad (4.10)$$

$$w_i^c = w_i^m = \frac{1}{2(L + \lambda)} \quad i = 1 \cdots 2L \quad (4.11)$$

where  $\lambda = \alpha^2(L + k) - L$  is a scaling parameter.  $\alpha$  determines the spread of the sigma points around and is usually set to a small positive value (e.g., 1e-3).  $k$  is a secondary scaling parameter which is usually set to 0, and  $\beta$  is used to incorporate prior knowledge of the distribution of  $x$  (for Gaussian distributions,  $\beta = 2$  is optimal).  $(\sqrt{(L + \lambda)P_x})_i$  is the  $i$ th row of the matrix square root.

The general architecture of the prognostic approach to estimate fuel cell and battery SOHs using UKF is shown in Figure 4.2 [201]. Through the input reference currents of fuel cell and battery ( $u_k$ ) and the real output voltages ( $y_k$ ) measured by sensors, UKF is used to estimate and modify the unobserved state parameters ( $x_k$ ) of their degradation model. With the right estimated state parameters, their SOHs can be determined.

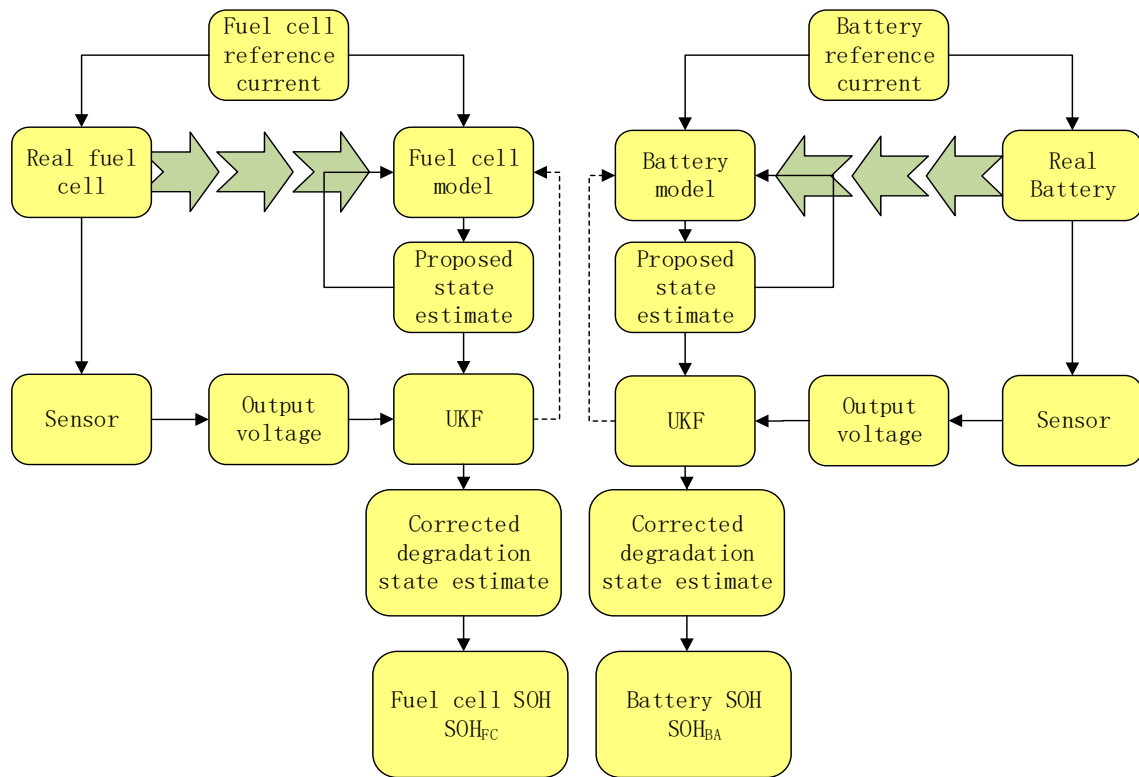


Figure 4.2: The general architecture of prognostic approach for estimation of power sources SOHs

### 4.3 Fuel cell degradation and on line state of health estimation

Upon long term operation of PEMFC, its main components including membrane, electrodes, bipolar plates, gas diffusion layers, and sealing gaskets would undergo mechanical, chemical and electrochemical degradation changes resulting in the decrease of fuel cell performance over time[202]. The presented fuel cell degradation model is designed based on the built fuel cell model in Section 3.2.2. The sample time of fuel cell aging process is much higher than the dynamical model. So for the degradation model, all the dynamical change of fuel cell is neglected. The static voltage of the PEMFC can be described in equation (4.12)[203]

$$E = N_{cell} * \left( E_{rev} - A * \ln\left(\frac{I_{FC}}{I_0}\right) - R * I_{FC} - B * \ln\left(1 - \frac{I_{FC}}{I_{max}}\right) \right) \quad (4.12)$$

According to the previous study of [204] [205], the resistance  $R$  and maximum current  $i_{max}$  have large variations along with fuel cell degradation, which are chosen as the degradation state parameters. Their variations with time can be described in equation (4.13) and (4.14)[206]

$$R(t) = R_0 (1 + \alpha(t)), \quad I_{max}(t) = I_{max0} (1 - \alpha(t)) \quad (4.13)$$

$$\alpha(t) = \beta * t \quad (4.14)$$

where  $R_0$  and  $I_{max0}$  are the initial value,  $\alpha$  and  $\beta$  represent degradation variance and degradation rate along with time. The fuel cell SOH can be defined in equation (4.15)

$$SOH_{FC} = \frac{\alpha(t) - \alpha_{min}}{\alpha_{max} - \alpha_{min}} \quad (4.15)$$

The estimation of  $SOH_{FC}$  relies on the precise estimation of  $\alpha$  and  $\beta$  through the following discrete nonlinear system in equation (4.16), (4.17)

$$x_{k+1} = A * x_k + w_k \quad (4.16)$$

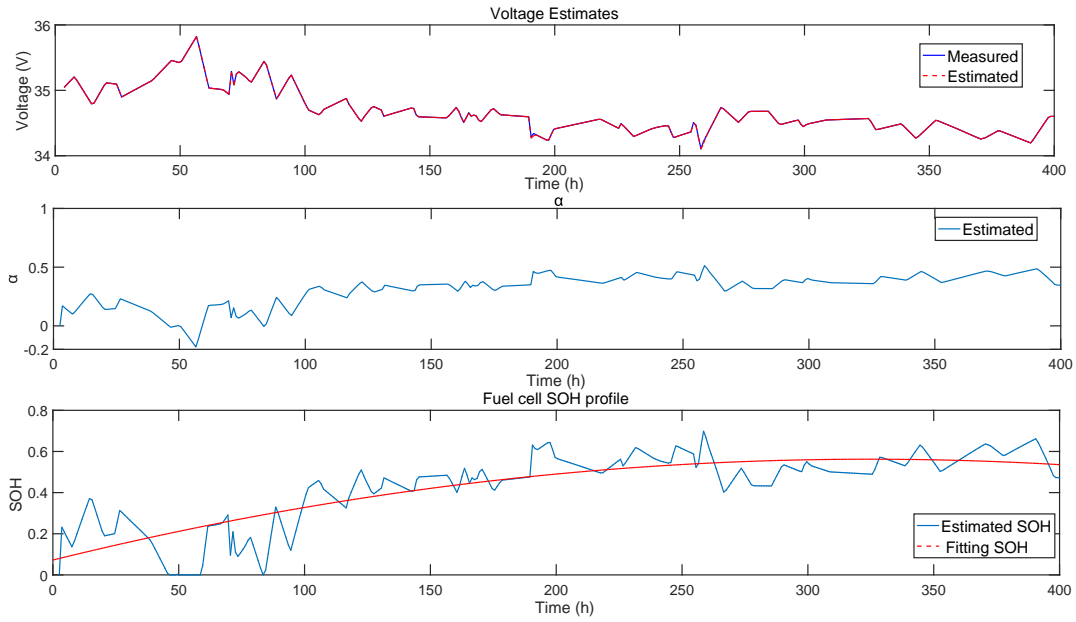
$$y_k = g(x_k, u_k) + v_k \quad (4.17)$$

where  $x_k = [\alpha, \beta]^T$  is the state variable,  $A = [1, T; 0, 1]$ ,  $y_k$  is the fuel cell voltage,  $w_k$  and  $v_k$  are process and observation noises,  $u_k$  is the input current load,  $g(x_k, u_k)$  is described as (4.12). In order to verify the validation of fuel cell degradation model, a PEMFC experimental degradation voltage dataset is used, which is achieved through a 400-h experimental degradation test on a 1.2 kW commercial Ballard NEXA PEM fuel cell stack. The fuel cell output current keeps at 12A for the whole experimental period. Fuel cell degradation model is used to estimate the fuel cell voltage along with the experimental test. The variation of degradation parameters of fuel cell degradation model is determined by UKF based on the on-line measured fuel cell voltage through voltage sensor. The measured and estimated fuel cell voltages, estimated degradation parameter and SOH along with time are shown in Figure 4.3.

It can be observed from Figure 4.3, the estimated fuel cell voltages through UKF accurately fit with the measured voltages from the experimental data, which can prove the accuracy of the online estimation model. The negative degradation parameter  $\alpha$  and its fluctuations are due to the reversal of fuel cell degradation. When  $\alpha$  is less than 0, its value is set as zero. With the estimated value of  $\alpha$ , the fuel cell SOH can be calculated through equation (4.15) and its range is (0,1). It also can be observed that the general trend of fuel cell SOH in red color increases along with time.

## 4.4 Battery degradation and on line state of health estimation

Regarding the battery model described in Section 3.2.4,  $q_{s,n}$ ,  $q_{b,n}$ ,  $q_{s,p}$ ,  $q_{b,p}$ ,  $V_{o,p}'$ ,  $V_{o,n}'$ ,  $V_r'$  are taken as states variables  $x$ , and battery output voltage  $V$  as the output variable

Figure 4.3: Estimation of the stack voltage, degradation parameter  $\alpha$  and SOH

y. Along with battery degradation, some physical ageing phenomenon can be observed such as the solid electrolyte interface (SEI) layer growth, lithium corrosion, lithium loss of lithium plating and changes in diffusion property[207]. The battery model fitting results for the aged battery can be seen in 4.4.

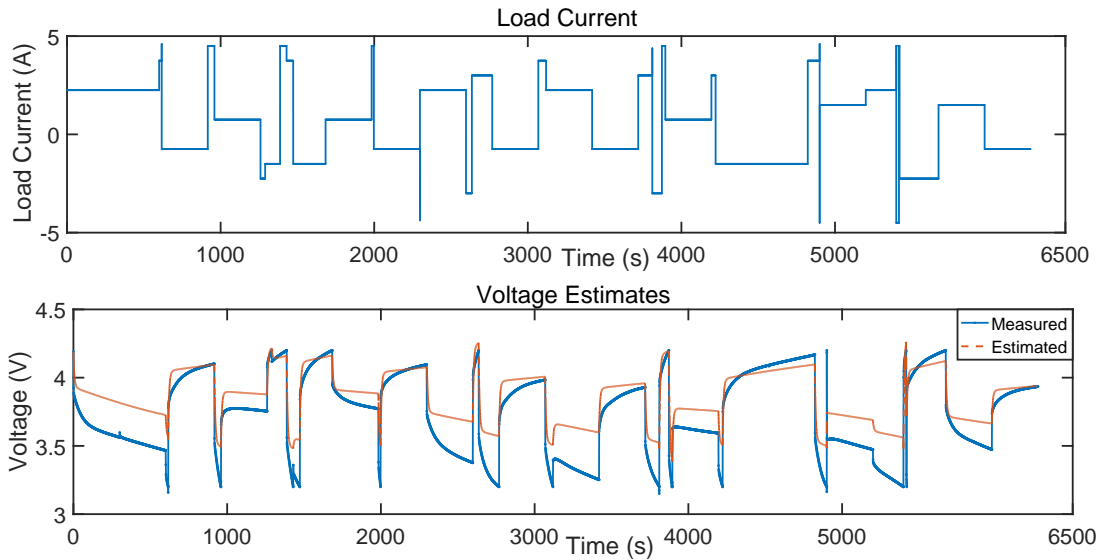


Figure 4.4: Battery model fitting for the aged battery

It can be observed that the errors between the estimated battery voltage and real measured voltage is large so some parameters of battery model should be changed along with battery aging. For the electro-chemistry based model, the maximum charge  $q_{max}$ , which stands for the loss of active Li ions due to degradation, the internal resistance  $R$  representing SEI layer growth and other factors and the diffusion constant  $D$  are selected as the aging parameters of battery ageing model. Along with the degradation,  $q_{max}$  decreases,

$R$  and  $D$  increase. The state of health of battery can be calculated according to  $q_{max}$ , defined in equation (4.18)

$$SOH_{BA} = \frac{q_{max}^{int} - q(t)}{q_{max}^{int} - q_{max}^{min}} \quad (4.18)$$

where  $q_{max}^{int}$  battery initial maximum charge,  $q_{max}^{min}$  is defined as the 50% of the  $q_{max}^{int}$ , which is also the threshold of battery end of life.  $q(t)$  is battery maximum charge at time  $t$ .

The aging parameters ( $q_{max}$ ,  $R$ ,  $D$ ) change in time as a function of usage. The dynamical change rate can be described as:

$$q_{max}' = w_q |i_{app}| \quad (4.19)$$

$$R' = w_R |i_{app}| \quad (4.20)$$

$$D' = w_D |i_{app}| \quad (4.21)$$

where  $i_{app}$  is the applied current,  $w_q$ ,  $w_R$  and  $w_D$  are the aging rate parameters.

The experimental test of random charge/discharge sequences of battery can well simulate battery operations in the vehicle due to its randomness. Therefore, a 3140 minutes experimental test data is used to verify the validation of battery degradation model. The modification of battery degradation parameters is determined by UKF based on the on-line measured battery voltages from the 3140 minutes experimental test. The measured and estimated battery voltages, estimated degradation parameters  $q_{max}$  and its SOHs along with time are shown in Figure 4.5 and Figure 4.6.

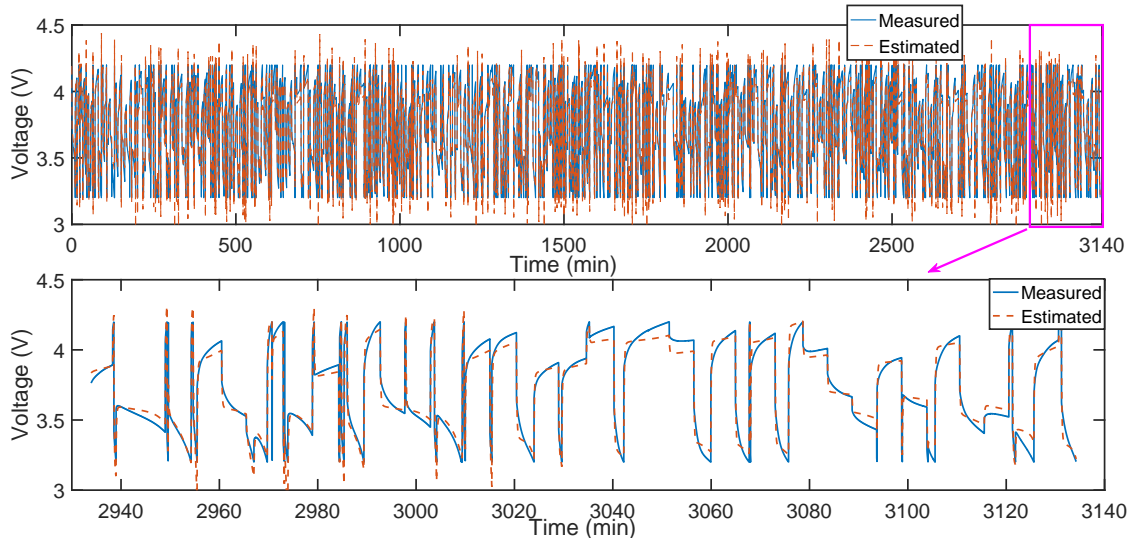


Figure 4.5: Battery degradation model fit for aged battery

With the added degradation state parameters, the battery voltage estimated by UKF and its degradation model can match well with the measured voltage over the random charge/discharge sequences. Some errors are still present which are due to temperature effects. The internal battery temperature changes over time are not considered in the degradation model. The change of battery charge/discharge currents leads to the variation

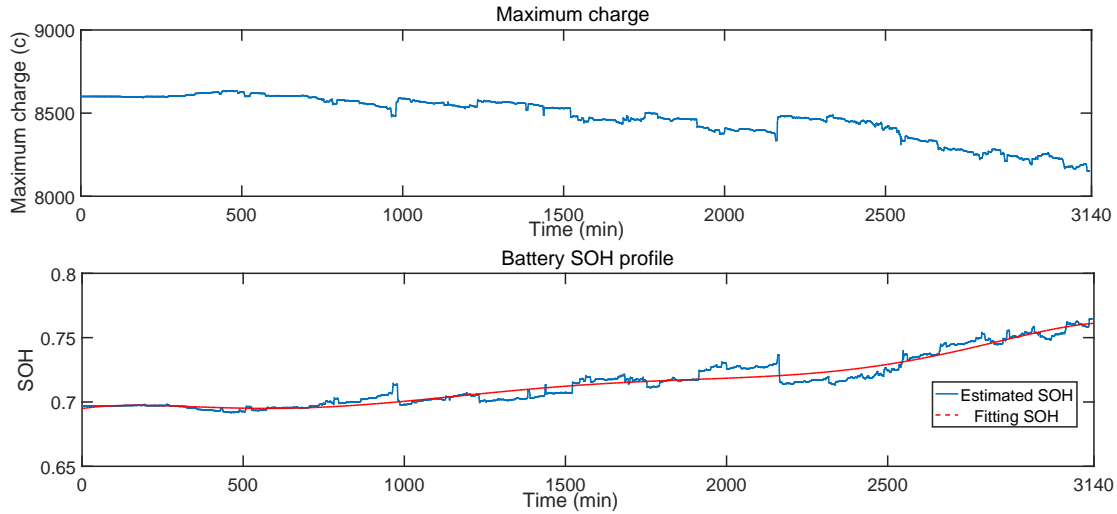


Figure 4.6: On-line UKF estimates of the degradation state parameter and SOH

of battery degradation state, which results in the fluctuation of the decreasing trend of  $q_{max}$  in Figure 4.6. According to the estimated  $q_{max}$  value, battery SOH can be calculated through equation (4.18) and its range is (0,1). Even though there are some fluctuations of SOH, the whole trend of battery, which is shown as the line in red color, increases along with time meaning the increase of battery degradation. Meanwhile, the battery SOC also can be precisely estimated with decreasing  $q_{max}$  along with time based on equation (3.44).

## 4.5 ECMS with power sources degradation

### 4.5.1 The effect of power sources degradation on ECMS

Along with fuel cell degradation, the fuel cell output voltage decreases, but auxiliary power doesn't change, so efficiency decreases. When fuel cell is fully degraded, its SOH is equal to 1 means the fuel cell voltage has decreased 10%, the efficiency changes in Figure 4.7.

It can be observed that the efficiency of aged fuel cell is all less than new fuel cell. The maximum efficiency decreases from 42.83% to 41.37%, but the maximum efficiency point occurs at the same current point 9.5A. So, the parameter  $\eta_{opt}$  and  $\eta_{max}$  of  $K_{FC}$  should change with fuel cell degradation degree.

In order to analyze the effects of power sources degradation on the designed ECMS, four degradation conditions of fuel cell and battery are considered in Table 4.1. The simulation results for four conditions are shown in Figure 4.8, in order to facilitate describing different conditions, they are defined as FHBH, FDBH, FHBD and FDBD respectively. The simulation results are shown in Table 4.2. Every condition is analyzed respectively in detail.

From Figure 4.8 and Table 4.2, it can be observed that the fuel cell of FHBH starts at 443s and it fluctuates around the maximum efficiency point due to battery and supercapacitor SOC variations. The battery final SOC is almost equal to its initial value. FHBH has the least maximum battery SOC variation which is defined as the difference between

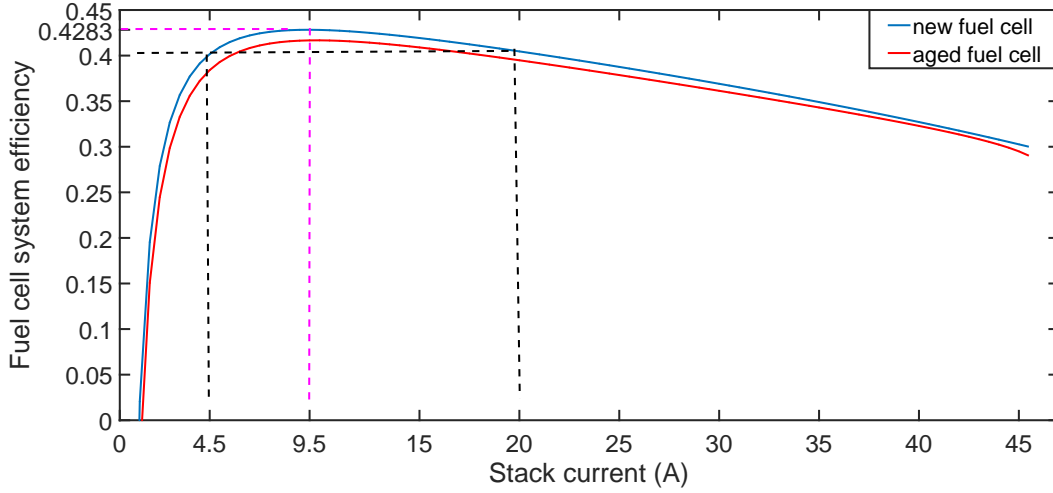


Figure 4.7: Comparative results of fuel cell system efficiency between new fuel cell and aged one

Table 4.1: Four degradation conditions of power sources

Condition	$SOH_{FC}$	$SOH_{BA}$
FHBH	0	0
FHBD	0	1
FDBH	1	0
FDBD	1	1

Table 4.2: Simulation results of ECMS for four conditions

	FHBH	FDBH	FHBD	FDBD
hydrogen consumption (g)	15.1	14.0	16.0	16.1
battery initial SOC	0.8	0.8	0.8	0.8
battery final SOC	0.7939	0.7849	0.7934	0.7809
battery SOC variation	0.0147	0.0225	0.0279	0.363
supercapacitor initial SOC	0.8	0.8	0.8	0.8
supercapacitor final SOC	0.7115	0.3699	0.6661	0.2363
supercapacitor SOC variation	0.5884	0.6072	0.5969	0.6223

maximum battery SOC and minimum battery SOC during the whole drive cycle period.

Compared to FHBH, the fuel cell of FHBD starts earlier, the battery final SOC is almost equal to FHBH. But due to the decrease of battery capacity and the increase of battery resistance along with its degradation, the battery SOC variation for the whole drive cycle is larger than FHBH, meanwhile, this also leads to larger fluctuation amplitude of fuel cell current. Final hydrogen consumption of FHBD is 16g increasing 5.625% than FHBH.

Compared to the other three conditions, the fuel cell of FDBH starts at the latest, which is due to the decrease of fuel cell efficiency and the increase of EF. The lower battery SOC is needed to trigger the operation of fuel cell. The fuel cell current of FDBH is larger than FHBH on the whole due to low battery SOC. Final battery SOC FDBH is 0.7849 and the difference between the initial and final value increases by 59.6% than FHBH, which

cannot meet the battery charge sustenance requirement.

FDBD has the largest battery and supercapacitor SOC variations and the final SOC's are the least. FDBD also has the most hydrogen consumption and fuel cell current is larger than the other three conditions when fuel cell is started.

Through the analysis of four degradation conditions, it can be concluded that compared to the health state, the battery degradation leads to more variable battery SOC, more fluctuation of fuel cell current around maximum efficiency point, more hydrogen consumption and earlier fuel cell start-up, but final battery SOC is not affected. Fuel cell degradation makes its maximum efficiency value decrease but corresponding fuel cell current doesn't change. The trigger time of fuel cell start-up is delayed and battery final SOC changes much to the initial SOC, which cannot be allowed for the charge sustenance of FCHEV. In the real situation, fuel cell and battery degrade together and the operation results of the vehicle are worse than single power source degradation.

#### 4.5.2 Adaptive equivalent consumption minimization strategy

Equivalent factor is an important parameter for the equivalent consumption minimization strategy. For an assigned known driving mission, a constant equivalent factor is enough to reach an optimal solution. But when fuel cell and battery degrade, the former constant equivalent factor cannot guarantee the charge-sustenance and optimal fuel consumption. In order to solve this problem, adaptive equivalent consumption minimization strategy (AECMS) is proposed through adjusting equivalent factors according to SOHs of power sources [157]. The variation of equivalent factors is defined in equation (4.22)(4.23)

$$\lambda_{BA} = \lambda_{BA0} * (1 + 0.193 * SOH_{FC}) * (1 + 0.193 * SOH_{BA}) \quad (4.22)$$

$$\lambda_{SC} = \lambda_{SC0} * (1 + 0.193 * SOH_{FC}) * (1 + 0.193 * SOH_{BA}) \quad (4.23)$$

where  $\lambda_{BA0}$  and  $\lambda_{SC0}$  are initial battery and supercapacitor equivalent factors.

The degradation of battery leads to the increase of fuel cell current variation in the whole drive cycle, which means the increase of fuel cell degradation rate. In order to increase fuel cell lifetime, fuel cell dynamical change rate limitation in equation (2.1) is adjusted according to battery SOH in equation (4.24)

$$dI = dI_0 * (1 - 0.5 * SOH_{BA}) \quad (4.24)$$

The architecture of the AECMS control system for FCHEV is shown in Figure 4.9. Based on the built degradation model of power sources and UKF, their SOHs are estimated. The equivalent factor and dynamical change rate of fuel cell are changed according to their SOHs to make sure the normal operation of the vehicle, increase the durability of power sources, and keep the stability of control system.

## 4.6 Simulation results and analyses

The simulation results of equivalent consumption minimization strategy are shown in Figure 4.10 and Table 4.3.

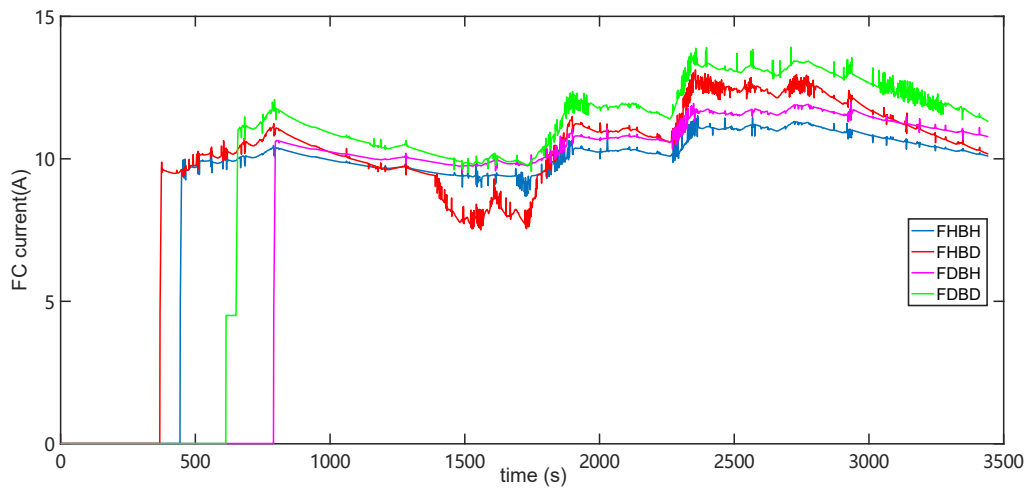
Table 4.3: Simulation results of AECMS for four conditions

	FHBH	FDBH	FHBD	FDBD
hydrogen consumption (g)	15.1	17.7	17.4	19.8
battery initial SOC	0.8	0.8	0.8	0.8
battery final SOC	0.7939	0.7953	0.8	0.8
battery SOC variation	0.0147	0.0157	0.0245	0.0258
supercapacitor initial SOC	0.8	0.8	0.8	0.8
supercapacitor final SOC	0.7113	0.7620	0.8	0.8
supercapacitor SOC variation	0.5884	0.5967	0.6183	0.6032

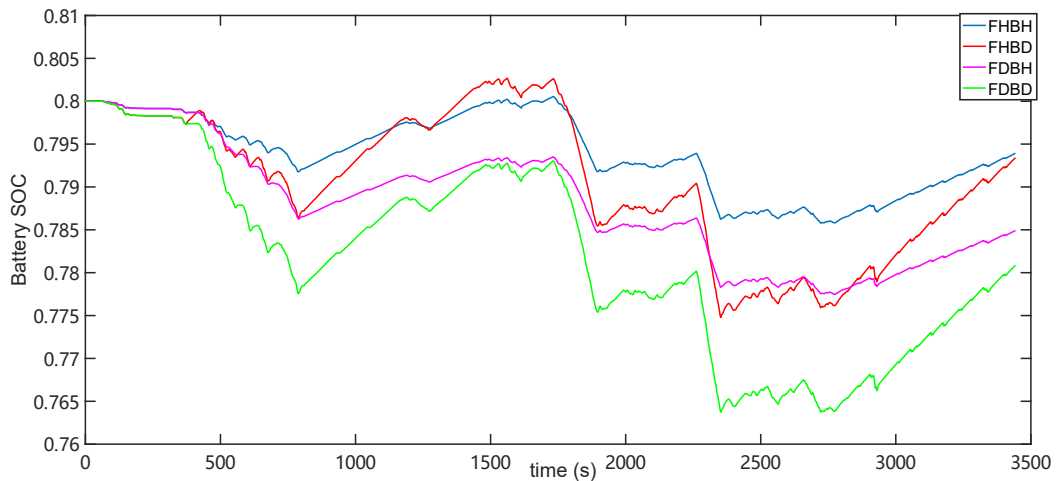
From Figure 4.10 and Table 4.3, it can be observed that all battery final SOCs of three degradation conditions of fuel cell and battery are above 0.79 meaning that the charge sustenance requirement of energy storage sources is met. AECMS is the further development of designed SECMS in Section 3.3.1 based on the online estimation of SOHs of fuel cell and battery, which has been proved that it can be used into the real vehicle through the real experimental degradation data. AECMS plays the full potential of fuel cell, battery and supercapacitor: fuel cell supplies steady energy and seeks for the maximum efficiency in the high efficiency zone, battery is operated as the main energy buffer and its charge sustenance is kept at the end of drive cycle and supercapacitor supplies peak power. The designed AECMS can make sure the normal operation of vehicle even though power sources have degraded seriously. It should be mentioned that when fuel cell and battery SOHs reach 1, it doesn't mean the fuel cell and battery cannot work anymore and it just means that the probability that power sources fail is very high. In case of serious damage and bringing inconvenient to normal life, power sources should be replaced in advance.

## 4.7 Conclusion

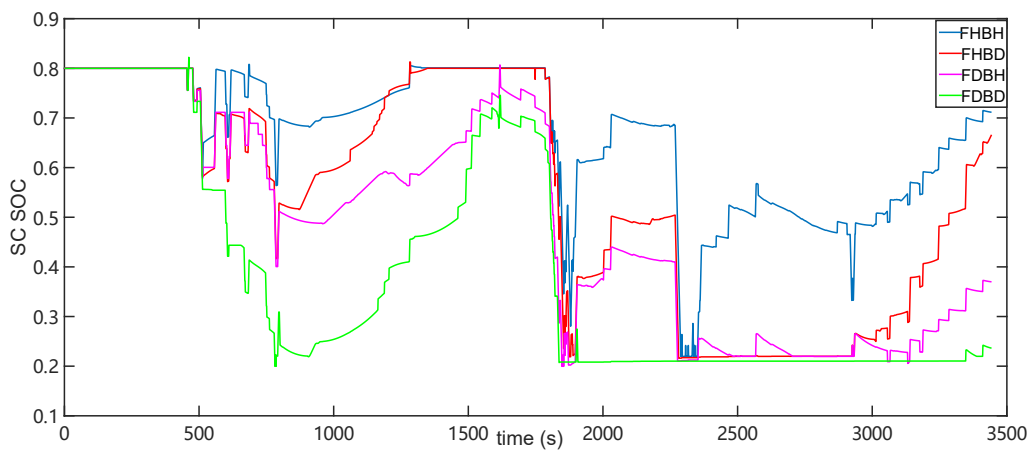
Along with vehicle operation, fuel cell and battery degrade which affects the normal operation of designed SECMS. So UKF is chosen to estimate the state of health of power sources due to its low computation cost and high precision and then the state of health are considered into SECMS. Four conditions of power sources degradation are simulated and according to simulation results, the effects of power sources degradation on SECMS are analyzed. The equivalent factor and dynamical change rate of fuel cell are tuned along with the degradation state of power sources to ensure the charge sustenance of battery and the increase of fuel cell lifetime, which lead to the development of AECMS based on the SECMS.



(a) Fuel cell current profile along the cycle



(b) Battery SOC profile along the cycle



(c) Supercapacitor SOC profile along the cycle

Figure 4.8: Comparative results of ECMS under different power sources degradation conditions

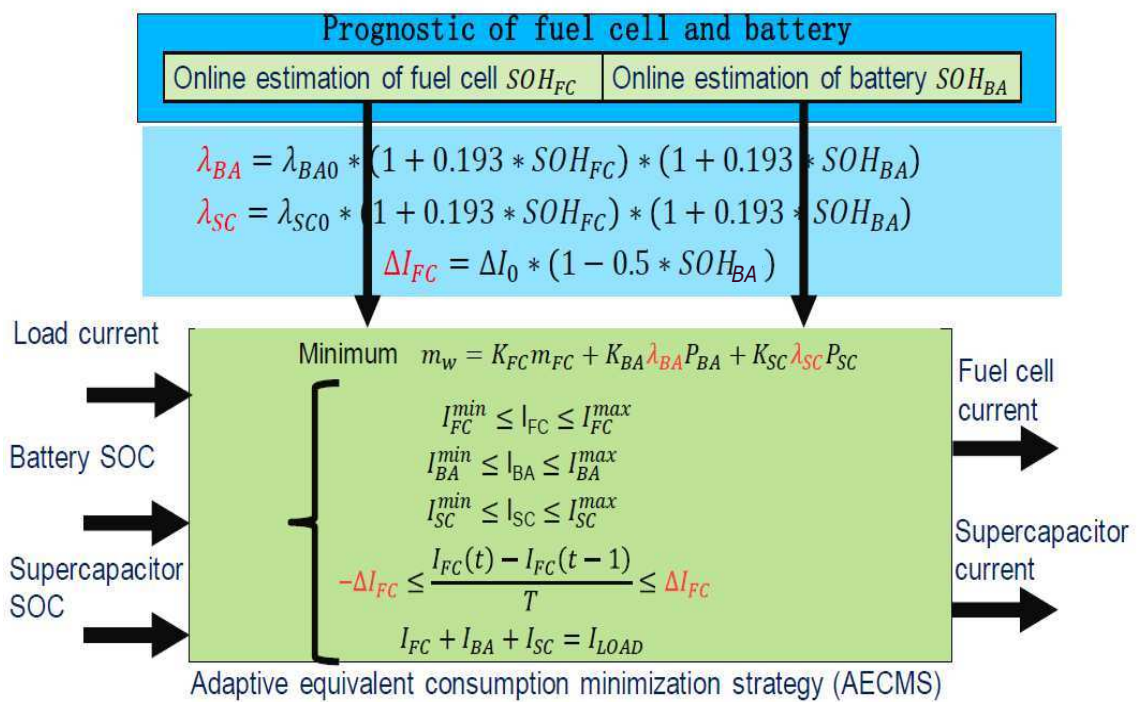
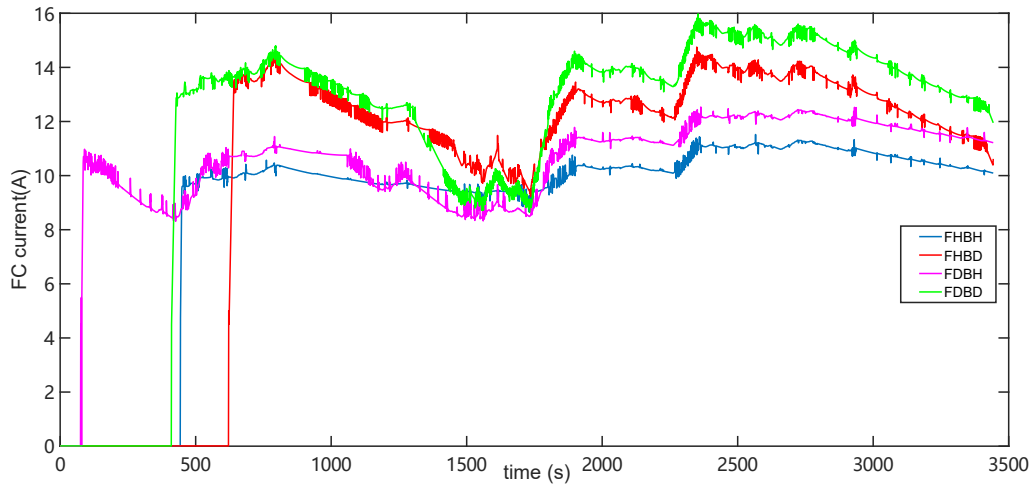
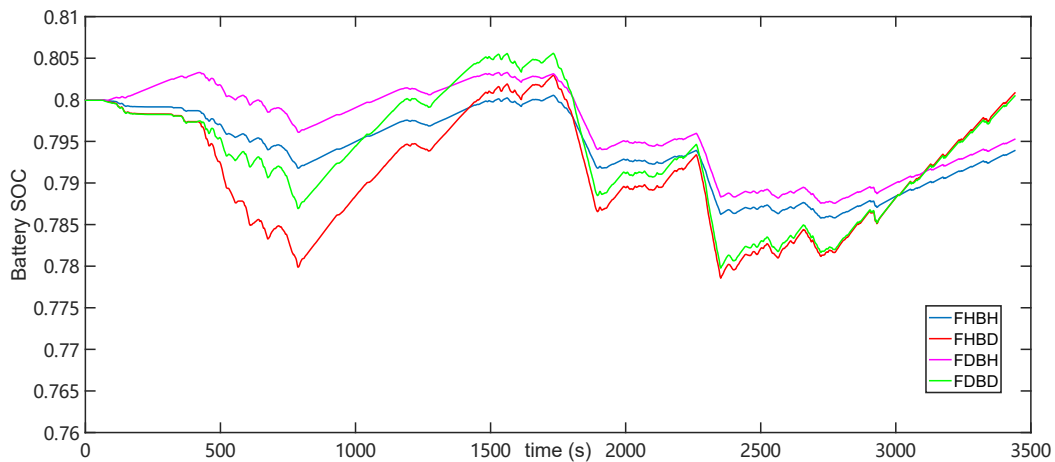


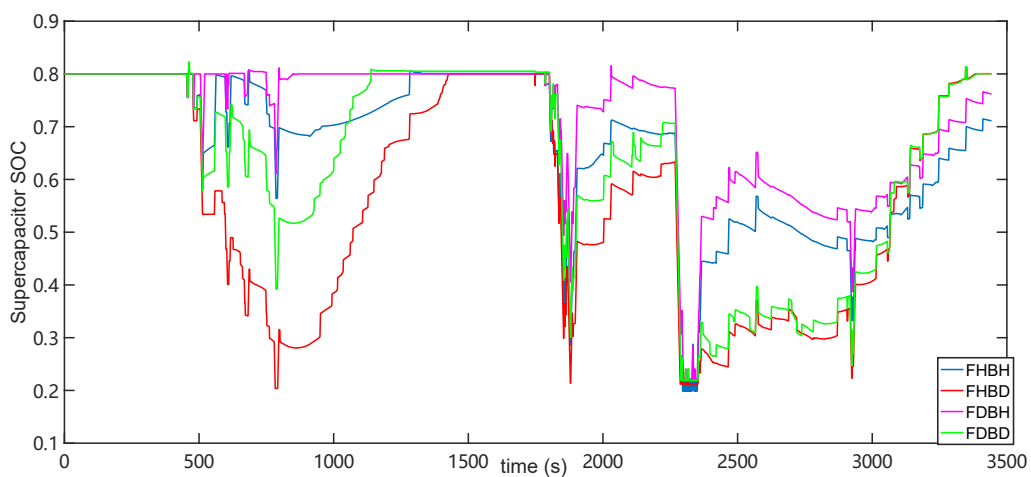
Figure 4.9: Control system of AECMS for FCHEV



(a) Fuel cell current profile along the cycle



(b) Battery SOC profile along the cycle



(c) Supercapacitor SOC profile along the cycle

Figure 4.10: Comparative results of AECMS under different power sources degradation conditions

## Experimental validation

### 5.1 Introduction

In order to experimentally validate the developed energy management strategies in the previous chapter, a test bench is needed. The experimental conditions are quite different from those in simulation and particularly for the control of power sources. The fuel cell system and energy storage sources are controlled by their own control system. The test bench is composed of the software system and hardware system. Figure 5.1 shows the schematics of the rapid-prototyping test bench used to validate the energy management system. The software part of the test bench includes the control program, which will be downloaded and operates in the dSPACE MicroAutobox, and ControlDesk software to monitor, modify and record the operation variables. The control program is built in Matlab/Simulink. Hardware system includes main equipment like MicroAutobox, power sources, DC/DC converters, sensors, power supply and electrical load.

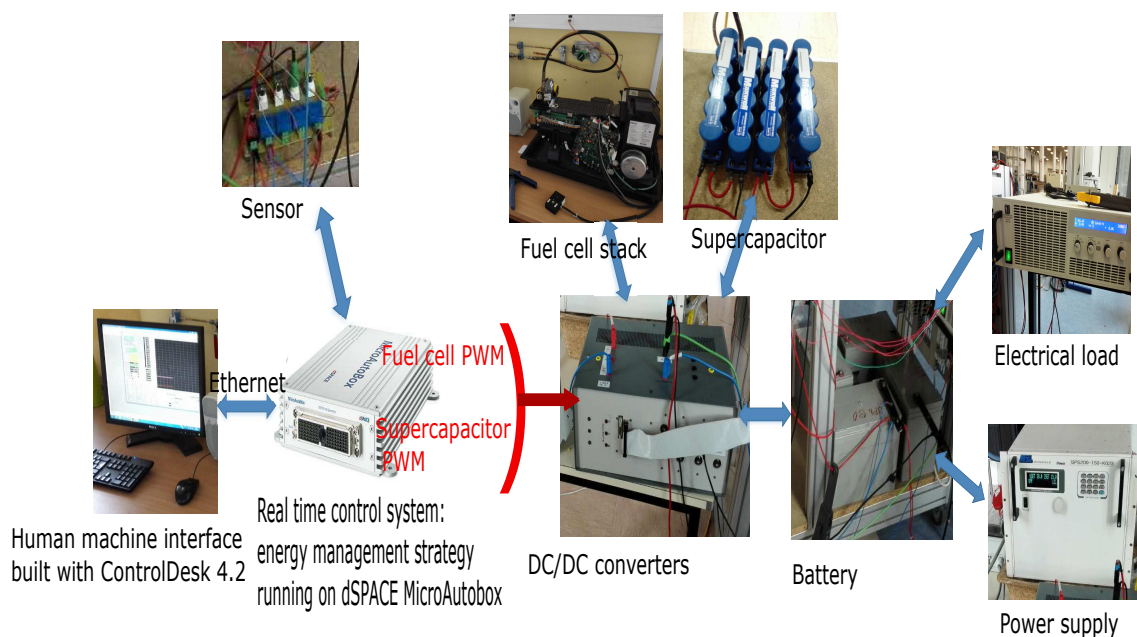


Figure 5.1: Schematics of the rapid-prototyping test bench used to validate the energy management system

## 5.2 Test bench

### 5.2.1 Software system

The dSPACE system provides fast processor and comprehensive real time interface which is installed directly in the personal computer. dSPACE real time interface allows the user to automatically implement MATLAB/Simulink models on dSPACE hardware via code generated by Real-Time Workshop. In order to test the designed energy management strategy, which is built in the Simulink, the entire I/O blocks are needed to read the information of sensors and output the control signals to the actuators. I/O blocks can be simply dragged from the real time interface I/O library to build the I/O model in the Simulink. The input I/O model convert analog signal to digital signal. On the contrary, the output I/O model is the digital-to-analog converter. Transformation functions are needed from I/O simulation block value to the real measurement signal value from sensors for both input and output I/O model. At the same time, a filter is needed to connect with input block to filter sensor noise. Input and output models are shown in Figure 5.2 and Figure 5.3.

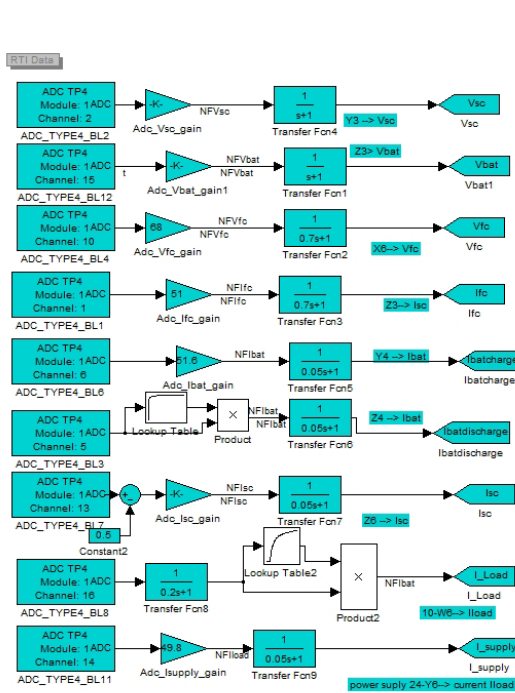


Figure 5.2: Input I/O model

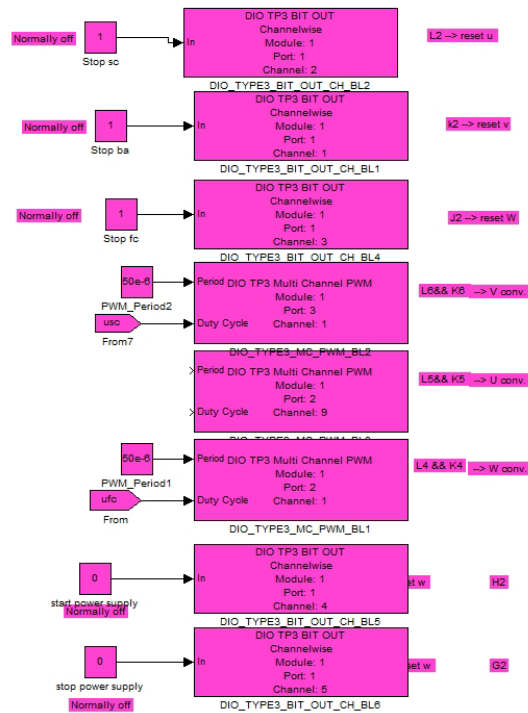


Figure 5.3: Output I/O model

The designed energy management strategies cannot be experimentally tested directly and other assisting controls are needed to ensure the normal operation of the test bench's components and control the fuel cell and supercapacitor currents. Therefore a hierarchical control architecture taken by the software system is proposed which consists of a two-level control loop: the high-level control loop corresponding to energy management strategy and the low-level control loop mainly corresponding to DC/DC converter control, which is shown in Figure 5.4. The low-level control also includes the control of power supply and electronic load to supply power profile of the drive cycle.

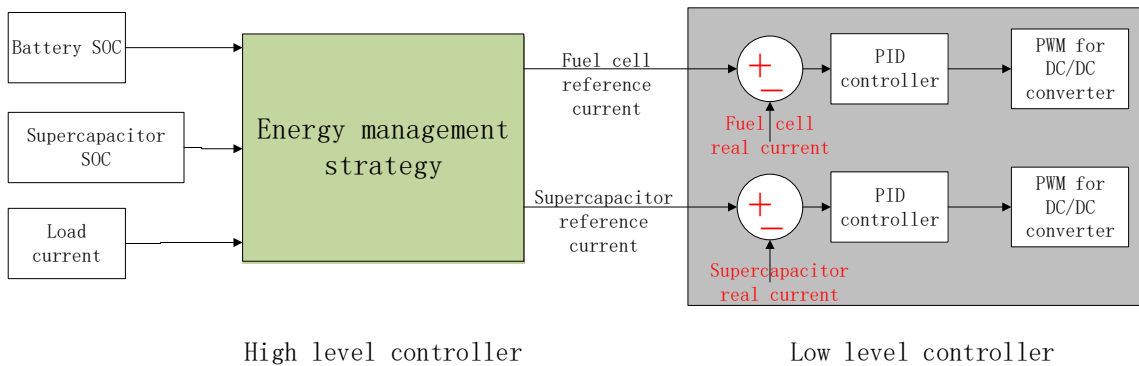


Figure 5.4: Hierarchical control architecture

The hierarchical control is implemented using a dSPACE AutoBox II programmable controller, which is a system based on Matlab/Simulink environment. For the low-level control, once the reference currents of fuel cell and supercapacitor are defined by the high-level control loop, two classical PI controllers are applied to adjust duty cycles of PWM signals to control the real fuel cell and supercapacitor output currents to track reference currents. The PWM signals are produced by MicroAutoBox II and are inputted into corresponding DC/DC converters connected to fuel cell and supercapacitor respectively. The low-level control loop is shown in the red zone in Figure 5.4.

### 5.2.2 Hardware system

This section details the hardware part of the studied system. The test bench is composed of three power sources: fuel cell, battery and supercapacitor. Fuel cell and supercapacitor are connected in parallel to the DC bus through DC/DC boost converters and buck/boost converter respectively. Battery is connected to DC bus directly. Power supply and electronic load cooperate to supply power requirement of the drive cycle. Some sensors to detect the current and voltage of components are also essential for the test bench. Rapid prototyping platform based MicroAutoBox II and human machine interface (HMI) through the computer are also needed. The architecture of the test bench is shown in Figure 5.5.

The fuel cell stack is commercialized 1.2 kW Ballard NEXA PEMFC, which has 47 cells. Four battery packs are connected in series. Overall capacity and voltage of battery packs are 90Ah and 48V respectively. The supercapacitor package is composed of four Maxwell supercapacitors, which is two strings of two supercapacitors in parallel. The rated capacitance of each supercapacitor is 58F.

A boost DC/DC converter for fuel cell and a buck/boost DC/DC converter for supercapacitor are packed into one box in parallel architecture as shown in Figure 5.6. The DC bus voltage is held by battery voltage. Each DC/DC converter consists of two IGBT transistors which are operated by two complementary PWM signals from MicroAutoBox II.

Power supply and electronic load cooperate as the drive cycle simulator and are programmed to supply negative current and positive current of drive cycle respectively, which are both connected to the DC bus directly. The control methods for power supply and electronic load are decided by their production company. The drive cycle chosen to test

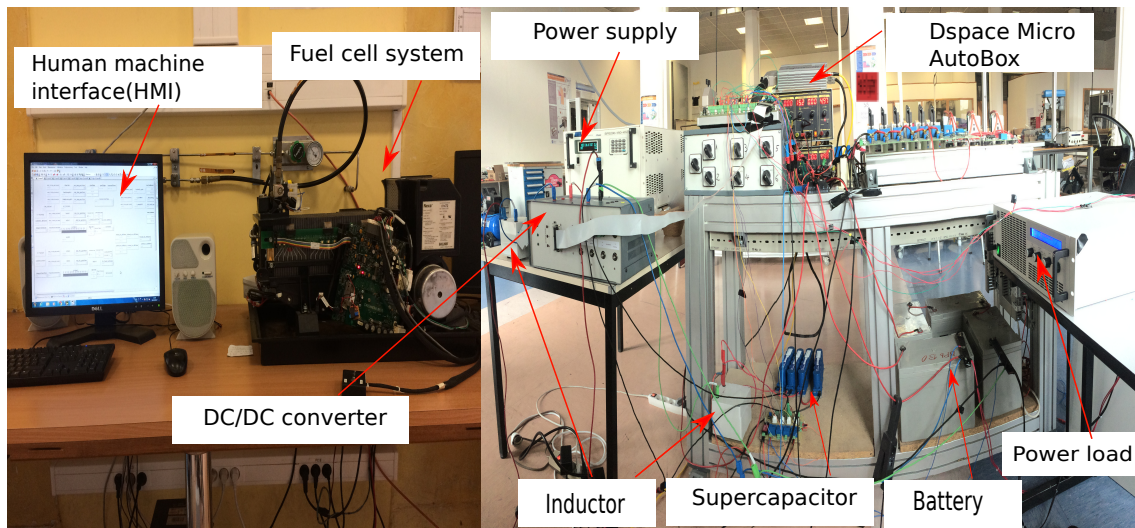


Figure 5.5: Test bench architecture



Figure 5.6: DC/DC converters

the energy management strategies is programmed in the low-level control loop and also downloaded into MicroAutoBox II. The power profile is provided as power values along with time from Matlab workspace. DC bus current profile can be calculated through battery voltage in real time. The current control signals are transformed and inputted into the power supply and the electronic load through MicroAutoBox II. Real output currents from the power supply and electronic load are tested by their inside sensors and are gathered by MicroAutoBox II as feedback. The control of power supply and electronic load by MicroAutoBox II are shown in Figure 5.7. Taking electronic load control for example, the MicroAutoBox II is connected to 15 poles Sub-D socket on the back side of the electronic load which is provided for remote control of the electronic load via analog signals or

switching conditions. The input voltage range of the electronic load from 15 poles Sub-D socket is 0-10 V, which corresponds to 0-100% maximum input current of the electronic load. The MicroAutoBox II controls the electronic load current through adjusting the voltage values that are inputted to the electric load through 15 poles Sub-D socket. The control to the power supply is similar to the electronic load.

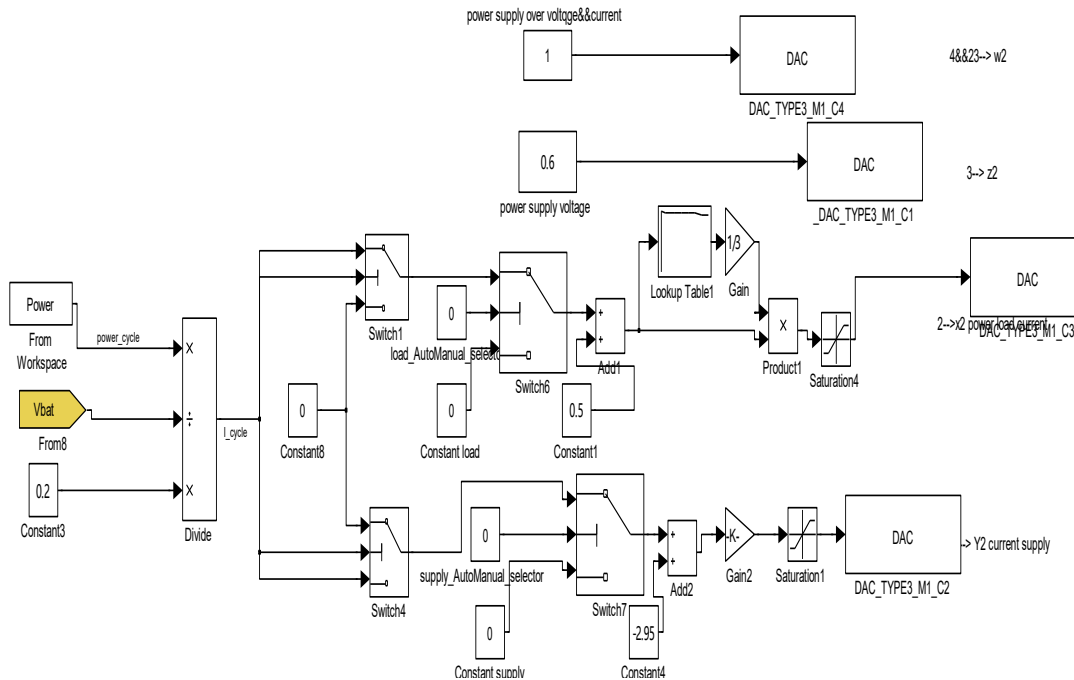


Figure 5.7: Control of power supply and electronic load through MicroAutoBox II

MicroAutoBox II shown in Figure 5.8 is a real-time system for performing fast function prototyping in full pass and bypass scenarios. It operates without user intervention, just like an ECU. MicroAutoBox II can be used for many different rapid control prototyping applications such as power train, chassis control, body control, advanced driver assistance systems, electric drives control, X-by-wire applications, and aerospace applications. MicroAutoBox II from dSPACE is used as the control unit due to its ability to be programmed by Matlab/Simulink directly. Through the dSPACE prototyping system, new control strategies can be developed, optimized and tested in a real environment quickly without manual programming. Easy-to-use library with numerous interface functionalities lets you connect inputs and outputs to the model. It should be mentioned that all sensor signals should be converted into digital form by using built-in 16-bit analog to digital converters and are retrieved by applying suitable mathematical operations. With all gathered control signals needed by energy management strategy, the reference currents of fuel cell and supercapacitor are calculated, through two PI controllers. 20 KHz PWM signal is inputted into the corresponding DC/DC converter through the prototyping system.

Some measurement instruments and sensors are used to measure current and voltage of relevant components. For the low-level control, the currents of all power sources are measured. Fuel cell current and supercapacitor current are used as feedback signals in PI controllers of Figure 5.4. Battery current is directly used to estimate the battery SOC. For the high-level control, both DC bus voltage and supercapacitor voltage are measured, where the first one is also the battery voltage and the second one is used to estimate supercapacitor SOC. Some sensor signals are not in the range  $[0, 4.5V]$ , which is only



Figure 5.8: MicroAutoBox II

accepted range for MicroAutoBox II. Some transform instruments are designed to do the transformation from high voltage into low voltage. The current and voltage sensors are shown in Figure 5.9.

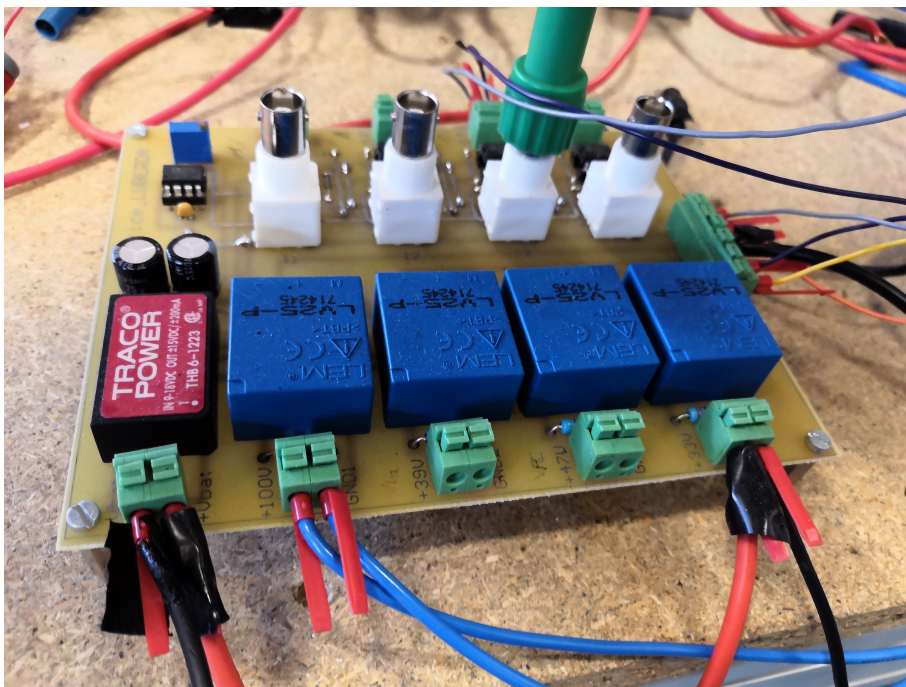


Figure 5.9: Current and voltage sensors

Human machine interface in the computer is designed using the ControlDesk 4.2 program in Figure 5.10. ControlDesk 4.2 is the dSPACE experiment software for seamless ECU development. It performs all the necessary tasks and gives you a single working environment, from the start of experimentation right to the end. Its usage is simple just based on drag and drop. It allows the development of a complete interface in a very short time (much shorter than an interface in C or C++ for example).

ControlDesk 4.2 allows communication with MicroAutoBox II in order to visualize



The load power profile of the drive cycle can be calculated according to the power train model in Section 3.2.1. According to the parameters of the power train, the load power profile is downsized shown in Figure 5.11. The DC bus voltage is held by battery. So Figure 5.12(a) shows the bus voltages of three control strategies corresponding to the drive cycle. Due to the charge/discharge of battery, its voltages fluctuate around 50V. Due to different battery current profile achieved through three energy management strategies, the battery voltages of three energy management strategies are also different but the difference is small.

Based on the load power profile and battery voltage profile, the load current profile on DC bus can be calculated shown in Figure 5.12(b). In the test bench, the negative current of bus representing the braking energy of the vehicle is recycled by the electronic load and the positive current meaning the forwarding energy is supplied by the power supply. Reference current in blue color is required reference current of the drive cycle. Red positive current and green negative current are controlled to track reference current. From the zoomed load current, it can be observed that the current profile of drive cycle can be well supplied through the power supply and electronic load.

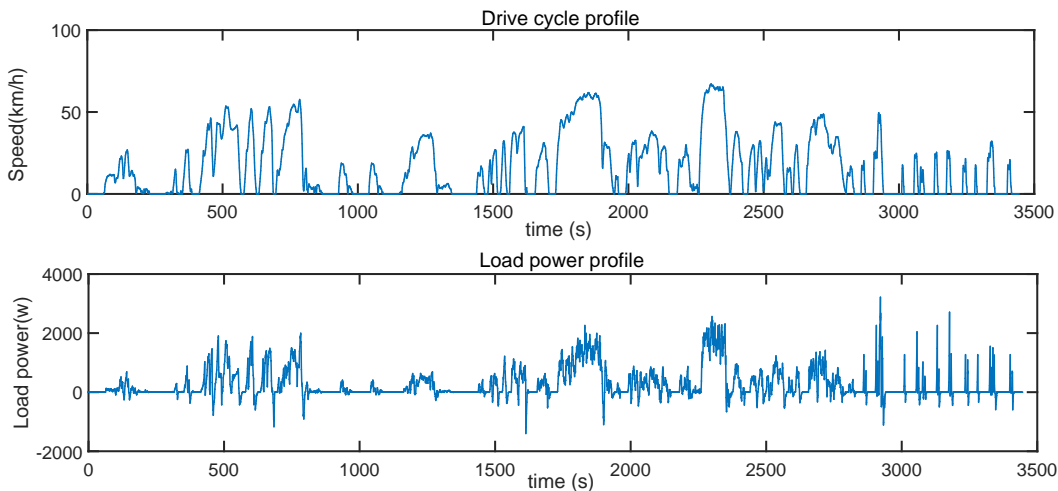


Figure 5.11: Drive cycle profile and load power profile

From the experimental test on the built test bench, the comparative results of battery SOC for experiment and simulation are shown in Figure 5.13. The comparisons of fuel cell current, battery current and supercapacitor current for experiment and simulation results of SECMS are shown in Figure 5.14.

From Figure 5.13 and Figure 5.14, it can be observed that regarding SCEMS, the experimental results of fuel cell current and battery current are similar to simulation results. The experimental results of fuel cell current are a little higher than simulation results but the differences are all lower than 0.5A. The final simulation result of battery SOC is 0.792 similar to the experiment value 0.7915. The difference is negligible. Supercapacitor current is sensitive to the current requirement of the drive cycle, fuel cell current and battery SOC, therefore small sensor noise and process calculation noise lead to the little difference between experimental supercapacitor current and simulated one of SECMS. Considering low energy density of supercapacitor and its role as the supplier of peak power, this difference can be neglected.

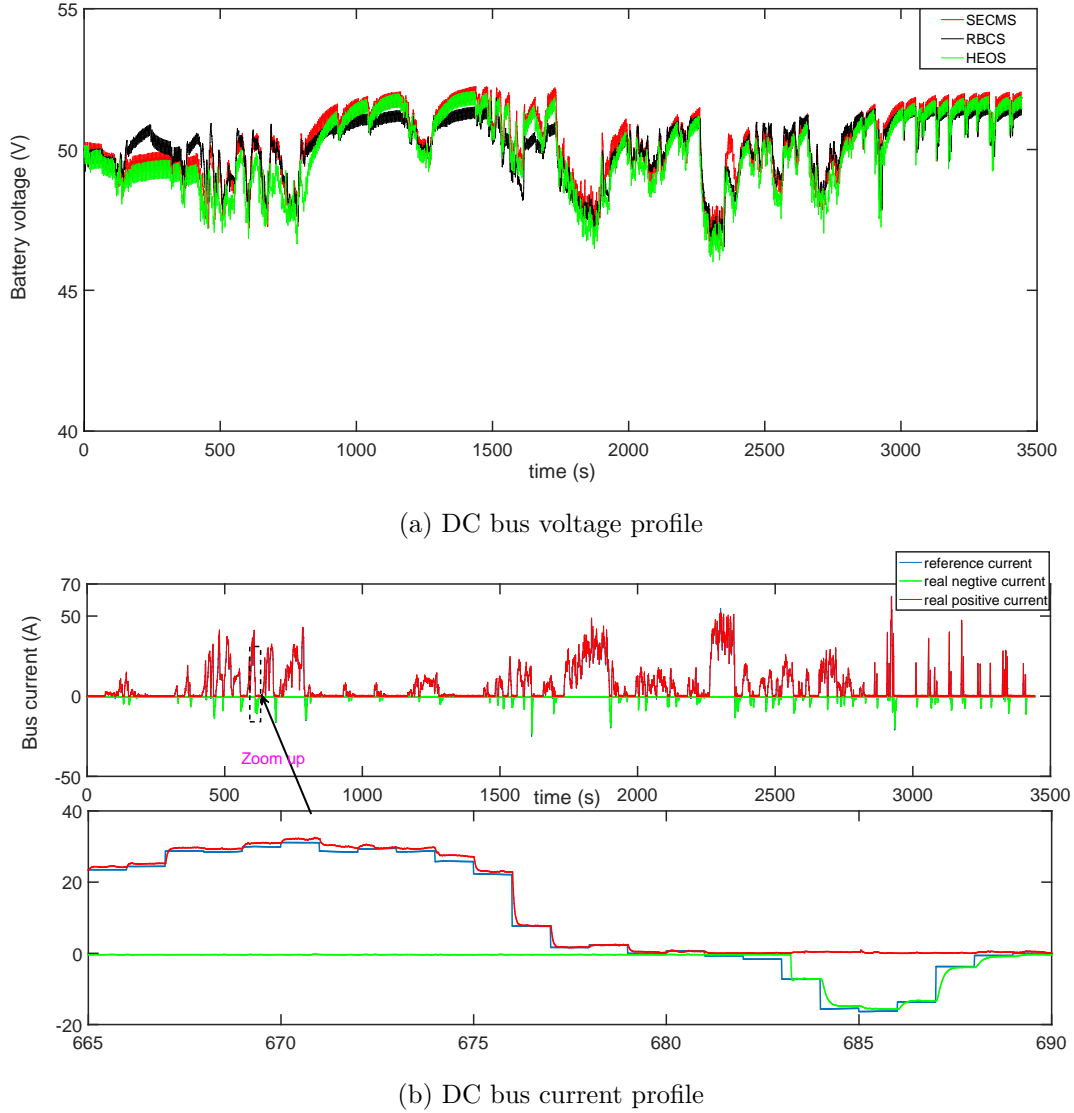


Figure 5.12: DC bus voltage profile and current profile

From the experimental test of the emulated driving cycle, the battery SOC, supercapacitor SOC, fuel cell current, battery current and supercapacitor current for three control strategies are shown in Figure 5.15 and Figure 5.16. The experimental comparison results are shown as Table 5.1.

Table 5.1: Experimental results

EMSs	SECMS	RBCS	HEOS
Initial supercapacitor and battery SOC	0.8	0.8	0.8
Final supercapacitor SOC	0.5865	0.8304	0.8199
Final battery SOC	0.7915	0.7946	0.7906
Hydrogen consumption (L)	194.07	210.35	194.77
Equivalent hydrogen consumption (L)	225.06	230.02	228.42

As shown in Figure 5.15, battery SOC and supercapacitor SOC of three control strate-

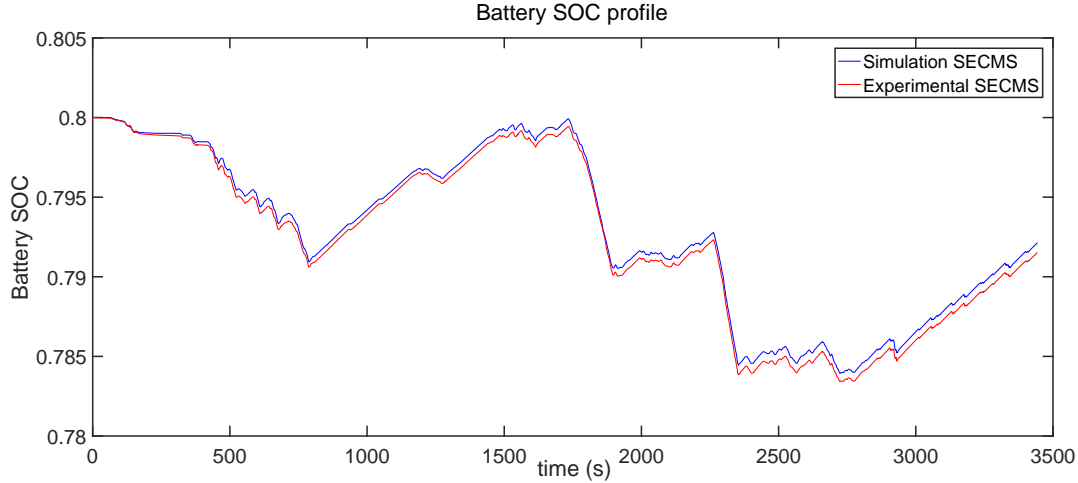


Figure 5.13: Comparison of experiment and simulation results of battery SOC

gies are in the limited range (0.2, 0.8) and (0.1, 0.9) respectively. According to Table 5.1, the final battery SOC of three control strategies are almost equal to initial values. The difference between initial battery SOC and final battery SOC of HEOS is the largest among three control strategies. The hydrogen consumption of Table 5.1 represents fuel cell real hydrogen consumption at the end of drive cycle. The final battery SOC, supercapacitor SOC and hydrogen consumption at the end of the drive cycle are different for three control strategies. In order to make a fair comparison of hydrogen consumption, the final battery and supercapacitor SOC variation should also be considered into the equivalent hydrogen consumption. Because three battery final SOC are all less than the initial value, when drive cycle is over, fuel cell is operated at maximum efficiency point 9.5A to charge battery until its SOC value increases to initial SOC value. Supercapacitor also charges or discharges to let its SOC be back to 0.8. The sum of hydrogen consumption to charge battery SOC back to initial SOC and hydrogen consumption for the end of drive cycle is defined as the equivalent hydrogen consumption. It can be observed that equivalent hydrogen consumption of SECMS is the least, RBCS is the most. Taking RBCS as the basis, the decrements of SECMS and HEOS are 2.16% and 0.69%. Compared to HEOS, ECMS decreases 1.47%.

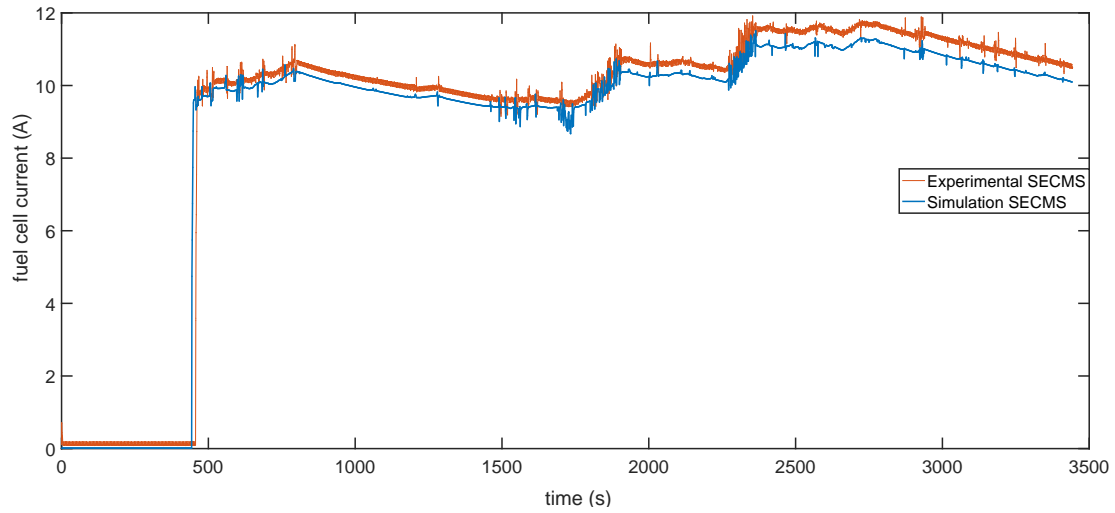
As shown in Figure 5.16 (a), all fuel cells of three strategies are operated in high efficiency zone [0.4 0.428]. Regarding SECMS and HEOS, fuel cell currents are around maximum efficiency point. The fuel cell of SECMS and HEOS start at 454.8s and 462.9s respectively and they keep working until the end of the drive cycle. The current of RBCS changes along with current demand at DC bus. It can be noted that the fuel cell degradation of RBCS is the highest due to its high dynamical change of current reference. In Figure 5.16 (c), supercapacitor only supplies peak power conforming to original design objective. It also can be observed that supercapacitor charge/discharge at different time and hold different period of time for three strategies. Battery passively supplies other DC bus current besides fuel cell current and supercapacitor current on the DC bus in Figure 5.16(b). In Figure 5.17, the fuel cell reference currents of SECMS and HEOS are shown. It can be observed that HEOS has more current spikes than SECMS. The current spikes of HEOS are supplied by supercapacitor of SECMS to ensure the steady of fuel cell current. In the whole, SECMS consumes the least hydrogen, has the most steady current

change and less on/off cycles. HEOS has similar fuel cell current as SECMS but with more spike current change and consumes more hydrogen. RBCS has the highest hydrogen consumption. The fuel cell dynamical current changes much and frequent on/off cycles are included which mean that it has the most degradation for the overall drive cycle.

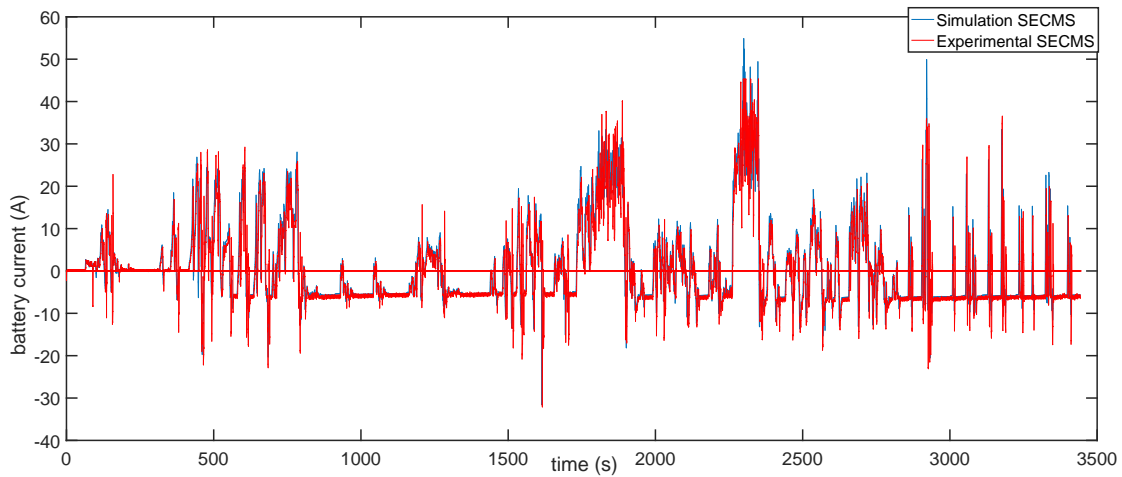
## 5.4 Conclusion

This chapter has presented the test bench used to validate the designed energy management strategies. The test bench includes the software system and hardware system. The software system takes hierarchical control architecture. The high-level is the designed energy management strategy and the low level is assisting control to the energy management strategy which includes two PID controllers to control the DC/DC converters and other controllers to control the power supply, electronic load, transformation of input sensor signals and transformation of output control signals. The equipment of the hardware system such as power sources, sensors, power supply, power supply and rapid prototyping unit are specified. SECMS can then be experimentally tested and comparative results can prove the precision of the simulation model of the fuel cell hybrid electric vehicle and reliability of the test bench.

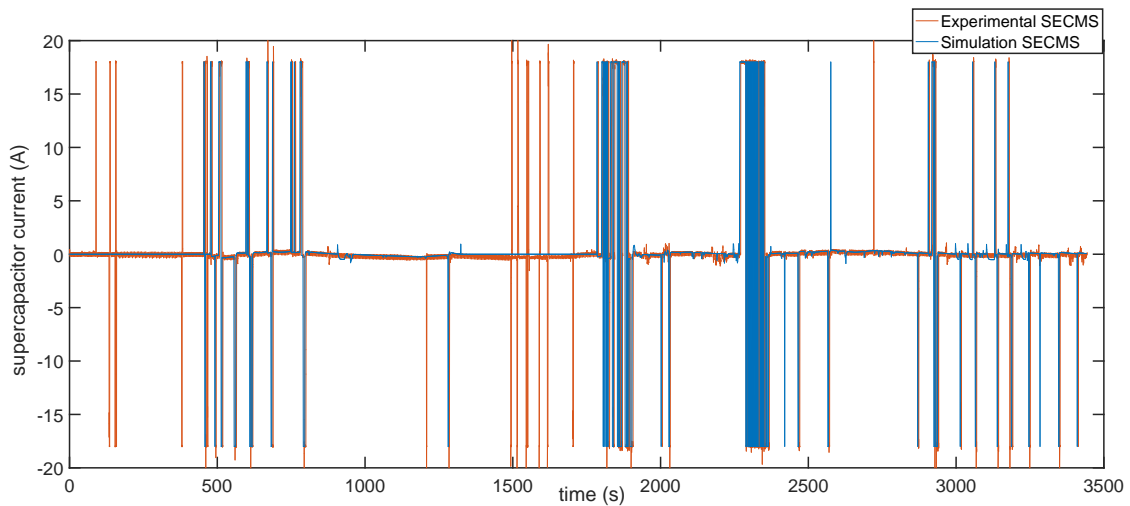
For the SECMS strategy, fuel cell is operated to seek for the maximum efficiency point in the defined high efficiency zone, while the battery assumes as the main energy storage source to buffer energy demand by vehicle and the supercapacitor dedicates to provide the peak power. In order to prove the superiority of the new approach, the RBCS and HEOS also have been implemented in the test-bench with same drive cycle. The experimental results show that the proposed SECMS has the least hydrogen consumption and offers the longest durability of fuel cell.



(a) Fuel cell current profile along the cycle

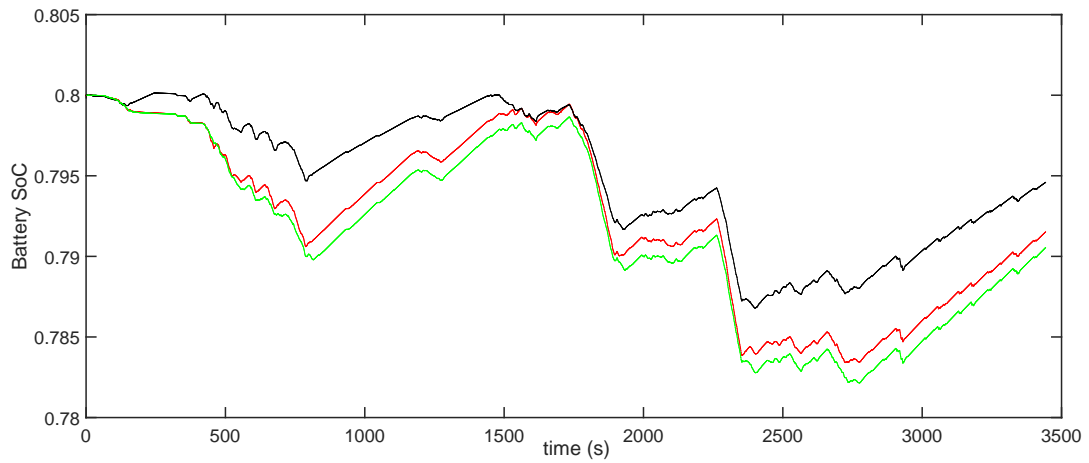


(b) Battery current profile along the cycle

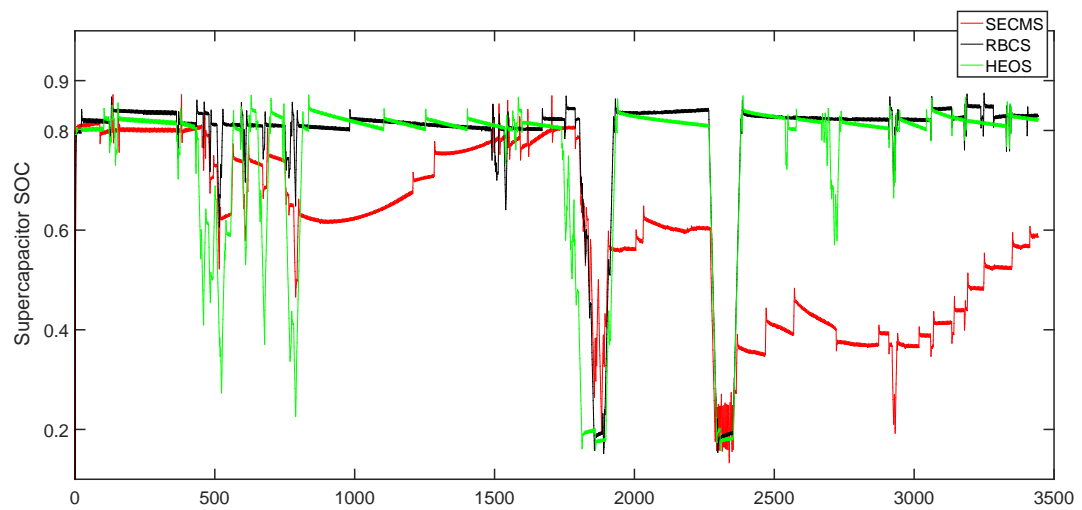


(c) Supercapacitor current profile along the cycle

Figure 5.14: Comparison of experiment and simulation results of SECMS

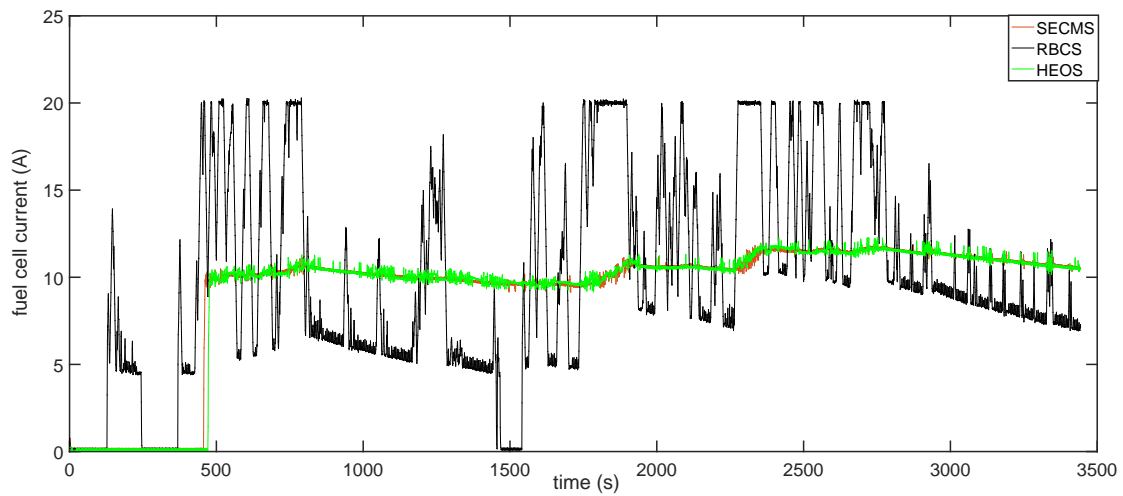


(a) Battery SoC profile along the cycle

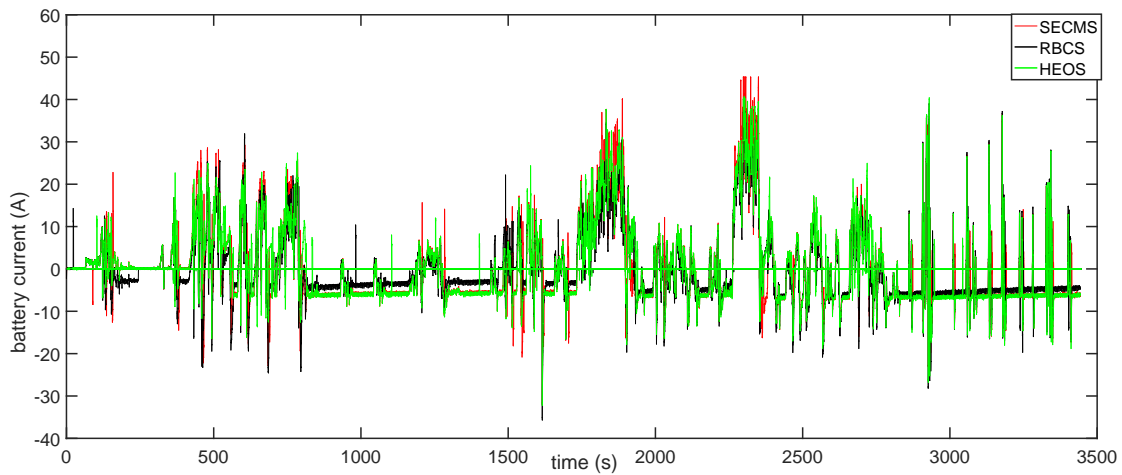


(b) Supercapacitor SOC along the cycle

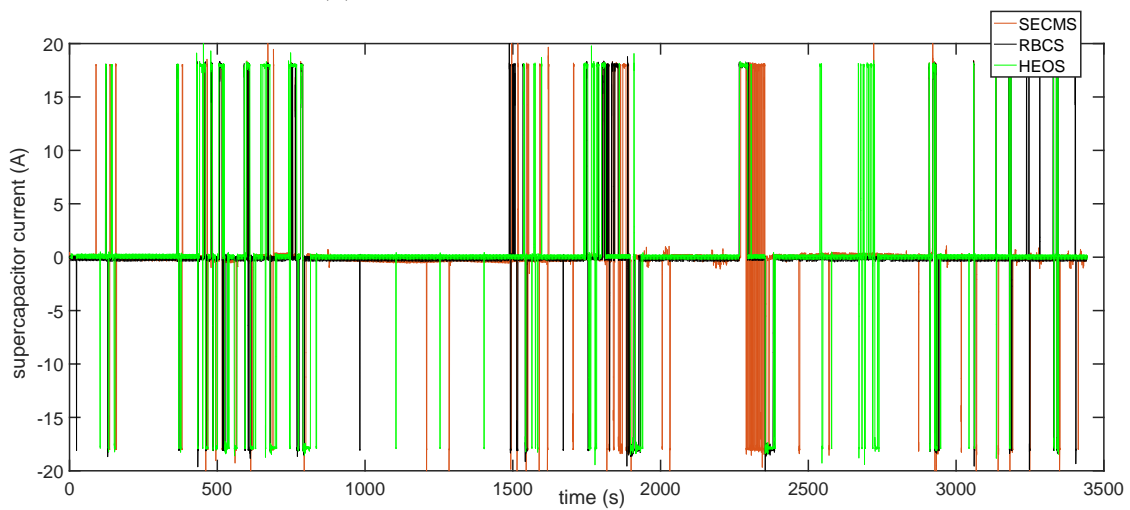
Figure 5.15: Experimental results of battery SOC and supercapacitor SOC



(a) Fuel cell current profile along the cycle



(b) Battery current profile along the cycle



(c) Supercapacitor current profile along the cycle

Figure 5.16: Experimental results of fuel cell, battery and supercapacitor current for three control strategies

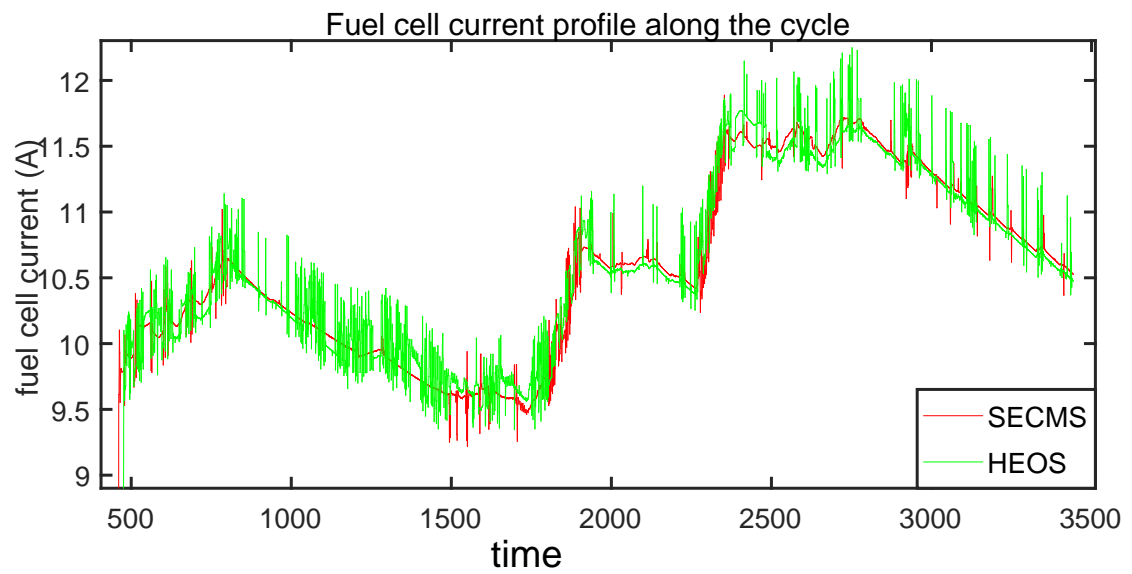


Figure 5.17: Comparison of fuel cell reference currents for SECMS and HEOS



## General conclusion

This dissertation has focused on the energy management strategies for fuel cell hybrid electric vehicle powered by fuel cell, battery and supercapacitor. In order to keep the stability of energy management strategy under the condition of power sources' degradation, the state of health of power sources are estimated on-line and are also considered into energy management strategy. At first, a start-of-the-art review of fuel cell hybrid electric vehicles is presented. Since the advantages of hydrogen: energy saving due to the high efficiency of fuel cell, energy security due to not relying on fossil fuels, and reducing carbon production in power transportation, a number of automobile manufacturers and various government agencies put forward many projects to develop fuel cell technology for use in the transportation system. The main projects to develop fuel cell vehicles of USA, Europe, Japan and China are introduced and technical targets of fuel cell vehicles of four countries are summarized.

Then, since fuel cell cannot supply high dynamical change power and recycles braking energy, energy storage sources are chosen to operate with fuel cell. However, fuel cell hybrid electric vehicle architecture with multiple power sources complicates the development of energy management strategy. In order to facilitate the design of energy management strategy, the characteristics of power sources are presented. Energy management strategies are classified into rule based strategy, frequency based strategy and optimization based strategy. The detail operation methods and advantages/disadvantages of every kind of energy management strategies are introduced. The objectives and methods to fulfill them are also reviewed for different energy management strategies.

Afterward, based on the state-of-the-art review of energy management strategies, equivalent consumption minimization strategy is chosen for fuel cell hybrid electric vehicle with fuel cell, battery and supercapacitor three power sources. Due to the low energy density of supecapacitor, its equivalent hydrogen consumption is neglected in most references, which not only counters to the aim of minimizing whole hydrogen consumption but also increases the complication of energy management strategy due to the need of an additional energy management strategy to calculate supercapacitor power demand. Thus, a SECMS strategy is proposed to consider the energy cost of all three power sources into the objective function to solve this problem. At the same time, a RBCS and HEOS strategies are also compared to demonstrate the superiority of SECMS in minimizing the hydrogen consumption and prolonging fuel cell lifetime.

Next, the power sources degradation was taken into account in the energy management strategies. Because the unscented Kalman filter has not only higher accuracy than extended Kalman filter but also lower computation cost than particle filter, it is chosen to

estimate the state of health of fuel cell and battery. Through the analysis of power sources degradation on SECMS strategy, it could be concluded that battery degradation leads to more variable battery state of charge, more fluctuations of fuel cell current around maximum efficiency point, more hydrogen consumption and earlier fuel cell operation. The degradation of fuel cell mainly affects the efficiency of fuel cell stack, equivalent factors and charge sustenance of battery. With the on-line estimated state of health, AECMS is designed based on the tune of fuel cell efficiency and equivalent factors with the degradation of power sources. In order to prolong the lifetime of fuel cell, its dynamical change rate is also adjusted according to its state of health. The simulation results show that the AECMS can ensure the normal operation of vehicle, the charge sustenance of battery and the increase of fuel cell durability.

Finally, in order to validate the proposed energy management strategies, a test bench is built. Its both hardware system and software system are introduced in detail. A hierarchical control architecture is set for the software system. The designed energy management strategies belong to the high-level of the hierarchical control system. Reference currents of fuel cell and supercapacitor are determined by this high level control. A low level control is designed based on PID control strategy to generate corresponding PWMs to control the outputs of DC/DC converter to follow the reference currents. The components of the hardware system like power sources, power supply, electronic load and sensors are presented. The validation of power supply and electronic load to emulate the power profile of the drive cycle is proved. The simulation results of SECMS and experimental results are compared and the results show that a good agreement proving the precision of models and the reliability of the test bench. RBCS and HEOS are also tested on the test bench. The experimental comparative study shows that SECMS is operated at around maximum efficiency, supercapacitor supplies peak power, battery works as the main energy buffer. The charge sustenance objective of battery is fulfilled. Compared with RBCS and HEOS, SECMS hydrogen consumption decreases 2.16% and 1.47% respectively. SECMS also has the most stable fuel cell current, so the degradation of fuel cell due to dynamical current change is the least. The neglect of supercapacitor equivalent hydrogen consumption in the equivalent consumption minimization strategy is not optimal, which also can be proved through the comparison of SECMS and HEOS.

This dissertation mainly introduces the AECMS for fuel cell hybrid electric vehicle powered by fuel cell battery and supercapacitor considering power sources degradation. Minimizing hydrogen consumption, seeking for maximum efficiency of fuel cell and increasing the stability of energy management strategy and lifetime of power sources are reached through the AECMS. However, there are a number of challenges and improvements that can be considered in the future works:

Besides the state of health of power sources, the equivalent factor of equivalent consumption minimization strategy is also affected by the drive cycles, which should keep accordance with the features of current driving cycle and adjust its value in real time. Drive cycle recognition and prediction can be helpful to find optimal equivalent factors, so multiple power sources can achieve optimal power distribution and the fuel economy, stability and charge sustenance of energy storage sources can be improved with tuning equivalent factor. Drive cycle recognition and prediction can be considered in the energy management strategy in the future works. The designed AECMS was only tested in the built test bench. Applying it into the real vehicle will be done in the following works, which will be more challenge and conversing to prove its validity.

Minimizing hydrogen consumption, keeping the stability of energy management strategy and increasing fuel cell lifetime were the objectives of AECMS. In the future works, minimizing the overall cost of the vehicle including hydrogen consumption cost, power sources' lifetime cost can also be considered into the objectives to improve the system.

Also, it may be interesting to apply the proposed energy management strategy to other drive train architectures of FCHEV like multiple fuel cell stacks. In addition to the control challenge, the numerical simulations and experimental emulation will also be a big challenge.



# Publications of PhD dissertation

The thesis's contributions lead to several publications :

International Journal with proceeding:

- H. Li, A. Ravey, A. N'Diaye, and A. Djerdir, "A novel equivalent consumption minimization strategy for hybrid electric vehicle powered by fuel cell, battery and supercapacitor," *Journal of Power Sources*, vol. 395, pp. 262-270, 2018.
- H. Li, A. Ravey, A. N'Diaye, and A. Djerdir, "Online adaptive equivalent consumption minimization strategy for fuel cell hybrid electric vehicle considering power sources degradation," *Energy Conversion and Management*.(Accept)

International Conference with proceeding:

- H. Li, A. Ravey, A. N. Diaye, and A. Djerdir, "A Review of energy management strategy for Fuel Cell Hybrid Electric Vehicle," in *2017 IEEE Vehicle Power and Propulsion Conference (VPPC)*, 2017, pp. 1-6.
- H. Li, A. Ravey, A. N. Diaye, and A. Djerdir, "Equivalent consumption minimization strategy for fuel cell hybrid electric vehicle considering fuel cell degradation," in *2017 IEEE Transportation Electrification Conference and Expo (ITEC)*, 2017, pp. 540-544.
- H. Li, A. Ravey, A. N. Diaye, and A. Djerdir, "State of health estimation of lithium-ion batteries under variable load profile," in *IECON 2017 - 43rd Annual Conference of the IEEE Industrial Electronics Society*, 2017, pp. 5287-5291.
- H. Li, A. Ravey, A. N. Diaye, and A. Djerdir, "Equivalent consumption minimization strategy for hybrid electric vehicle powered by fuel cell, battery and supercapacitor," in *IECON 2016 - 42nd Annual Conference of the IEEE Industrial Electronics Society*, 2016, pp. 4401-4406.



# Bibliography

- [1] Das, H. S., Tan, C. W., and Yatim, A. H. M. [Fuel cell hybrid electric vehicles: A review on power conditioning units and topologies](#). *Renewable and Sustainable Energy Reviews* 76 (2017), 268–291.
- [2] Hwang, J.-J., Chen, Y.-J., and Kuo, J.-K. [The study on the power management system in a fuel cell hybrid vehicle](#). *International Journal of Hydrogen Energy* 37, 5 (2012), 4476–4489.
- [3] Li, H., Ravey, A., Diaye, A. N., and Djerdir, A. [A review of energy management strategy for fuel cell hybrid electric vehicle](#). In *2017 IEEE Vehicle Power and Propulsion Conference (VPPC)*, pp. 1–6.
- [4] M. Sabri, M. F., Danapalasingam, K. A., and Rahmat, M. F. [A review on hybrid electric vehicles architecture and energy management strategies](#). *Renewable and Sustainable Energy Reviews* 53 (2016), 1433–1442.
- [5] Fernández, R. I., Cilleruelo, F. B., and Martínez, I. V. [A new approach to battery powered electric vehicles: A hydrogen fuel-cell-based range extender system](#). *International Journal of Hydrogen Energy* 41, 8 (2016), 4808–4819.
- [6] Hwang, J.-J., Hu, J.-S., and Lin, C.-H. [Design of a range extension strategy for power decentralized fuel cell/battery electric vehicles](#). *International Journal of Hydrogen Energy* 40, 35 (2015), 11704–11712.
- [7] Sohn, Y.-J., Kim, M., and Lee, W.-Y. [The computer-aided analysis for the driving stability of a plug-in fuel cell vehicle using a proton exchange membrane fuel cell](#). *International Journal of Hydrogen Energy* 37, 2 (2012), 1893–1904.
- [8] Chan, C. C. [The state of the art of electric, hybrid, and fuel cell vehicles](#). *Proceedings of the IEEE* 95, 4 (2007), 704–718.
- [9] Marks, C., Rishavy, E. A., and Wyczalek, F. A. [Electrovan-a fuel cell powered vehicle](#). In *SAE Technical Paper Series*, SAE International.
- [10] Fletcher, T. P. [Optimal energy management strategy for a fuel cell hybrid electric vehicle](#). Thesis, 2017.
- [11] Qin, N., Raissi, A., and Brooker, P. [Analysis of fuel cell vehicle developments](#). The Florida Solar Energy Center (FSEC) (2014).
- [12] Kreuer, K.-D. [Fuel cells: selected entries from the encyclopedia of sustainability science and technology](#). Springer Science & Business Media, 2012.
- [13] None, N. [2016 annual progress report: Doe hydrogen and fuel cells program](#). Report, 2017-03-09 2017.

- [14] United States Environmental Protection Agency and US Department of Energy. [Compare fuel cell vehicles](https://www.fueleconomy.gov/feg/fcv_sbs.shtml). [https://www.fueleconomy.gov/feg/fcv\\_sbs.shtml](https://www.fueleconomy.gov/feg/fcv_sbs.shtml).
- [15] Larminie, J., and Dicks, A. [Fuel cell systems explained](#), vol. 2. 2003.
- [16] Sharaf, O. Z., and Orhan, M. F. [An overview of fuel cell technology: Fundamentals and applications](#). *Renewable and Sustainable Energy Reviews* 32 (2014), 810–853.
- [17] Khaligh, A., and Li, Z. [Battery, ultracapacitor, fuel cell, and hybrid energy storage systems for electric, hybrid electric, fuel cell, and plug-in hybrid electric vehicles: State of the art](#). *IEEE Transactions on Vehicular Technology* 59, 6 (2010), 2806–2814.
- [18] Jyotheeswara Reddy, K., and Natarajan, S. [Energy sources and multi-input dc-dc converters used in hybrid electric vehicle applications – a review](#). *International Journal of Hydrogen Energy* 43, 36 (2018), 17387–17408.
- [19] Ravey, A. [Design and control strategy of powertrain in hybrid electric vehicles](#). Theses, Université de Technologie de Belfort-Montbéliard, Dec. 2012.
- [20] Deng, J., Bae, C., Marcicki, J., Masias, A., and Miller, T. [Safety modelling and testing of lithium-ion batteries in electrified vehicles](#). *Nature Energy* 3, 4 (2018), 261–266.
- [21] Trovão, J. P., Silva, M. A., Antunes, C. H., and Dubois, M. R. [Stability enhancement of the motor drive dc input voltage of an electric vehicle using on-board hybrid energy storage systems](#). *Applied Energy* 205 (2017), 244–259.
- [22] Veneri, O., Capasso, C., and Patalano, S. [Experimental investigation into the effectiveness of a super-capacitor based hybrid energy storage system for urban commercial vehicles](#). *Applied Energy* 227 (2018), 312–323.
- [23] Deng, D. [Li-ion batteries: basics, progress, and challenges](#). *Energy Science & Engineering* 3, 5 (2015), 385–418.
- [24] Capasso, C., Lauria, D., and Veneri, O. [Experimental evaluation of model-based control strategies of sodium-nickel chloride battery plus supercapacitor hybrid storage systems for urban electric vehicles](#). *Applied Energy* 228 (2018), 2478–2489.
- [25] Ruan, J., Walker, P. D., Zhang, N., and Wu, J. [An investigation of hybrid energy storage system in multi-speed electric vehicle](#). *Energy* 140 (2017), 291–306.
- [26] Mekhilef, S., Saidur, R., and Safari, A. [Comparative study of different fuel cell technologies](#). *Renewable and Sustainable Energy Reviews* 16, 1 (2012), 981–989.
- [27] Elmer, T., Worall, M., Wu, S., and Riffat, S. B. [Fuel cell technology for domestic built environment applications: State-of-the-art review](#). *Renewable and Sustainable Energy Reviews* 42 (2015), 913–931.
- [28] Wang, H., Wang, Q., and Hu, B. [A review of developments in energy storage systems for hybrid excavators](#). *Automation in Construction* 80 (2017), 1–10.
- [29] Lü, X., Qu, Y., Wang, Y., Qin, C., and Liu, G. [A comprehensive review on hybrid power system for pemfc-hev: Issues and strategies](#). *Energy Conversion and Management* 171 (2018), 1273–1291.

- [30] Zhang, C., Jiang, J., Gao, Y., Zhang, W., Liu, Q., and Hu, X. [Charging optimization in lithium-ion batteries based on temperature rise and charge time](#). *Applied Energy* 194 (2017), 569–577.
- [31] Zhang, S., Xiong, R., and Cao, J. [Battery durability and longevity based power management for plug-in hybrid electric vehicle with hybrid energy storage system](#). *Applied Energy* 179 (2016), 316–328.
- [32] Wang, G., Yu, Y., Liu, H., Gong, C., Wen, S., Wang, X., and Tu, Z. [Progress on design and development of polymer electrolyte membrane fuel cell systems for vehicle applications: A review](#). *Fuel Processing Technology* 179 (2018), 203–228.
- [33] None, N. [2017 annual progress report: Doe hydrogen and fuel cells program](#). Report, 2017-05 2018.
- [34] Satyapal, S. [Us department of energy hydrogen and fuel cells program](#).
- [35] David Peterson, R. F. [Historical fuel cell and hydrogen budgets](#). Report, 2017-7-12 2017.
- [36] [Budget](#). <https://www.hydrogen.energy.gov/budget.html>, June 2017.
- [37] U.S.Department of Energy. [Fuel cell technologies program multi-year research, development and demonstration plan](#). Report, 2005.
- [38] [Hydrogen and fuels cells for transport - european commission](#). <https://www.hydrogen.energy.gov/budget.html>.
- [39] Undertaking, S. J. [Annual work plan](#). S2R JU Governing Board, Brussels (2016).
- [40] [Summary of the strategic road map for hydrogen and fuel cells](#). Report, Agency for Natural Resources and Energy, June 23, 2014.
- [41] Ministerial Council on Renewable Energy, Hydrogen and Related Issues. [Basic hydrogen strategy.pdf](#). Report, 2017.
- [42] Energy, A. f. N. R. a. [Summary of the strategic road map for hydrogen and fuel cells](#). Report, 2014.
- [43] [http://www.meti.go.jp/english/press/2016/0322\\_05.html](http://www.meti.go.jp/english/press/2016/0322_05.html), March 22, 2016.
- [44] Behling, N., Williams, M. C., and Managi, S. [Fuel cells and the hydrogen revolution: Analysis of a strategic plan in japan](#). *Economic Analysis and Policy* 48 (2015), 204–221.
- [45] Kendall, M. [Fuel cell development for new energy vehicles \(nevs\) and clean air in china](#). *Progress in Natural Science: Materials International* (2018).
- [46] [China’s hydrogen energy and fuel cell industry innovation strategic alliance was formally established](#). [http://www.xinhuanet.com/energy/2018-02/11/c\\_1122402144.htm](http://www.xinhuanet.com/energy/2018-02/11/c_1122402144.htm), 2018.
- [47] <http://xxgk.miit.gov.cn/gdnps/wjfbContent.jsp?id=6064786>, 2018.

- [48] Rajabzadeh, M., Bathaee, S. M. T., and Aliakbar Golkar, M. [Dynamic modeling and nonlinear control of fuel cell vehicles with different hybrid power sources](#). *International Journal of Hydrogen Energy* 41, 4 (2016), 3185–3198.
- [49] Papageorgopoulos, D. C. [Advancements and prospects of doe fuel cell research and development activities](#). In *Meeting Abstracts*, The Electrochemical Society, pp. 1614–1614.
- [50] Chen, H., Pei, P., and Song, M. [Lifetime prediction and the economic lifetime of proton exchange membrane fuel cells](#). *Applied Energy* 142 (2015), 154–163.
- [51] de Bruijn, F. A., Dam, V. A. T., and Janssen, G. J. M. [Review: Durability and degradation issues of pem fuel cell components](#). *Fuel Cells* 8, 1 (2008), 3–22.
- [52] Li, J., Hu, Z., Xu, L., Ouyang, M., Fang, C., Hu, J., Cheng, S., Po, H., Zhang, W., and Jiang, H. [Fuel cell system degradation analysis of a chinese plug-in hybrid fuel cell city bus](#). *International Journal of Hydrogen Energy* 41, 34 (2016), 15295–15310.
- [53] Hu, X., Johannesson, L., Murgovski, N., and Egardt, B. [Longevity-conscious dimensioning and power management of the hybrid energy storage system in a fuel cell hybrid electric bus](#). *Applied Energy* 137 (2015), 913–924.
- [54] Yuan, X.-Z., Li, H., Zhang, S., Martin, J., and Wang, H. [A review of polymer electrolyte membrane fuel cell durability test protocols](#). *Journal of Power Sources* 196, 22 (2011), 9107–9116.
- [55] Placca, L., and Kouta, R. [Fault tree analysis for pem fuel cell degradation process modelling](#). *International Journal of Hydrogen Energy* 36, 19 (2011), 12393–12405.
- [56] Liu, D., and Case, S. [Durability study of proton exchange membrane fuel cells under dynamic testing conditions with cyclic current profile](#). *Journal of Power Sources* 162, 1 (2006), 521–531.
- [57] Sulaiman, N., Hannan, M. A., Mohamed, A., Majlan, E. H., and Wan Daud, W. R. [A review on energy management system for fuel cell hybrid electric vehicle: Issues and challenges](#). *Renewable and Sustainable Energy Reviews* 52 (2015), 802–814.
- [58] Burke, A. F. [Batteries and ultracapacitors for electric, hybrid, and fuel cell vehicles](#). *Proceedings of the Ieee* 95, 4 (2007), 806–820.
- [59] Odeim, F., Roes, J., and Heinzl, A. [Power management optimization of an experimental fuel cell/battery/supercapacitor hybrid system](#). *Energies* 8, 7 (2015), 6302–6327.
- [60] Panday, A., and Bansal, H. O. [A review of optimal energy management strategies for hybrid electric vehicle](#). *International Journal of Vehicular Technology* 2014 (2014), 1–19.
- [61] Cuma, M. U., and Koroglu, T. [A comprehensive review on estimation strategies used in hybrid and battery electric vehicles](#). *Renewable and Sustainable Energy Reviews* 42 (2015), 517–531.
- [62] Jalil, N., Kheir, N. A., and Salman, M. [A rule-based energy management strategy for a series hybrid vehicle](#). In *Proceedings of the 1997 American Control Conference (Cat. No.97CH36041)*, vol. 1, pp. 689–693 vol.1.

- [63] Shabbir, W., and Evangelou, S. A. [Exclusive operation strategy for the supervisory control of series hybrid electric vehicles](#). *IEEE Transactions on Control Systems Technology* (2016), 1–9.
- [64] Ahmadi, S., and Bathaee, S. M. T. [Multi-objective genetic optimization of the fuel cell hybrid vehicle supervisory system: Fuzzy logic and operating mode control strategies](#). *International Journal of Hydrogen Energy* 40, 36 (2015), 12512–12521.
- [65] Fadel, A., and Zhou, B. [An experimental and analytical comparison study of power management methodologies of fuel cell–battery hybrid vehicles](#). *Journal of Power Sources* 196, 6 (2011), 3271–3279.
- [66] Lachhab, I., and Krichen, L. [An improved energy management strategy for fc/uc hybrid electric vehicles propelled by motor-wheels](#). *International Journal of Hydrogen Energy* 39, 1 (2014), 571–581.
- [67] Aouzellag, H., Ghedamsi, K., and Aouzellag, D. [Energy management and fault tolerant control strategies for fuel cell/ultra-capacitor hybrid electric vehicles to enhance autonomy, efficiency and life time of the fuel cell system](#). *International Journal of Hydrogen Energy* 40, 22 (2015), 7204–7213.
- [68] Yun, H., Liu, S., Zhao, Y., Xie, J., Liu, C., Hou, Z., and Wang, K. [Energy management for fuel cell hybrid vehicles based on a stiffness coefficient model](#). *International Journal of Hydrogen Energy* 40, 1 (2015), 633–641.
- [69] Li, Q., Yang, H., Han, Y., Li, M., and Chen, W. [A state machine strategy based on droop control for an energy management system of pemfc-battery-supercapacitor hybrid tramway](#). *International Journal of Hydrogen Energy* 41, 36 (2016), 16148–16159.
- [70] Li, Q., Chen, W., Li, Y., Liu, S., and Huang, J. [Energy management strategy for fuel cell/battery/ultracapacitor hybrid vehicle based on fuzzy logic](#). *International Journal of Electrical Power & Energy Systems* 43, 1 (2012), 514–525.
- [71] Mohammadi, M., Kraa, O., Becherif, M., Aboubou, A., Ayad, M. Y., and Bahri, M. [Fuzzy logic and passivity-based controller applied to electric vehicle using fuel cell and supercapacitors hybrid source](#). *Energy Procedia* 50 (2014), 619–626.
- [72] Ravey, A., Mohammadi, A., and Bouquain, D. [Control strategy of fuel cell electric vehicle including degradation process](#). In *Industrial Electronics Society, IECON 2015 - 41st Annual Conference of the IEEE*, pp. 003508–003513.
- [73] Odeim, F., Roes, J., Wülbeck, L., and Heinzl, A. [Power management optimization of fuel cell/battery hybrid vehicles with experimental validation](#). *Journal of Power Sources* 252 (2014), 333–343.
- [74] Caux, S., Hankache, W., Fadel, M., and Hissel, D. [On-line fuzzy energy management for hybrid fuel cell systems](#). *International Journal of Hydrogen Energy* 35, 5 (2010), 2134–2143.
- [75] Ryu, J., Park, Y., and Sunwoo, M. [Electric powertrain modeling of a fuel cell hybrid electric vehicle and development of a power distribution algorithm based on driving mode recognition](#). *Journal of Power Sources* 195, 17 (2010), 5735–5748.

- [76] Li, C.-Y., and Liu, G.-P. [Optimal fuzzy power control and management of fuel cell/battery hybrid vehicles](#). *Journal of Power Sources* 192, 2 (2009), 525–533.
- [77] Carignano, M. G., Costa-Castelló, R., Roda, V., Nigro, N. M., Junco, S., and Feroldi, D. [Energy management strategy for fuel cell-supercapacitor hybrid vehicles based on prediction of energy demand](#). *Journal of Power Sources* 360 (2017), 419–433.
- [78] Ibrahim, M., Jemei, S., Wimmer, G., Steiner, N. Y., Kokonendji, C. C., and Hissel, D. [Selection of mother wavelet and decomposition level for energy management in electrical vehicles including a fuel cell](#). *International Journal of Hydrogen Energy* 40, 45 (2015), 15823–15833.
- [79] Alloui, H., Achour, Y., Marouani, K., and Becherif, M. [Energy management based on frequency decoupling: Experimental results with fuel cell-electric vehicle emulator](#). In *2015 IEEE 81st Vehicular Technology Conference (VTC Spring)*, pp. 1–5.
- [80] Tani, A., Camara, M. B., and Dakyo, B. [Energy management based on frequency approach for hybrid electric vehicle applications: Fuel-cell/lithium-battery and ultracapacitors](#). *IEEE Transactions on Vehicular Technology* 61, 8 (2012), 3375–3386.
- [81] Alloui, H., Marouani, K., Becherif, M., Sid, M. N., and Benbouzid, M. E. H. [A control strategy scheme for fuel cell-vehicle based on frequency separation](#). *2014 International Conference on Green Energy* (2014).
- [82] Azib, T., Larouci, C., Chaibet, A., and Boukhniifer, M. [Online energy management strategy of a hybrid fuel cell/battery/ultracapacitor vehicular power system](#). *IEEE Transactions on Electrical and Electronic Engineering* 9, 5 (2014), 548–554.
- [83] Li, Q., Chen, W., Liu, Z., Li, M., and Ma, L. [Development of energy management system based on a power sharing strategy for a fuel cell-battery-supercapacitor hybrid tramway](#). *Journal of Power Sources* 279 (2015), 267–280.
- [84] Enang, W., and Bannister, C. [Modelling and control of hybrid electric vehicles \(a comprehensive review\)](#). *Renewable and Sustainable Energy Reviews* 74 (2017), 1210–1239.
- [85] Shaneb, O. A., Taylor, P. C., and Coates, G. [Optimal online operation of residential chp systems using linear programming](#). *Energy and Buildings* 44 (2012), 17–25.
- [86] Dinnawi, R., Fares, D., Chedid, R., Karaki, S., and Jabr, R. A. [Optimized energy management system for fuel cell hybrid vehicles](#). In *Mediterranean Electrotechnical Conference (MELECON), 2014 17th IEEE*, pp. 97–102.
- [87] Caux, S., Gaoua, Y., and Lopez, P. [A combinatorial optimisation approach to energy management strategy for a hybrid fuel cell vehicle](#). *Energy* 133 (2017), 219–230.
- [88] Salmasi, F. R. [Control strategies for hybrid electric vehicles: Evolution, classification, comparison, and future trends](#). *IEEE Transactions on Vehicular Technology* 56, 5 (2007), 2393–2404.
- [89] Zhang, X., and Mi, C. [Vehicle power management: modeling, control and optimization](#). Springer Science & Business Media, 2011.
- [90] Bertsekas, D. P., Bertsekas, D. P., Bertsekas, D. P., and Bertsekas, D. P. [Dynamic programming and optimal control](#), vol. 1. Athena scientific Belmont, MA, 1995.

- [91] Fletcher, T., Thring, R., and Watkinson, M. [An energy management strategy to concurrently optimise fuel consumption & pem fuel cell lifetime in a hybrid vehicle.](#) International Journal of Hydrogen Energy (2016).
- [92] Martel, F., Kelouwani, S., Dubé, Y., and Agbossou, K. [Optimal economy-based battery degradation management dynamics for fuel-cell plug-in hybrid electric vehicles.](#) Journal of Power Sources 274 (2015), 367–381.
- [93] Martel, F., Dubé, Y., Kelouwani, S., Jaguemont, J., and Agbossou, K. [Long-term assessment of economic plug-in hybrid electric vehicle battery lifetime degradation management through near optimal fuel cell load sharing.](#) Journal of Power Sources 318 (2016), 270–282.
- [94] Fares, D., Chedid, R., Panik, F., Karaki, S., and Jabr, R. [Dynamic programming technique for optimizing fuel cell hybrid vehicles.](#) International Journal of Hydrogen Energy 40, 24 (2015), 7777–7790.
- [95] Zhou, Z., and Mi, C. [Power management of phev using quadratic programming.](#) International Journal of Electric and Hybrid Vehicles 3, 3 (2011), 246–258.
- [96] Chrenko, D., Gan, S., Gutenkunst, C., Kriesten, R., and Moyne, L. L. [Novel classification of control strategies for hybrid electric vehicles.](#) In Vehicle Power and Propulsion Conference (VPPC), 2015 IEEE, pp. 1–6.
- [97] Ahmadi, S., Bathaee, S. M. T., and Hosseinpour, A. H. [Improving fuel economy and performance of a fuel-cell hybrid electric vehicle \(fuel-cell, battery, and ultra-capacitor\) using optimized energy management strategy.](#) Energy Conversion and Management 160 (2018), 74–84.
- [98] Eberhart, R., and Kennedy, J. [A new optimizer using particle swarm theory.](#) In Micro Machine and Human Science, 1995. MHS '95., Proceedings of the Sixth International Symposium on, pp. 39–43.
- [99] Bonyadi, M. R., and Michalewicz, Z. [Particle swarm optimization for single objective continuous space problems: A review.](#) Evolutionary Computation 25, 1 (2017), 1–54.
- [100] Zhang, Y., Wang, S., and Ji, G. [A comprehensive survey on particle swarm optimization algorithm and its applications.](#) Mathematical Problems in Engineering 2015 (2015).
- [101] Zhang, Y., Balochian, S., Agarwal, P., Bhatnagar, V., and Housheya, O. J. [Artificial intelligence and its applications.](#) Mathematical Problems in Engineering 2014 (2014), 10.
- [102] Khoucha, F., Habib, M., Benbouzid, M. E. H., and Kheloui, A. [Rule-based energy management strategy optimized using pso for fuel cell/battery electric vehicle.](#) 2015 3, 1 (2015).
- [103] Koubaa, R., and krichen, L. [Double layer metaheuristic based energy management strategy for a fuel cell/ultra-capacitor hybrid electric vehicle.](#) Energy 133 (2017), 1079–1093.
- [104] Ahmadi, S., Abdi, S., and Kakavand, M. [Maximum power point tracking of a proton exchange membrane fuel cell system using pso-pid controller.](#) International Journal of Hydrogen Energy 42, 32 (2017), 20430–20443.

- [105] Marini, F., and Walczak, B. [Particle swarm optimization \(pso\). a tutorial](#). *Chemo-metrics and Intelligent Laboratory Systems* 149 (2015), 153–165.
- [106] Li, M., Du, W. Q., and Nian, F. Z. [An adaptive particle swarm optimization algorithm based on directed weighted complex network](#). *Mathematical Problems in Engineering* 2014 (2014), 7.
- [107] Millo, F., Rolando, L., Fuso, R., Bergshoeff, E., and Shafiabady, F. [Analysis of different energy management strategies for complex hybrid electric vehicles](#). *Computer-Aided Design and Applications* 11, sup1 (2014), S1–S10.
- [108] Wang, H., Huang, Y., He, H., Lv, C., Liu, W., and Khajepour, A. [Chapter 5 - Energy Management of Hybrid Electric Vehicles A2 - Zhang, Hui](#). Woodhead Publishing, 2018, pp. 159–206.
- [109] Aiteur, I. E., Vlad, C., and Godoy, E. [Energy management and control of a fuel cell/supercapacitor multi-source system for electric vehicles](#). In *System Theory, Control and Computing (ICSTCC)*, 2015 19th International Conference on, pp. 797–802.
- [110] García, P., Torreglosa, J. P., Fernández, L. M., and Jurado, F. [Viability study of a fc-battery-sc tramway controlled by equivalent consumption minimization strategy](#). *International Journal of Hydrogen Energy* 37, 11 (2012), 9368–9382.
- [111] Geng, B., Mills, J. K., and Sun, D. [Two-stage energy management control of fuel cell plug-in hybrid electric vehicles considering fuel cell longevity](#). *IEEE Transactions on Vehicular Technology* 61, 2 (2012), 498–508.
- [112] Zhang, P., Yan, F., and Du, C. [A comprehensive analysis of energy management strategies for hybrid electric vehicles based on bibliometrics](#). *Renewable and Sustainable Energy Reviews* 48 (2015), 88–104.
- [113] Han, J., Park, Y., and Park, Y.-s. [A novel updating method of equivalent factor in ecms for prolonging the lifetime of battery in fuel cell hybrid electric vehicle](#). *IFAC Proceedings Volumes* 45, 30 (2012), 227–232.
- [114] Zhang, S., Xiong, R., and Zhang, C. [Pontryagin’s minimum principle-based power management of a dual-motor-driven electric bus](#). *Applied Energy* 159 (2015), 370–380.
- [115] Krotov, V. F. [Global Methods in Optimal Control Theory](#). Birkhäuser Boston, Boston, MA, 1993, pp. 74–121.
- [116] Zheng, C. H., Xu, G. Q., Park, Y. I., Lim, W. S., and Cha, S. W. [Prolonging fuel cell stack lifetime based on pontryagin’s minimum principle in fuel cell hybrid vehicles and its economic influence evaluation](#). *Journal of Power Sources* 248 (2014), 533–544.
- [117] Xu, L., Li, J., Ouyang, M., Hua, J., and Yang, G. [Multi-mode control strategy for fuel cell electric vehicles regarding fuel economy and durability](#). *International Journal of Hydrogen Energy* 39, 5 (2014), 2374–2389.
- [118] Ettahir, K., Boulon, L., and Agbossou, K. [Optimization-based energy management strategy for a fuel cell/battery hybrid power system](#). *Applied Energy* 163 (2016), 142–153.

- [119] Zheng, C., Cha, S. W., Park, Y.-i., Lim, W. S., and Xu, G. [Pmp-based power management strategy of fuel cell hybrid vehicles considering multi-objective optimization](#). *International Journal of Precision Engineering and Manufacturing* 14, 5 (2013), 845–853.
- [120] Serrao, L., Onori, S., and Rizzoni, G. [A comparative analysis of energy management strategies for hybrid electric vehicles](#). *Journal of Dynamic Systems, Measurement, and Control* 133, 3 (2011), 031012–031012–9.
- [121] Onori, S., and Tribioli, L. [Adaptive pontryagin’s minimum principle supervisory controller design for the plug-in hybrid gm chevrolet volt](#). *Applied Energy* 147 (2015), 224–234.
- [122] Simmons, K., Guezennec, Y., and Onori, S. [Modeling and energy management control design for a fuel cell hybrid passenger bus](#). *Journal of Power Sources* 246 (2014), 736–746.
- [123] Greenwell, W., and Vahidi, A. [Predictive control of voltage and current in a fuel cell-ultracapacitor hybrid](#). *IEEE Transactions on Industrial Electronics* 57, 6 (2010), 1954–1963.
- [124] Sultana, W. R., Sahoo, S. K., Sukchai, S., Yamuna, S., and Venkatesh, D. [A review on state of art development of model predictive control for renewable energy applications](#). *Renewable and Sustainable Energy Reviews* 76 (2017), 391–406.
- [125] Ziogou, C., Papadopoulou, S., Georgiadis, M. C., and Voutetakis, S. [On-line nonlinear model predictive control of a pem fuel cell system](#). *Journal of Process Control* 23, 4 (2013), 483–492.
- [126] Torreglosa, J. P., Garcia, P., Fernandez, L. M., and Jurado, F. [Predictive control for the energy management of a fuel-cell battery supercapacitor tramway](#). *IEEE Transactions on Industrial Informatics* 10, 1 (2014), 276–285.
- [127] Li, T., Liu, H., and Ding, D. [Predictive energy management of fuel cell supercapacitor hybrid construction equipment](#). *Energy* 149 (2018), 718–729.
- [128] Arce, A., del Real, A. J., and Bordons, C. [Mpc for battery/fuel cell hybrid vehicles including fuel cell dynamics and battery performance improvement](#). *Journal of Process Control* 19, 8 (2009), 1289–1304.
- [129] Zhang, S., Xiong, R., and Sun, F. [Model predictive control for power management in a plug-in hybrid electric vehicle with a hybrid energy storage system](#). *Applied Energy* 185 (2017), 1654–1662.
- [130] Camacho, E., Bordons, C., and Alba, C. [Model Predictive Control](#). Springer London, 2004.
- [131] Marcano, M., Matute, J. A., Lattarulo, R., Martí, E., and Pérez, J. [Low speed longitudinal control algorithms for automated vehicles in simulation and real platforms](#). *Complexity* 2018 (2018), 12.
- [132] Kathis, J. [Using model predictive control for cooperative traffic signal control](#). In *OPT-i 1st International Conference on Engineering and Applied Sciences Optimization - Proceedings* (2014), M. Karlaftis, N. Lagaros, and P. M., Eds.

- [133] Sid, M. N., Nounou, K., Becherif, M., Marouani, K., and Alloui, H. [Energy management and optimal control strategies of fuel cell/supercapacitors hybrid vehicle](#). In *Electrical Machines (ICEM), 2014 International Conference on*, pp. 2293–2298.
- [134] Zheng, C.-H., Lee, C.-M., Huang, Y.-C., and Lin, W.-S. [Adaptive optimal control algorithm for maturing energy management strategy in fuel-cell/li-ion-capacitor hybrid electric vehicles](#). In *2013 9th Asian Control Conference (ASCC)*, pp. 1–7.
- [135] Ansarey, M., Shariat Panahi, M., Ziarati, H., and Mahjoob, M. [Optimal energy management in a dual-storage fuel-cell hybrid vehicle using multi-dimensional dynamic programming](#). *Journal of Power Sources* 250 (2014), 359–371.
- [136] Li, H., Ravey, A., N'Diaye, A., and Djerdir, A. [Equivalent consumption minimization strategy for hybrid electric vehicle powered by fuel cell, battery and supercapacitor](#). In *IECON 2016 - 42nd Annual Conference of the IEEE Industrial Electronics Society (Oct 2016)*, pp. 4401–4406.
- [137] Torreglosa, J. P., Jurado, F., García, P., and Fernández, L. M. [Hybrid fuel cell and battery tramway control based on an equivalent consumption minimization strategy](#). *Control Engineering Practice* 19, 10 (2011), 1182–1194.
- [138] Hannan, M. A., Azidin, F. A., and Mohamed, A. [Hybrid electric vehicles and their challenges: A review](#). *Renewable and Sustainable Energy Reviews* 29 (2014), 135–150.
- [139] Solano, J., Hissel, D., and Pera, M. C. [Energy management of an hybrid electric vehicle in degraded operation](#). In *2014 IEEE Vehicle Power and Propulsion Conference (VPPC)*, pp. 1–4.
- [140] Solano, J., Hissel, D., and Pera, M. [Fail-safe power for hybrid electric vehicles: Implementing a self-sustained global energy management system](#). *IEEE Vehicular Technology Magazine* 13, 2 (2018), 34–39.
- [141] Zheng, C. H., Kim, N. W., Park, Y. I., Lim, W. S., Cha, S. W., and Xu, G. Q. [The effect of battery temperature on total fuel consumption of fuel cell hybrid vehicles](#). *International Journal of Hydrogen Energy* 38, 13 (2013), 5192–5200.
- [142] Li, H., Ravey, A., Diaye, A. N., and Djerdir, A. [Equivalent consumption minimization strategy for fuel cell hybrid electric vehicle considering fuel cell degradation](#). In *2017 IEEE Transportation Electrification Conference and Expo (ITEC)*, pp. 540–544.
- [143] García, P., Torreglosa, J. P., Fernández, L. M., and Jurado, F. [Control strategies for high-power electric vehicles powered by hydrogen fuel cell, battery and supercapacitor](#). *Expert Systems with Applications* 40, 12 (2013), 4791–4804.
- [144] Feroldi, D., and Carignano, M. [Sizing for fuel cell/supercapacitor hybrid vehicles based on stochastic driving cycles](#). *Applied Energy* 183 (2016), 645–658.
- [145] Ettihir, K., Higueta Cano, M., Boulon, L., and Agbossou, K. [Design of an adaptive ems for fuel cell vehicles](#). *International Journal of Hydrogen Energy* (2016).
- [146] Bizon, N., and Thounthong, P. [Real-time strategies to optimize the fueling of the fuel cell hybrid power source: A review of issues, challenges and a new approach](#). *Renewable and Sustainable Energy Reviews* 91 (2018), 1089–1102.

- [147] Bizon, N. [Energy optimization of fuel cell system by using global extremum seeking algorithm](#). *Applied Energy* 206 (2017), 458–474.
- [148] Bizon, N. [Real-time optimization strategy for fuel cell hybrid power sources with load-following control of the fuel or air flow](#). *Energy Conversion and Management* 157 (2018), 13–27.
- [149] Hemi, H., Ghouili, J., and Cheriti, A. [Combination of markov chain and optimal control solved by pontryagin’s minimum principle for a fuel cell/supercapacitor vehicle](#). *Energy Conversion and Management* 91 (2015), 387–393.
- [150] Pelletier, S., Jabali, O., Laporte, G., and Veneroni, M. [Battery degradation and behaviour for electric vehicles: Review and numerical analyses of several models](#). *Transportation Research Part B-Methodological* 103 (2017), 158–187.
- [151] Zhang, L., Hu, X., Wang, Z., Sun, F., and Dorrell, D. G. [A review of supercapacitor modeling, estimation, and applications: A control/management perspective](#). *Renewable and Sustainable Energy Reviews* 81, Part 2 (2018), 1868–1878.
- [152] Pei, P., and Chen, H. [Main factors affecting the lifetime of proton exchange membrane fuel cells in vehicle applications: A review](#). *Applied Energy* 125 (2014), 60–75.
- [153] Pei, P., Chang, Q., and Tang, T. [A quick evaluating method for automotive fuel cell lifetime](#). *International Journal of Hydrogen Energy* 33, 14 (2008), 3829–3836.
- [154] Li, T., Liu, H., Zhao, D., and Wang, L. [Design and analysis of a fuel cell supercapacitor hybrid construction vehicle](#). *International Journal of Hydrogen Energy* 41, 28 (2016), 12307–12319.
- [155] Hu, X., Murgovski, N., Johannesson, L. M., and Egardt, B. [Optimal dimensioning and power management of a fuel cell/battery hybrid bus via convex programming](#). *IEEE/ASME Transactions on Mechatronics* 20, 1 (2015), 457–468.
- [156] Zheng, C. H., Oh, C. E., Park, Y. I., and Cha, S. W. [Fuel economy evaluation of fuel cell hybrid vehicles based on equivalent fuel consumption](#). *International Journal of Hydrogen Energy* 37, 2 (2012), 1790–1796.
- [157] Han, J., Park, Y., and Kum, D. [Optimal adaptation of equivalent factor of equivalent consumption minimization strategy for fuel cell hybrid electric vehicles under active state inequality constraints](#). *Journal of Power Sources* 267 (2014), 491–502.
- [158] Xu, L., Yang, F., Li, J., Ouyang, M., and Hua, J. [Real time optimal energy management strategy targeting at minimizing daily operation cost for a plug-in fuel cell city bus](#). *International Journal of Hydrogen Energy* 37, 20 (2012), 15380–15392.
- [159] Daigle, M. J., and Kulkarni, C. S. [Electrochemistry-based battery modeling for prognostics](#).
- [160] Hou, Z., Wang, R., Wang, K., Shi, W., Xing, D., and Jiang, H. [Failure mode investigation of fuel cell for vehicle application](#). *Frontiers in Energy* 11, 3 (2017), 318–325.
- [161] Jakob, W., and Blume, C. [Pareto optimization or cascaded weighted sum: A comparison of concepts](#). *Algorithms* 7, 1 (2014), 166–185.

- [162] Kim, I. Y., and de Weck, O. L. [Adaptive weighted sum method for multiobjective optimization: a new method for pareto front generation](#). *Structural and Multidisciplinary Optimization* 31, 2 (2006), 105–116.
- [163] Onori, S., Serrao, L., and Rizzoni, G. [Hybrid electric vehicles: Energy management strategies](#). Springer, 2016.
- [164] Tani, A., Camara, M. B., and Dakyo, B. [Energy management based on frequency approach for hybrid electric vehicle applications: Fuel-cell/lithium-battery and ultracapacitors](#). *IEEE Transactions on Vehicular Technology* 61, 8 (2012), 3375–3386.
- [165] Gao, F., Blunier, B., and Miraoui, A. [Proton exchange membrane fuel cells modeling](#). John Wiley & Sons, 2013.
- [166] Kim, J., Kim, M., Kang, T., Sohn, Y.-J., Song, T., and Choi, K. H. [Degradation modeling and operational optimization for improving the lifetime of high-temperature pem \(proton exchange membrane\) fuel cells](#). *Energy* 66 (2014), 41–49.
- [167] Breaz, E., Gao, F., Blunier, B., and Tirnovan, R. [Mathematical modeling of proton exchange membrane fuel cell with integrated humidifier for mobile applications](#). In *2012 IEEE Transportation Electrification Conference and Expo (ITEC)*, pp. 1–6.
- [168] Fei, G., Blunier, B., and Miraoui, A. [Pem fuel cell stack modeling for real-time emulation in hardware-in-the-loop applications](#). *IEEE Transactions on Energy Conversion* 26, 1 (2011), 184–194.
- [169] McCall, J. [Genetic algorithms for modelling and optimisation](#). *Journal of Computational and Applied Mathematics* 184, 1 (2005), 205–222.
- [170] You, G. W., Park, S., and Oh, D. [Diagnosis of electric vehicle batteries using recurrent neural networks](#). *IEEE Transactions on Industrial Electronics* 64, 6 (2017), 4885–4893.
- [171] Basualdo, M., Feroldi, D., and Outbib, R. [Pem fuel cells with bio-ethanol processor systems](#). *Springer* 10 (2012), 978–1.
- [172] Larminie, J., Dicks, A., and McDonald, M. S. [Fuel cell systems explained](#), vol. 2. J. Wiley Chichester, UK, 2003.
- [173] Zheng, C., Oh, C., Park, Y., and Cha, S. [Fuel economy evaluation of fuel cell hybrid vehicles based on equivalent fuel consumption](#). *International Journal of Hydrogen Energy* 37, 2 (2012), 1790 – 1796. *10th International Conference on Clean Energy 2010*.
- [174] Daigle, M. J., and Kulkarni, C. S. [Electrochemistry-based battery modeling for prognostics](#).
- [175] Richardson, R. R., Osborne, M. A., and Howey, D. A. [Gaussian process regression for forecasting battery state of health](#). *Journal of Power Sources* 357 (2017), 209–219.
- [176] Bole, B., Kulkarni, C. S., and Daigle, M. [Adaptation of an electrochemistry-based li-ion battery model to account for deterioration observed under randomized use](#). Tech. rep., SGT, Inc. Moffett Field United States, 2014.

- [177] Karthikeyan, D. K., Sikha, G., and White, R. E. [Thermodynamic model development for lithium intercalation electrodes](#). *Journal of Power Sources* 185, 2 (2008), 1398–1407.
- [178] Li, H., Ravey, A., N'Diaye, A., and Djerdir, A. [State of health estimation of lithium-ion batteries under variable load profile](#). In *IECON 2017 - 43rd Annual Conference of the IEEE Industrial Electronics Society* (Oct 2017), pp. 5287–5291.
- [179] Gao, Y. [Graphene and polymer composites for supercapacitor applications: a review](#). *Nanoscale Research Letters* 12, 1 (2017), 387.
- [180] Li, H., Ravey, A., N'Diaye, A., and Djerdir, A. [Equivalent consumption minimization strategy for fuel cell hybrid electric vehicle considering fuel cell degradation](#). In *2017 IEEE Transportation Electrification Conference and Expo (ITEC)* (June 2017), pp. 540–544.
- [181] Solano Martínez, J., John, R. I., Hissel, D., and Péra, M.-C. [A survey-based type-2 fuzzy logic system for energy management in hybrid electrical vehicles](#). *Information Sciences* 190 (2012), 192–207.
- [182] Hemi, H., Ghouili, J., and Cheriti, A. [A real time fuzzy logic power management strategy for a fuel cell vehicle](#). *Energy Conversion and Management* 80 (2014), 63–70.
- [183] Yu, Z., Zinger, D., and Bose, A. [An innovative optimal power allocation strategy for fuel cell, battery and supercapacitor hybrid electric vehicle](#). *Journal of Power Sources* 196, 4 (2011), 2351–2359.
- [184] García, P., Torreglosa, J. P., Fernández, L. M., and Jurado, F. [Viability study of a fc-battery-sc tramway controlled by equivalent consumption minimization strategy](#). *International Journal of Hydrogen Energy* 37, 11 (2012), 9368–9382.
- [185] Zhang, W., Li, J., Xu, L., and Ouyang, M. [Optimization for a fuel cell/battery/capacity tram with equivalent consumption minimization strategy](#). *Energy Conversion and Management* 134, Supplement C (2017), 59 – 69.
- [186] Onori, S., Serrao, L., and Rizzoni, G. [Hybrid electric vehicles: Energy management strategies](#), 2015.
- [187] Xing, X. Q., Lum, K. W., Poh, H. J., and Wu, Y. L. [Geometry optimization for proton-exchange membrane fuel cells with sequential quadratic programming method](#). *Journal of Power Sources* 186, 1 (2009), 10–21.
- [188] Brundell-Freij, K., and Ericsson, E. [Influence of street characteristics, driver category and car performance on urban driving patterns](#). *Transportation Research Part D: Transport and Environment* 10, 3 (2005), 213–229.
- [189] Sutharssan, T., Montalvao, D., Chen, Y. K., Wang, W. C., Pisac, C., and Elemara, H. [A review on prognostics and health monitoring of proton exchange membrane fuel cell](#). *Renewable and Sustainable Energy Reviews* 75 (2017), 440–450.
- [190] Saha, B., and Goebel, K. [Model adaptation for prognostics in a particle filtering framework](#). *International Journal of Prognostics and Health Management* 2 (2011), 61.

- [191] Daigle, M., Saha, B., and Goebel, K. [A comparison of filter-based approaches for model-based prognostics](#). In 2012 IEEE Aerospace Conference (March 2012), pp. 1–10.
- [192] Sankararaman, S., Daigle, M. J., and Goebel, K. [Uncertainty quantification in remaining useful life prediction using first-order reliability methods](#). IEEE Transactions on Reliability 63, 2 (2014), 603–619.
- [193] Chelidze, D. [Multimode damage tracking and failure prognosis in electromechanical systems](#). In Component and Systems Diagnostics, Prognostics, and Health Management II, vol. 4733, International Society for Optics and Photonics, pp. 1–13.
- [194] Celaya, J., Kulkarni, C., Biswas, G., Saha, S., and Goebel, K. [A model-based prognostics methodology for electrolytic capacitors based on electrical overstress accelerated aging](#).
- [195] Haykin, S. [Kalman filtering and neural networks](#), vol. 47. John Wiley & Sons, 2004.
- [196] Wan, E. A., and Merwe, R. V. D. [The unscented kalman filter for nonlinear estimation](#). In Proceedings of the IEEE 2000 Adaptive Systems for Signal Processing, Communications, and Control Symposium (Cat. No.00EX373), pp. 153–158.
- [197] Goebel, K., Saha, B., Saxena, A., Celaya, J. R., and Christophersen, J. P. [Prognostics in battery health management](#). IEEE instrumentation & measurement magazine 11, 4 (2008).
- [198] Daigle, M., Roychoudhury, I., and Bregon, A. [Model-based prognostics of hybrid systems](#).
- [199] Wan, E. A., and Merwe, R. V. D. [The unscented kalman filter for nonlinear estimation](#). In Proceedings of the IEEE 2000 Adaptive Systems for Signal Processing, Communications, and Control Symposium (Cat. No.00EX373) (2000), pp. 153–158.
- [200] Wan, E., and Merwe, R. V. D. [Chapter 7 the unscented kalman filter](#). In Kalman Filtering and Neural Networks (2001), Wiley, pp. 221–280.
- [201] Sierra, G., Orchard, M., Goebel, K., and Kulkarni, C. [Battery health management for small-size rotary-wing electric unmanned aerial vehicles: An efficient approach for constrained computing platforms](#). Reliability Engineering & System Safety 182 (2019), 166–178.
- [202] Gazdzick, P., Mitzel, J., Garcia Sanchez, D., Schulze, M., and Friedrich, K. A. [Evaluation of reversible and irreversible degradation rates of polymer electrolyte membrane fuel cells tested in automotive conditions](#). Journal of Power Sources 327 (2016), 86–95.
- [203] Larminie, J., and Dicks, A. [Fuel Cell Systems Explained](#). J. Wiley, 2003.
- [204] Jouin, M., Gouriveau, R., Hissel, D., Péra, M.-C., and Zerhouni, N. [Degradations analysis and aging modeling for health assessment and prognostics of pemfc](#). Reliability Engineering & System Safety 148 (2016), 78–95.

- [205] Bressel, M., Hilairet, M., Hissel, D., and Bouamama, B. O. [Remaining useful life prediction and uncertainty quantification of proton exchange membrane fuel cell under variable load](#). *IEEE Transactions on Industrial Electronics* 63, 4 (2016), 2569–2577.
- [206] Bressel, M., Hilairet, M., Hissel, D., and Ould Bouamama, B. [Extended kalman filter for prognostic of proton exchange membrane fuel cell](#). *Applied Energy* 164 (2016), 220–227.
- [207] Yang, R., Xiong, R., He, H., Mu, H., and Wang, C. [A novel method on estimating the degradation and state of charge of lithium-ion batteries used for electrical vehicles](#). *Applied Energy* 207 (2017), 336–345.



# List of Figures

1.1	Toyota Mirai . . . . .	8
1.2	The schematic diagram of fuel cell . . . . .	10
1.3	Three architectures of FCHEV [29] . . . . .	12
1.4	Electrical Chain Components Evaluation vehicle . . . . .	14
1.5	F-CITY H2 . . . . .	15
1.6	3 vehicles of the Mobypost fleet . . . . .	15
1.7	Mobypost project . . . . .	16
1.8	Hydrogen and fuel cell budget . . . . .	18
1.9	Hydrogen/Fuel cell Strategy Road map[41] . . . . .	20
1.10	Hydrogen/Fuel cell Strategy Road map about FCV and hydrogen stations[42]	21
1.11	Development objectives of hydrogen fuel cell vehicles in China . . . . .	25
2.1	Energy management strategy . . . . .	29
2.2	PID control strategy . . . . .	30
2.3	Operating mode control . . . . .	31
2.4	Fuzzy membership function of battery SOC . . . . .	32
2.5	Fuzzy rules . . . . .	32
2.6	Speed profile of drive cycle . . . . .	33
2.7	Comparative simulations of SOC . . . . .	33
2.8	n level filtering: decomposition [78] . . . . .	34
2.9	n level filtering: reconstruction [78] . . . . .	35
2.10	Wavelet transform for the Fuel cells-batteries-supercapacitors-architecture [78] . . . . .	35
2.11	Accumulated running cost of each controller[91] . . . . .	38
2.12	Energy management system proposed for the hybrid tramway[110] . . . . .	41
2.13	Simulation results for fuel cell and battery power[110] . . . . .	42
2.14	(a)Supercapacitor power, (b) Power dissipated in the braking resistor dissipated power, and (c) total power of the energy sources[110] . . . . .	43
2.15	Response of fuel-cell hybrid vehicle with hybrid storage system[135] . . . . .	47

2.16	The experimental results of EMS without a supercapacitor. The (a) power distribution and (b) battery voltage[139, 140] . . . . .	49
2.17	The experimental results of EMS without a supercapacitor. The (a) power distribution and (b) battery voltage[139, 140] . . . . .	49
2.18	Frequency decomposing technique for frequency based strategy [82] . . . . .	54
2.19	Lithium-ion battery experimental lifecycle according to DOD [93] . . . . .	55
2.20	FUDS cycle-sprinter power allocation of the sources[94] . . . . .	57
2.21	Optimization results of EMS [59]. (a) Comparison between the Pareto front and the performance of randomly tuned parameters; (b) Optimal strategy parameters for the Pareto front . . . . .	60
2.22	Experimental evaluation of the power management strategy over Manhattan drive cycle [59] . . . . .	61
3.1	Powertrain architecture . . . . .	70
3.2	Schematic representation of the forces acting on a vehicle in motion . . . . .	71
3.3	Structural and functional decomposition of a fuel cell stack[165] . . . . .	73
3.4	Representation of the different losses on the polarization curve[165] . . . . .	73
3.5	Ballard NEXA TM fuel cell stack . . . . .	75
3.6	Fuel cell polarization curve . . . . .	76
3.7	Fuel cell system efficiency curve along with stack current . . . . .	78
3.8	Battery model . . . . .	79
3.9	Model validation for variable loading . . . . .	82
3.10	Supercapacitor model . . . . .	83
3.11	2-quadrant DC/DC buck/boost converter for supercapacitor . . . . .	83
3.12	Architecture of rule based control strategy . . . . .	87
3.13	Flow chart of operating mode control strategy . . . . .	88
3.14	HEOS architecture . . . . .	89
3.15	WVUCITY drive cycle . . . . .	90
3.16	New York Bus drive cycle . . . . .	90
3.17	LA92 drive cycle . . . . .	90
3.18	Load power profile for composite drive cycle of WVUCITY, New York Bus and LA92 drive cycle . . . . .	91
3.19	Simulation results of battery SOC and supercapacitor SOC . . . . .	92
3.20	Simulation results of fuel cell, battery and supercapacitor currents for three control strategies . . . . .	93
4.1	Model-based prognostics architecture. . . . .	96

4.2	The general architecture of prognostic approach for estimation of power sources SOHs . . . . .	98
4.3	Estimation of the stack voltage, degradation parameter $\alpha$ and SOH . . . . .	100
4.4	Battery model fitting for the aged battery . . . . .	100
4.5	Battery degradation model fit for aged battery . . . . .	101
4.6	On-line UKF estimates of the degradation state parameter and SOH . . . . .	102
4.7	Comparative results of fuel cell system efficiency between new fuel cell and aged one . . . . .	103
4.8	Comparative results of ECMS under different power sources degradation conditions . . . . .	106
4.9	Control system of AECMS for FCHEV . . . . .	107
4.10	Comparative results of AECMS under different power sources degradation conditions . . . . .	108
5.1	Schematics of the rapid-prototyping test bench used to validate the energy management system . . . . .	109
5.2	Input I/O model . . . . .	110
5.3	Output I/O model . . . . .	110
5.4	Hierarchical control architecture . . . . .	111
5.5	Test bench architecture . . . . .	112
5.6	DC/DC converters . . . . .	112
5.7	Control of power supply and electronic load through MicroAutoBox II . . . . .	113
5.8	MicroAutoBox II . . . . .	114
5.9	Current and voltage sensors . . . . .	114
5.10	Human machine interface in ControlDesk 4.2 . . . . .	115
5.11	Drive cycle profile and load power profile . . . . .	116
5.12	DC bus voltage profile and current profile . . . . .	117
5.13	Comparison of experiment and simulation results of battery SOC . . . . .	118
5.14	Comparison of experiment and simulation results of SECMS . . . . .	120
5.15	Experimental results of battery SOC and supercapacitor SOC . . . . .	121
5.16	Experimental results of fuel cell, battery and supercapacitor current for three control strategies . . . . .	122
5.17	Comparison of fuel cell reference currents for SECMS and HEOS . . . . .	123



# List of Tables

1.1	Real-world demonstration projects of fuel cell vehicles and their specifications[11]	7
1.2	Comparison of three commercial vehicles[14]	9
1.3	Comparison of different kinds of fuel cells [26, 27, 16]	11
1.4	Comparison of batteries and supercapacitor[28]	11
1.5	Technical targets of integrated transportation fuel cell power systems[32]	17
2.1	Highway/FUDS driving cycle comparative results	57
2.2	EMS for different objectives	62
3.1	Fuel cell parameters	75
3.2	Cooling fan speed and stack temperature	77
3.3	Constraints for battery and supercapacitor	86
3.4	Parameters for three drive cycles	91
3.5	Comparative results for three EMSs	92
4.1	Four degradation conditions of power sources	103
4.2	Simulation results of ECMS for four conditions	103
4.3	Simulation results of AECMS for four conditions	105
5.1	Experimental results	117



# Abstract

Global warming, environmental pollution and exhaustion of petroleum energies have risen their attention to humanity over the world. Fuel cell hybrid electric vehicle (FCHEV) taking hydrogen as fuel and have zero emission, is thought by public and private organizations as one of the best ways to solve these problems. This PhD dissertation considers a FCHEV with three power sources: fuel cell, battery and supercapacitor, which increases the difficulty to design an energy management strategy (EMS) to split the power between the different power sources.

Among the EMS available in the current literature, the Equivalent consumption minimization strategy (ECMS) was selected because it allows a local optimization without relying on prior knowledge of driving condition while giving optimal results. Due to the low energy density of supercapacitor, its equivalent hydrogen consumption is neglected in most bibliographic references, which not only counter to the aim of minimizing whole hydrogen consumption but also increase the complication of EMS due to the need of an additional EMS to calculate supercapacitor power demand. Thus, a sequential quadratic programming ECMS (SECMS) strategy is proposed to consider the energy cost of all three power sources into the objective function. A rule based control strategy (RBCS) and hybrid strategy (HEOS) are also designed in order to be compared with SECMS. Degradation of energy sources represents a major challenge for the stability of the developed SECMS system. So, based on online estimating state of health of fuel cell and battery, an adaptive ECMS (AECMS) has been designed by adjusting the equivalent factor and dynamical change rate of fuel cell. The simulation results show that the AECMS can ensure the charge sustenance of battery and the increase of fuel cell durability.

To validate the proposed energy management algorithms and the numerical models, an experimental test bench has been built around the real time interface dSPACE. The comparison of the simulation and experimental results showed that the proposed SECMS is operated at around maximum efficiency, supercapacitor supplies peak power, battery works as the energy buffer. It has been proved that the neglect of supercapacitor equivalent hydrogen consumption in ECMS leads to not optimal operation. Compared with RBCS and HEOS, SECMS has least hydrogen consumption and most stable fuel cell current.

Keywords: Fuel cell hybrid electric vehicles, Equivalent consumption minimization strategy, Degradation of power sources, On-line estimation of state of health, Adaptive equivalent consumption minimum strategy, Experimental validation, dSPACE.



Le réchauffement climatique, la pollution de l'environnement et l'épuisement des énergies pétrolières ont attiré l'attention de l'humanité dans le monde entier. Les véhicules électriques hybrides à pile à combustible (FCHEV), utilisant l'hydrogène comme carburant et n'émettant aucune émission, sont considérés par les organismes publics et privés comme l'un des meilleurs moyens de résoudre ces problèmes. Cette thèse de doctorat considère un FCHEV avec trois sources d'énergie: pile à combustible, batterie et supercondensateur, ce qui complique l'élaboration d'une stratégie de gestion de l'énergie (EMS) pour répartir la puissance entre différentes sources d'alimentation. Parmi les méthodes de gestion de l'énergie de la littérature actuelle, la stratégie de minimisation de la consommation équivalente (ECMS) a été sélectionnée car elle permet une optimisation locale sans connaissance préalable des conditions de conduite et cela en donnant des résultats optimaux.

En raison de la faible densité énergétique du supercondensateur, sa consommation équivalente d'hydrogène est négligée dans la plupart des références bibliographiques, ce qui va non seulement à l'encontre de l'objectif de minimiser la consommation totale d'hydrogène, mais accroît également la complexité du système EMS en raison du besoin d'un système EMS supplémentaire pour calculer la demande en puissance du supercondensateur. Ainsi, une stratégie ECMS à programmation quadratique séquentielle (SECMS) est proposée pour prendre en compte le coût énergétique des trois sources d'énergie dans la fonction objectif. Une stratégie de contrôle basée sur des règles (RBCS) et une stratégie hybride (HEOS) a été également conçues pour être comparée à SECMS. La dégradation des sources d'énergie représente un défi majeur pour la stabilité du système SECMS développé. Basé sur l'estimation en ligne de l'état de santé de la pile à combustible et de la batterie, le système ECMS adaptatif (AECMS) a été implémenté en ajustant le facteur équivalent et le taux de changement dynamique de la pile à combustible. Les résultats de la simulation montrent que l'AECMS peut assurer le maintien de la charge de la batterie et l'augmentation de la durabilité de la pile à combustible.

Pour valider les algorithmes de gestion de l'énergie et les modèles numériques proposés, un banc d'essai expérimental a été construit autour de l'interface temps réel dSPACE. La comparaison des résultats de la simulation numérique et des résultats expérimentaux a montré que le système SECMS proposé fonctionne à un rendement maximal, que le supercondensateur fournit la puissance de pointe et que la batterie fonctionne comme un tampon d'énergie. Il a été prouvé que la négligence de la consommation d'hydrogène équivalente au supercondensateur dans l'ECMS conduit à un fonctionnement non optimal. Comparé à RBCS et HEOS, la SECMS a le moins d'hydrogène consommé et le courant de pile à combustible le plus stable.

Mots clés : Véhicules hybrides à pile à combustible, minimisation de l'énergie équivalente consommée, dégradation des sources de puissance, estimation en ligne de l'état de santé, minimisation adaptative de l'énergie équivalente consommée, Validation expérimentale, dSPACE.



